

Durham E-Theses

New polymer and derivative chemistry of icosahedral carboranes

Stephenson, Ian Richard

How to cite:

Stephenson, Ian Richard (1988) *New polymer and derivative chemistry of icosahedral carboranes*, Durham theses, Durham University. Available at Durham E-Theses Online:
<http://etheses.dur.ac.uk/6637/>

Use policy

The full-text may be used and/or reproduced, and given to third parties in any format or medium, without prior permission or charge, for personal research or study, educational, or not-for-profit purposes provided that:

- a full bibliographic reference is made to the original source
- a [link](#) is made to the metadata record in Durham E-Theses
- the full-text is not changed in any way

The full-text must not be sold in any format or medium without the formal permission of the copyright holders.

Please consult the [full Durham E-Theses policy](#) for further details.

NEW POLYMER AND DERIVATIVE CHEMISTRY
OF ICOSAHEDRAL CARBORANES

By Ian Richard Stephenson B.Sc (Dunelm)
Grey College

The copyright of this thesis rests with the author.
No quotation from it should be published without
his prior written consent and information derived
from it should be acknowledged.

A thesis submitted to the University of Durham
in candidature for the Degree of Doctor of Philosophy

April 1988



To my family

DECLARATION

The work described in this thesis was carried out in the University of Durham between September 1984 and September 1987. It has not been submitted, either completely or in part, for another degree in this or any other University and is the original work of the author except where acknowledged by reference. Some aspects of the work have formed the basis for the following publications:

'Structure and bonding of the Lithium Tetrahydroborate Tetramethylethylene diamine Adduct $[\text{TMEDA} \cdot \text{LiBH}_4]_2$, a Centrosymmetric dimer containing Doubly and Triply Bridging Hydrogen atoms'
D.R. Armstrong, W. Clegg, H.M. Colquhoun, J.A. Daniels, R.E. Mulvey, I.R. Stephenson, K. Wade, J. Chem. Soc. Chem. Commun. 1987, 630.

'A Pentuply-bridging Carbonyl Group:Crystal and Molecular Structure of a Salt of the 1-oxo-2-phenyl-1,2-dicarba-dodecaborate (12) anion, $[\text{LH}]^+ [\text{O}(\text{Ph})\text{C}_2\text{B}_{10}\text{H}_{10}]^-$ L=1,8-NNN¹N¹-tetramethylnaphthalenediamine'
D.A. Brown, W. Clegg, H.M. Colquhoun, J.A. Daniels, I.R. Stephenson, K. Wade, J. Chem. Soc. Chem. Commun. 1987, 889.

ACKNOWLEDGEMENTS

I would like to express my sincere thanks to Professor K. Wade for his patient and enthusiastic supervision during this work. I am also indebted to Dr. H.M. Colquhoun and Dr. J.A. Daniels of ICI plc for the invaluable help and advice they have readily given throughout this project.

I would also like to thank all the spectroscopists, analysts and other technical staff in the Durham University Chemistry department, and in particular Mr. B. Hall, for all their assistance. I am also very grateful to Dr. W. Clegg of Newcastle University for his crystallographic work, to Dr. D. Reed of Edinburgh University for high field N.M.R. spectra and to Professor E.H. Wong of Durham (New Hampshire) and Dr. R.E. Mulvey for their helpful discussions. In addition, I would like to thank all my colleagues in the Chemistry department for their support and friendship over the past three years.

A grant from the S.E.R.C., and C.A.S.E. award from ICI plc are gratefully acknowledged.

Finally I would like to sincerely thank Chris Reid for typing this thesis.

CONTENTS

Abstract

Abbreviations and nomenclature

	<u>Page</u>
Chapter 1 <u>Introduction</u>	1
1.2 Icosahedral Carboranes: a brief review	1
1.2.1 General Chemistry of Carboranes	1
1.2.2 Potential applications of Carboranes	6
1.3 The Preparation and Properties of Aromatic (polyetherketones)	8
1.4 Scope of the present work	11
1.5 References	13
Chapter 2 <u>The Preparation and Characterisation of Icosahedral Carboranes</u>	
2.1 Introduction	16
2.2 Carborane Preparation	16
2.2.1 The reaction of Decaborane with acetylene	16
2.2.2 Thermal isomerisation of icosahedral carboranes	22
2.2.3 Carborane derivatives prepared	24
<hr/>	
2.3 Characterisation of Carboranes	26
2.3.1 Infra Red Spectroscopy	26
2.3.2 Nuclear Magnetic Resonance Spectroscopy	27
2.3.3 Mass Spectrometry	28
2.4 Experimental	34
2.5 References	49

	<u>Page</u>
Chapter 3 <u>Model polymerisation reactions and monomer synthesis</u>	
3.1 Introduction	52
3.2 Polymerisation Reactions	53
3.2.1 Nucleophilic Polycondensation : Polyetherification	53
3.2.2 Electrophilic Polycondensation : polyacylation	54
3.3 Model Reactions	57
3.3.1 The electronic properties of the carborane cage	57
3.3.2 The reactivity of the cage	58
3.3.3 Nucleophilic model reactions	59
3.3.4 Electrophilic model reactions	61
3.3.5 Conclusions	65
3.3.5.1 The feasibility of the different routes to aromatic poly(carboranyl-etherketones)	66
3.3.5.2 The choice of linkage used for carborane incorporation	66
3.4 Monomer synthesis	68
3.4.1 Target molecules and synthesis strategy	68
3.4.1.1 Preparation of diaryl acetylenes	69
3.4.2 Summary of synthesis carried out	73
3.5 Experimental	76
3.6 References	106
Chapter 4 <u>The synthesis and characterisation of poly(carboranyl- etherketones)</u>	
4.1 Introduction	110
4.2 Polymer Preparation	110
4.3 Polymer Characterisation	112
4.3.1 Molecular weight determination	112
4.3.1.1 Solution viscosities	115
4.3.1.2 Gel Permeation Chromatography	117

	<u>Page</u>
4.3.2 Spectroscopic Characterisation	118
4.3.2.1 Infra Red Spectroscopy	120
4.3.2.2 ¹³ C NMR	121
4.3.2.3 ¹ H NMR	125
4.3.3 Calorimetric and Thermal Characterisation of polymers	127
4.3.3.1 DSC studies	127
4.3.3.2 TGA studies	133
4.4 Experimental	140
4.5 Conclusions and Future Work	144
4.6 References	148
Chapter 5 <u>Studies on C-hydroxy Carboranes</u>	
5.1 Introduction	150
5.2 C-oxygen derivatives of icosahedral carboranes	150
5.3 Preparation and properties of C-hydroxy carboranes	153
5.3.1 Preparation of C-hydroxy carboranes	153
5.3.2 Properties of C-hydroxy carboranes	155
5.3.3 The effects of deprotonation on C-hydroxy derivatives	156
5.4 The crystal and molecular structure of the proton sponge salt of 1-hydroxy-2-phenyl-ortho- carborane	161
5.5 Experimental	172
5.6 Conclusions and Future Work	185
5.7 References	188
Chapter 6 <u>NMR and Theoretical Studies on Icosahedral Carboranes</u>	
6.1 Introduction	190
6.2 ¹¹ NMR studies on Icosahedral Carborane derivatives	191

	<u>Page</u>
6.3 Results	193
6.3.1 Experimental	193
6.3.2 Assignment of Spectra - The use of ^{11}B - ^{11}B 2D COSY NMR	193
6.3.3 Discussion	211
6.4 Theoretical studies on Icosahedral Carboranes	219
6.4.1 Results from theoretical calculations	221
6.4.2 Discussion	224
6.5 Proton NMR Studies on Icosahedral Carboranes	231
6.5.1 Results: interpretation of ^1H NMR spectra	232
6.5.2 Discussion	236
6.6 Conclusions and Future Work	240
6.7 References	242
Appendix A	<u>Studies into the interaction between lithium and boron hydride anions</u>
A.1 Introduction	244
A.2 Discussion	245
A.3 Additional studies carried out	248
Appendix B	General Techniques 255
Appendix C	Colloquia 257

New Polymer and Derivative Chemistry of Icosahedral Carboranes

I.R. Stephenson, B.Sc.

Abstract

This thesis describes research carried out to establish routes to, and syntheses and characterisation of aromatic poly(etherketones), with icosahedral carboranes ($C_2B_{10}H_{12}$) incorporated into the polymer backbone (poly(carboranyletherketones)). Several sidelines which have stemmed from this work are also described.

A brief literature review and discussion of project objectives introduces the work. The mechanism of formation and the general characterisation of icosahedral carboranes is then discussed along with a description of various syntheses of C-carborane derivatives.

Chapter 3 describes a series of model reactions performed to test the feasibility of the various routes available for the preparation of poly(carboranyletherketones). Electrophilic polyacylation in superacid solution was found to be the most convenient method. Hence monomers (suitably substituted derivatives of 1,2-diphenyl-ortho-carborane) were prepared for polymer synthesis under these conditions.

Chapter 4 outlines the preparation and characterisation of four poly(carboranyletherketones). These polymers are shown by NMR to have the expected structures. Their solution and calorimetric characteristics show the polymers to be totally amorphous, with the polymer chains being stiffened by the presence of the 1,2-diphenyl-ortho-carborane unit. The thermal % weight loss from these polymers both in air and in nitrogen is substantially less than that shown by parent poly(etherketones).

Various C-hydroxy carboranes ($R(OH)C_2B_{10}H_{10}$) and their trialkylammonium salts have been prepared and used to examine the effects of electron delocalisation into the carborane cage. Evidence for this originally provided by I.R. data is backed up by the molecular structure of the proton sponge salt $Ph(O)C_2B_{10}H_{10}^- C_{14}H_{19}N_2^+$. This structure shows novel cage distortions which are rationalised by frontier orbital considerations. Attempts to monitor electron delocalisation into the cage using ^{11}B NMR, have led to a detailed NMR study of a series of carborane derivatives. As a result, various substituent effects have been highlighted. These effects have been qualitatively related to the change in polarity of the cage, using MOBI calculations to estimate changes in charge distribution throughout the cage.

Finally, Appendix A summarises some additional studies, carried out to determine the ways lithium interacts with boron hydride anions BH_4^- and $B_{10}H_{10}^{2-}$.

Abbreviations and Nomenclature

Standard Reagents:

Cp	Cyclopentadiene
DMA	Dimethylacetamide
DMF	Dimethylformamide
PS	Proton sponge, N,N,N',N'-tetramethylnaphthalenediamine
Py	Pyridine
EDETA	Pentamethyldiethylenetriamine
TMEDA	Tetramethylethylenediamine
HMPA	Hexamethylphosphoramide
THF	Tetrahydrofuran
TMS	Tetramethylsilane
TFSA	Trifluoromethanesulphonic acid
HOMO	Highest occupied molecular orbital
LOMO	Lowest unoccupied molecular orbital

Discussion of Spectroscopy

I.R. Infra Red: cm^{-1} wavenumber; s - strong absorption; m - medium; w - weak; sh - shoulder.

N.M.R. Nuclear Magnetic Resonance; δ - chemical shift in ppm (parts per million); J - coupling constant (Hertz); s - singlet; d - doublet; t - triplet; m - multiplet, etc.; d/s - doublet (singlet on decoupling)

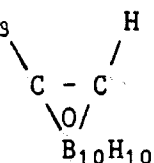
Mass Spectrometry E.I. - Electron Impact; C.I. - Chemical Ionisation; M - Molecular ion; m/e - mass ion.

Nomenclature of Carboranes

<u>Full name</u>	<u>Abbreviated Name</u>	<u>Symbols</u>
1,2 dicarba-closo-dodecaborane(12)	ortho-carborane	$\begin{array}{c} \text{HC} - \text{C-H} \\ \diagdown \quad / \\ \text{O} \\ \text{B}_{10}\text{H}_{10} \end{array} \quad \ominus$
1,7 dicarba-closo-dodecaborane(12)	meta-carborane	$\text{HCB}_{10}\text{H}_{10}\text{CH} \quad \ominus'$
1,12 dicarba-closo-dodecaborane(12)	para-carborane	$\text{HCB}_{10}\text{H}_{10}\text{CH} \quad \ominus''$

Carboranes are referred to by their abbreviated names in the text and in most publications. Some Russian literature however uses the term 'Barene' to describe the closo $\text{C}_2\text{B}_{10}\text{H}_{12}$ cage. Carborane derivatives are named according to the position and nature of substituents attached to the cage.

Hence CH_3 H = 1-methyl-ortho-carborane, etc.



Polymers

For brevities sake all polymers are referred to using abbreviations.

Hence PEEK (see Figure 1.1) represents poly(etheretherketone).

Chemical identifiers of polymers are derived from the polymer structure hence PEEK = poly(oxy-1,4 phenylene-oxy-1,4 phenylene-carbonyl-1,4 phenylene) etc.

CHAPTER 1

INTRODUCTION

1.1 INTRODUCTION TO CHAPTER 1

This chapter introduces the reader to the work described in this thesis by briefly reviewing, separately, the two main areas covered in this study. These are the chemistry of icosahedral carboranes and of aromatic poly(etherketones). It then brings these two areas together in a summary of the primary objectives and achievements of the present work. Many of the articles referred to in this chapter are fairly general, giving the reader a lead into more specialised literature if required.

1.2 Icosahedral Carboranes : a brief overview

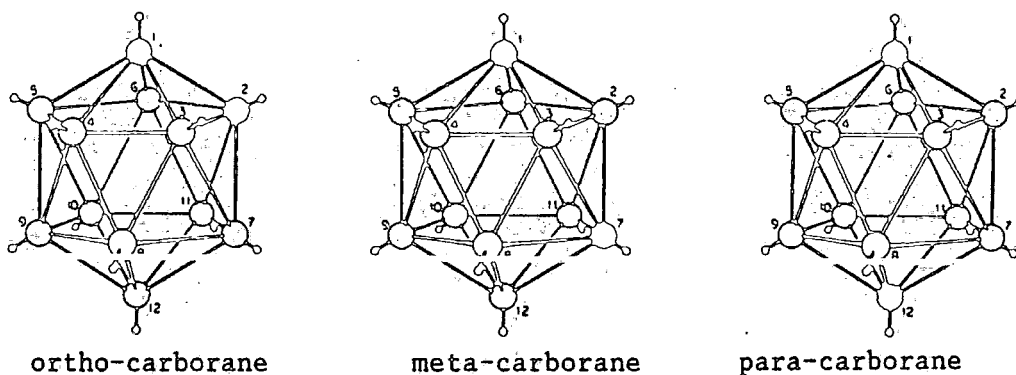
1.2.1 General Chemistry of Carboranes

The term carborane is used collectively to describe the carbon-boron-hydrogen cluster compounds in which one or more carbon atoms form an integral part of the framework. The dicarbaboranes (containing two carbon atoms) are the most common and these fall into three classes of general formula: $C_2B_{n-2}H_n$ ($n = 5-12$), $C_2B_{n-x}H_{n+4-x}$ ($x = 1, 2 \dots, n = 5-12$) and $C_2B_{n-x}H_{n+6-x}$ ($x = 0, 1, 2 \dots, n = 5-12$). These classes are termed closo (closed), nido (nest like) and arachno (web like) thus reflecting three structural categories. These categories have been rationalised in terms of the number of electrons in the molecule for cluster bonding according to electron counting rules¹. Hence closo structures contain $(n+1)$ electron pairs for cluster bonding, nido $(n+2)$ and arachno $(n+3)$.

The most chemically and thermally stable class are the closo compounds, and out of this series, most interest has been focused on the icosahedral dicarbo-closo- dodecaboranes ($C_2B_{10}H_{12}$) of which there are three isomers (see Figure 1.1). These compounds, which form the basis of the present study,



Figure 1.1



have over the years proved to be the most convenient to investigate because of their remarkable stability and their accessibility.

The first work on icosahedral carboranes was carried out in the late fifties in the United States during investigations into developing high energy rocket fuels from boranes and their derivatives². Much of this early work was not declassified until 1963 when three independent groups reported the discovery of ortho-carborane simultaneously^{3,4,5}. Since their discovery, carboranes have and still do provide challenges not only to synthetic organic and inorganic chemists but also to theoretical chemists trying to understand the mechanisms by which various polyhedra are formed and the bonding that holds them together^{6,7}. As such their now very wide chemistry has formed the basis of a number of comprehensive reviews^{2,8-11}.

The icosahedral cage is remarkably thermally stable and chemically robust when compared to the boranes from which it is derived and this has been attributed to the highly delocalised pseudo aromatic structure it possesses. The ortho-carborane cage is generated by the reaction of decaborane, in the presence of a Lewis base, with acetylenes. This reaction has been used extensively in this study and is discussed in detail

in Chapter 2. The meta-carborane isomer is most conveniently generated by the thermal isomerisation of the ortho isomer (see Section 2.2.2) above 400°C. The meta isomer is also produced in small amounts (16%) during the pyrolysis of nido - CB_5H_9 although this method is not satisfactory for the routine preparation of this compound¹². Para-carborane is produced, along with appreciable cage degradation by heating the meta isomer above 600°C (see Section 2.2.2). These thermal isomerisations may be reversed by reduction of the meta or para cages to their corresponding dianions $\text{C}_2\text{B}_{10}\text{H}_{12}^{2-}$ using sodium in liquid ammonia. These dianions then rearrange and on oxidation back to the neutral species give the ortho or meta isomers respectively^{13,14,15}. The action of strong nucleophiles causes the removal of a boron atom from the cage to give nido-dicarbaundecaborate anions ($\text{C}_2\text{B}_9\text{H}_{12}^-$) (see Section 3.3.2). These anions and the compounds derived from them are more reactive than their closo parents.

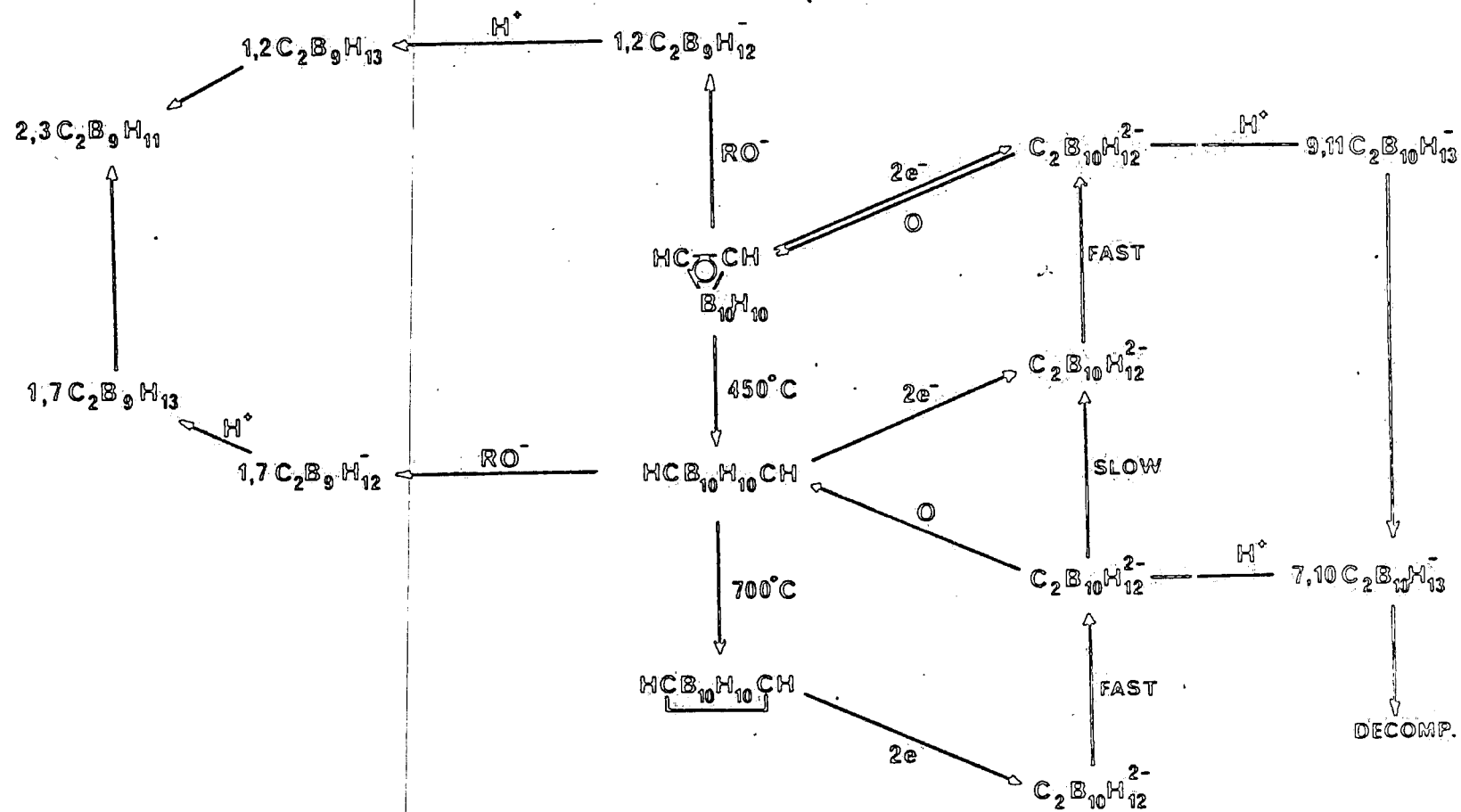
One particularly interesting and widely investigated property of these icosahedral fragments is their ability to bond to metals and other elements producing hetero cluster species^{8,16}. Production of such compounds has been instrumental in highlighting trends between boron clusters and other cluster compounds. This has allowed many classes of cluster compounds to be considered as members of the same family all conforming to a common structural and bonding pattern^{1,16}.

Some of the transformations that the ortho-cage, and compounds derived from it, undergo are summarised in figure 1.2^{8,9,15}. An extensive exopolyhedral derivative chemistry of icosahedral carboranes has been developed since their discovery, permitted by the chemical stability of the C_2B_{10} cage. Functionality can be introduced at the carbon atoms of the cage by using substituted acetylenes when preparing the ortho-isomer, (see Chapters 2 and 3). In addition the cage is electron

withdrawing with respect to substituents at its carbon atoms. Therefore hydrogen terminally attached to the carbon atom is mildly acidic. Hence metallation of the carbon atoms using organolithium reagents, gives C-lithio derivatives which are versatile precursors to a variety of C-organic, C-non-metallic^{2,8-11} and C- σ -bonded main group and transition metal derivatives¹⁷.

The derivative chemistry at the boron atoms of the cage is also quite varied and extensive. Electrophilic halogenation of the cage has long been known to occur and selective halogenation has been used to confirm calculated electron distributions in the ortho-carborane cage^{18,19}. Alkylation of the boron atoms remote from the carbon atoms of the cage can be achieved electrophilically²⁰ and B(3) alkylated or arylated derivatives of ortho carborane can be prepared by reacting organoboron dihalides ($\text{R}(\text{BHal})_2$) with the corresponding dicarbollide anions ($\text{C}_2\text{B}_9\text{H}_{11}^{2-}$)²¹⁻²³. Metallation of boron atoms of all three isomers using $\text{Hg}(\text{CF}_3\text{CO}_2)_2$ ²⁴ or $\text{Tl}(\text{CF}_3\text{CO}_2)_3$ ²⁵ give metal derivatives that constitute versatile precursors to a whole range of other B carboranyl derivatives.

Figure 1.2 Some of the transformations the ortho carborane cage undergoes



1.2.2 Potential applications of Carboranes

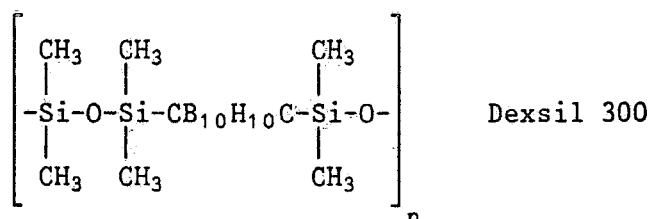
As mentioned in the previous section, the discovery of carboranes stemmed from attempts to develop high energy fuels for rocket propulsion from boranes and their derivatives. Although extensive research was carried out in this area it has seemed to yield limited success².

A number of studies have been carried out to investigate the influence of fairly bulky icosahedral carborane groups on the reactivity of certain biologically active molecules. Structure/activity relationships in biologically active peptides have been probed using species modified by incorporating carborane containing amino salts into the peptide chain²⁶. Also the influence of pendant carborane groups on the metal binding action of porphyrins has been investigated²⁷.

The use of Boron Neutron Capture Therapy (BNCT) as a cure for cancer has been postulated for some time²⁸. The prerequisite for the success of this technique is to introduce a sufficient quantity of ^{10}B atoms (10^8 - 10^9) into tumour cells so that when irradiated with thermal neutrons they will react to give a lethal dose of a radiation destroying the cell^{29,30}. To this end, a variety of boron compounds have been developed including mono-clonal antibodies containing decaborane residues³⁰ and tumour specific steroids with pendant ortho carborane groups attached. Although BNCT is far from being widely used as a safe cure for cancer, it is nevertheless an area of ongoing interest around the world³². Icosahedral carboranes lend themselves to such an application because of the relatively high boron content of the cage, the stability of the cluster and the large amount of derivative chemistry that can be performed on the cage.

The most effort has been devoted to exploiting the outstanding

chemical and thermal stability of carboranes by incorporating them into a variety of polymers. The most well known and thoroughly characterised class of carborane polymers are the commercially available Dexsil series which consist of meta-carborane cages incorporated into a polysiloxane backbone, e.g. Dexsil 300³³⁻³⁵:



These polymers have been used in a variety of coating and sealant roles, but are probably most widely used nowadays as stationary phases in G.C. columns.

The carborane cage has been incorporated into a variety of other inorganic and organic polymer systems often with the desired stabilising effect^{8, 35, 36}. This seems to occur firstly by the cage acting as a stabilising additive effectively producing a polymer composite material³⁷. Secondly the cage is sometimes seen to act as an "energy sink" chemically stabilising the polymer chain into which it is incorporated, presumably through the inductive influence of the cage. This latter mechanism is invoked to explain the outstanding stability of the Dexsils.

As mentioned previously, fragments derived from icosahedral carboranes and other carborane systems have reactivity towards transition metals not shown by the closo parents. Exploitation of this reactivity in some polymer systems has been the subject of limited studies which have afforded materials with some interesting catalytic and electronic properties³⁸⁻⁴¹, suggesting there is wide scope for further work in this area.

1.3. The Preparation and Properties of Aromatic poly(etherketones)

In recent years much research has been directed at developing new high performance polymers capable of withstanding higher temperatures and stress, such as polyarylates, polyimides and poly(ethersulphones)⁴². The latest in this family of high performance polymers are the aromatic poly(etherketones). These thermoplastic materials have very high thermal and chemical stability, exceptional toughness, strength and load bearing capabilities. They also have good radiation and fire resistance and since they are highly crystalline, they have good solvent resistance. These properties result in the aromatic poly(etherketones) being the most outstanding thermoplastic materials commercially available today⁴³.

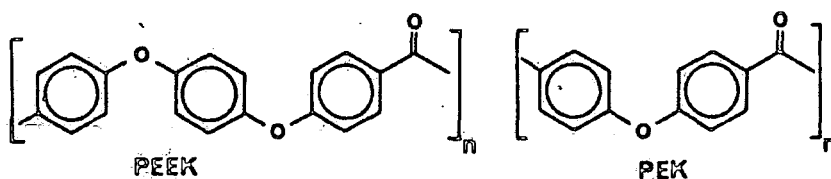
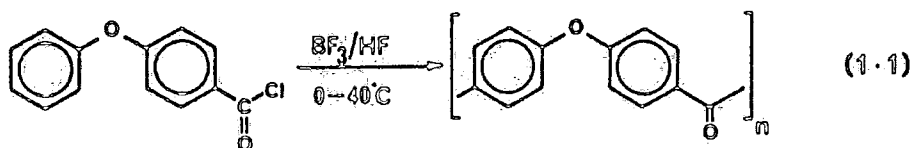


Figure 1.3 Commercially available poly(etherketones)

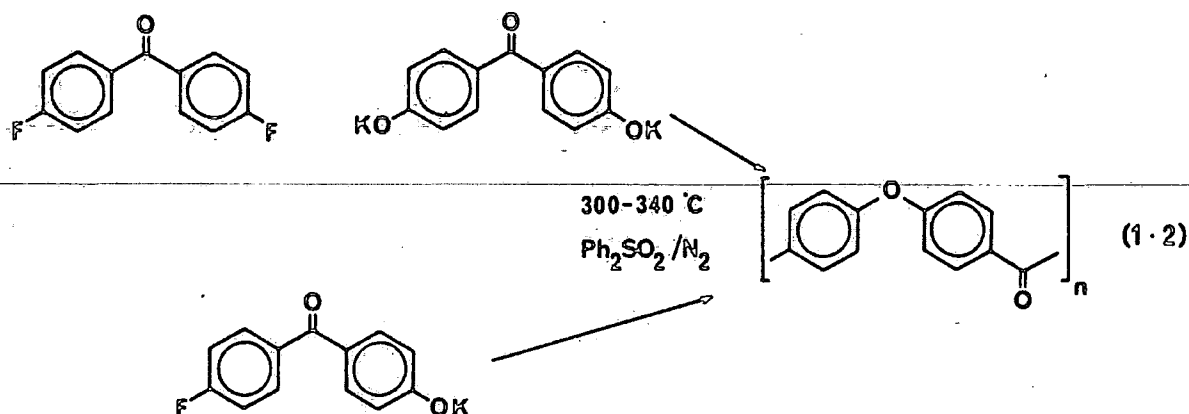
These polymers are prepared using two different routes:

- (i) Electrophilic polycondensation (polyacylation),
- (ii) Nucleophilic polycondensation (polyetherification). The first preparation of poly(etherketones) involved Friedel-Crafts polycondensations of aryl carboxylic acid or acid chloride derivatives in nitrobenzene⁴⁴, dichloromethane⁴⁵ or polyphosphoric acid⁴⁶. These reactions all resulted in the formation of low molecular weight material, because of the low solubility of the polymers in these solvents causing premature crystallisation of polymer and a low degree of polymerisation. The first preparation of high molecular weight poly(etherketones) was effected using BF_3 as the catalyst in HF as solvent⁴⁷ (see equation 1.1).



More recently, electrophilic polycondensation of aryl carboxylic acids and ethers in trifluoromethane sulphonic acid ($\text{CF}_3\text{SO}_3\text{H}$, TFSA) which acts both as solvent and catalyst has been used as a convenient route into poly(etherketones), (see Chapters 3 and 4)⁴⁸. TFSA, a commercially available superacid^{49,50} is more suitable than HF for laboratory scale work as it is non corrosive to glassware and the triflate anion CF_3SO_3^- is essentially non toxic.

The nucleophilic polycondensation of alkali metal phenoxides of 4-hydroxy phenylketones and 4-fluoro-phenylketones (discussed in detail in section 3.2.1) requires a solvent that is dipolar and aprotic. Diphenylsulphone is the solvent most commonly used which dissolves polymers at temperatures approaching their melting points, hence high temperatures are needed for polymer formation by this route, (equation 1.2)⁴⁹.



1.4 Scope of the present work

The primary objective of this study has been to devise routes to and thus to prepare aromatic poly(etherketones) with icosahedral carboranes incorporated into the polymer backbone, (aromatic poly(carboranyletherketones)) and to examine their chemical, thermal and physical properties. The impetus behind this has been the thought that combining these two exceptionally stable systems could in principle produce materials of yet greater stability.

Central to the study has been the preparation of a range of ortho-carborane derivatives as starting materials, model compounds and monomers. Chapter 2 therefore discusses the formation and characterisation of such carborane derivatives in some detail.

Chapter 3 describes investigations carried out to probe the feasibility of using the two different routes to prepare aromatic poly(etherketones) outlined in the previous section. As a result of these investigations potential monomers were identified and prepared as outlined. The syntheses and characterisation of four different poly(carboranyletherketones) are described in Chapter 4, and their properties compared with those of the parent poly(etherketones).

Chapters 5 and 6 discuss work peripheral to the main research theme, resulting from our original interest in the potential of α -hydroxy derivatives of ortho-carborane $R(HO)C_2B_{10}H_{10}$ as monomers. Deprotonation of such hydroxy species by trialkylamine bases produces anions which have been used to examine the effects of electron delocalisation into the cage. Effects of delocalisation on the structure of the cage are illustrated by the molecular structure of the anion $PhC_2B_{10}H_{10}O^-$ which shows intriguing distortions rationalised by frontier orbital considerations. Substituent effects have been identified in the NMR spectra of these carborane derivatives and these are discussed in Chapter 6.

Finally local interest in lithium chemistry prompted a brief investigation into the interactions occurring between lithium cations and some boron hydride anions. This has led to the discovery of a novel structure for the lithium borohydride adduct $[\text{LiBH}_4 \cdot \text{TMEDA}]_2$. This work is covered in Appendix A as it is not directly related to the central theme of this study.

1.5 References

1. K. Wade, Chem. Commun. 1971, 792.
2. R.L. Hughes, I.C. Smith, E.W. Lawless, Production of the Boranes and related research, Academic Press, 1967.
3. T.L. Hoying, J.W. Alger, S.L. Clark, D.J. Mangold, H. Goldstein, M. Hillman, R.J. Polak, J.W. Szymanski, Inorg. Chem. 1963, 2, 1089.
4. M.M. Fein, J. Bobinski, N. Mayes, N.N. Schwartz, M.S. Cohen, Inorg. Chem. 1963, 2, 1111.
5. L.I. Zakharkin, V.I. Stanko, V.A. Brattsev, Yu. A. & O. Yu. Okhlobystin, Bull. Acad. Sci. U.S.S.R. Chem. Div., 1966, 2074.
6. W.N. Lipscomb, Science, 1977, 196, 1047.
7. A.J. Stone, Polyhedron, 1984, 3, 1299.
8. R.W. Jotham in Mellor's Comprehensive Treatise on Inorganic and Theoretical Chemistry, 1981, V, Part B1, Section B8, 450, Longmans.
9. R.N. Grimes, Carboranes, Academic Press, N.Y. 1970.
10. D.T. Howarth, Endeavour, 1972, 31, 16.
11. V.I. Bregadze, O. Yu. Okhlobystin, Organomet. Chem. Rev. 1969, 4, 345.
12. R.R. Reitz, M.F. Hawthorne, Inorg. Chem. 1974, 13, 755.
13. D. Grafstein, J. Dvorak, Inorg. Chem. 1963, 2, 1128.
14. L.I. Zakharkin, V.N. Kalinin, Izvest. Akad. Nauk. S.S.S.R. Ser. Khim. 1969, 194.
15. G.B. Dunks, R.J. Wiersema, M.F. Hawthorne, J. Amer. Chem. Soc. 1973, 95, 3173.
16. Metal Interactions with Boron Clusters, Ed. R.N. Grimes, Plenum Press, 1982.
17. Ref. 16, Chapter 5.
18. J.A. Potenza, W.N. Lipscomb, J. Amer. Chem. Soc. 1964, 86, 1874.
19. J.A. Potenza, W.N. Lipscomb, G.D. Vickers, H.A. Schroeder, J. Amer. Chem. Soc. 1966, 88, 628.

20. L.I. Zakharkin, I.V. Pisareva, R. Kh. Bikkineev, Bull. Acad. Sci. U.S.S.R. Chem. Div., 1977, 26, 577.
21. L.I. Zakharkin, V.S. Kozlova, J. Gen. Chem. U.S.S.R., 1972, 42, 472.
22. M.F. Hawthorne, P.A. Wegner, J. Amer. Chem. Soc. 1968, 90, 896.
23. M.F. Hawthorne, P.A. Wegner, J. Amer. Chem. Soc. 1968, 90, 4302.
24. V.I. Bregadze, V.Ts. Kampel, N.N. Godovikov, J. Organomet. Chem., 1976, 112, 249. V.I. Bregadze, V.Ts. Kampel, N.N. Godovikov, J. Organomet. Chem. 1977, 136, 281.
25. V.I. Bregadze, V.Ts. Kampel, A.Ya. Usyatinskii, J. Organomet. Chem. 1978, 154, C1.
26. R. Schwyer, K. Quang Do, A.N. Eberle, J. Fauchere, Helv. Chim. Acta, 1981, 64, 2078.
27. R.C. Haushalter, W.M. Bulter, R.W. Rudolph, J. Amer. Chem. Soc., 1981, 103, 2620.
28. A.H. Soloway in Progress in Boron Chemistry, Ed. H. Steinberg, A.I. McCloskey, 1964, 1, Ch. 4, Pergamon.
29. A.H. Soloway, A. Fazlul, R.F. Barth, W.E. Carey, Pharm. Int., 1984, 5, 91.
30. R.F. Barth, A. Fazlul, A.H. Soloway, D.M. Adams, Z. Stepiewski, Hybridoma, 1986, 5, 43 (Chem. Abs. 1986, 105, 148943s).
31. S.B. Kahl, Synth. appl. Isot. Labelled Cpds. Proc. Int. Symp. 1982, (publ. 1983), 181, Elsevier (Chem. Abs. 99, 38697q).
32. G. Constantine (Harwell) Paper submitted at Intraboron VI, Strathclyde, Sept. 1987.
33. Ref. 42, Chapter 7.
34. E.N. Peters, J. Macromol. Sci - Rev. Macromol. Chem. 1979, C17, 173.
35. J.F. Ditter, J.R. Wasson, Gmelin Handbook Anorg. Chem. Borverbindungen. 1975, 27(6), 69.
36. N.I. Bekasova, Russian Chem. rev. 1984, 53, 61, (Transl. from Usp. Khim. 1984, 53, 107).
37. Yu.M. Rodionov, S.I. Danilov, Dokl. Akad. Nauk. S.S.S.R. 1986, 288, 143 (Engl. 132).

38. V.N. Kalinin, O.A. Mel'nik, A. Sakharova, T.M. Frunze, L.I. Zakjarkin, N.V. Borunova, V.Z. Sharf, Bull. Acad. Sci. U.S.S.R. Chem. Div. 1985, 35, 2258.
39. E.S. Chandrasekarran, D.A. Thompson, R.A. Rudolph, Inorg. Chem. 1978, 17, 760.
40. B.A. Sosinsky, W.C. Kalb, R.A. Gray, V.A. Ueki, M.F. Hawthorne, J. Amer. Chem. Soc. 1977, 99, 6768.
41. W. Siebert, Angew. Chem. Int. Ed. Engl. 1985, 24, 943.
42. J.P. Critchley, G.J. Knight, W. Wright, Heat Resistant Polymers, Technologically useful materials, Plenum, N.Y. 1983.
43. A.G. Wood, Modern Plastics International, 1987 (June), 88.
44. W.H. Bonner, U.S. Pat. 3065205, 1962.
45. I. Goodman, J.E. McIntyre, W. Russell, Br. Pat. Appl. 971227, 1964.
46. Y. Iwakura, K. Uno, J. Takiguchi, J. Polym. Sci. A-I, 1968, 6, 3345.
47. B.M. Marks, U.S. Pat. 3442857, 1969.
48. H.M. Colquhoun, Polym. Preprints, 1984, 25, 17.
49. G.A. Olah, G.K. Prakash, J. Sommer, Superacids, Wiley Interscience, 1985.
50. R.D. Howells, J.D. McDown, Chem. Rev. 1977, 77, 69.
51. T.E. Attwood, P.C. Dawson, J.L. Freeman, L.R.J. Hoy, J.B. Rose, P.A. Staniland, Polymer, 1981, 22, 1096.
52. D.R. Kelsey, L.M. Robeson, R.A. Clendinning, C.S. Blackwell, Macromolecules, 1987, 20, 1204.

CHAPTER 2

PREPARATION AND CHARACTERISATION OF
ICOSAHEDRAL CARBORANES

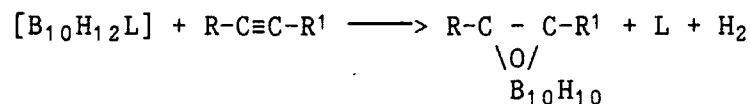
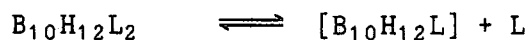
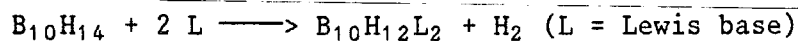
2.1 INTRODUCTION

This chapter discusses the preparation and characterisation of some C-substituted icosahedral carborane derivatives. It addresses the problem of the mechanism of formation of the ortho-carborane cage through the reaction of decaborane and acetylenes, and it also discusses the mechanism of the thermal isomerisation of the ortho isomer to give the corresponding meta and para isomers. In addition, the techniques that have been used to characterise the carboranes prepared are analysed as a lead in to the final experimental section which outlines the syntheses of several carborane derivatives.

2.2 Carborane Preparation

2.2.1 The reaction of decaborane with acetylene

As indicated in Chapter 1, the most effective way of generating the ortho-carborane cage is by reacting decaborane, in the presence of a Lewis base, with acetylene derivatives. The kinetics of this reaction have been studied by several workers, and the following mechanism (Scheme 1) has been proposed as a result^{1,2,3}:



Scheme 1

The final carborane forming reaction is the rate determining step.

The reactive intermediate in this reaction is the mono-ligand adduct. The importance of this intermediate in other reactions of bis-ligand adducts has been confirmed kinetically, for instance in their transformation to $B_{10}H_{10}^{2-}$ anion⁴ and in ligand exchange reactions⁵. The exact structure of the intermediate is not known although several configurations have been postulated⁶. Figure 2.1 shows a diagram of the nido decaborane cage which on reaction with Lewis base gives the arachno bis ligand adduct. A likely structure of the intermediate could be derived from the bis ligand by removing one ligand to produce a nido species, isoelectronic with decaborane but with bridging hydrogens situated as in the bis ligand adduct. A stable compound of formula $B_{10}H_{12}(Me_2S)$ can be prepared from the parent $B_{10}H_{12}(Me_2S)_2$ ⁷, or directly from decaborane⁸. Its structure has been inferred from comparisons made between the ¹³C NMR data obtained for this compound and the crystallographically characterised species $5(Me_2S) 9(C_6H_{11}) B_{10}H_{12}$, made by the hydroboration of cyclohexene with $B_{10}H_{12}(Me_2S)_2$ (see figure 2.2)⁹. This compound has been shown not to be the reactive isomer involved in the carborane forming reaction since it only reacts slowly with acetylenes to generate ortho carborane derivatives in very low yields, and it will only react with dimethyl sulphide to regenerate the bis ligand parent at elevated temperatures¹.

Since the form of the reactive intermediate is unclear, so too is the way that it interacts with acetylenes to generate carboranes. The formation of a second intermediate complex, between the mono ligand adduct and the acetylene, has been proposed. This introduces a second step into Scheme 1 (Scheme 2).

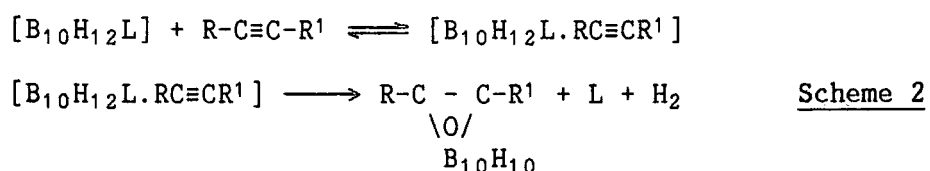


Figure 2.1

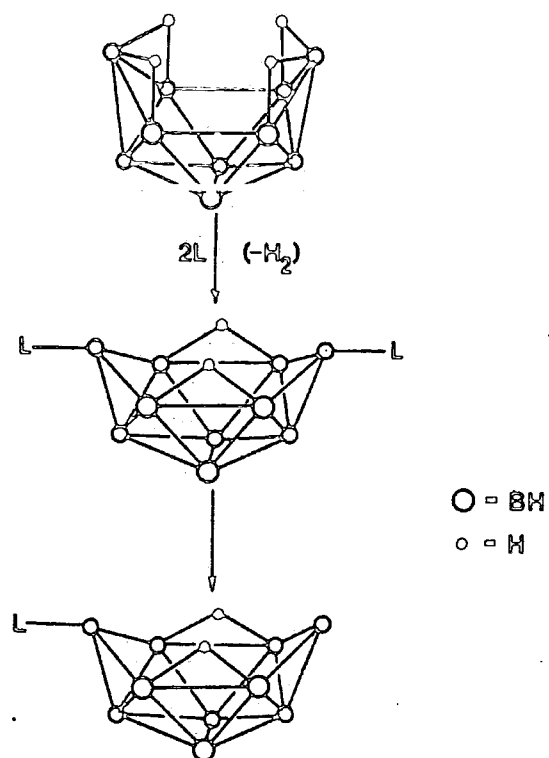
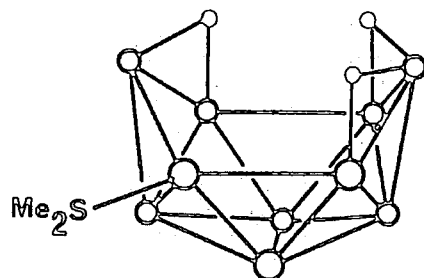


Figure 2.2



This process would be kinetically indistinguishable from the first mechanism, however it has prompted the suggestion that in this new complex, the acetylene lies across the open face of the B_{10} moiety allowing endo attack to take place. The loss of L and a molecule of hydrogen accompanied by minor C and B rearrangement would then afford the C_2B_{10} cage.

More recently, an attempt to understand this endo attack of the acetylene group on the B_{10} open face has been made, using frontier orbital considerations¹⁰. For this interaction to be feasible, the HOMOs and the LUMOs of the two species need to be of compatible symmetry. Figure 2.3 shows the configuration of HOMOs and LUMOs of decaborane¹¹ and the acetylene group.

On generating the arachno bis ligand adduct, the LUMO of the decaborane cage is occupied becoming the HOMO of the new species. Assuming the configuration and relative energies of these orbitals remains constant, removal of one ligand produces a B_{10} moiety isoelectronic with decaborane and which has a LUMO of identical configuration to that of decaborane, only it has a vacant lobe at B(6). It can be seen straight away that on symmetry grounds, this vacant lobe can accommodate electron donation from the acetylene HOMO, giving rise to the interaction shown in figure 2.4. The HOMO of the mono-ligand adduct will be the same as for the decaborane cage also. As such it is of a form that means back donation from it into the LUMO of the acetylene moiety is also symmetry allowed (see figure 2.5). The orientation of the C_2 species produced by these interactions would be exactly that required for closure to give the C_2B_{10} cage. This approach therefore illustrates quite clearly how the endo attack may occur.

To complete the cage formation, this interaction would be followed by or would be part of a concerted process involving elimination of the remaining ligand and a molecule of hydrogen.

Figure 2.3

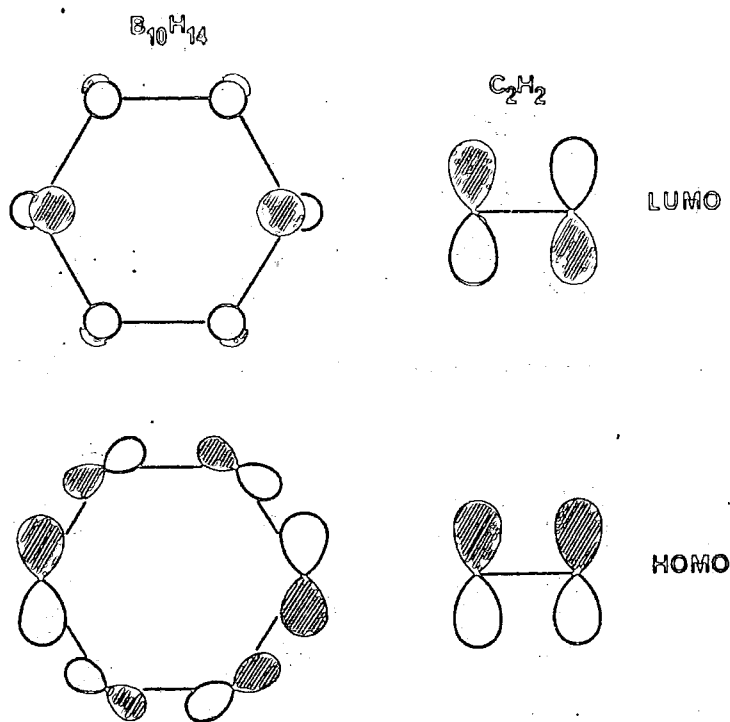


Figure 2.4

$LUMO_{B_{10}} + HOMO_{C_2H_2}$

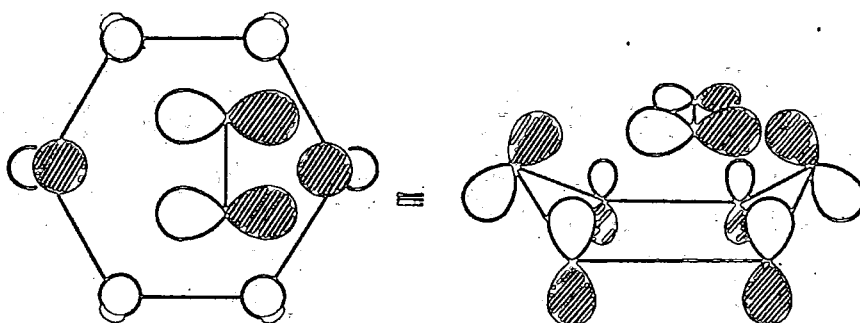
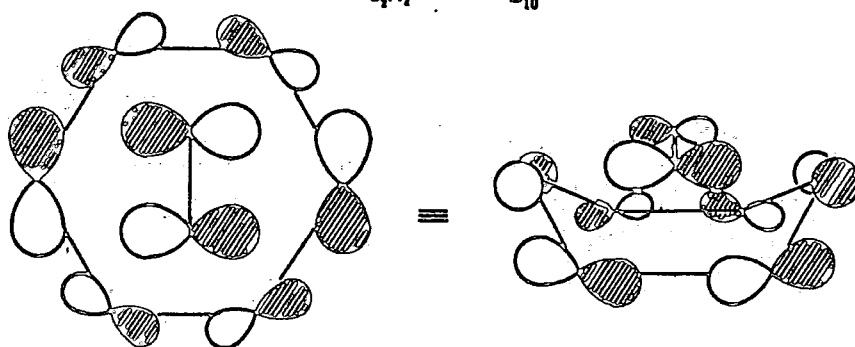


Figure 2.5

$LUMO_{C_2H_2} + HOMO_{B_{10}}$



$B_{10} - B_{10}H_{12} \cdot L$

Deuteration studies have shown that the hydrogen evolved in this reaction comes only from the B_{10} cage¹. They do not show whether bridging or terminal hydrogens are lost, although it seems most feasible from the likely orientation of the bridging hydrogens, that these would be preferentially displaced.

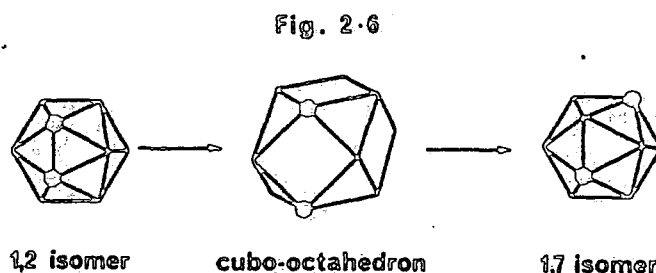
The nature of the acetylene derivative used can influence the yield of carborane obtained. Acetylene groups possessing electron donating substituents tend to give poor yields. It is widely known that nucleophilic acetylenes are much more susceptible to hydroboration². Also cyclohexene is readily hydroborated by $B_{10}H_{12}(Me_2S)_2$ ⁹, and more recently the reactions of bis(trimethylsilyl) acetylene and (trimethylsilyl) propyne with $B_{10}H_{12}(Me_2S)_2$ were found to produce no ortho-carborane derivatives at all. Instead, hydroboration of the acetylene groups occurred, accompanied by sulphide and silyl group migration to produce 5(Me_2S)-6-alkenyl-decaborane derivatives almost exclusively. The reaction with bis(trimethylsilyl) acetylene was also found to produce the novel mono-carbon carborane 9-(Me_2S)-7-(Me_3SiCH)- $CB_{10}H_{10}$ ¹³. These observations coupled with results from attempts to characterise the byproducts from carborane syntheses^{1,2} indicate that hydroboration of the acetylene group is the main reaction competing with carborane formation. In addition, acetylenes that have functional groups with appreciable protic acidity cannot be used in carborane formation as these groups tend to degrade the decaborane prior to reaction with the acetylene. Therefore acetylenic alcohols and carboxylic acids need to be suitably protected before carborane syntheses are attempted using them.

The most effective bases for carborane formation have been found to be nitriles such as acetonitrile, dialkyl sulphides and *N,N* dimethylaniline¹⁴. Protophilic bases such as triethylamine are not suitable as they deprotonate the $B_{10}H_{12}L_2$ species to give

$B_{10}H_{10}^{2-}$ salts¹⁵. The preparation of $B_{10}H_{12}L_2$ adducts prior to carborane synthesis is not essential, the treatment of decaborane with acetylenes in the presence of free Lewis base also being effective. It should be noted however that because of the nature of the reactive intermediate in this reaction, a presence of excess Lewis base will inhibit the rate of carborane formation.

2.2.2 Thermal isomerisation of icosahedral carboranes

The thermal isomerisation of ortho carborane to the meta isomer was first observed during an attempt to dimerise and/or polymerise ortho-carborane by pyrolytic dehydrogenation¹⁶. The seemingly most widely accepted mechanism for this rearrangement was proposed before the reaction had actually been performed¹⁷ and involves a co-operative diamond square diamond (DSD) rearrangement passing through a cubo-octahedral intermediate (figure 2.6).

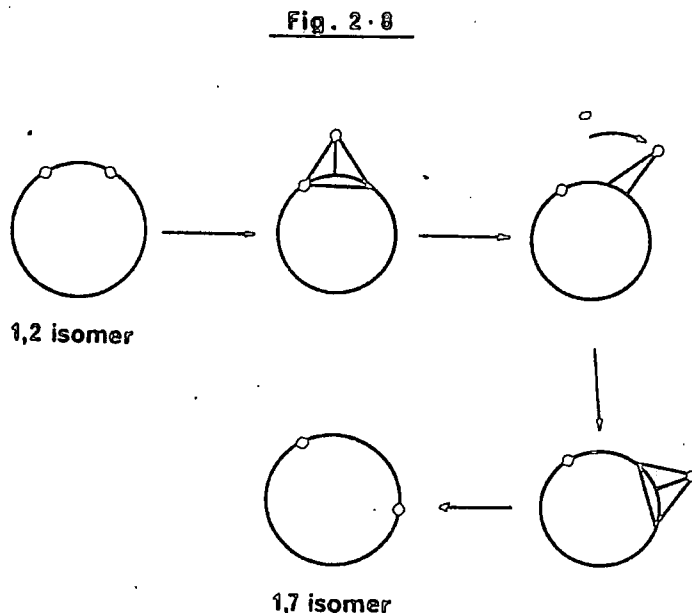
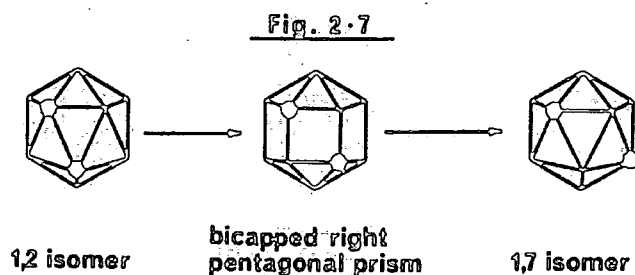


The fact that the reverse isomerisations para \rightarrow meta \rightarrow ortho cannot be accomplished thermally is an indication of the increased thermodynamic stability of isomers whose carbon atoms are more removed from each other. Although experimental heats of formation of these isomers are not available for direct verification of these relative stabilities, the sequence has been interpreted in terms of molecular orbital energy calculations^{18,19}. More recently predictions of stabilities made using the rule of topological charge stabilisation have

been found to agree well with the observed sequence²⁰.

The transformation of the meta to the para isomer, first observed by Papetti et al²², cannot be explained using the DSD mechanism alone. Also the fact that considerably higher temperatures are needed to induce this isomerisation, which occurs with a large amount of cage degradation, suggests another mechanism is occurring.

The mutual rotation of the two pentagonal bipyramidal halves of the cage, passing through a bicapped right pentagonal prism (figure 2.7)^{16,21}, and the rotation of a triangular face in the cubo-octahedral intermediate, have been introduced as alternatives to explain the formation of the para isomer. Finally a more recent proposal involving single edge cleavage has been suggested as being more energetically favourable than the mechanisms outlined above which involve cleavage of five or six contacts²³ (see figure 2.8).



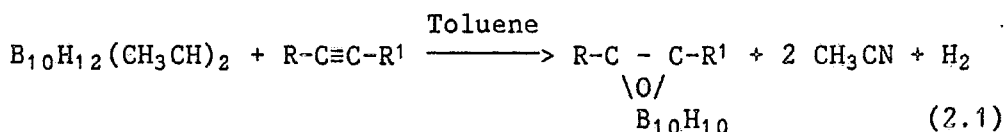
2.2.3 Carborane derivatives prepared

Table 2.1 lists some of the carborane derivatives whose syntheses have been carried out in the present work and which are described in the experimental section (2.4).

Table 2.1

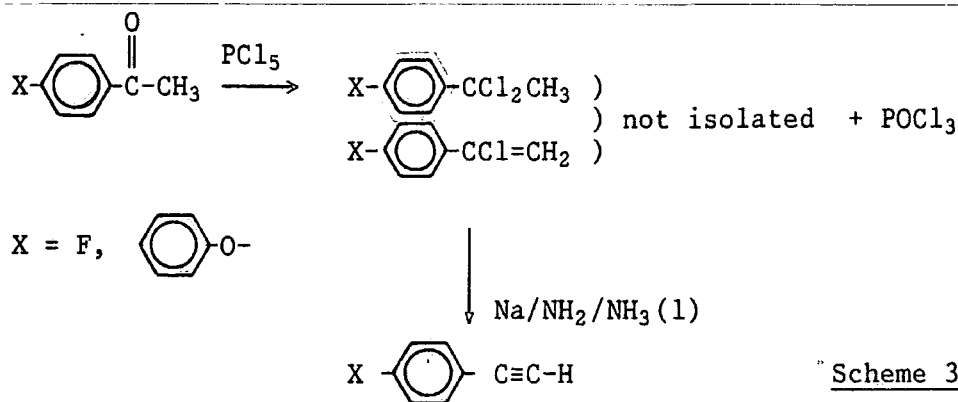
Compound	References
$\text{BrCH}_2 - \underset{\substack{\diagdown \text{O} \\ \text{B}_{10}\text{H}_{10}}}{\text{C}} - \text{C} - \text{H} \quad (\text{I})$	24
$\text{CH}_3 - \underset{\substack{\diagdown \text{O} \\ \text{B}_{10}\text{H}_{10}}}{\text{C}} - \text{C} - \text{H} \quad (\text{II})$	24, 25, 26
$\text{C}_6\text{H}_5 - \underset{\substack{\diagdown \text{O} \\ \text{B}_{10}\text{H}_{10}}}{\text{C}} - \text{C} - \text{H} \quad (\text{III})$	25, 27
$\text{C}_6\text{H}_5 - \underset{\substack{\diagdown \text{O} \\ \text{B}_{10}\text{H}_{10}}}{\text{C}} - \text{C} - \text{C}_6\text{H}_5 \quad (\text{IV})$	25
$\text{F} - \text{C}_6\text{H}_4 - \underset{\substack{\diagdown \text{O} \\ \text{B}_{10}\text{H}_{10}}}{\text{C}} - \text{C} - \text{H} \quad (\text{V})$	28, 29
$\text{C}_6\text{H}_5 - \text{O} - \text{C}_6\text{H}_4 - \underset{\substack{\diagdown \text{O} \\ \text{B}_{10}\text{H}_{10}}}{\text{C}} - \text{C} - \text{H} \quad (\text{VI})$	
$\text{C}_6\text{H}_5 - \text{CB}_{10}\text{H}_{10}\text{CH} \quad (\text{VII})$	30

All the ortho carborane derivatives, with exception of 1-methyl-ortho-carborane (II), have been prepared by the reaction of bis(acetonitrile) decaborane with the corresponding acetylene species (equation 2.1).



The 1-methyl derivative (II) was prepared by the acid hydrolysis of the Grignard derivative derived from 1-bromomethyl-ortho-carborane (I). The yields of (II) produced by the reaction of propyne with bis(acetonitrile) decaborane are poor (30%)²⁵. Propargyl bromide ($\text{BrCH}_2\text{C}\equiv\text{CH}$) gives a much greater yield of carborane because the acetylene group in this compound is less nucleophilic than in propyne because of the electron withdrawing influence of the bromine atom, making it less susceptible to hydroboration. The conversion of (I) into (II) is virtually quantitative, making this route much more efficient.

Prior to the preparation of 1-(4-fluorophenyl)-ortho-carborane (V) and 1-(4-phenoxyphenyl)-ortho-carborane (VI), the corresponding mono-aryl acetylenes needed to be prepared. This can be achieved by the bromination of styrene derivatives followed by dehydrobromination or by chlorination of methyl ketones followed by dehydrochlorination^{28, 32}. The latter method has been used in the present study and the reaction sequence employed is summarised in Scheme 3.

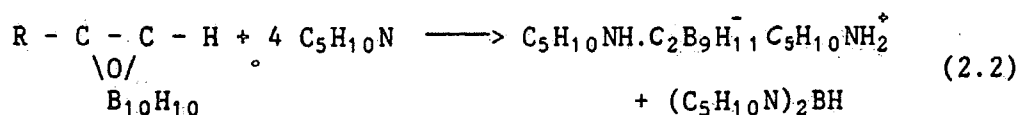


Scheme 3

The dehydrochlorination step can be accomplished using ethanolic potassium hydroxide^{28, 32} in principle, although in preparing the

derivatives above this was found to give poor yields of the acetylenes because of formation of vinyl ether side products. More satisfactory yields and higher purity products were obtained using sodium amide in liquid ammonia.

The isomerisation of small batches (1-2 g) of 1-phenyl-ortho-carborane (III) to its meta isomer (VII) was most conveniently carried out in Carius tubes sealed under vacuum, rather than in more conventionally used stainless steel autoclaves under an atmosphere of argon³⁰. Autoclave reactions gave low yields (below 50%), with the production of a totally insoluble and infusible glass which could not be satisfactorily characterised. The removal of small amounts of the residual ortho isomer was effected by treating a hexane solution of the reaction mixture with piperidine. The piperidine reacts specifically with the ortho isomer (equation 2.2) to give a residue that is water soluble and so may be readily removed by aqueous extraction of the reaction mixture³¹.



Purification may also be achieved using column chromatography on alumina³⁰.

2.3 Characterisation of Carboranes

This section outlines the use of techniques, other than elemental analysis, routinely employed in this and other studies to characterise carborane derivatives.

2.3.1 Infra Red Spectroscopy

I.R. is mainly used as a fingerprint technique to identify particular carborane derivatives^{33, 34} and for monitoring

isomerisation reactions¹⁶ (compare data given for 1-phenyl-ortho-carborane (III) and its meta isomer (VII) in Sections 2.4.4. and 2.4.8. respectively).

The most clearly assignable features in the I.R. spectrum of the carborane cage are sharp C-H stretching modes at 3080-3060 cm^{-1} and B-H stretching modes between 2600-2500 cm^{-1} . A strong absorption at around 750 cm^{-1} is usually visible also, due to the asymmetrical stretching mode of the icosahedral cage.

2.3.2 Nuclear Magnetic Resonance Spectroscopy

i) ^{11}B NMR³⁵

This is discussed in detail in Chapter 6. The ^{11}B nucleus is easy to observe on account of its high relative abundance and receptivity. ^{11}B NMR has therefore been widely used to monitor substitution reactions at both boron and carbon atoms of the cage. It is also probably the most effective technique available for identifying cage transformations, i.e. isomerisation or cage degradation reactions.

ii) ^{13}C NMR³⁶

The main interest in the ^{13}C nucleus has been derived from trying to explain its chemical shift ($\delta(^{13}\text{C})$) in various derivatives. A relationship between $\delta(^{13}\text{C})$ and co-ordination number occurs in carboranes so that higher co-ordinate carbon will resonate at lower frequency³⁷. This is also the case for $\delta(^{11}\text{B})$ ³⁸, and so a correlation between $\delta(^{13}\text{C})$ and $\delta(^{11}\text{B})$ in isoelectronic species has been established³⁹.

A fairly extensive study of the ^{13}C NMR of icosahedral carboranes³⁹ has shown that changes in $\delta(^{13}\text{C})$ on attaching substituents to the cage carbon atoms, closely resemble

changes seen in aliphatic model systems. Ortho, meta and para (antipodal) substituent effects have also been identified³⁹. The antipodal effect also occurs in ^{11}B NMR and is discussed in detail in Chapter 6.

The information obtained from ^{13}C NMR is complementary to that given by other techniques and so has not been used extensively to characterise the carboranes described in this chapter.

2.3.3 Mass Spectrometry

Mass spectrometry is extremely useful for the characterisation of carborane derivatives^{40,41}. The cage is stable under electron impact (E.I.) and so E.I. spectra invariably show very intense molecular ion peaks. These are readily identified since the B_{10} cage produces a very characteristic isotope distribution pattern, due to the presence of two isotopes ^{10}B and ^{11}B . The relative abundances ($^{10}\text{B} = 18.33\%$, $^{11}\text{B} = 81.17\%$) mean that the base peak in the molecular ion signal corresponds to the ion with an isotope ratio of $8^{11}\text{B} : 2^{10}\text{B}$, and the highest mass peak to the $^{11}\text{B}_{10}$ species.

Figure 2.9 shows the E.I. spectrum of 1,2-diphenyl-ortho-carborane (IV) which provides a typical example. The base peak at m/e 296 corresponds to the species $^{12}\text{C}_{14}^{11}\text{B}_8^{10}\text{B}_2^1\text{H}_{20}$ with the peak of $^{12}\text{C}_2^{11}\text{B}_{10}^1\text{H}_{20}$ species occurring at m/e 298. Weaker peaks at m/e 299 and 300 occur due to the presence of the ^{13}C isotope. Figure 2.10 shows the result of an isotope cluster abundance calculation, emphasising the peak pattern statistically expected for the 1,2 diphenyl-ortho-carborane molecule. The E.I. spectrum also shows fragmentation of the cage, and although this process is not fully understood, it is thought to be initially caused by dehydrogenation of the cluster⁴². The cage can also withstand the removal of a second electron under E.I. without appreciable

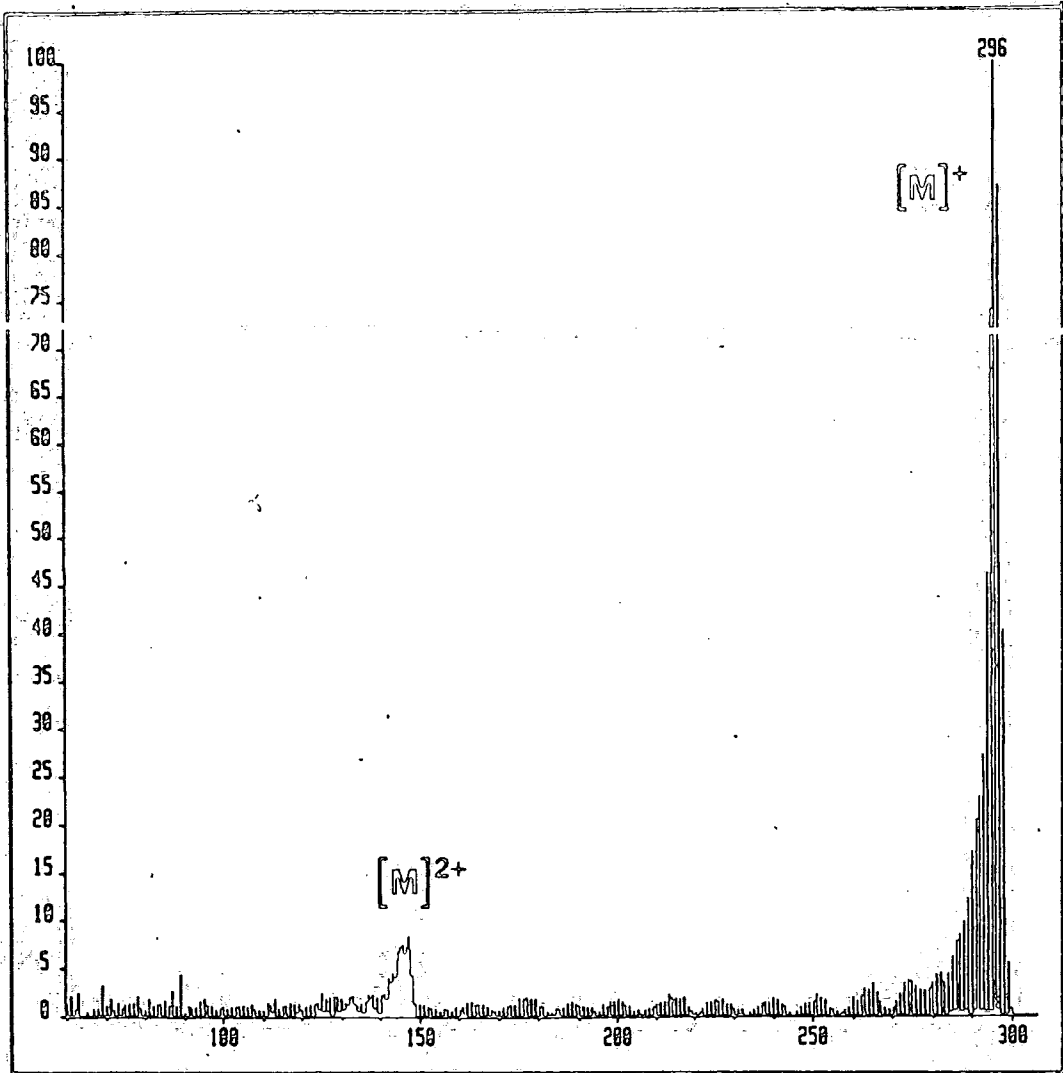


Figure 2.9 E.I. Mass Spectrum of VI

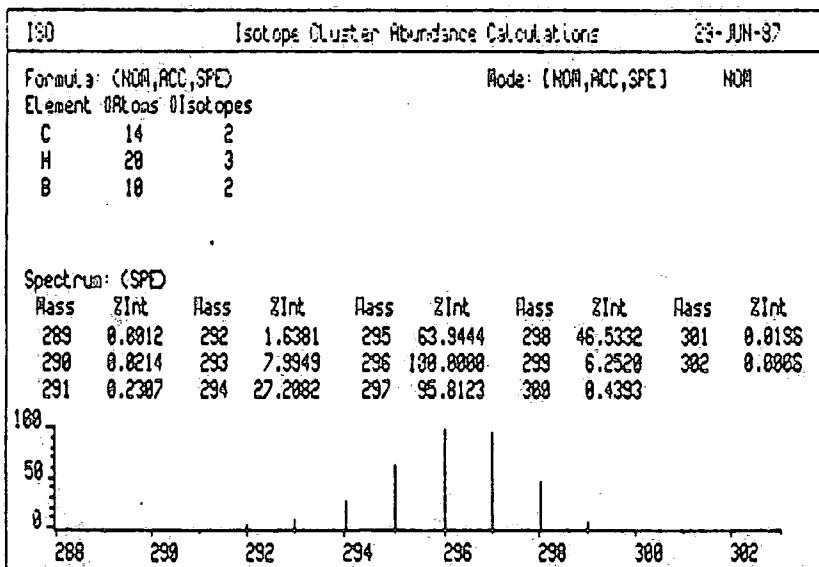
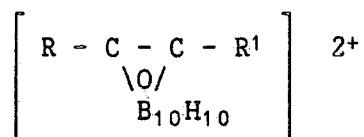


Figure 2.10

fragmentation, producing doubly charged molecular ions:

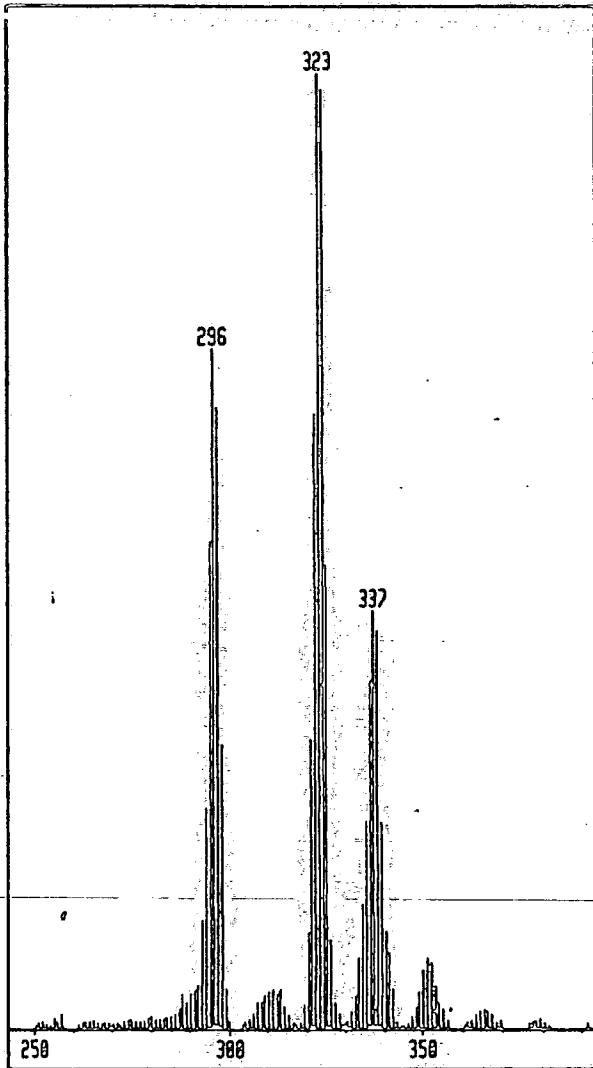
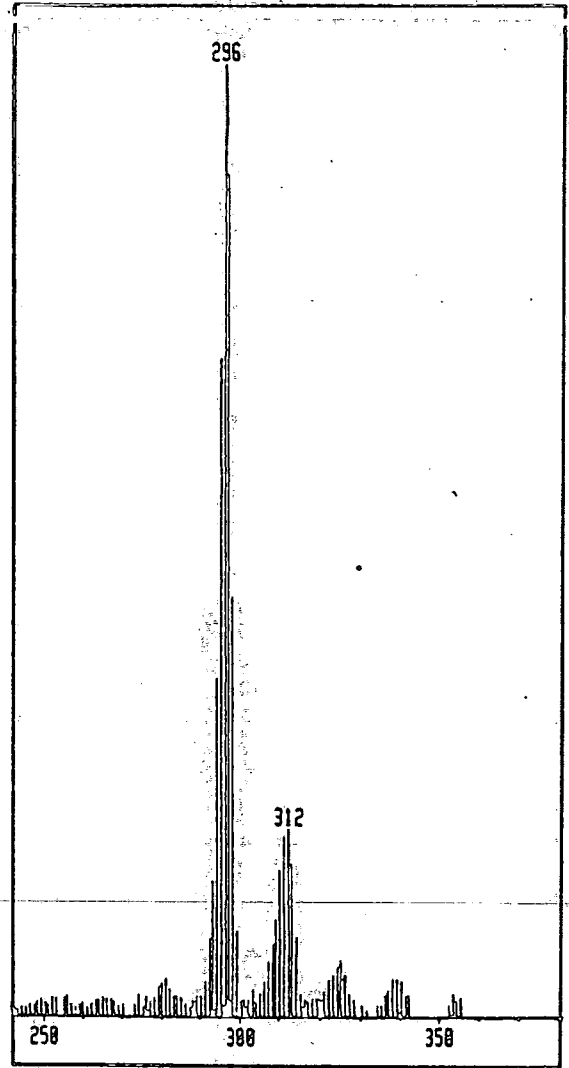


This gives rise to half mass peaks. These can be seen in figure 2.9 between m/e 144-149 (more correctly $m/2e$ 288-298). This group are readily identified as M^{2+} peaks since every peak within the cluster occurs every half mass unit because of the $2+$ charge.

Positive Chemical Ionisation mass spectra (C.I.)^{43,44} of several carborane derivatives have also been examined during this study. This technique involves the protonation of the sample by a reagent gas prior to scanning, giving rise to $(M + H)^+$ peaks. It therefore depends on the proton affinity of the sample relative to the reactive ions produced by electron bombardment of the reagent gas. This study has shown that carboranes behave unusually under these conditions.

Figures 2.11 and 2.12 show the C.I. spectra of (VI), using isobutane and ammonia respectively, as reagent gases. Negligible protonation of the sample molecules has occurred, shown by the presence of peaks around m/e 296 in both spectra (protonation would have resulted in the peak at m/e 297 in these clusters, being the most intense). The spectra are also complicated by the combination of reagent gas and sample fragments producing quasi-molecular ions of higher mass.

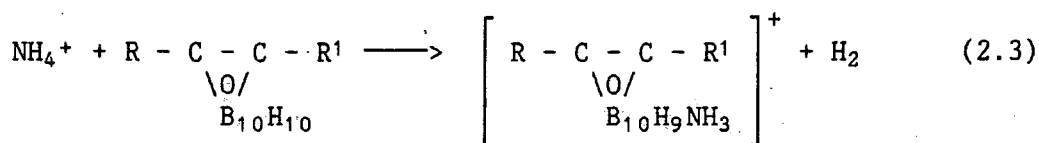
During the C.I. experiment, isobutane produces the tertiary butyl cation as the main reactive species. This can combine with sample molecules giving rise to $(M + 57)$ peaks corresponding to the complex $[M + (\text{CH}_3)_3\text{C}]^+$. A cluster of $(M + 57)$ peaks is visible in figure 2.11 around m/e 352. The peaks of greater intensity below this, around m/e 323 ($M + 25$) and m/e 337 ($M + 41$), are more

Figure 2.11Figure 2.12

C.I. Mass Spectra of VI

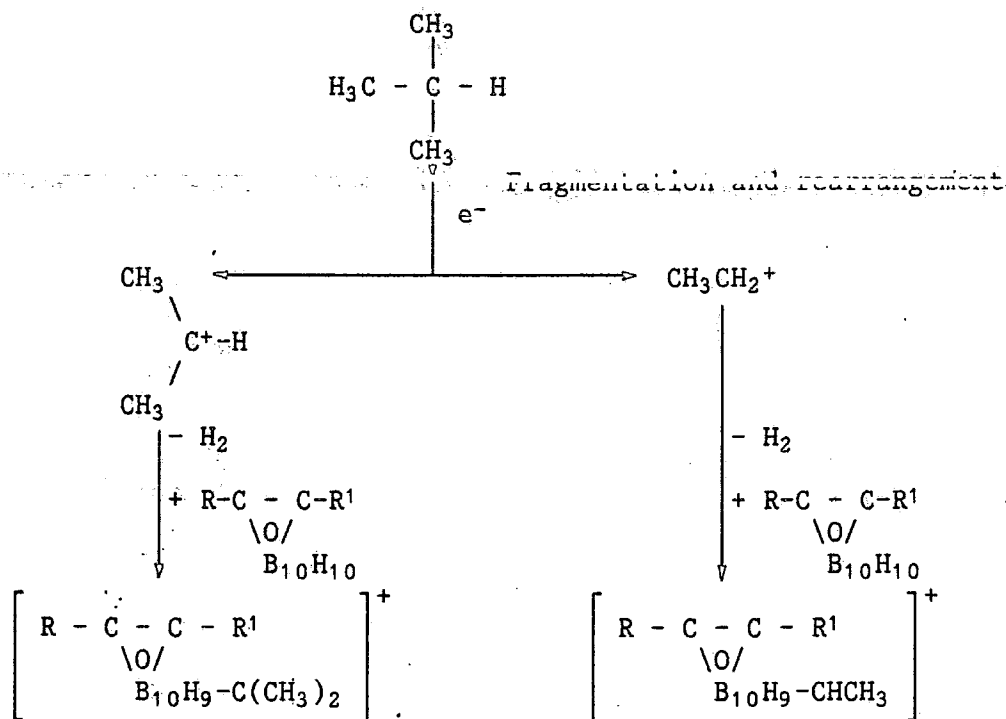
unusual in that they do not coincide with combination complexes commonly seen in isobutane C.I. spectra^{43,44}. When ammonia is used as the reagent gas, the most abundant reactive species is the NH_4^+ ion and so the occurrence of the combination complex $(\text{M} + \text{NH}_4)^+$ is common. In figure 2.12 a cluster of peaks around m/e 312 ($\text{M} + 16$) is visible, obviously not the expected $(\text{M} + \text{NH}_4)^+$ complex which would give rise to $(\text{M} + 18)$ peaks.

All the carboranes described in this chapter produced these quasi-molecular ions under C.I. conditions. Their occurrence is not fully understood at present. It seems feasible that they are produced as a result of condensation reactions between reagent gas fragments and the sample molecules. This would involve elimination of molecular hydrogen and functionalisation of the cage boron atoms. For example the NH_4^+ ion could be reacting as in equation 2.3.



Similarly the $(\text{M} + 25)$ and $(\text{M} + 41)$ peaks seen in the isobutane C.I. spectrum may be produced by the reaction of ethyl and propyl cations (formed by the fragmentation of isobutane under E.I.) with the carborane cage (see scheme 4).

Scheme 4



This condensation reaction seems particularly feasible for the NH_4^+ ion firstly because the hydrogen atoms of the cage are slightly negatively charged inducing an electrostatic interaction with the cation. Secondly the elimination of hydrogen would create a vacant site on the icosahedral surface to allow a Lewis acid/Lewis base interaction between the ammonia and carborane residue to produce a stable positively charged adduct. This reaction would presumably be encouraged by the electron deficiency of the cage. This observation may therefore have implications for the C.I. mass spectra of other formally electron deficient compounds containing hydridic hydrogen.

For the purpose of unambiguously characterising icosahedral carboranes, it can be seen from figures 2.9, 2.11 and 2.12 that the most effective technique is E.I. Therefore only the E.I. spectra of the carboranes prepared are discussed in the experimental section.

2.4 Experimental

2.4.1 Purification and use of decaborane¹⁴

Decaborane is a toxic volatile solid described as having a pungent chocolate like odour. Its minimum detectable concentration in air has been estimated at 0.7 ppm whereas the maximum allowable concentration for an 8 hour daily exposure is 0.05 ppm^{4,5}. Therefore all supplies of the compound have been stored in well ventilated cupboards and all manipulations carried out in well ventilated fume hoods. Other hazardous properties of decaborane include its flammability, its violent reaction with oxidising agents such as nitric acid, and the tendency of crude material to explode in air at temperatures approaching 100°C. Dissolving decaborane in chlorinated solvents such as carbon tetrachloride or ethers such as dioxane can result in the production of shock sensitive solutions and residues and so the most commonly used solvents for decaborane are hydrocarbons such as pentane or toluene.

Commercially obtained decaborane, or pure material that has been stored for a period of weeks contains a small proportion of polymeric material which can greatly reduce the yield of carborane prepared by its reaction with acetylenes. Purification may be accomplished by recrystallisation from benzene or pentane. However, the most convenient laboratory scale method for purifying decaborane has been found to be vacuum sublimation which is relatively quick and minimises exposure of workers to the material.

Typically, 10 to 12 g batches of crude decaborane were placed in a purpose built sublimation apparatus that had been purged with nitrogen. The system was evacuated on a vacuum line, assembled in a fume hood, to 0.001 mmHg and the apparatus heated to 80°C. The

pure decaborane was collected on a cold finger cooled with liquid nitrogen over a period of one to two hours, in yields between 85-90%, melting point 99°C (lit 99.7°C⁴⁵).

All apparatus exposed to decaborane was decontaminated prior to conventional washing by treatment with aqueous methanol or ammonia solution for 24 hours.

2.4.2 Preparation of bis-(acetonitrile) decaborane

Preparation of preformed bis-(acetonitrile) decaborane is not essential for the synthesis of carboranes, this may be done in situ. However storage of the decaborane in the form of its stable bis-acetonitrile adduct eliminates the need for its constant resublimation.

24.6 g (0.202 moles) of sublimed decaborane was dissolved in 50 mls of freshly dried acetonitrile and 20 mls of dry toluene. The pale yellow solution was refluxed under a nitrogen atmosphere for six hours affording a white precipitate. The mixture was cooled to room temperature and the precipitate was filtered off, washed twice with fresh toluene and dried under vacuum. The resulting white powder was identified as bis-(acetonitrile) decaborane. Yield 34.68 g (0.172 moles), 85%. The product was characterised as follows.

Analysis Found: C, 22.9; H, 8.5; B, 52.8; N, 13.6 % $C_4H_{18}B_{10}N_2$
Requires: C, 23.7; H, 8.8; B, 53.4; N, 13.8%.

Infra Red (Nujol) (cm^{-1}) : 2980-2820 (s) (C-H stretch); 2520 (s) 2480 (sh) (B-H stretch); 2370 (w); 2330 (w); 1500 (s); 1400 (m); 1345; 1117; 1076; 1030; 1015 (sh); 995 (s); 970; 949; 937; 927; 872 (w); 792; 775; 745; 672; 650; 525 (br); 488; 445;

N.B. No $C\equiv N$ stretch seen.

2.4.3 Preparation of 1-methyl ortho carborane (II)²⁴

i) Preparation of 1-bromomethyl-ortho-carborane (I)

A solution of propargyl bromide (13.5 mls, 0.179 moles) in 30 mls of dry toluene was added in three portions to a stirred slurry of bis-(acetonitrile) decaborane (36.17 g, 0.179 moles) in dry toluene under nitrogen. Each addition was made over one hour, the solution being heated to reflux for one hour between additions. The mixture was refluxed for a further 35 hours under nitrogen producing an orange solution. The solution was cooled and the solvents removed under vacuum leaving a viscous brown oil which solidified on standing. The solid was melted and extracted four times with 100 ml portions of dry hexane. The hexane extracts were combined, filtered, washed four times each with 100 ml portions of 10% sodium hydroxide (aq) and distilled water and dried over anhydrous magnesium sulphate. The hexane solution was filtered, the solvent removed under vacuum and the residue distilled under reduced pressure (85-90°C 1 mmHg) to give a colourless low melting waxy solid identified as 1-bromomethyl-ortho-carborane. Yield 33.58 g (0.142 moles) 79.3% (lit 83%), melting point (46-48°C). Product characterised as follows:

Analysis Found : C, 15.1; H, 5.9; B, 45.5; Br, 33.8

% $C_3B_{10}H_{13}Br$ Requires : C, 15.2; H, 5.5; B, 45.6;

Br, 33.7 %

Infra Red (Contact film) (cm^{-1}) : 3065 (s) (carboranyl C-H stretch); 3020; 2975 (aliphatic C-H stretch); 2590 (s) (B-H stretch); 2225 (w.br); 2120 (w.br); 1925 (w.br); 1850 (w.br); 1720; 1430 (s); 1362; 1252 (s); 1222; 1191; 1125 (s); 1064 (s); 1020 (s); 1005; 974 (w); 936; 920; 881 (w); 843 (w); 821; 810 (sh); 784; 765 (sh); 727 (s) (cage vibration); 684; 668; 640; 562; 530 (w); 502; 452 (w).

ii) Conversion of 1-bromomethyl-ortho carborane (I) to 1-methyl-ortho-carborane (II)

1-bromomethyl-ortho-carborane (48.96 g, 0.207 moles), dissolved in 300 mls of anhydrous diethyl ether, was added dropwise to a refluxing mixture of dry magnesium turnings (7.5 g) diethyl ether (50 mls) and iodine (1 crystal) under a dry nitrogen atmosphere. Having completed the addition, the mixture was refluxed for three hours, cooled to room temperature and the ether solution decanted into a beaker containing 800 g of crushed ice. The mixture was acidified with 3M hydrochloric acid and the two resulting layers separated. The aqueous layer was washed three times with diethyl ether and all ether extracts were combined, dried over anhydrous magnesium sulphate and filtered. The solvent was distilled off leaving a white solid which was purified by sublimation (1 mmHg 100-130°C) producing a white crystalline solid identified as 1-methyl-ortho-carborane. Yield 29.20 g (0.185 moles) 89.3% (lit 93%). Melting point 215-217°C, (lit 218-219°C). Product characterised as follows:

Analysis Found : C, 22.2; H, 9.2; B, 66.9 %. $C_3B_{10}H_{14}$

Requires: C, 22.8; H, 8.9; B, 68.4%.

Infra Red (Nujol) (cm^{-1}); 3055 (carboranyl C-H stretch), 3000-2800 (s) (aliphatic CH stretch); 2575 (s) (B-H stretch); 1840 (w); 1450 (s); 1374 (s); 1227 (w); 1132; 1095; 1080 (sh); 1032; 1017; 997; 972; 933; 915 (sh); 880 (sh); 785; 767 (sh); 722 (s) (cage vibration); 673 (w); 653 (w); 494 (w); 460 (w).

N.M.R. ^{11}B and 1H NMR are discussed in detail in Chapter 6.

Mass Spectrum (E.I.) A highest mass peak at m/e 160 was observed corresponding to $^{12}C_3^{11}B_{10}^1H_{14}$, along with the usual isotope distribution pattern for the B_{10} cage between m/e 150-160. Characteristic cage fragmentation was also observed and $\frac{1}{2}$ mass peaks were seen between m/e 75-80 (m/2e 150-160).

2.4.4. Preparation of 1-phenyl-ortho-carborane (III)²⁵

Freshly distilled phenylacetylene (17.8 mls, 0.143 moles) in 40 mls of dry toluene was added to bis-(acetonitrile) decaborane (28.89 g, 0.143 moles) slurried with dry toluene, under nitrogen. The mixture was heated cautiously initiating an exothermic reaction which quickly subsided. The resulting orange solution was refluxed for 24 hours, cooled and 40 mls of methanol added and the solution stirred until the evolution of hydrogen stopped. The solvents were removed under vacuum producing a viscous orange oil. This was vacuum distilled (120-125°C 0.1 mmHg) producing an off-white low melting solid which was dissolved in 30 mls of methanol and stirred for 12 hours to ensure complete degradation of any decaborane residues. The methanol was removed under vacuum and the resulting off-white solid recrystallised from hexane giving colourless crystals identified as 1-phenyl-ortho-carborane. Yield 16.15 g (73 μ moles), 51.3% (lit 65%). Melting point 68-70°C (lit 69-70°C). Product characterised as follows:

Analysis Found: C, 43.7; H, 8.0; B, 48.9%. $C_8B_{10}H_{16}$

Requires: C, 43.6; H, 7.3; B, 49.1%

Infra Red (Nujol) (cm^{-1}): 3060 (s) (carboranyl C-H stretch); 2620-2540 (s) (B-H stretch); 1581 (w) (C=C stretch); 1490; 1458 (sh); 1447 (s); 1374; 1337; 1314; 1276; 1260; 1193; 1160; 1120; 1105; 1070 (s); 1037; 1020; 1004 (s); 933; 918; 873; 860 (sh); 799; 753 (s); 732 (s); 725; 688 (s) (cage vibration); 663; 598; 560; 484.

NMR 1H and ^{11}B spectra are discussed in Chapter 6.

^{13}C { 1H broad band noise} 62.896 MHz. Solvent $CDCl_3$. Referenced externally to TMS at 0.00 ppm: (ppm) Carboranyl carbon atoms; 77.06, s, C(1) (under solvent signal, located by re-running sample in CD_3COCD_3); 60.17, (s), C(2). Phenyl carbon atoms: 133.46, (s), C(1); 129.93, (s), C(2); 128.88, (s), C(3); 127.53 (s), C(4).

Mass spectrum (E.I.) A highest mass peak at m/e 222 was observed corresponding to $^{12}C_8^{11}B_{10}^1H_{16}$ accompanied by the characteristic isotope distribution pattern for the B_{10} cage between m/e 212-222. Characteristic fragmentation of the cage, and $\frac{1}{2}$ mass peaks

between m/e 106-111 (m/2e 212-222) were also seen.

2.4.5 Preparation of 1,2-diphenyl-ortho-carborane (IV)²⁵

Diphenyl acetylene (16.10 g, 90 mmols) dissolved in 60 mls of dry toluene, was added to a slurry of bis-(acetonitrile) decaborane (18.20 g, 90 mmols) in 40 mls of dry toluene under nitrogen. The mixture was refluxed for 24 hours producing a dark red solution. This was cooled to room temperature, 50 mls of methanol added and the mixture stirred for a further 12 hours. The solvents were removed under vacuum leaving a red/brown solid which was ground to a powder and refluxed with hexane. The hexane solution was filtered off and the residual solid was further extracted in a soxhlet apparatus with hexane for 24 hours. The hexane extracts were combined and the solvent removed under vacuum leaving a yellow solid. This was dissolved in methanol and the solution stirred for 12 hours. The methanol was then removed and the solid produced recrystallised from fresh hexane producing off-white crystals identified as 1,2-diphenyl-ortho-carborane. Yield 18.38 g, (61.1 mmols), 69% (lit 70%). Melting point 145-146°C (lit 148-149°C). Product characterised as follows:

Analysis found: C, 54.9; H, 6.5; B, 36.0%. $C_{14}B_{10}H_{20}$ Requires: C, 56.7; H, 6.7; B, 36.5%.

Infra Red (Nujol) (cm^{-1}): 3055 (sh) (aromatic C-H stretch); 2630 (m); 2570 (s); 2550 (sh) (B-H stretch); 1575 (w) (C=C stretch); 1485 (sh); 1455 (sh); 1443 (s); 1373; 1331; 1260; 1189; 1160; 1109; 1073; 1030; 1002; 970 (w); 929 (sh); 919; 889; 870; 802; 780; 755 (s); 730; 687 (s) (cage vibration); 657 (w); 597; 579; 509; 471.

^{11}B NMR. { 1H broad band noise} 115.55 MHz, solvent C_6D_6 Referenced externally to $BF_3 \cdot Et_2O$ at 0.00 ppm.

Resonance Pattern	δ (^{11}B) ppm	Integral	Assignment*
s	- 1.12	2B	B(9,12)
s	- 8.02	4B	B(4,5,7,11)
s	- 9.17	2B	B(8,10)
s	-10.46	4B	B(3,6)

* Nomenclature as in Chapter 6, figure 6.1

Mass Spectrum

See Section 2.3.3 and figure 2.8.

2.4.6 Preparation of 1-(4-fluorophenyl)-ortho-carborane (V)

i) Preparation of 4-fluorophenylacetylene²⁸

4-fluoroacetophenone (20 mls, 0.165 moles) was slowly added to phosphorous pentachloride (35.5 g, 0.171 moles) under nitrogen producing an exothermic reaction evolving hydrogen chloride gas. The reaction subsided after approximately 10 minutes producing a yellow solution which was heated to 100°C (water bath) for 2 hours. The mixture was cooled and reaction byproduct, phosphorous oxychloride, removed under vacuum (identified by I.R.). The residue was then distilled under vacuum (30-50°C, 0.01 mmHg) producing 17.35 gm of the chloride mixture which was used as prepared.

Approximately 200 mls of liquid ammonia was condensed into a cooled flask (dry ice) equipped with a dry ice/acetone condenser (all apparatus was previously purged with

nitrogen). 0.2 g of iron III nitrate nona-hydrate was added to the ammonia followed by slow addition of sodium pieces (6 g, 0.26 moles). The resulting mixture was stirred until the conversion of sodium to sodium amide was complete (indicated by the disappearance of the blue sodium solution and appearance of the grey sodium amide suspension). The chloride mixture in 60 mls of dry diethyl ether, was added slowly over one hour to the vigorously stirred sodium amide suspension. The mixture was then allowed to reflux for two hours and finally left, allowing the ammonia to evaporate away. 200 mls of 10% ammonium chloride solution and 50 mls of diethyl ether were added to the resulting residue and the ether layer separated. The aqueous layer was extracted a further two times with diethyl ether, all the other extracts were combined, washed twice each with aqueous sodium chloride and distilled water, dried over anhydrous magnesium sulphate and filtered affording a dark brown solution. The ether solvent was removed under reduced vacuum, producing a colourless liquid (22-24°C, 0.1 mmHg) identified as 4-fluorophenylacetylene, yield 3.30 g (27.5 mmoles) 16.7%. (A smaller fraction (50-60°, 0.1 mmHg) was produced identified by I.R. as unreacted 4-fluoroacetophenone). The acetylene derivative was characterised as follows:

Analysis % Found: C, 80.9; H, 4.5; F, 15.8. C_8H_5F requires: C, 80.0; H, 4.2; F, 15.8.

I.R. (contact film) (cm^{-1}): 3280 (s) ($\equiv C-H$ stretch); 3040 (w) (arom. C-H stretch); 2105 ($C\equiv C$ stretch); 1880 (w,br); 1680 (w,br); 1597 ($C\equiv C$ stretch); 1497; 1262 (sh); 1228 (s) (C-F stretch?); 1157; 1092; 1015 (w); 847 (s); 820 (sh); 759; 710 (sh); 680 (sh); 660 (br); 615 (br); 530.

ii) Reaction of 4-fluorophenylacetylene with bis(acetonitrile) decaborane

4-fluorophenylacetylene (3.10 g, 25.8 mmoles) in 20 mls of

dry toluene was added to a slurry of bis-(acetonitrile) decaborane (5.28 g, 25.8 mmoles) in 30 mls of toluene and the mixture refluxed for 24 hours producing an orange solution. The mixture was cooled, decaborane residues degraded with 30 mls of methanol as before, and the solvents removed under vacuum. The orange solid produced was extracted three times with boiling hexane. The hexane extracts produced were combined, washed three times with 10% sodium hydroxide, dried over anhydrous magnesium sulphate and filtered. The hexane solution produced was concentrated under vacuum affording colourless crystals identified as 4-fluorophenyl-ortho-carborane. Yield 3.07 g (12.9 mmoles) 50% (lit. 83%). Melting point 138-139°C (lit. 140-141°C). Product characterised as follows:

Analysis Found: C, 40.6; H, 5.9; B, 45.3; F, 7.8%; $C_8B_{10}H_{15}F$.
Requires: C, 40.3; H, 6.3; B, 45.4; F, 8.0%

I.R. (Nujol) (cm^{-1}): 3068 (Carboranyl C-H stretch); 2620 (sh); 2600 (s); 2570 (s); (B-H stable); 1610 ($C=C$ stretch); 1510 (s); 1460 (s); 1412; 1378; 1368 (sh); 1307; 1260 (sh); 1247 (s) (C-F stretch?); 1172 (s); 1160; 1125 (w); 1115 (w,sh); 1075; 1024; 1005; 925 (w,br); 880; 844 (s); 810; 732; 725 (sh); 710 (w); 689 (w); 642 (w); 566 (w); 551 (s); 530 (w); 515 (s).

N.M.R. ^{19}F { 1H } 235.342 MHz. Solvent $CDCl_3$. Referenced externally to CDF_3 at 0.00 ppm: (ppm), s, -111.12.

^{11}B { 1H broad band noise} 80.24 MHz Solvent C_6D_6 . Referenced externally to $BF_3 \cdot Et_2O$ at 0.00 ppm.

Resonance Pattern	δ ppm	Integral	Assignment
s	- 1.30	1B	B(9)
s	- 3.60	1B	B(12)
s	- 8.29	2B	B(8,10)
s	-10.27	2B	B(4,5)
s(sh)	-10.90	2B	B(3,6)
s	-12.19	2B	B(7,11)

Mass Spectrum (E.I.) A highest mass peak was observed at m/e 240 ($^{12}\text{C}_8^{1}\text{H}_{15}^{11}\text{B}_{10}^{19}\text{F}$) accompanied by the usual isotope distribution pattern between m/e 230-240, and cage fragmentation. Weak $\frac{1}{2}$ mass peaks could also be seen at m/e 115-120 (m/2e 230-240).

2.4.7 Preparation of 1-(4-phenoxyphenyl)-ortho-carborane (VI)

i) Preparation of 4-phenoxyphenylacetylene

4-phenoxyacetophenone (40.38 g, 0.19 moles) and phosphorous pentachloride (44.46 g, 0.21 moles) were mixed under nitrogen. The mixture was heated gently, melting the acetophenone derivative, and inducing an exothermic reaction evolving a large amount of hydrogen chloride gas. This subsided after 10 minutes and the resulting solution was heated to 100°C (water bath) for 2 hours producing a black liquid. This was cooled and the phosphorous oxychloride removed under vacuum. The liquid was then poured onto 300 mls ice/water and the mixture extracted three times with diethyl ether. The ether extracts were combined, washed with

distilled water, dried over anhydrous magnesium sulphate and filtered producing a dark brown solution.

A suspension of sodium amide in liquid ammonia was prepared as in Section 2.3.6 (i) (from 12 g of sodium (0.52 moles), 500 mls of liquid ammonia and 0.3 g iron III nitrate nonahydrate). The ether solution prepared from the reaction of the acetophenone derivative with phosphorous pentachloride, was slowly added to the vigorously stirred sodium amide suspension over one hour. The mixture was then allowed to reflux for two hours, the ammonia allowed to evaporate away and the mixture worked up as before (Section 2.3.6 (i)), affording a viscous black oil. This was distilled under vacuum producing a yellow oil (120-125°C 0.1 mmHg) which was identified as 4-phenoxyphenylacetylene. Yield 18.25 g (94 mmoles) 49.5%. Product characterised as follows:

Analysis Found: C, 85.0; H, 5.8%. $C_{14}H_{10}O$ Requires C, 86.6; H, 5.2%.

I.R. (contact film) (cm^{-1}): 3275 (s) ($\equiv C-H$ stretch); 3035 (aromatic C-H stretch); 2975 (w); 2425 (w); 2390 (w); 2105 ($C\equiv C$ stretch); 2015 (w); 1980 (w.br); 1635 (sh); 1583 (s) ($C=C$ stretch); 1473 (s); 1455 (sh); 1407 (w); 1370 (w); 1328 (sh); 1275; 1235 (s) (C-O-C asymmetric stretch); 1197; 1164 (s); 1100; 1070; 1022; 1013; 957; 940; 905; 869; 838; 801; 761; 688; 655; 645 (w); 605 (br); 527; 500; 427 (w).

1H N.M.R. 60 MHz. Solvent $CDCl_3$. Referenced to internal TMS at 0.00 ppm: 6.5-7.5 ppm (m) Integral 9H (Aromatic protons); 3.00 ppm (s) Integral 1H (Acetylenic proton).

ii) Reaction of 4-phenoxyphenylacetylene with bis-(acetonitrile) decaborane

4-phenoxyphenylacetylene (7.18 g, 37 mmol) in 30 ml of dry toluene was added to a slurry of bis(acetonitrile) decaborane (7.47 g, 37 mmol) in 20 ml of toluene and the mixture refluxed for 24 hours producing a brown solution. This reaction mixture was worked up in the same way as for the preparation of 4-fluorophenyl-ortho-carborane (Section 2.3.6 (ii)). The pale yellow hexane solution produced was concentrated under vacuum and chilled (-30°C), giving a white powder which was filtered off and recrystallised from dry methanol to give colourless crystals identified as 4-phenoxyphenyl-ortho-carborane. Yield, 4.65 g (15 mmol), 40%. Melting point: $92-93^{\circ}\text{C}$. Product characterised as follows:

Analysis. Found: C, 54.8; H, 6.9; B, 35.1%. $\text{C}_{14}\text{H}_{20}\text{B}_{10}\text{O}$
Requires: C, 53.8; H, 6.4; B, 34.6%.

I.R. (Nujol) (cm^{-1}): 3058 (carboranyl C-H stretch); 3000-2800 (Nujol); 2580 (s); 550 (sh) (B-H stretch); 1607 (w); 1586 (C=C stretch); 1510 (sh); 1500 (sh); 1482; 1467; 1415 (w); 1375; 1312 (w.sh); 1305 (w); 1286; 1245 (s) (C-O-C asymmetric stretch); 1205 (s); 1178; 1162; 1125 (w.br); 1072; 1023; 1003; 910; 884; 868; 841; 794; 775 (w.sh); 755 (s); 825; 821 (sh); 693; 650 (w); 575 (w); 558 (w); 511; 485.

Mass Spectrum (E.I.) A highest mass peak was seen at m/e 314 ($^{12}\text{C}_{14}^{1}\text{H}_{20}^{11}\text{B}_{10}\text{O}$) with the usual isotope distribution pattern between m/e 304-314, and fragmentation of the cage. Very weak $\frac{1}{2}$ mass peaks were seen between m/e 152-157 ($m/2e$ 304-305).

NMR ^{13}C { ^1H broad band noise} 62.896 MHz, solvent CDCl_3 . Referenced externally to TMS at 0.00 ppm. (ppm): Carboranyl carbon atoms: 155.63, (s), C(1); 130.03, (s), C(4); 124.47, (s), C(3,5); 119.86, (s), C(2,6). Phenylene carbon atoms: 159.23, (s), C(4); 129.39, (s), C(2,6); 127.46, (s), C(1);

117.78, (s), C(3,5).

^{11}B N.M.R { ^1H broad band noise} 115.545 MHz, solvent C_6D_6 referenced externally to $\text{BF}_3 \cdot \text{Et}_2\text{O}$ at 0.00 ppm.

Resonance Pattern	δ ppm	Integral	Assignment
s	- 0.81	1B	B(9)
s	- 3.32	1B	B(12)
s	- 7.89	2B	B(8,10)
s	- 9.72	2B	B(4,5)
s	-10.54	2B	B(3,6)
s	-11.70	2B	B(7,11)

2.4.8 Isomerisation of 1-phenyl-ortho-carborane (III) to 1-phenyl-meta carborane VII³⁰

A 16 mm bore Carius tube was charged with 1-phenyl-ortho-carborane (2.05 g, 9.4 mmoles) and sealed under vacuum. The tube was placed inside a close-fitting steel jacket and heated in a furnace to 450°C for 24 hours. The tube was allowed to cool to room temperature and then opened (hot spotted with the bottom of the tube immersed in liquid nitrogen). The contents of the tube were extracted three times with boiling hexane and the extracts combined, filtered and hexane removed under vacuum leaving a colourless oil which crystallised on standing affording colourless crystals. T.L.C. on silica using hexane as the elutant showed the sample to be contaminated with a small amount of starting material. (R.f. values: 1-phenyl-ortho-carborane 0.24, 1-

phenyl-meta-carborane 0.32). The solid was dissolved in 30 mls fresh hexane and piperidine (2.75 mls, 37.6 mmoles) added. The mixture was refluxed for two hours producing a small amount of brown oil. The mixture was cooled and extracted three times with 2M hydrochloric acid. The colourless hexane solution produced was separated, washed with distilled water, dried over anhydrous magnesium sulphate and filtered. Removal of the hexane under vacuum produced a white powder identified as 1-phenyl-meta-carborane. Yield 1.46 g (6.6 mmoles), 70.6%. Melting point: 53-56°C (lit. 55-56°C). Data from elemental analysis and mass spectrometry was in agreement with the formula $C_8H_{16}B_{10}$. These techniques make no distinction between the two isomers. Product characterised as follows:

I.R. (Contact film) (cm^{-1}): 3060 (s); (Carboranyl C-H stretch); 2920 (w.br); 2850 (w.br); 2600 (s) (B-H stretch); 1590 (br) C=C stretch; 1495; 1447; 1400 (w); 1337 (w); 1319 (w); 1270 (w.br); 1210 (w.br); 1193 (w); 1160 (w); 1126; 1082; 1047; 1028; 1010; 1003; 975 (w.br); 937 (w); 925 (w); 900 (w.sh); 876; 838; 810 (w.br); 790 (w.br); 843 (sh); 834 (s); 695 (s) (Cage vibration); 665; 605; 580; 530; 493; 480 (w.sh); 468; 435 (w.br).

^{11}B NMR [1H broad band noise] 80.24 MHz, solvent C_6D_6 referenced externally to $BF_3 \cdot Et_2O$ at 0.00 ppm.

Resonance Pattern	S ppm	Integral	Assignment*
s	- 3.48	1B	B(5)
s	- 8.36	1B	B(12)
s	- 9.92	4B	
s	-13.02	2B	
s	-14.85	2B	

* ^{11}B - ^{11}B 2D COSY NMR data is required to allow complete assignment of all the resonances in the ^{11}B spectrum of VII. Even without full assignment however it can be clearly seen from comparing this spectrum with that of the parent ortho derivative (see Section 6.3.2 (iii)) that the isomerisation reaction has been successful.

2.5. REFERENCES

1. W.E. Hill, F.A. Johnson, R.W. Novak, Inorg. Chem. 1975, 14, 1244.
2. W.E. Hill, F.A. Johnson, N.S. Hosmane in I.U.P.A.C. Boron Chemistry 4, Ed. R.W. Parry, G. Kodama, 1979, 3.
3. B.L. Korunskii, V.N. Kalinin, G.V. Sitonia, F.I. Dubovitskii, I.T. Zakharkin, Bull. Acad. Sci. U.S.S.R. Chem. Div. 1971, 20, 1712.
4. M.F. Hawthorne, R.L. Pilling, R.N. Grimes, J. Amer. Chem. Soc. 1967, 89, 1067.
5. M.F. Hawthorne, R.L. Pilling, R.C. Vasavada, J. Amer. Chem. Soc. 1967, 89, 1075.
6. M. Thorton-Pett, M.A. Beckett, J.D. Kennedy, J. Chem. Soc. Dalton Trans. 1986, 303.
7. W.H. Noth, E.L. Muetterties, J. Inorg. Nucl. Chem. 1960, 20, 66.
8. B. Stibr, J. Plesek, S. Hermanek, Collect. Czech. Chem. Commun, 1972, 37, 2696.
9. E.I. Tolpin, E. Mizusawa, D.S. Becker, J. Vensel, Inorg. Chem. 1980, 19, 1182; E. Mizusawa, S.E. Rudnick, K. Eriks, Inorg. Chem. 1980, 19, 1188.
10. K. Wade, E.H. Wong, unpublished results (1987).
11. M.F. Guest, I.H. Hillier, J. Chem. Soc. Farraday Trans, 1974, 2004.
12. H.C. Brown, "Hydroboration", W.A. Benjamin, New York, 1962.
13. R.L. Ernest, W. Quintana, R. Rosen, P.J. Carroll, L.G. Sneddon, Organometallics, 1987, 6 (1), 80.
14. M.M. Fein, J. Bobinski, N. Mayes, N. Schwartz, M.S. Cohen, Inorg. Chem. 1963, 2, 1111.
15. M.F. Hawthorne, A.R. Pitochelli, J. Amer. Chem. Soc. 1959, 81, 5519.
16. D. Grafstein, J. Dvorak, Inorg. Chem. 1963, 2, 1128.
17. W.N. Lipscomb, Science, 1966, 153, 373.
18. R. Hoffman, W.N. Lipscomb, J. Chem. Phys. 1962, 36, 2179.
19. R. Hoffman, W.N. Lipscomb, Inorg. Chem. 1963, 2, 231.

20. J.J. Ott, B.M. Gimarc, Inorg. Chem. 1986, 108, 4303.
21. L.I. Zakharkin, V.N. Kalinin, Dokl. Akad. Nauk. S.S.S.R. 1966, 169, 590.
22. S. Papetti, T.L. Heying, J. Amer. Chem. Soc. 1964, 86, 2295.
23. B.F.G. Johnson, J. Chem. Soc. Chem. Commun. 1986, 27.
24. M.F. Hawthorne, T.D. Andrews, P.M. Garrett, F.P. Olsen, M. Reintjes, F.N. Tebbe, L.F. Warren, P.A. Wegner, D.C. Young, Inorg. Syntheses, 1967, 10, 91.
25. E.V. Stanko, V. Kopylov, A. Klimova, J. Gen. Chem. U.S.S.R. 1965, 35, 1437.
26. L.I. Zakharkin, A.A. Ponomarenko, O. Yu. Okhlobystin, Bull. Acad. Sci. U.S.S.R. Chem. Div. 1964, 2107.
27. L.I. Zakharkin, V.I. Bregadze, O. Yu. Okhlobystin, J. Organomet. Chem. 1966, 6, 228.
28. L.I. Zakharkin, V.N. Kalinin, A.P. Snyakin, B.A. Kvasov, J. Organomet. Chem. 1969, 18, 19.
29. M.F. Hawthorne, T.E. Berry, P.A. Wagner, J. Amer. Chem. Soc. 1965, 87, 4746.
30. L.I. Zakharkin, V.N. Kalinin, Bull. Acad. Sci. U.S.S.R. Chem. Div. 1965, 2173.
31. L.I. Zakharkin, V.N. Kalinin, Tetr. Letts, 1965, 7, 407.
32. D. Mesnard, F. Bernadou, L. Miginiac, J. Chem. Res (S), 1981, 270.
33. L.A. Leites, L.E. Vinogradova, V.T. Aleksanyan, S.S. Bukalov, Bull. Acad. Sci. U.S.S.R. Chem. Div. 1976, 2311.
34. L.A. Leites, L.E. Vinogradova, V.N. Kalinin, L.I. Zakharkin, Bull. Acad. Sci. U.S.S.R. Chem. Div. 1968, 970.
35. J.D. Kennedy, Multinuclear NMR (NMR in Inorganic and Organometallic Chemistry) Ed. J. Mason, Plenum, 1986 (in press) Chapter 8.
36. B. Wrackmeyer, Prog. N.M.R. Spectros. 1979, 12, 227.
37. L.J. Todd, Pure Appl. Chem. 1972, 30, 587.
38. R.E. Williams, Prog. in Boron Chem. 1970, 2, 103.

39. L.J. Todd, A.R. Siedle, G.M. Bodner, S.B. Kahl, J.P. Hickey, J. Magn. Reson. 1976, 23, 301.
40. R.H. Cragg, A.F. Weston, J. Organomet. Chem. 1974, 67, 161.
41. J.F. Ditter, F.J. Gerhart, R.E. Williams, Adv. Chem. Ser. 1968, 72, 191.
42. N.I. Vasyukova, Yu. S. Nekrasov, Yu. N. Sukharev, V.A. Mazunov, Yu. L. Sergeer, Bull. Acad. Sci. U.S.S.R. Chem. Div. 1985, 34, 1223.
43. A.G. Harrison, Chemical Ionisation Mass Spectrometry, 1983, CRC Press.
44. M.E. Rose, R.A.W. Johnstone, Mass Spectroscopy for Chemists and Biochemists. Cambridge University Press, 1982, Chapter 7.
45. R.L. Hughes, I.C. Smith, E.W. Lawless, Production of the Boranes and Related Research, 1967, Academic Press, New York and London.
46. W.N. Lipscomb, Boron Hydrides, Benjamin, New York, 1967.

CHAPTER 3

MODEL POLYMERISATION REACTIONS AND
MONOMER SYNTHESIS

3.1 INTRODUCTION

This chapter firstly describes investigations carried out to deduce the most effective route to aromatic poly(carboranyleterketones) and secondly the preparation of monomers targetted as a result of these studies. The chapter begins by discussing the reactions used to prepare aromatic poly(etherketones) in more detail. These are:

- i) Nucleophilic polycondensation of 4-halogeno-phenyl ketones and phenoxide derivatives - polyetherification;
- ii) Electrophilic polycondensation of aromatic carboxylic acid and aromatic ether derivatives - polyacylation.

The mechanisms of these reactions are outlined, and limitations likely to be imposed on them by the presence of the carborane cage in monomers are discussed. The properties of the cage influencing the different reaction routes are the reactivity of the cage towards nucleophiles, and the electron withdrawing nature of the polyhedron which could in theory encourage polyetherification and inhibit polyacylation.

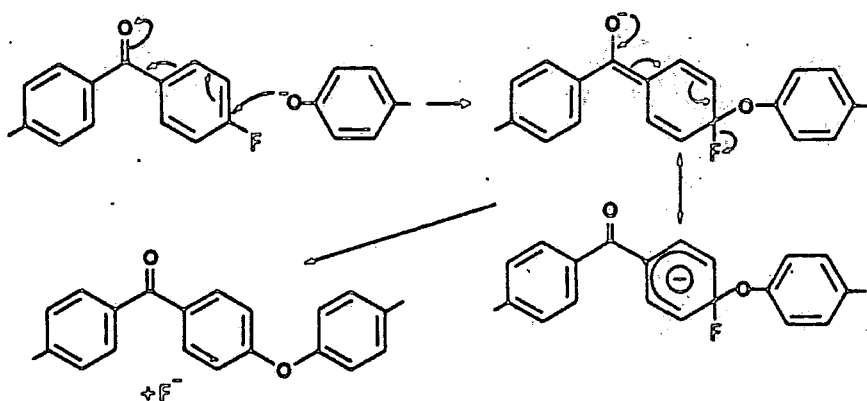
The results from test reactions show that polyacylation is the only feasible route to the desired polymers. The merit of the various linkages that could be used for cage incorporation are discussed, the ketone link being ruled out because of its reactivity when adjacent to the cage. The ether link is also ruled out because of the difficulty in preparing suitable monomers (C-hydroxy derivatives) and because of the possibility of competing cage degradation in reactions using these as monomers. The use of suitably substituted diaryl carborane derivatives are therefore seen as the most effective polymer precursors. Potential monomers are thus identified and their preparations are discussed. The final section of the chapter gives experimental details of all reactions described in previous discussion.

3.2 Polymerisation Reactions

3.2.1 Nucleophilic Polycondensation : Polyetherification

As mentioned in Chapter 1, aromatic poly(etherketones) are most effectively prepared on a commercial scale by the polycondensation of 4-halogeno phenyl ketones with alkali metal salts of 4-hydroxyphenyl compounds. Elimination of the alkali metal halide generates ether linkages between monomer units¹ (see Scheme 1).

Scheme 1



For this reaction to proceed, the halogen needs to be sufficiently activated to promote nucleophilic attack. This activation is provided by the carbonyl group which conjugatively stabilises the benzenide intermediate formed prior to ether formation² (see Scheme 1). The nature of the halogen used is also important. The reactivities of the different halides in the nucleophilic ether formation follow the sequence $F \gg CI > Br > I^3$. This pattern suggests that the condensation is a two stage process with attack of the nucleophile being the rate determining step. C-halogen bond cleavage cannot be rate determining since if it were the halogen reactivities would be reversed to correspond with the increasing C-halogen bond strength. The much greater reactivity of the fluoro species is due to the electronegative fluorine atom

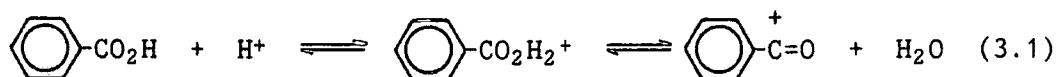
rendering the carbon atom to which it is attached more positive, and therefore much more susceptible to attack by phenoxide ion. The presence of the fluorine atom will also help to stabilise the anionic intermediate formed in the reaction³. The position of the halogen atom relative to the activating group is also important since stabilisation of the intermediate occurs through the mesomeric effect. Hence only ortho and para substituted derivatives are effective in ether synthesis. The para derivatives are more reactive as they are less sterically hindered than the ortho derivatives.

4-fluoro phenylketones are used for the preparation of high molecular weight aromatic poly(etherketones). Aromatic poly(ethersulphones) may be produced using 4-chlorophenylsulphone derivatives because of the greater activating power of the sulphone linkage^{4,5}.

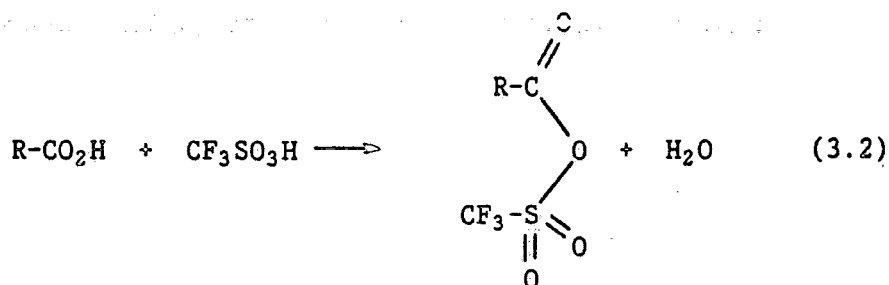
3.2.2 Electrophilic Polycondensation : Polyacylation

Although there are several methods available for preparing aromatic poly(etherketones) electrophilically (see Chapter 1), the most convenient route has been found to be the polycondensation of aryl ethers with benzoic acid derivatives in trifluoromethanesulphonic acid (Triflic acid) or TFSA⁶. This acid acts both as a catalyst and solvent for the reaction and it is conveniently removed on completion of a polymer synthesis by quenching the reaction mixture with water.

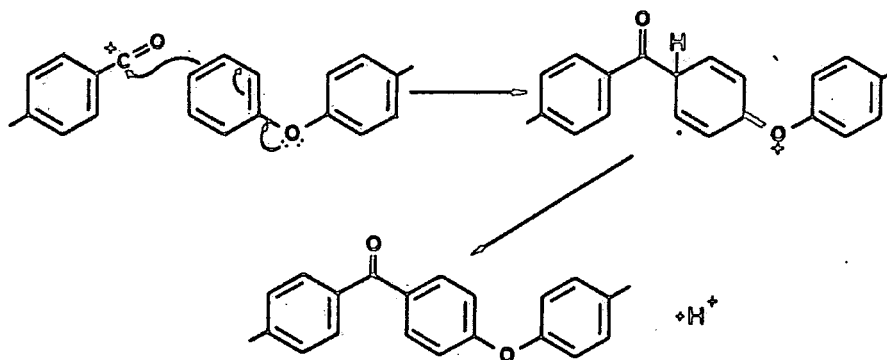
The condensation reaction is believed to involve production of the acylium ion Ar-CO^+ through protonation of the carboxylic acid moiety, followed by elimination of a molecule of water (equation 3.1).



This cation then electrophilically attacks the aryl ether, to generate the ketone linkage. The ether group plays an important role in activating towards electrophilic attack the phenyl ring to which it is attached. A possible rationale for this activation is given in Scheme 2. It should be noted that mixed anhydrides of carboxylic acids and TFSA (equation 3.2)



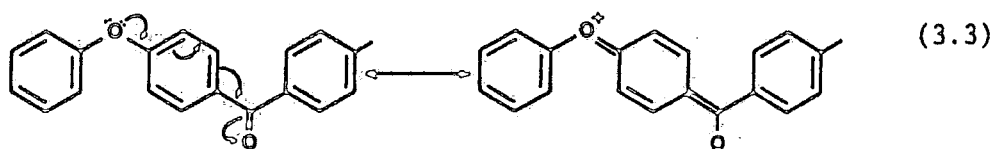
Scheme 2



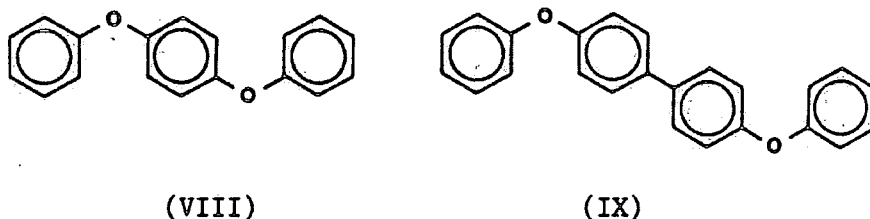
have also been shown to be powerful acylating agents⁷ leading to their being proposed as alternative intermediate species in the acylation of aromatic hydrocarbons by carboxylic acids in TFSA⁸.

The identities of the aromatic ethers and benzoic acids used in this polyacylation reaction are very important. In principle diphenyl ether has two para positions available for acylation, however in practice only one position is substituted⁶. It will not readily react with a second acid molecule because the vacant para site becomes deactivated as a result of the electron withdrawing influence of the carbonyl group (equation 3.3). If

the ether groups

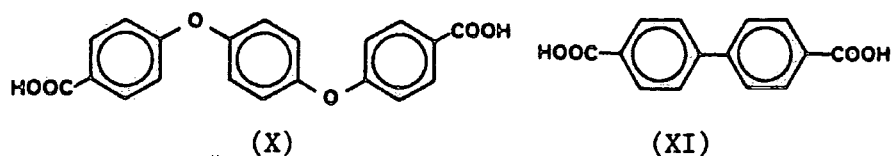


are independent however, diacylation can occur and polymerisation will take place as with the species 1,4 diphenoxybenzene (VIII) and 4,4' diphenoxybiphenyl (IX). In these compounds, the



charge induced at one ether linkage upon acylation is too distant from the second ether group to cause deactivation⁶.

Terephthalic acid (X) fails to acylate aromatic ethers at all in TFSA. Indeed electronwithdrawing substituents situated para to the carboxyl group generally deactivate the acid towards the acylation reaction by a factor that corresponds fairly well to the Hammett σ value of the substituent⁶. This supports the proposal that the reactive intermediate in the acylation reaction is the acylium ion since this species would be expected to be destabilised by electronwithdrawing substituents. Acids possessing neutral or electron donating substituents para to the carboxyl group are therefore most suitable as monomers, e.g. 4,4' (diphenoxybenzene)-dicarboxylic acid (X) and 4,4' dicarboxybiphenyl.

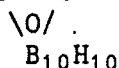


3.3 Model Reactions

In order to test the feasibility of using the reactions described in Section 3.2 to prepare aromatic poly(carboranyletherketones), a series of model reactions have been performed. Before these are outlined however, the properties of the carborane cage that are likely to influence these reactions are discussed.

3.3.1 The electronic properties of the carborane cage

The ortho carborane cage has long been known to be electronwithdrawing with respect to substituents at its carbon atoms⁹. This is indicated for instance by the ease with which the carbon atoms of the cage are metallated by alkyl lithium reagents (see Chapter 1), and by the acidity of carboranyl carboxylic acids (HC - C - CO₂H, pK_a = 2.49^{10,11})

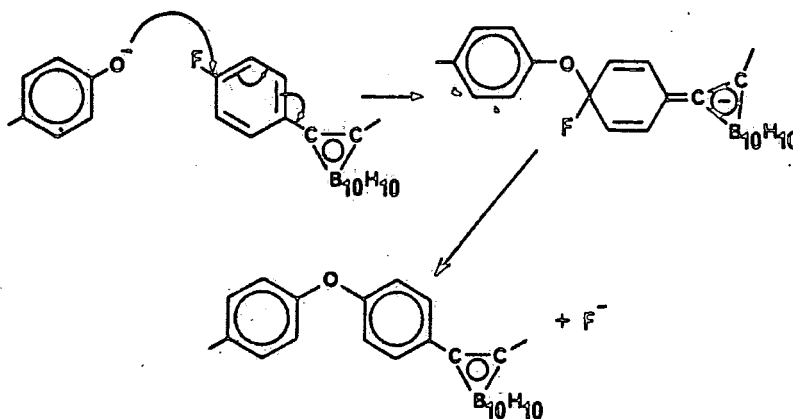


A Hammett σ value of +0.49 has been calculated for the ortho carborane nucleus¹² indicating its strongly electronwithdrawing nature (c.f. $\sigma_{\text{Cl}} = +0.23$, $\sigma_{\text{CF}_3} = +0.54$). Various studies to determine the extent to which the cage interacts with the π electron system of aryl substituents have also been undertaken. The calculation of the inductive and resonance reactivity parameters, σ_{I} and σ_{R} , of the cage have been performed using ¹⁹F NMR data obtained from 4-(fluorophenyl)-carborane derivatives^{13,14}. σ_{I} gives a measure of the inductive influence of the cage on an aromatic substituent, and σ_{R} an estimate of the ability of the cage to interact with an aryl π system¹⁵. Also the extent to which the cage conjugates with an aryl π system has been monitored using ultra violet absorption spectroscopy¹⁶. All these studies suggest that the electronwithdrawal occurs virtually entirely by an inductive mechanism and that conjugation between the cage and neutral aryl substituents is negligible.

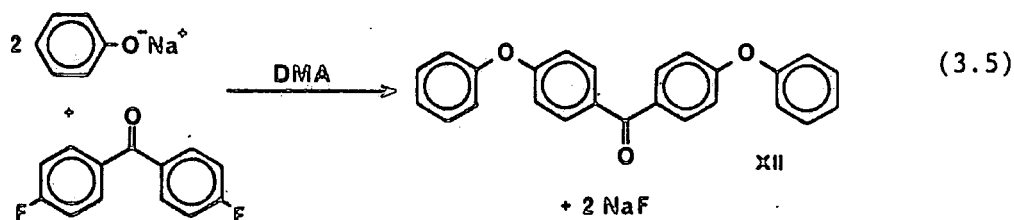
3.3.3 Nucleophilic model reactions

The fact that the ortho-carborane cage is strongly electron withdrawing, and that it is susceptible to nucleophilic attack in its own right, both have a direct bearing on the use of the nucleophilic polycondensation route to prepare aromatic poly(carboranyloxyketones). We originally supposed that the cage might substantially activate a 4-fluorophenyl substituent attached to its carbon atoms, by electronwithdrawal into the cage. This would induce nucleophilic displacement of the para fluorine atom generating an ether link, and so facilitating polymer formation (scheme 3). Also, the attack on the cage by the phenoxide nucleophile would be in obvious competition with the nucleophilic displacement reaction.

Scheme 3



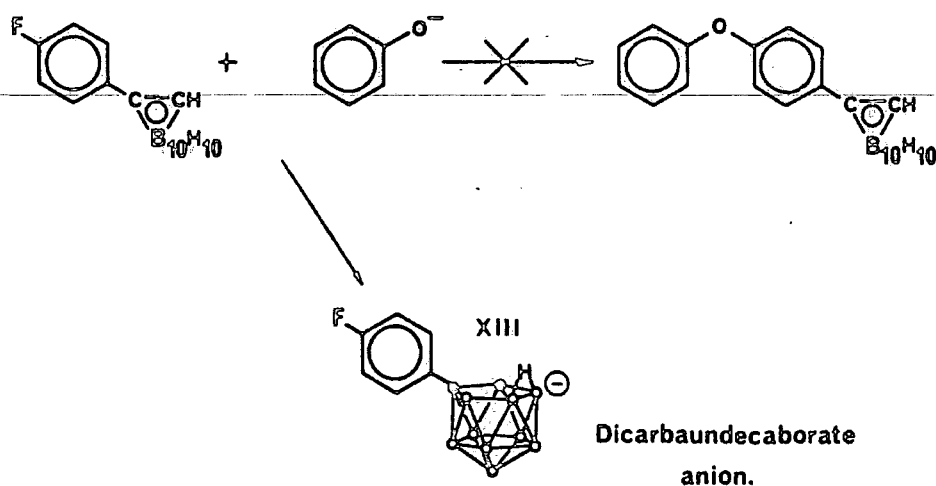
The process which occurs was deduced by examining the reaction between sodium phenoxide and 1-(4-fluorophenyl)-ortho-carborane (prepared as in Section 2.4.6). The conditions used were determined by carrying out a control reaction between sodium phenoxide and the PEEK co-monomer 4,4' difluorobenzophenone to produce 4,4'-diphenoxybenzophenone (XII) (equation 3.5).



This reaction was carried out in DMA at 175°C for eight hours affording (XII) in 80% yield. The high temperature used in this reaction mimicked the conditions encountered in typical polymerisation reactions to a certain extent, and the use of DMA as the reaction solvent simplified the reaction work up which involved quenching the reaction mixture with water followed by conventional extraction procedures.

Exposure of 1-(4-fluorophenyl)-ortho-carborane to identical reaction conditions did not produce the 1-(4-phenoxyphenyl)-ortho-carborane derivative. The only carborane-containing material recovered was identified as the 1-(4-fluorophenyl)-1,2-dicarbaundecaborate anion, isolated as its tetramethylammonium salt (XIII) (see Scheme 4). The reactivity of the cage towards the phenoxide nucleophile was further confirmed by treating 1,2-(diphenyl)-ortho-carborane with sodium phenoxide in DMA at room temperature. Stirring the solution for 48 hours brought about an approximate 18% conversion of the carborane to the 1,2(C₆H₅)₂C₂B₉H₁₀⁻ salt (XIV). These reactions illustrate that the reactivity of the cage is likely to render this reaction route unsuitable for the preparation of the desired polymers.

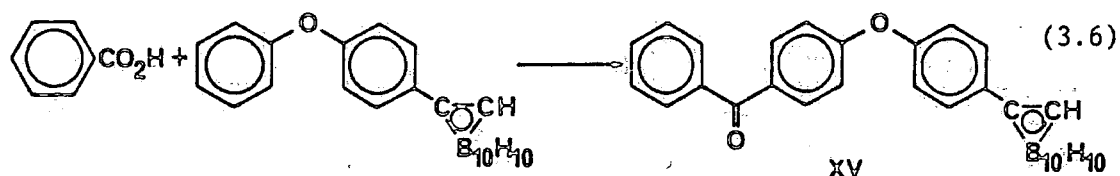
Scheme 4



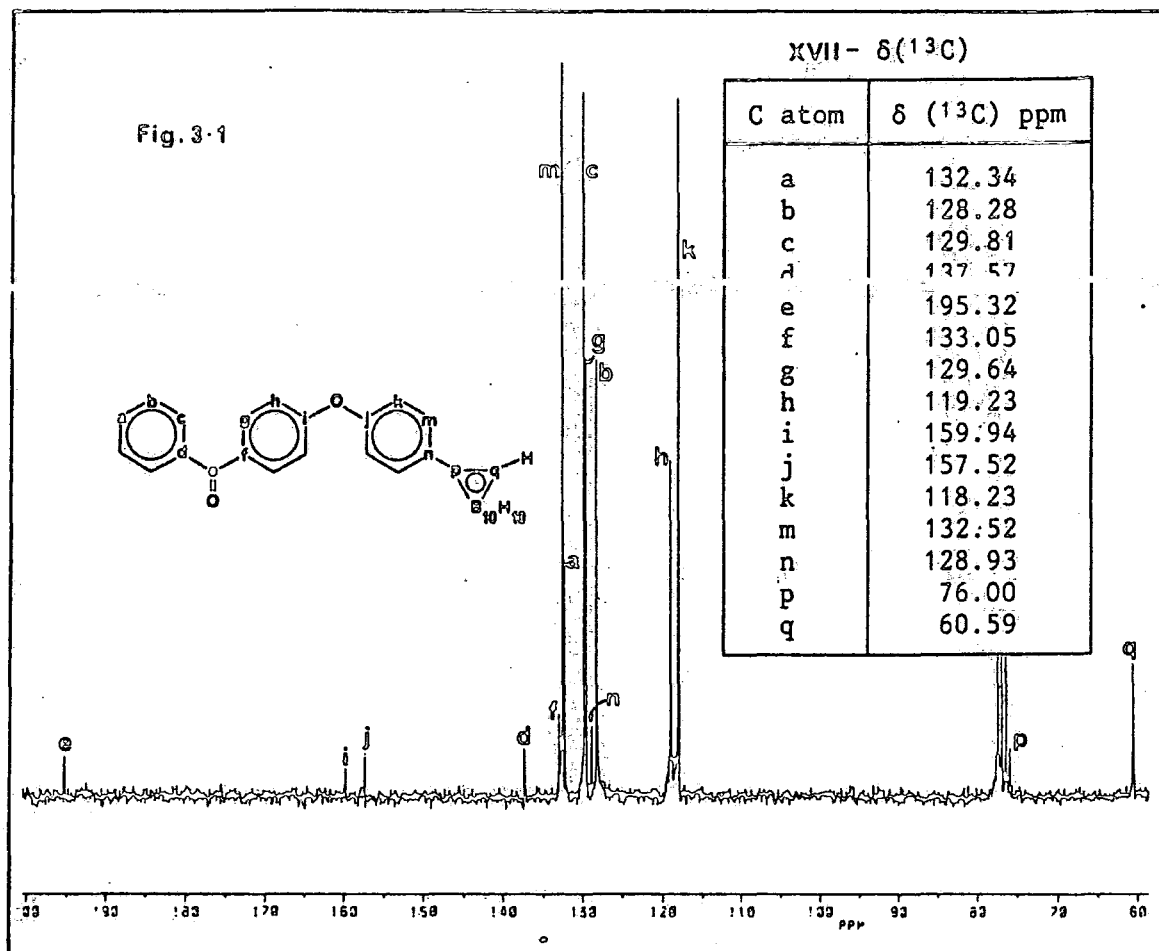
3.3.4 Electrophilic model reactions

Again, the fact that the cage is electronwithdrawing has a bearing on the effectiveness of the aromatic ether and carboxylic acid derivatives of carboranes for use in electrophilic polycondensation reactions. As pointed out before, electron withdrawal will deactivate ethers to electrophilic attack, and will inhibit the activity of carboxylic acids as acylating agents.

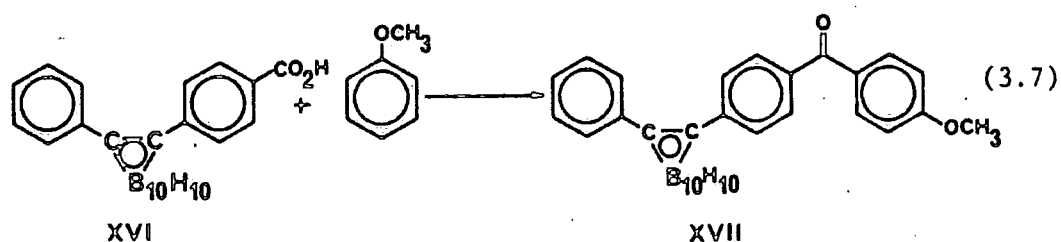
The reactivity of the carboranyl-aryl-ether-moiety was investigated by the attempted acylation of 4-(phenoxyphenyl)-ortho-carborane (preparation described in Section 2.4.7) with benzoic acid in TFSA. This produced the ketone (XV) in 95% yield (equation 3.6).



Substitution occurs exclusively at the 4 position of the phenoxy group as confirmed by ^{13}C NMR. The ^{13}C spectrum of (XV) is shown in Figure (3.1) to illustrate this. Assignments were made using the model compounds diphenyl ether and the unreacted phenoxy derivative and by applying the principle of substituent additivity⁴².



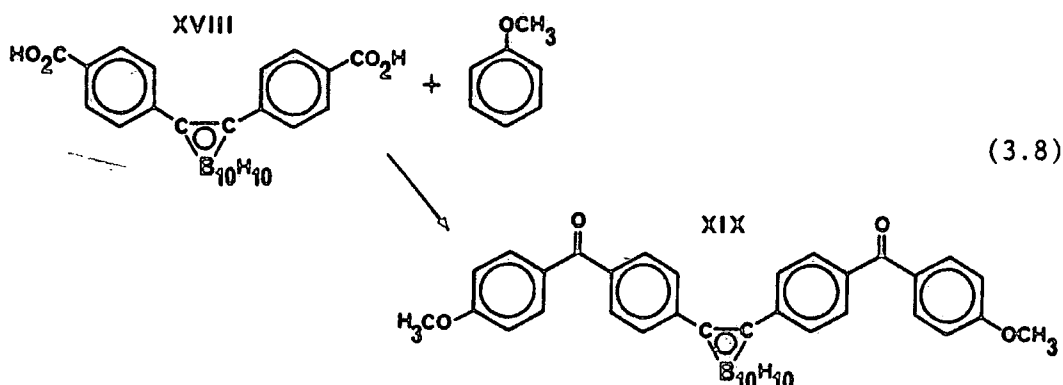
Aromatic carboxylic acids of sufficient reactivity will react with methoxybenzene (anisole) to generate the corresponding 4-methoxy ketone derivatives⁶. This reaction has been employed in the present study to investigate the ability of carboranyl carboxylic acids to act as acylating agents. The acid 1-(4-carboxyphenyl) 2-(phenyl)-ortho-carborane (XVI), (details of the preparation of which are given in Sections 3.4.2 and 3.5.7) was treated with an equimolar amount of anisole in TFSA producing the methoxy ketone derivative (XVII) in 78% yield (equation 3.7).



The rate of this reaction can in principle be followed by ^1H NMR since the resonance of the methyl protons of anisole is shielded by approximately 0.5 ppm upon acylation of the anisole molecule. The rate is therefore monitored by observing the disappearance of the free anisole CH_3 resonance and the appearance of the CH_3 resonance of the acylated product. Using this method, the rates of reaction of various para-substituted benzoic acids have been measured⁶ and their reactivity found to correspond approximately with the Hammett σ value of the substituent.

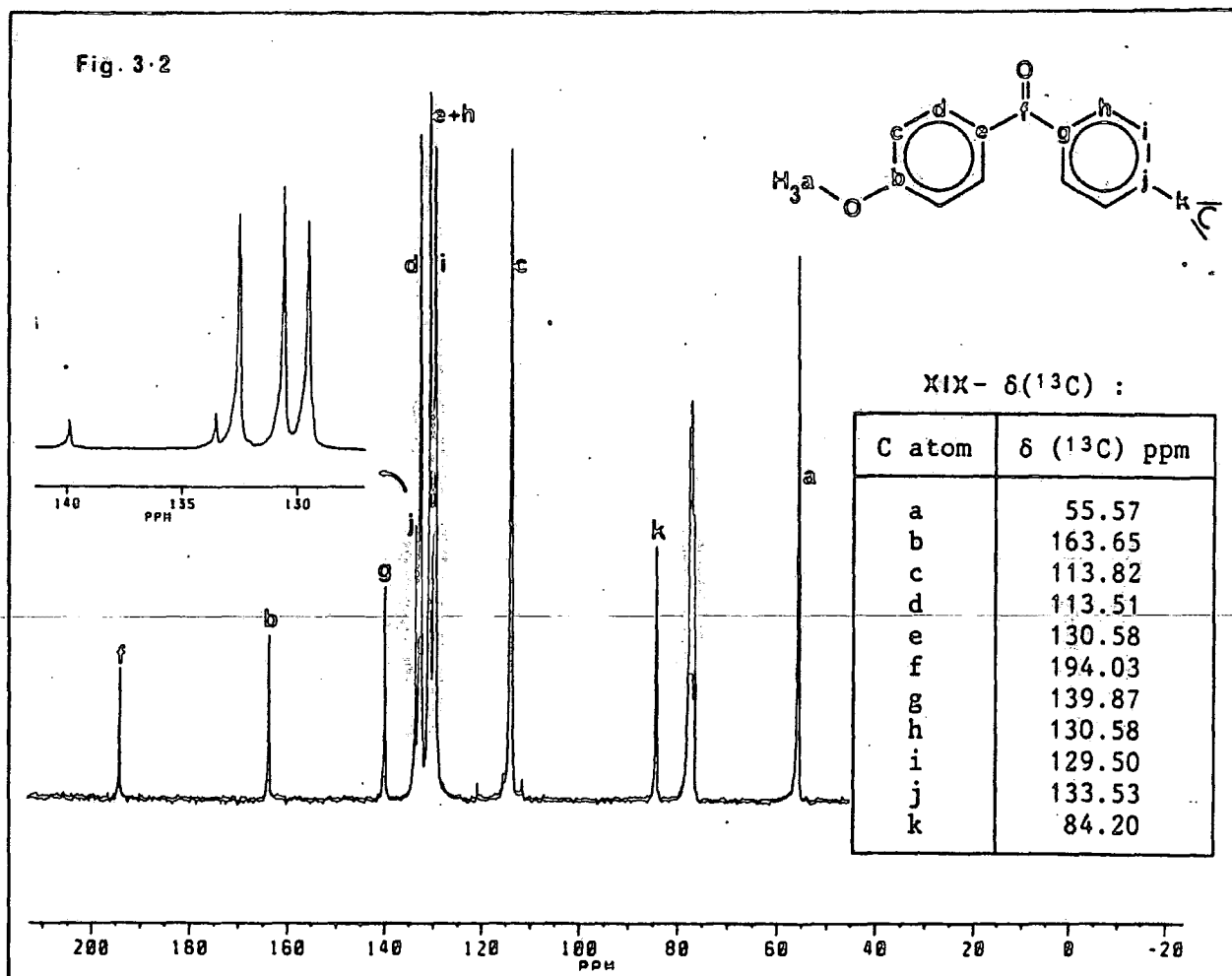
Attempts, during the present study, to monitor the reaction between acid (XVI) and anisole in this manner, were thwarted since the carborane derivative is not readily soluble in TFSA. The corresponding diacid 1,2-bis(4-carboxyphenyl)-ortho-carborane (XVIII) is readily soluble in TFSA however, and its rate of reaction has been measured as the reaction half life of a solution, 0.5 M in (XVIII) and 1 M in anisole at 30°C ($t_{1/2}$ was taken as the point at which the integral of the free anisole CH_3 signal was equal to that of the methoxy ketone CH_3 signal). The half life for this solution was found to be approximately 35 minutes. This compares fairly well with the data obtained for other benzoic acid derivatives (e.g. 4-(chloro)benzoic acid and 4-(trifluoromethyl)-benzoic acid $\sigma_{\text{Cl}} = +0.23$, $t_{1/2} = 15$ minutes, $\sigma_{\text{CF}_3} = +0.54$, $t_{1/2} = 150$ minutes)⁶. It also indicates that the 4-carboxyphenyl moiety when attached to the ortho-carborane cage acts as a deactivated acylating agent.

The product of the reaction between the diacid (XVIII) and anisole was isolated and characterised (equation 3.8).



The ^{13}C NMR spectrum of (XIX) (shown in figure 3.2) shows that the anisole has been acylated exclusively at the 4 position.

Attempts were also made to react meta-carborane 1,7 dicarboxylic acid $\text{HO}_2\text{CCB}_{10}\text{H}_{10}\text{CCO}_2\text{H}$ with anisole. These two compounds were found not to react at all as shown by characterisation of only unreacted starting material from reaction mixtures, and by ^1H NMR. This is undoubtedly due to the deactivating effect of the relatively strongly electron withdrawing meta carborane cage. This also clearly implies that the 1,2 ortho-carborane dicarboxylic acid isomer will be unreactive also.



3.3.5 Conclusions

3.3.5.1 The feasibility of the different routes to aromatic poly(carboranyletherketones)

The reactions described in Section 3.3.3 indicate that the ortho-carborane cage is too reactive towards the phenoxide nucleophile to allow polyetherification to be effective in polymer formation. The possible activating effect of the cage on the 4-fluorophenyl substituent has not been demonstrated because of the reactivity of the cage. However the fact that none of the 1-(4-phenoxyphenyl)-1,2-dicarbaundecaborate anion (see Scheme 4) or its carborane parent (VI) were isolated suggests that the activation by the cage was insufficient to promote nucleophilic displacement of the para fluorine substituent. The extent of the interaction between the aryl π system and the cage in the 1-(4-fluorophenyl) derivative will be influential in any activation by the cage, since activation occurs through the mesomeric effect. Hence the fact that no fluorine displacement has taken place in the 1-(4-fluorophenyl) derivative would be consistent with the negligible π interaction between aryl substituents and the cage observed by other workers^{13,14,16}. It is interesting to note that in contrast to its closo parent, the nido dicarbaundecaborate anion interacts quite strongly with the π system of aryl substituents^{14,16}. However since the species is anionic, it is electron donating and so will deactivate a 1-(4-fluorophenyl) substituent towards nucleophilic attack.

We originally postulated that the C-hydroxy carboranes might be active, in the form of their alkali metal salts, as nucleophiles. This would have enabled the incorporation of carboranes into aromatic poly(etherketones) through direct ether linking units. These compounds have been studied in

the present work (see Chapters 5 and 6), although the findings outlined in Section 3.3.3 discouraged us from carrying out a detailed investigation into their use as monomers.

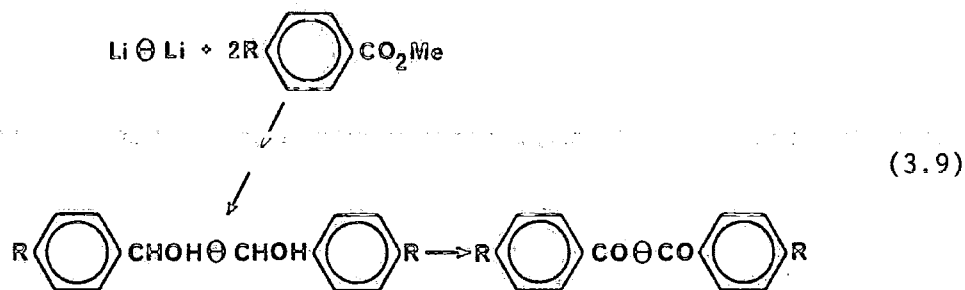
The present study has concentrated on derivatives of ortho carborane. However, the reactivity of the meta and para carborane cages towards strong nucleophiles^{20,21} also, suggests that the nucleophilic route would once again be ineffective for the incorporation of these isomers into aromatic poly(etherketones).

The electrophilic model reactions however, show firstly that despite the electron withdrawing nature of the cage, 1-(4-phenoxyphenyl)-carborane derivatives are reactive enough to be readily acylated in TFSA. Secondly they show that although 1-(4-carboxyphenyl)-carborane derivatives are deactivated as acylating agents (again because of the influence of the cage) they are nevertheless reactive enough to undergo condensation with aromatic ethers. These observations lead us to concentrate on the electrophilic route for the synthesis of aromatic poly(carboranyletherketones).

3.3.5.2 The choice of linkage used for carborane incorporation

In principle the cage could be incorporated into the poly(etherketone) backbone through direct ether linkages, direct ketone linkages or using substituted diaryl carborane derivatives (through a C-C linkage). The use of the ether linkage is not feasible at present as indicated in the preceding section. The ketone link could in principle be used by employing suitably substituted dibenzoyl derivatives in electrophilic polymerisations. These could be prepared by the action of benzoate esters on dilithio carborane

derivatives, followed by subsequent oxidation of the resultant tertiary alcohol²² (equation 3.9).



Since the cage is electronwithdrawing however, the carbonyl to cage link is reactive towards nucleophiles. Hence carboranyl ketones are readily cleaved with alkali for instance^{23,24}, giving the free carborane and the corresponding benzoic acid derivative. It seems unlikely therefore that the carboranyl ketone link would favourably enhance the chemical and thermal properties of aromatic poly(etherketones).

The C-C bond between the cage and aryl substituents is very thermally stable and chemically inert. Also as indicated before, diarylcarborane derivatives can be conveniently prepared from the corresponding diaryl acetylenes. This has resulted in the monomers prepared all consisting of substituted diaryl ortho-carborane derivatives for use in electrophilic polymerisations.

3.4 Monomer synthesis

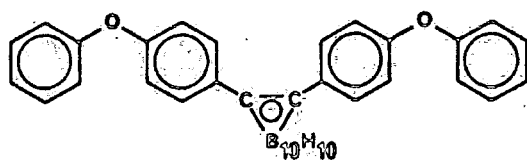
3.4.1 Target molecules and synthesis strategy

On the basis of the conclusions made in Section 3.3, the following compounds were singled out as potential monomers for electrophilic polycondensation in TFSA:

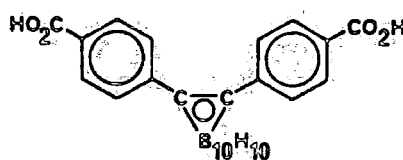
1,2-bis(4-phenoxyphenyl)-ortho-carborane (XX),

1,2-bis(4-carboxyphenyl)-ortho-carborane (XVIII) and

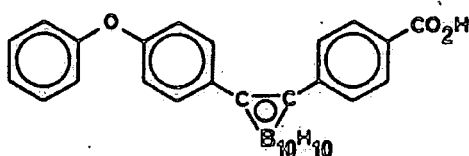
1-(4-carboxyphenyl)-2-(4-phenoxyphenyl)-ortho-carborane (XXI)



(XX)



(XVIII)

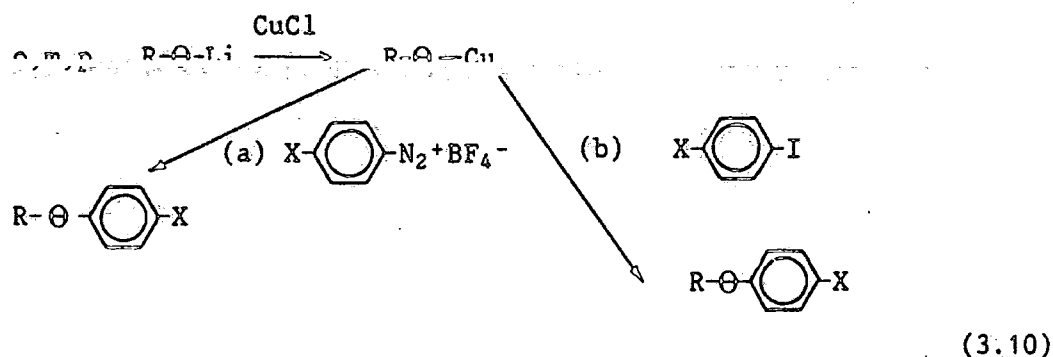


(XXI)

Compounds (XX) and (XVIII) have been prepared during this study, however attempts to prepare the final mono-acid (XXI) have not proved successful as yet. The preparation of the 1-(4-carboxyphenyl)-2-phenyl-ortho-carborane (XVI) will also be discussed in this section.

The syntheses of all these compounds have involved reacting the corresponding acetylenes with decaborane in the presence of a Lewis base. As mentioned in Section 2.2.1, decaborane is degraded by the carboxyl group and so carboxylic acids have to be synthesised by generating the carboxyl group after the cage has been formed. Alternative syntheses of diaryl carboranes through

direct functionalisation of the preformed cage have been reported. These involve the reaction of carboranyl copper reagents with (a) aryl diazonium tetrafluoroborates²⁵ and (b) aryl iodides²⁶ (equation 3.10)



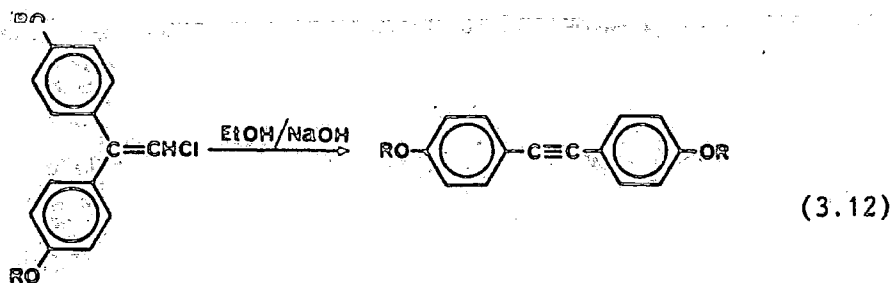
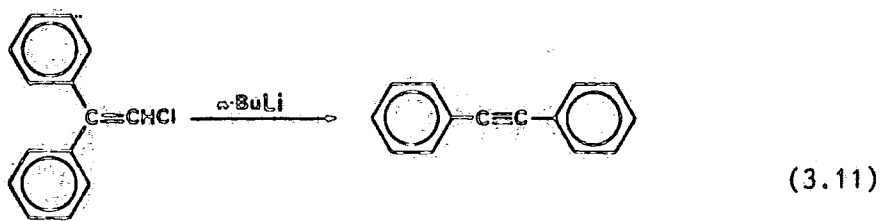
These methods however have not been widely employed for the preparation of aryl carborane derivatives. Also attempts during the present study to prepare aryl meta carborane derivatives via route (b) have not been successful.

3.4.1.1. Preparation of diaryl acetylenes

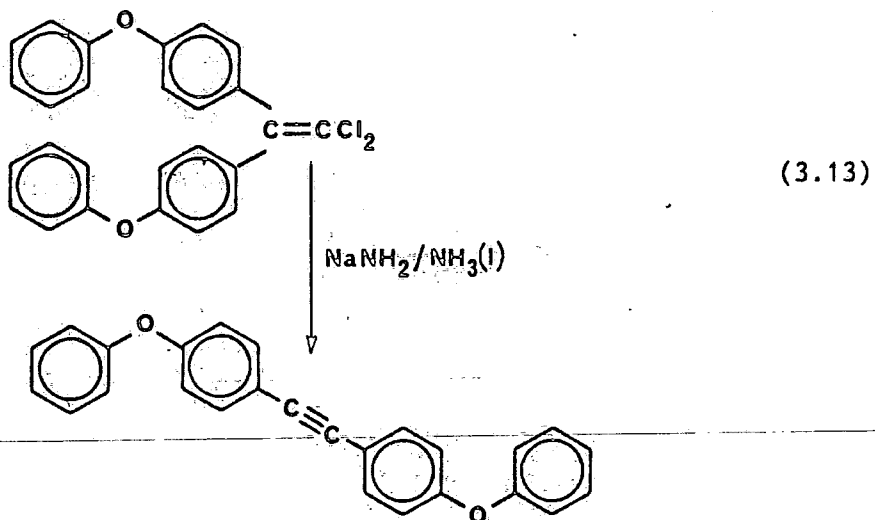
Diaryl acetylenes may be prepared in a variety of ways and these may be divided into two classes: (i) Elimination reactions to generate the acetylene group. (ii) Coupling reactions between aryl substrates and the preformed acetylene group.

i) Elimination reactions

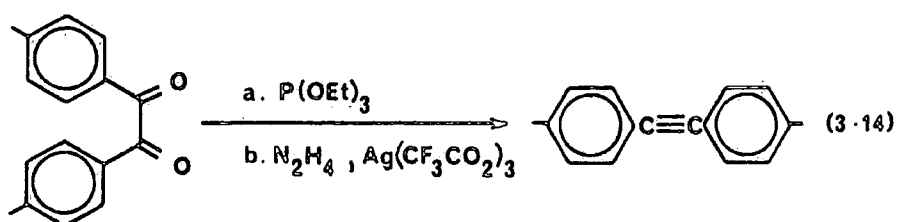
Dehydrohalogenation can be used to prepare diaryl acetylenes. For instance, brominated stilbenes are converted to the corresponding acetylene by the action of strong base²⁷. Also treatment of 1,1 diaryl haloethenes with various bases, producing dehydrohalogenation and aryl group migration, have also been employed. (Equations 3.11 and 3.12)^{28,29}.



A preparation of the acetylene precursor to (XX) has been reported using a similar route³⁰, (equation 3.13).

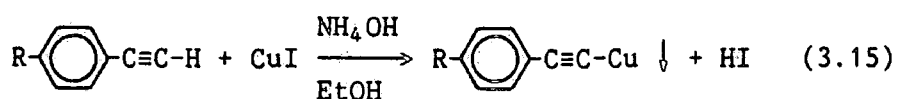


Elimination of oxygen from diarylethanedione derivatives (benzils) by treatment with either (a) triethylphosphate³¹ or (b) reaction with hydrazine, followed by oxidation of the resultant dihydrazone with silver trifluoroacetate³², also gives diarylacetylenes in reasonable yields (equation (3.14)).

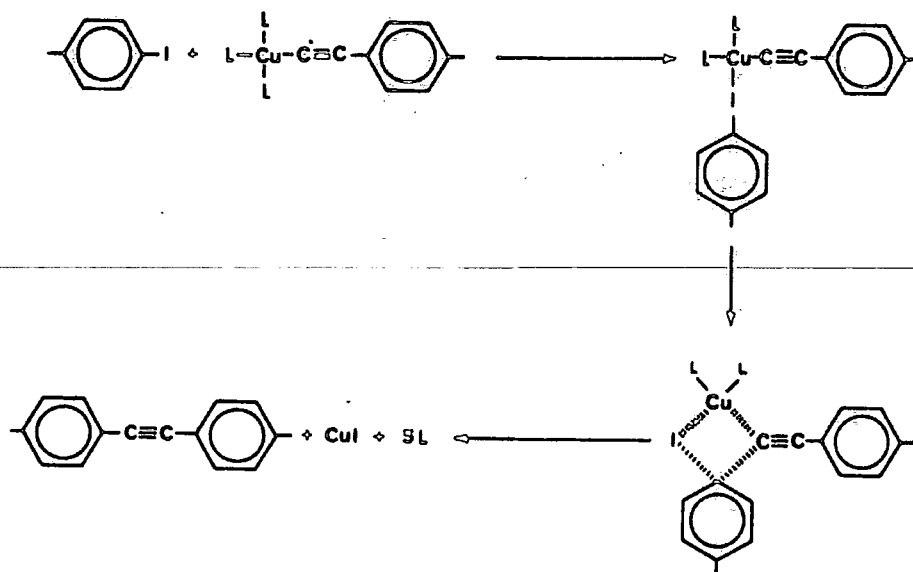


b) Coupling reactions

Diaryl acetylenes are conveniently prepared by the reaction between aryl ethynyl copper derivatives and aryl iodides in pyridine under an inert atmosphere (Scheme 6)³³. The aryl ethynyl copper precursors are readily synthesised by the reaction of monoaryl acetylenes in ethanol, with aqueous ammoniacal cuprous iodide (Equation 3.15)³⁴. (See Section 3.5.7(ii)) or by the action of cuprous tert. butoxide on acetylenes in the THF³⁵.

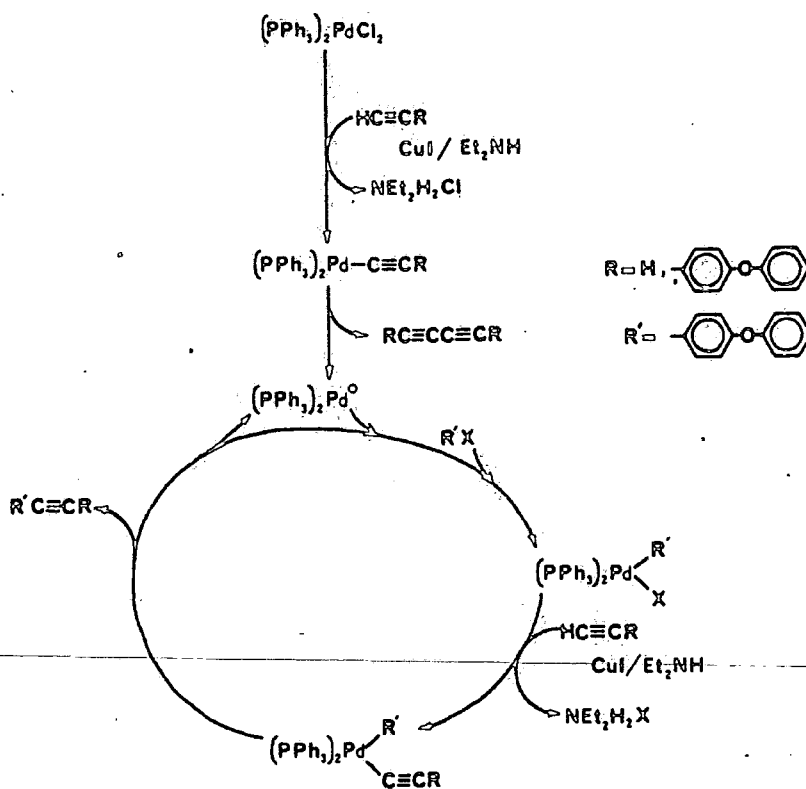


Scheme 6



Direct arylation of unsubstituted acetylenes by aryl iodides can also be achieved, in the presence of palladium catalysts and cuprous iodide^{36,37}. Indeed free acetylene is readily converted to symmetrically substituted diaryl derivatives by reaction with aryl iodides, catalysed by bis(triphenylphosphine) palladium dichloride and cuprous iodide in diethylamine³⁸ (the proposed mechanism for this reaction is given in Scheme 7).

Scheme 7



Owing to the availability or ease of preparation of precursors for these coupling reactions, and due to the improved yields attainable by these routes, all syntheses of diaryl acetylenes carried out in this study have used these methods as opposed to the elimination reactions described before.

3.4.2 Summary of the syntheses carried out

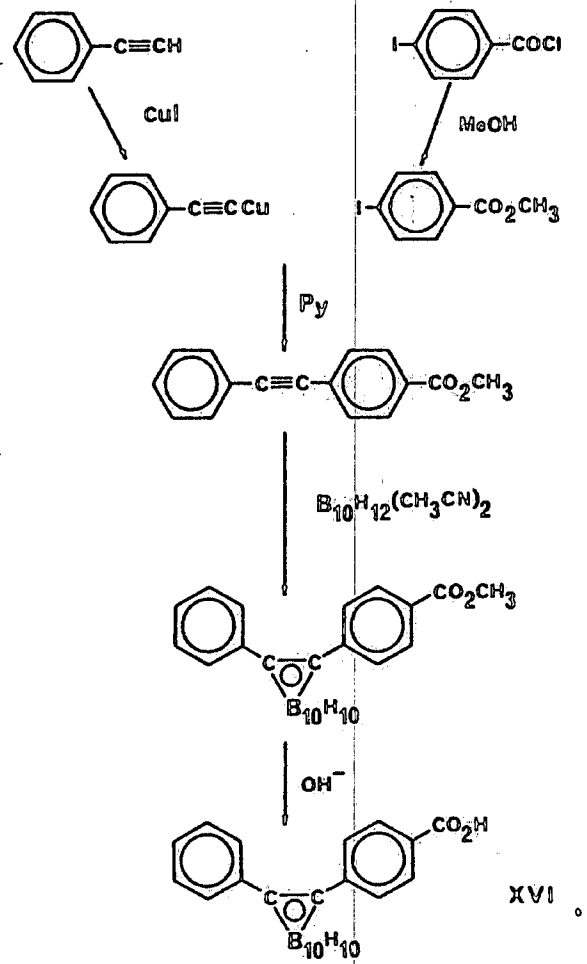
The routes used in this study to prepare compounds (XVI), (XVIII) and (XX), from commercially available materials, are summarised in Schemes 8, 9 and 10. Full details of the reactions shown are given in the Experimental Section (3.5).

Attempts to prepare the ether-acid monomer (XXI), involved the syntheses of three previously uncharacterised ortho carborane derivatives 1,4-(methylcarboxy)phenyl-2-(4-phenoxyphenyl)-ortho-carborane (XXII), 1-(4-methylphenyl)-2-(4-phenoxyphenyl)-ortho-carborane (XXIII) and 1-(4-bromophenyl)-2-(4-phenoxyphenyl)-ortho-carborane (XXIV).

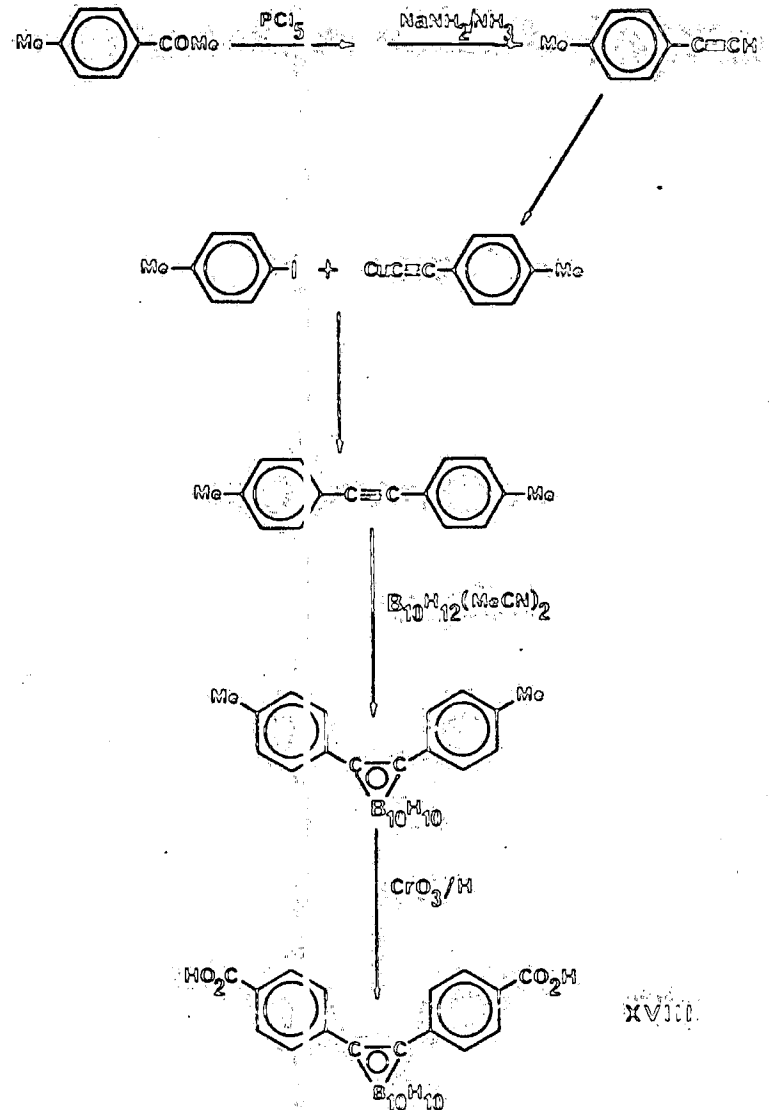
The syntheses of these compounds are summarised in Schemes 11-13 with full details presented in Sections 3.5.10 to 3.5.12.

Attempts to hydrolyse the ester (XXII) under identical conditions to those used in the preparation of the mono-acid (XVI) (see Section 3.5.7 (iv)) failed to produce the desired carboxylic, the unchanged ester being recovered in each case (addition of dioxane or methanol to increase solvation of the reactant had no effect on the reaction). Hydrolysis under acid conditions (50%

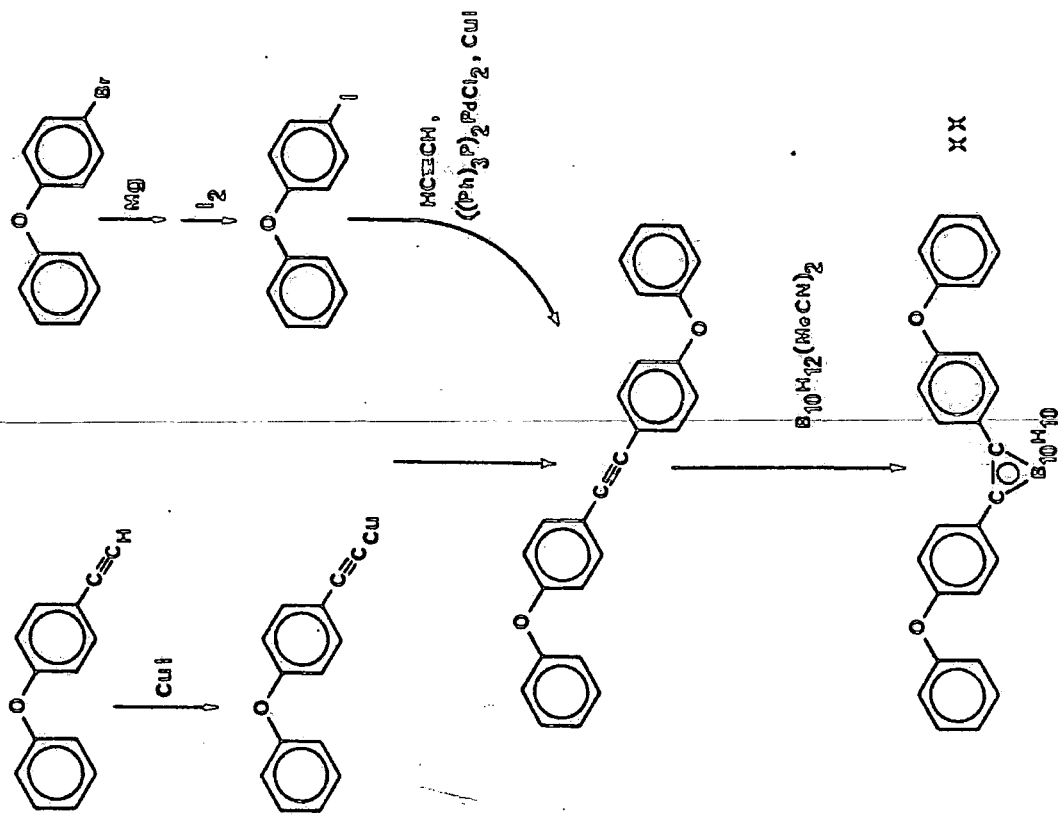
Scheme 8



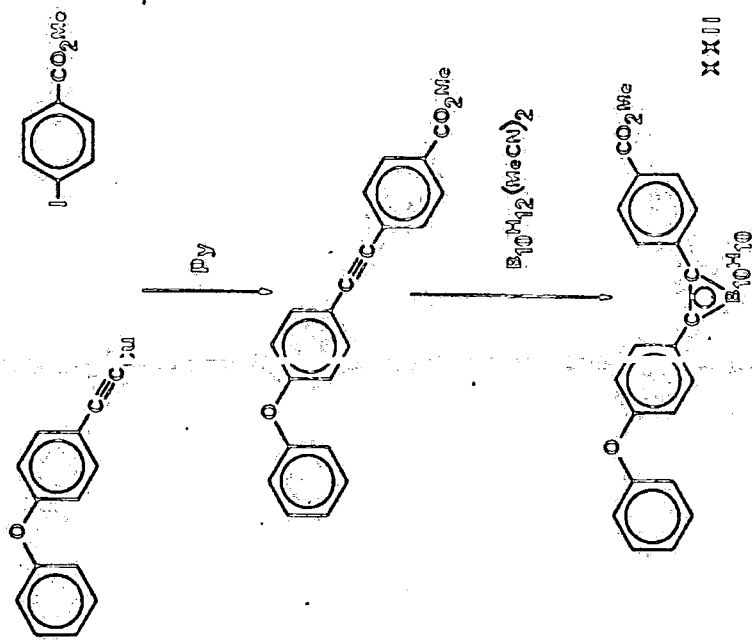
Scheme 9



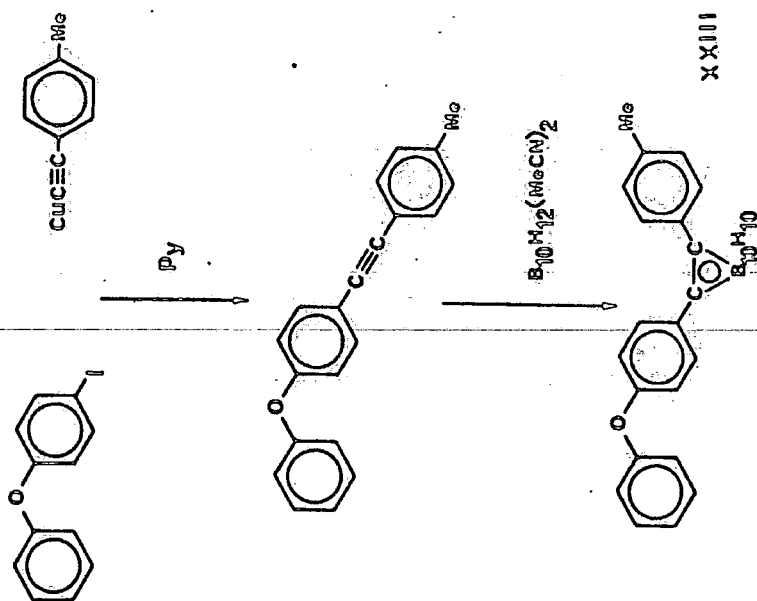
Scheme 10



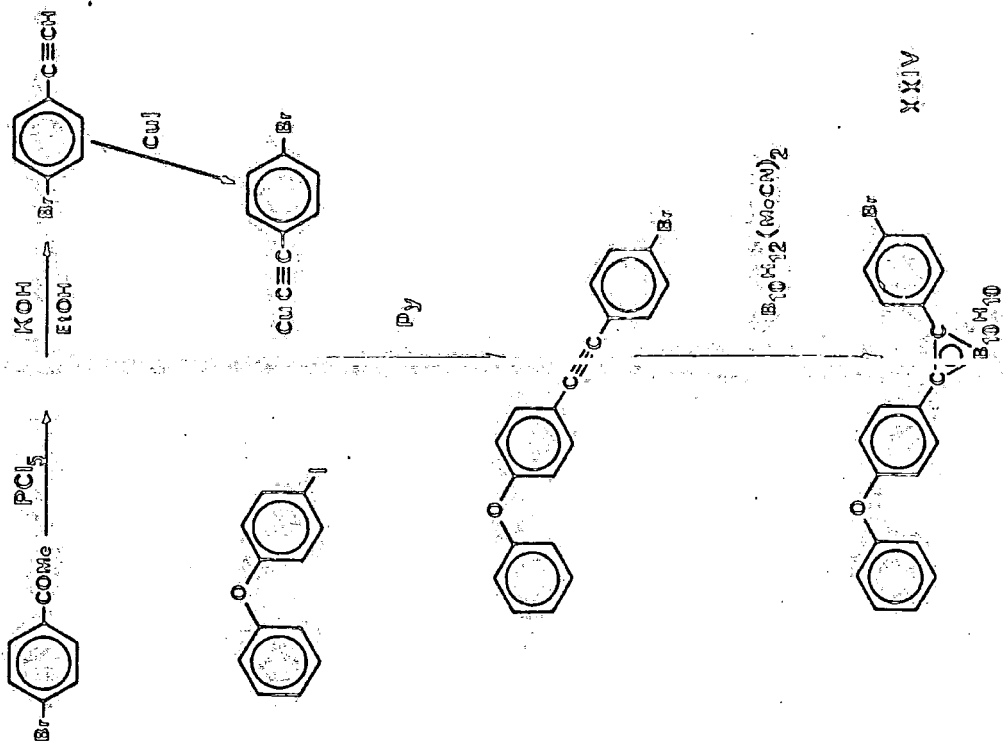
Scheme 11



Scheme 12



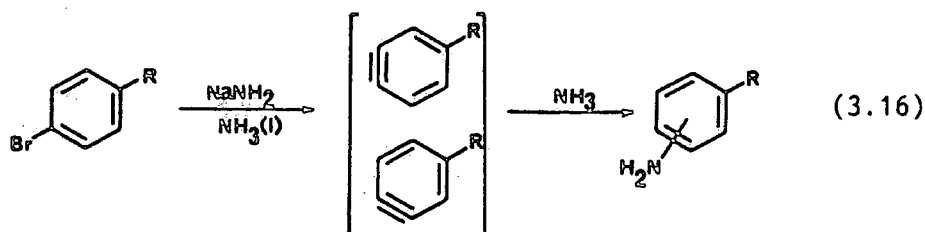
Scheme 13



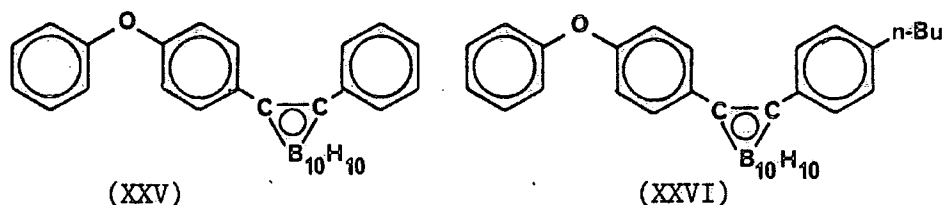
H_2SO_4 , dioxane 100°C) was also unsuccessful, the unchanged ester being recovered again.

The 4-methylphenyl derivative (XXIII) was seen as a particularly useful precursor since its likely thermal stability would have permitted its thermal isomerisation to the meta isomer, thus providing a route into the corresponding meta-carborane monomer. Exposing (XXIII) to the same oxidising conditions as used in the preparation of the diacid (XVIII) showed evidence for the oxidation reaction occurring (reaction mixtures turning green indicating the presence of chromium (III) residues). None of the acid (XXI) could be isolated from the reaction mixture either by filtration or ether extraction. It should be noted here that in some cases the cage is susceptible to oxidation by chromic acid, giving water soluble B-hydroxy compounds³⁹. Hence it is possible that the cage in (XXIII) is not able to withstand the conditions used (see Section 3.5.8(v)).

The preparation of bromide (XXIV) required the prior synthesis of 4-bromophenyl-acetylene. This was prepared from the acetophenone derivative by chlorination followed by dehydrochlorination. The dehydrochlorination step was carried out using ethanolic potassium hydroxide. This is because sodium amide in liquid ammonia will dehydrobrominate aryl bromides to give benzyne intermediates which react non specifically with ammonia producing 3 and 4 substituted aniline derivatives (equation 3.16).



Subsequent attempts to convert (XXIV) to the acid (XXI) by metallation of the bromide followed by carboxylation, have not been successful to date. The bromide was found to be unreactive towards magnesium, possibly due to the para electron withdrawing carborane substituent which might be expected to deactivate the bromide towards this metallation. The action of n-butyl-lithium followed by freshly sublimed dry ice failed to give (XXI). Analysis of the reaction mixtures produced (I.R. and Mass Spectrometry) showed the hydrolysis product (XXV) and the alkylation product (XXVI) to be the only carborane containing species present.



The routes explored to the mono acid (XXI) not being effective could be a reflection of the limitations imposed by the presence of the carborane cage. These would include the reactivity of the cage to base which has implications for the conditions used for base hydrolysis of esters, the inductive effect of the cage and solubility (particularly where aqueous conditions are being used). The work carried out in this present study should not be regarded as exhaustive however. For instance the hydrolysis of other esters under a variety of other non basic conditions remain to be tried⁴⁰. In addition, the transition metal phase transfer catalysed carbonylation of aryl bromides has been developed as a versatile route to carboxylic acids⁴¹ and may be effective in converting (XXIV) into (XXI).

3.5 Experimental Section

3.5.1 The reaction between sodium phenoxide and 4,4' difluorobenzophenone : Preparation of 4,4' benzophenone (XII)

Sodium phenoxide* (1.27 g, 10.95 mmoles) was slurried with 10 mls of freshly distilled DMA under nitrogen (the phenoxide appeared to be slightly soluble). 4,4' difluorobenzophenone (1.19 g, 5.45 mmoles) dissolved in 20 mls of DMA was added to the stirring phenoxide suspension producing a pale yellow, cloudy solution. The mixture was heated under nitrogen with stirring, at 175°C for 8 hours affording a pale yellow solution and a white precipitate. The mixture was cooled, filtered and the resultant solution was poured in 100 mls of distilled water producing a white precipitate (the solid residue from the filtration was washed with acetone, dried and identified (elemental analysis) as sodium fluoride (0.454 g, 10.81 mmoles, 98.7% of theory)). The aqueous suspension was extracted three times with toluene. The toluene extracts were combined, washed three times each with 10% sodium hydroxide and distilled water, dried over anhydrous magnesium sulphate and filtered. The resulting colourless toluene solution was concentrated under vacuum and chilled (-30°C) affording a white powder identified as 4,4' diphenoxybenzophenone. Yield 3.08 g (8.42 mmoles) 77%, melting point 143-144°C. Characterised as follows:

Analysis Found: C, 82.2; H, 4.7%. $C_{25}H_{18}O_3$ Requires: C, 82.0; H, 4.9%.

Infra Red (Nujol) (cm^{-1}): 3027 (w) 3017 (w) (Aromatic C-H stretch); 3000-2760 (s) (Nujol); 1639 (s) (C=O stretch); 1587 (s); 1496 (w.sh); 1485 (w); 1450 (Nujol); 1410 (w); 1373 (Nujol); 1310 (m); 1288; 1261 (s) (C-O-C stretch); 1197 (w); 1163 (m); 1149 (m); 1112; 1071; 1021; 960 (w); 935; 900; 872; 854 (s); 841 (s); 823 (sh); 796 (m); 763 (s); 747 (s); ; 692 (m); 679 (m); 625

(w); 582 (w); 502; 488.

- * Sodium phenoxide was prepared by adding phenol to an equimolar amount of sodium methoxide in methanol, followed by removal of methanol under vacuum. The phenoxide was handled in a glove box.

3.5.2 The reaction between sodium phenoxide and 1-(4-fluorophenyl)-ortho-carborane: Preparation of tetramethylammonium 1-(4-fluorophenyl)-1,2 dicarbaundecaborate (XIII)

1-(4-fluorophenyl)-ortho-carborane (0.41 g, 1.74 mmoles) dissolved in 15 mls of DMA was added to a suspension of sodium phenoxide (0.198 g, 1.74 mmoles) in DMA (10 mls) under dry nitrogen, producing a pale yellow solution. The mixture was heated with stirring for 7 hours at 175°C, cooled and poured into 100 mls of distilled water. The solution was acidified with a few drops of dilute HCl and extracted three times with ether. The ether extracts were combined, washed three times each with dilute sodium hydroxide (no phenol was detected upon acidification of the sodium hydroxide washings) and distilled water and dried over anhydrous magnesium sulphate. The solution was then filtered and the solvent removed under reduced pressure leaving an off white solid. The residue showed no movement on a silica gel plate eluted with dichloromethane (Rf values : 1-(4-fluorophenyl)ortho-carborane = 1-(4-phenoxyphenyl)-ortho-carborane = 0.67, phenol = 0.30 - all species run on the same plate). The solid was dissolved in hot distilled water and filtered. Tetramethylammonium bromide (0.3 g, 19.5 mmoles) dissolved in distilled water was added to the solution affording a thick white precipitate. This was filtered off, washed with fresh distilled water and recrystallised from ethanol/water producing colourless crystals identified as tetramethylammonium 1-(4-fluorophenyl)-1,2-

dicarbaundecaborate.

Yield 0.23 g (7.64 mmoles), 44%. Melting point: decomposed 325-330°C, (lit (13) - decomposes at 330°C). Characterised as follows :

Analysis: Found: C, 47.9; H, 9.5; B, 31.0; N, 4.4%

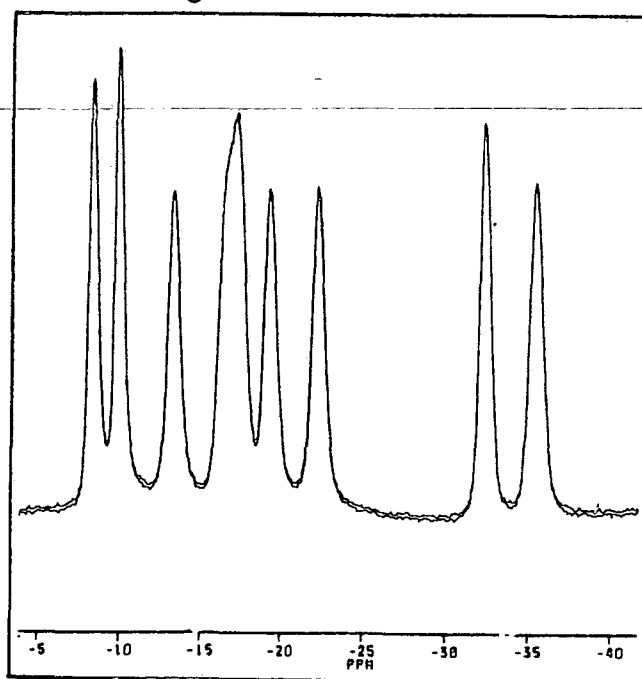
$C_{12}H_{27}B_9NF$. Requires: C, 47.8; H, 9.0; B, 32.3; N, 4.6; F, 6.3%

Infra Red (Nujol) (cm^{-1}): 3040 (w.sh) (Aromatic CH stretch); 2517 (s) (BH stretch); 1590 (w) (C=C stretch); 1507 (sh); 1500 (sh); 1477 (s.sh); 1227 (m); 1217 (m); 1158 (m); 1095 (w); 1070; 1026; 1014; 980 (w); 950 (s); 884 (w); 850 (sh); 832; 809; 720; 527 (w); 497 (w); 474 (w);

^{19}F NMR: 235.3412 MHz, solvent THF, referenced externally to $CFCl_3$ at 0.00 ppm: (ppm) -120.61 (s)

^{11}B NMR: { 1H broadband noise} 80.239 MHz, solvent D_6 acetone, referenced externally to $BF_3 \cdot Et_2O$ at 0.00 ppm. See figure 3.3. From the symmetry considerations the ^{11}B spectrum is expected to show nine resonances each one corresponding to one boron atom of the cage. The spectrum shows eight in reality, the resonance at -17.34 ppm is a coincidental combination of resonances of two inequivalent nuclei. (c.f. data for the carborane parent section 2.4.6).

Figure 3.3



Mass Spectrum (E.I) The compound was not sufficiently volatile in solid form to give a satisfactory mass spectrum, A THF solution of the salt showed a strong molecular ion peak with the characteristic carborane isotope distribution pattern between m/e 220 and 228 (base peak at m/e 226) corresponding to the E.I. fragment of the $F-C_6H_4-C_2B_9H_{11}$ species.

3.5.3 Reaction of sodium phenoxide with 1,2-diphenyl-ortho-carborane. Preparation of triethylammonium 1,2-diphenyl-1,2-dicarbaundecaborate (XIV)

1,2-diphenyl-ortho-carborane (prepared as in Section 2.4) (2.17 gm, 7.33 mmoles) dissolved in DMA (20 mls) was added to a suspension of sodium phenoxide (0.85 g, 7.33 mmoles) under nitrogen, producing an orange solution. The solution was stirred at room temperature under nitrogen for 48 hours and then poured into 100 mls of distilled water producing a pale yellow precipitate. The aqueous suspension was washed three times with diethyl ether and the ether washings combined, washed with 10% aqueous sodium hydroxide and water and dried over anhydrous magnesium sulphate. The solution was filtered and the solvent removed under reduced pressure leaving a solid residue. This was extracted with boiling hexane resulting in solvation of part of the residue. The hexane solution was filtered off, concentrated in vacuo producing a sticky white solid which after repeated recrystallisation from fresh hexane affording colourless crystals identified as 1,2-diphenyl-ortho-carborane (0.36 g, 1.22 mmoles).

The residue remaining from the hexane extraction was taken up in boiling distilled water and the solution filtered. Tetramethylammonium bromide (1.20 g, 7.8 mmoles) in distilled water was added to the aqueous extract affording a thick

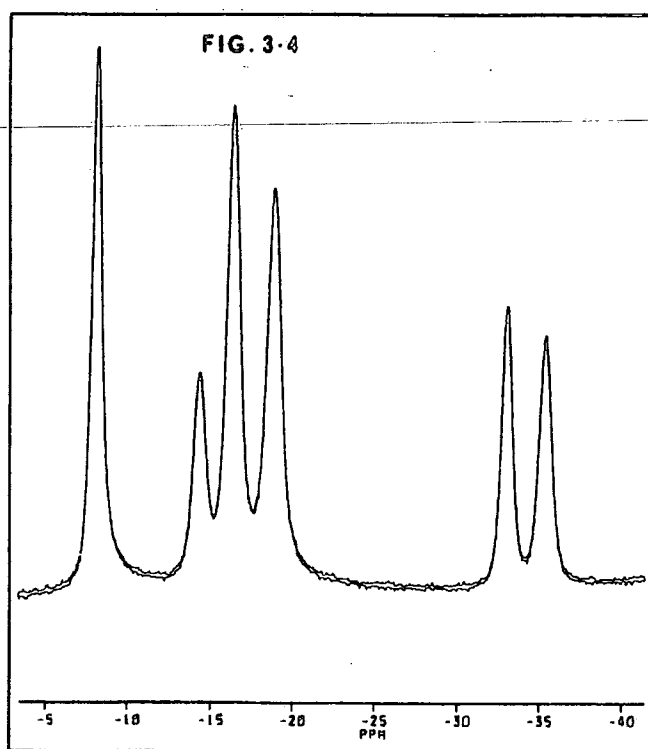
white precipitate which was filtered off and washed with distilled water. Attempts to recrystallise the solid from acetone/water were not successful, the solid was recrystallised from ethanol/water producing colourless crystals identified as tetramethylammonium 1,2-diphenyl-1,2-dicarbaundecaborate, yield 0.48 gm, (1.33 mmoles), 18.2%.

Melting point: decomposed 300°-304°C. Characterised as follows:

Analysis Found: C, 57.5; H, 9.3; B, 27.5; N, 3.4%. $C_{18}H_{32}B_9N$
Requires: C, 60.2; H, 8.9; B, 27.1; N, 3.9%.

Infra Red (Nujol) (cm^{-1}): 3070 (w.sh) 3050 (w.sh) 3008 (w) (Aromatic C-H stretch); 3000-2760 (s) (Nujol); 2580 (sh) .2510 (vs) (B-H stretch); 1595; 1572 (w); 1480 (vs); 1460 (sh); 1442 (s); 1414 (w); 1375 (m); 1365 (sh); 1310 (w); 1280 (w); 1255 (w); 1770 (w); 1067 (m); 1030 (w.sh); 1020; 950 (s); 890 (w); 764 (s); 720 (w); 697 (s); 475 (w).

^{11}B NMR 80.239 MHz, solvent D_6 acetone, referenced externally to $BF_3 \cdot Et_2O$ at 0.00 ppm. See figure 3.4 The spectrum is expected to show three resonances of integral 2B and three of integral 1B since the anion has three equivalent pairs of boron atoms and three unique atoms. This is seen (c.f. data for the carborane parent section 2.4.5).



Mass Spectrum The main feature was a cluster of peaks between m/e 278-287 with the characteristic carborane isotope pattern corresponding to the E.I. fragment of the $\text{PH}_2\text{C}_2\text{B}_9\text{H}_{10}^-$ species. Also observed weak peaks at m/e 69 (Me_3N^+) and below due to fragmentation of the Me_4N cation and traces of solvent.

3.5.4 The reaction between 1-(4-phenoxyphenyl)-ortho-carborane and benzoic acid : Preparation of 1-(4-benzoyl-4-phenoxyphenyl)-ortho-carborane (XV)

TFSA (5 mls) was added to a mixture of 1-(4-phenoxyphenyl)-ortho-carborane (0.385 g, 1.23 mmoles) and benzoic acid (0.151 g, 1.24 mmoles) under nitrogen. The mixture was stirred at room temperature under nitrogen until all the carborane derivative had dissolved producing an orange solution. This solution was allowed to stand for 12 hours and was then poured into 30 mls of distilled water affording a white precipitate which was filtered off, washed on the frit with 10% aqueous sodium hydroxide and distilled water and dried under vacuum. The dried product was recrystallised from hexane/acetone giving colourless crystals identified as (XV).

Yield: 0.499 (11.99 mmoles), 97%. Melting point 138-140°C.

Characterised as follows:

Analysis: Found, C, 60.3; H, 5.9; B, 26.0%. $\text{C}_{21}\text{H}_{24}\text{B}_{10}\text{O}_2$

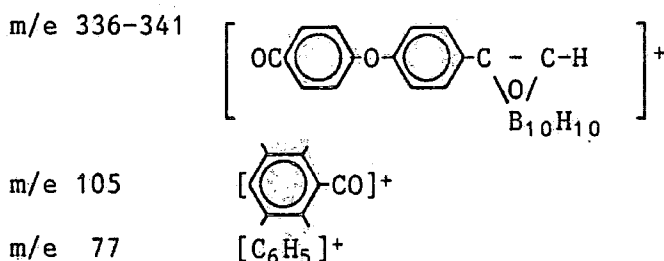
Requires: C, 60.6; H, 5.7; B, 26.0%.

Infra Red (Nujol) (cm^{-1}): 3055 (m) (Carboranyl C-H stretch); 3000-2750 (s) (Nujol); 2565 (s.br) (B-H stretch); 1642 (C=O stretch), 1610 (w.sh), 1587 (m), 1575 (sh); 1490; 1445; 1412 (w); 1373; 1315 (w.sh); 1308 (m); 1278 (s); 1240 (s) (C-O-C stretch); 1200 (sh); 1175 (sh); 1170 (m); 1148; 1115 (w); 1072 (m); 1019 (w); 1002 (w); 972 (w); 952 (w); 938 (m); 925 (s); 885 (m); 857; 847 (s); 795; 740 (s); 720 (sh); 705 (s);

680 (w.sh); 632; 617; 595; 560 (w); 510 (m).

^{13}C NMR { ^1H broad band noise} 62.896 MHz, solvent CDCl_3 .
Referenced externally to TMS at 0.00 ppm, see figure 3.1.
(section 3.3.4).

Mass Spectrum A highest mass peak was observed at m/e 418
(very weak M+1 and M+2 peaks were seen due to the presence of
the ^{13}C isotope) corresponding to the species
 $^{12}\text{C}_{21}^{1}\text{H}_{24}^{11}\text{B}_{10}^{16}\text{O}_2$ accompanied by the usual isotope pattern
between m/e 413-418. Other intense fragments observed:



3.5.5 The reaction between 1-(4-carboxyphenyl)-2-(phenyl)-ortho-carborane (XVI) and anisole: Preparation of 1-(4'-methoxy-4-benzophenyl)-2-(phenyl)-ortho-carborane (XVII)

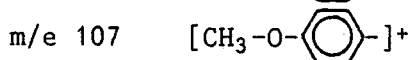
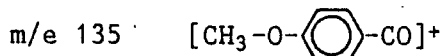
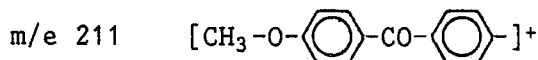
TFSA (1.0 mls) was added to a mixture of (XVI) (0.34 g, 1.00 mmoles) and anisole (0.108 g, 1.00 mmoles) under nitrogen. The mixture was stirred until all the carborane reactant had dissolved producing a yellow solution which was left to stand under nitrogen for 18 hours. The resulting red solution was then poured into distilled water producing a white precipitate. The suspension was extracted three times with diethyl ether, the ether extracts combined, washed three times each with 10% sodium hydroxide and water and dried over anhydrous magnesium sulphate. The solution was then filtered and the solvent removed under reduced pressure leaving an off white solid which was recrystallised twice from hexane affording colourless crystals identified as (XVII). Yield 0.34 g (0.79 mmoles) 79%. Melting point 160-163°C. Characterised as follows:

Analysis Found: C, 61.3; H, 5.9; B, 25.0%, $C_{22}H_{26}B_{10}O_2$.

Requires: C, 61.4; H, 6.1; B, 25.1%.

Infra Red (Nujol) (cm^{-1}): 3015 (w.sh) Aromatic (C-H stretch); 3000-2750 (s) (Nujol); 2650 (sh) 2620 (w) 2580 (s) 2520 (w) (B-H stretch); 1650 (C=O stretch); 1598 (s); 1567 (w); 1500 (w); 1586 (w); 1455 (s) (Nujol); 1416 (w); 1402; 1372 (Nujol); 1312; 1300 (m); 1287 (m); 1277 (s); 1257 (s) (C-O-C stretch); 1170 (s); 1160 (w); 1145 (m); 1104 (w); 1068; 1030; 1000 (w); 970 (w); 945 (w); 925 (m); 890; 868; 852 (m); 838; 810 (w); 794 (w); 776; 760; 725; 687 (m); 667; 638 (w); 620 (w); 600; 582 (w); 550 (w); 510 (w); 470 (w).

Mass Spectrum A highest mass peak at m/e 432 was observed corresponding to the species $^{12}C_{12}^{1}H_{26}^{11}B_{10}^{16}O_2$ accompanied by the usual isotope distribution pattern between m/e 428 and 432. Other intense fragments observed:



3.5.6 The reaction between 1,2 bis(4-carboxyphenyl)-ortho-carborane (XIX) and anisole: Preparation of 1,2 bis-(4-methoxy-4-benzophenyl)-ortho-carborane (XIX)

T.F.S.A. (10 mls) was added to a mixture of (XVIII) (0.28 g, 0.73 mmoles) and anisole (0.16 g, 1.48 mmoles) under nitrogen producing an orange solution. This was left to stand for 48 hours, turning dark orange and was then poured into distilled water producing an off white solid which was filtered off, washed with fresh distilled water and then refluxed for one hour with further distilled water, filtered, dried under vacuum and recrystallised from hexane/acetone affording off white crystals identified as (XIX). Yield 0.24 g (0.43 mmoles) 58.9%. Melting point: 168-170°C. Characterised as follows:

Analysis Found: C, 63.3; H, 5.7; B, 19.1%, $C_{30}H_{32}B_{10}O_4$.

Requires: C, 63.8; H, 5.7; B, 19.1%.

Infra Red (Nujol) (cm^{-1}): 3100 (w) 3005 (w.sh) (Aromatic C-H Stretch): 3000-2750 (s) (Nujol); 2680 (w) 2580 (s) (B-H stretch): 1647 (s) (C=O stretch): 1598 (s); 1510; 1461 (m); 1442; 1422; 1405; 1380; 1330 (sh); 1320 (m); 1302 (m); 1292 (m); 1286 (w); 1267 (s) (C-O-C stretch); 1187 (w); 1180 (s); 1158 (s); 1130 (w.sh); 1120; 1078; 1036 (s); 1010 (w); 980 (w); 967 (w); 937 (s); 897 (m); 876; 860 (s); 850 (s); 840 (s); 815 (w); 803 (w); 799 (w.sh); 770 (s); 740 (w); 730 (w); 707 (w); 690 (m); 678 (w.sh); 650; 626 (w); 605; 590; 565; 518; 500 (w); 465.

^{13}C NMR { 1H broad band noise} 62.896 MHz, solvent $CDCl_3$. Referenced externally to TMS at 0.00 ppm, see figure 3.2 (section 3.3.4)

Mass Spectrum A highest mass peak was observed at m/e 566 corresponding to the species $^{12}C_{30}^{1}H_{32}^{11}B_{10}^{16}O_4$ with the characteristic isotope distribution pattern between m/e 561 and 566.

3.5.7 Preparation of 1-(4-carboxyphenyl)-2-phenyl-ortho-carborane (XVI) (see Scheme 8)

i) The preparation of 4 iodo-methyl benzoate

4-Iodo-benzoyl chloride (21.75 g, 82.1 mmoles) was added to methanol (100 mls previously distilled and dried over A4 molecular sieve). The reactant temperature was moderated by immersing the reaction flask in an ice bath. On completing the addition of the chloride, the reactants were heated under reflux for two hours, cooled and poured into 500 mls of distilled water. The suspension was extracted three times with diethyl ether, the ether extracts combined, washed three times with dilute sodium bicarbonate solution and dried over

anhydrous magnesium sulphate. The ether solution was filtered, concentrated under reduced pressure and left to stand affording off-white crystals identified as 4-iodo-methylbenzoate. Yield 15.47 g (59 mmoles) 71.9%. Melting point 114°C (lit 114°C). Characterised as follows:

Analysis: Found C, 37.4; H, 2.4; I, 49.1%; $C_8H_7O_2I$.

Requires: C, 36.8; H, 2.7; I, 48.7.

Infra Red: (Nujol) (cm^{-1}): 300-2750 (s) Nujol; 1695 (s) (C=O stretch); 1578 (m); 1432; 1388; 1370 (sh); 1360 (sh); 1320 (sh); 1280 (s); 1268 (s) (C-C(=O)-O and O-C-C asymm. stretch); 1240 (sh); 1193 (m); 1177 (m); 1113 (s); 1105 (s); 1084 (sh); 1055 (sh); 1005 (s); 956 (w); 842 (m); 823; 753 (s); 720 (sh); 680 (w); 490 (w); 459 (w).

ii) Preparation of phenyl ethynyl copper

Cuprous iodide (17.20 g, 90.3 mmoles) dissolved in concentrated aqueous ammonia solution (0.88 M), was added dropwise to a mechanically stirred solution of phenyl acetylene (9.21 g, 90.3 mmoles) in ethanol (500 mls) producing a very heavy yellow precipitate (appears green due to the blue colour of the solution). The mixture was then stirred for one hour after which time the reactants were filtered leaving the solid copper derivative which was thoroughly washed five times each with water, ethanol and diethyl ether. The solid was dried for three hours under vacuum producing a fine, bright infusible yellow powder identified as phenyl ethynyl copper. Yield 10.1 g (61.4 mmoles) 68%.

Characterised as follows:

Analysis Found C, 58.1; H 3.1%, C_8H_5Cu . Requires: C, 58.3; H, 3.2; Cu, 38.6%.

Infra Red (KBr disc) (cm^{-1}): 3023 (w) (Aromatic C-H

stretch); 1070 (w); 1028 (w); 920 (sh); 907 (w); 750 (s); 685 (s); 522 (m); 510 (sh); 317 (w); 285 (w).

iii) Preparation of 4-(carboxymethyl)-diphenylacetylene

4-iodo-methylbenzoate (7.96 g, 30.4 mmol) dissolved in freshly distilled pyridine (20 ml) was added to a suspension of phenyl ethynyl copper (5.00 g, 30.4 mmol) in pyridine (80 ml) under dry nitrogen. The mixture was refluxed for 18 hours under nitrogen producing a dark brown solution which was cooled and poured into 300 ml of distilled water. The suspension was extracted with diethyl ether. The ether extracts were combined and washed with distilled water until the resulting aqueous washings were colourless. The ether solution was then dried over anhydrous magnesium sulphate. The solution was filtered and the ether removed under reduced pressure leaving an amber solid which when recrystallised from methanol, gave amber plates identified as 4-(carboxymethyl)-diphenylacetylene. Yield 2.93 g (12.4 mmol), 40.8%. Melting point 114-116°C. Characterised as follows: Analysis: C, 81.6; H 5.0%. $C_{16}H_{12}O_2$ Requires C, 81.4; H, 5.1%.

Infra Red (Nujol) (cm^{-1}): 3020 (w.sh) (Aromatic C-H stretch); 3000-2750 (s) (Nujol); 2219 (m) ($C\equiv C$ stretch); 1705 (s) ($C=O$ stretch); 1600; 1480 (w,sh); 1450 (sh); 1438 (m); 1403 (w); 1373 (w); 1310 (m); 1278 (s) ($C-O$ stretch); 1255 (m.sh); 1193; 1177 (m); 1160 (w.sh); 1142; 1110 (s); 1070 (w.sh); 1081; 1010 (w); 998 (w); 961 (w); 925 (w); 862 (m); 860 (m); 818 (w); 772 (s); 764 (s); 755 (sh); 695 (s); 514 (m).

iv) Preparation of 1-4(methylcarboxy)-phenyl-2 phenyl
-ortho-carborane

4-(methylcarboxy)-diphenylacetylene (2.64 gm, 11.2 mmoles) dissolved in dry toluene (15 mls) was added to a suspension of bis(acetonitrile) decaborane (2.29 g, 11.3 mmoles) in toluene (35 mls) under nitrogen. The mixture was stirred and refluxed under nitrogen for 24 hours producing a red solution which was cooled. The solvents were removed in vacuo leaving a red low melting solid. This was stirred with 30 mls of dry methanol for 18 hours affording an orange solution and a white solid. The solid was filtered off and recrystallised from methanol producing colourless plates identified as 1-4-(carboxymethyl-phenyl)-2-phenyl-ortho-carborane. Yield 1.45 g (4.1 mmoles) 36.6%. Melting point 138-139°C. Characterised as follows: C, 54.3; H, 5.9; B, 29.8%. $C_{16}H_{22}B_{10}O_2$ Requires: C, 54.3; H, 6.2, B, 30.5%. Infra. Red (Nujol) (cm^{-1}); 3000-2750 (Nujol); 2620 (w); 2580 (s); 2560 (s) (B-H stretch); 1720 (s) (C=O stretch); 1605 (w.br); 1485 (sh); 1455 (sh); 1445 (m); 1430 (m); 1404 (w); 1372; 1310 (sh); 1295 (sh); 1282 (s) (C-O stretch); 1236 (w.sh); 1188 (m); 1117 (m); 1072; 1060 (sh); 1018 (w); 1003 (w); 963 (w); 930 (w); 890; 860; 827; 800 (w); 782 (m); 760 (m); 730 (m); 720 (w); 700; 690; 578; 495 (w).

v) Preparation of 1-(4-carboxyphenyl)-2-phenyl-ortho-
carborane (XVI)

1-(4-(carboxymethyl) phenyl)-2-phenyl-ortho-carborane (1.38 g, 3.9 mmoles) was ground to a fine powder and added to 50 mls of 10% aqueous sodium hydroxide. The mixture was stirred and heated at 100°C for 8 hours producing a slightly cloudy solution. This was cooled,

washed twice with diethyl ether and acidified with hydrochloric acid producing a thick white precipitate. The suspension was extracted with diethyl ether, the ether solution dried over anhydrous magnesium sulphate, filtered and the solvent removed under reduced pressure leaving a white solid which when recrystallised from acetone/water afforded colourless crystals identified as (XVI). Yield 1.04 g (3.06 mmoles), 78%. Melting point 278-280°C. Characterised as follows:

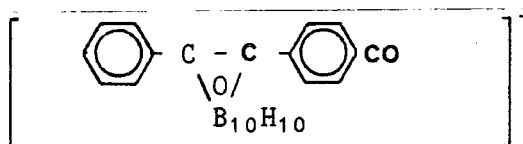
Analysis: Found: C, 52.6; H, 5.9; B, 31.5% $C_{15}H_{20}B_{10}O_2$.
Requires: C, 52.9; H, 5.9; B, 31.8%.

Infra Red: 3300-2300 (s.br) (O-H stretch); 2623 (w); 2590 (s); 2560 (s); (B-H stretch); 1687 (s) (C=O stretch); 1609 (C-C stretch); 1565 (w); 1485 (sh); 1446 (m); 1417 (s); 1372 (w); 1315 (w); 1283 (s) (C-O stretch); 1245 (sh); 1190; 1124; 1072 (m); 1020 (w); 1005 (w); 930 (m.br); 893 (m); 860 (m); 835 (w); 802; 782; 770; 764; 736; 726; 700 (s); 690 (s); 580 (m); 540 (m); 510 (w); 475.

Mass Spectrum. A highest mass peak was seen at m/e 343 corresponding to the M+1 peak of the species.

$^{12}C_{15}^{1}H_{20}^{11}B_{10}^{16}O_2$ (due to the presence of ^{13}C), accompanied by the characteristic carborane isotope distribution pattern. Other fragments also observed:

m/e 321-325



m/e 289 - 296 - due to loss of CO_2H and H_2 .

m/e 45 - $[CO_2H]^+$

3.5.8 Preparation of 1,2 bis(carboxyphenyl)-ortho-carborane (XVIII)
(see Scheme 9)

i) Preparation of 4-(methyl) phenyl acetylene

4-(methyl) acetophenone (50 mls, 0.375 moles) was converted to the acetylene derivative in the same way as described for the preparation of 4-fluorophenylacetylene (Section 2.4.6(i)). The colourless liquid was distilled at 90-95°C (19.5 mmHg) yield 13.17 g (0.114 moles) 30%. Characterised as follows:

Analysis. Found: C, 92.5; H, 6.8%. C_9H_8 Requires: C, 93.1; H, 6.9%.

Infra Red: (Contact film) (cm^{-1}): 3290 (s) (acetylenic C-H stretch); 3070 (sh); 3050 (sh); 3020 (Aromatic CH stretch); 2965 (m); 2925 (m); 2870 (Aliphatic CH stretch); 2110 (m) ($C\equiv C$ stretch); 1895 (w.br); 1605 (m); 1510 (m); 1450 (br); 1410 (w.sh); 1375 (w.sh); 1357 (w); 1268 (m); 1212 (w); 1182 (w); 1178 (w); 1118 (w); 1108 (w); 1040 (w); 1022; 950 (w); 900 (w.br); 820 (s); 788 (w); 725 (w); 655; 645; 610 (br); 569 (w); 532 (s); 517 (w); 462 (w); 410 (w).

1H NMR 60 MHz. solvent $CDCl_3$, referenced externally to TMS at 0.00 ppm, (ppm): 7.45-6.70 (m), Integral 4H (Aromatic H); 2.9 (s), Integral 1H (Acetylenic H); 2.23 (s) Integral 3H (Methyl H).

ii) Preparation of 4-(methyl) phenyl ethynyl copper

4-(methyl) phenyl acetylene (12.67, 0.109 moles) was converted to its ethynyl copper derivative in exactly the same way as in the preparation of phenyl ethynyl copper (Section 3.5.7(ii)). The product was isolated as a bright yellow infusible powder, yield 10.88 g, (60.9 mmoles), 55.9%. Characterised as follows:

Analysis Found: C, 56.7; H 3.4; Cu 30.8%. C_9H_7Cu .

Requires: C, 60.1; H, 3.9; Cu, 35.6%.

Infra Red (KBr disc) (cm^{-1}): 3010 (w) (Aromatic C-H stretch); 2905 (w) (Aliphatic C-H stretch); 1595 (w) (C-C stretch); 1500 (m); 1370 (w); 1188 (w); 1172; 1112; 1100 (w); 1032; 1018; 810 (s); 640 (w); 520 (m); 452; 415 (w).

iii) Preparation of bis-(4-methyl)-phenyl acetylene

4 iodo toluene (6.08 g, 28 mmoles) dissolved in pyridine (20 mls) was added to a stirred suspension of 4-(methyl) phenyl ethynyl copper (5.00 g, 28 mmoles) in pyridine (80 mls) under nitrogen. The mixture was refluxed for 18 hours under nitrogen producing a cloudy brown solution. This was cooled and poured into 500 mls of distilled water and the resulting suspension extracted three times with diethyl ether. The ether extracts were combined, washed three times each with 2 M hydrochloric acid, aqueous sodium bicarbonate and water. The amber ether solution was dried over anhydrous magnesium sulphate, filtered and the ether removed under reduced pressure leaving a solid which, recrystallised from methanol/toluene given amber plates identified as bis(4-methylphenyl) acetylene. Yield 3.99 gm (19.4 mmoles), 69.2%. Melting point 134-135°C (lit. 136°C). Characterised as follows:

Analysis; Found: C, 92.9; H, 6.4%. $C_{16}H_{18}$. Requires: C, 93.2; H, 6.8%.

Infra Red (Nujol) (cm^{-1}) 3025 (w.sh) (Aromatic C-H stretch); 3000-2750 (Nujol); 1517 (m); 1460 (s); 1378 (m) (Nujol); 1310 (w); 1210 (w); 1170 (w.br); 1125 (w); 1105 (w.sh); 1035 (w); 1020 (w); 840 (w); 820 (s); 725 (w); 518 (m); 470 (w.br).

iv) Preparation of 1,2 bis(4-methylphenyl)-ortho-carborane

Bis(4-methylphenyl) acetylene (4.20 g, 20.4 mmoles) was converted to the corresponding carborane derivative by reaction with bis(acetonitrile) decarborane (4.24 g, 21 mmoles) in the same way as described for the preparation of 1,2 diphenyl-ortho-carborane (Section 2.4.5). The crude carborane derivative was recrystallised from hexane giving colourless crystals identified as 1,2 bis(4-methylphenyl)-ortho-carborane, yield 2.20 g (6.8 mmoles), 33.3%. Melting point 172-173°C, (lit. 172-173°C). Characterised as follows:

Analysis. Found: C, 59.3; H, 7.8, B, 33.6, %. $C_{16}H_{24}B_{10}$
Requires: C, 59.6; H, 7.5; B, 33.5%.

Infra Red (Nujol) (cm^{-1}): 3040 (w) (Aromatic C-H stretch); 3000-2750 (Nujol); 2650 (m) 2640 (m) 2620 (sh) 2604 (s.sh) 2600 (s) 2570 (s) 2555 (s) (B-H stretching frequencies); 1905 (w.br); 1613; 1512 (m); 1450 (m) (Nujol); 1410 (w); 1378 (Nujol); 1317; 1286 (w); 1262 (w); 1230 (w); 1197 (s); 1136 (m); 1078 (s); 1048 (w); 1025 (w); 1015 (w); 1005 (w); 978 (w); 970 (w); 945 (w.sh); 930 (w); 897 (s); 880; 837 (s); 827 (s); 815 (sh); 790; 740 (sh); 732 (m); 714 (s); 652 (w.br); 687 (m); 620 (m); 496 (s); 432.

v) Preparation of 1,2 bis(carboxyphenyl)-ortho-carborane (XVIII)

Chromium trioxide (11.0 g, 0.11 m) was dissolved in 40 mls of acetic anhydride and added dropwise over a period of one hour, to a stirred mixture of 1,2 bis(4-methylphenyl)-ortho-carborane (2.10 g, 6.52 mmoles), glacial acetic acid (100 mls) and concentrated sulphuric acid (3 mls) producing an exothermic reaction, turning the red CrO_3 solution green. On completion of the

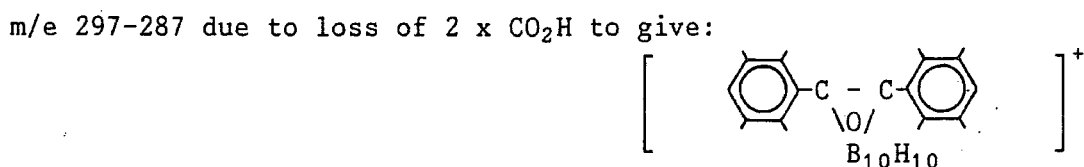
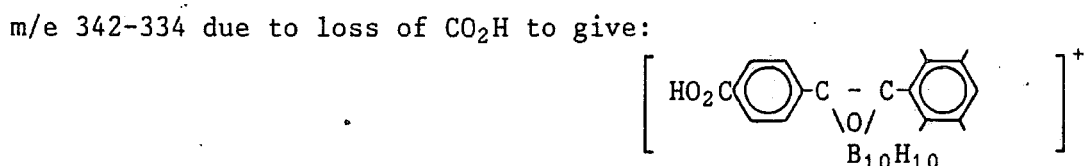
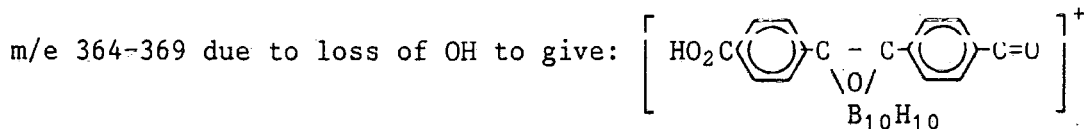
addition of chromium trioxide, the mixture was heated to 100°C for three hours, cooled and poured into 300 mls ice/water. The aqueous mixture was filtered leaving a green solid which was washed repeatedly with distilled water in an attempt to remove the green chromium residues. The pale green solid produced was then dissolved in a minimum amount of boiling sodium bicarbonate solution. The resulting solution was filtered hot and allowed to cool producing off white crystals of the disodium salt of the carboxylic acid. This was filtered off and dissolved in fresh distilled water. The solution was acidified with dilute hydrochloric acid producing an off white precipitate which was filtered off and recrystallised from acetone/water (3:1) producing a white powder which was dried under vacuum and identified as 1,2 bis(4-carboxy phenyl)-ortho-carborane. Yield 1.55 g (4.04 mmoles) 62% (lit. -70%). Melting point (determined using a Mettler TA3000 Differential Scanning Calorimeter) 395.5°C (lit. 350°C). Characterised as follows:

Analysis. Found: C, 50.4; H, 4.9; B, 28.3% $C_{16}H_{20}B_{10}O_4$. Requires C, 50.0; H, 5.2; B, 28.1%.

Infra Red (Nujol) (cm^{-1}): 3500-2200 (s.br) (Carboxyl OH stretch); 2650 (sh) 2600 (s) 2570 (sh) (B-H stretch); 1700 (s) (Carboxyl C=O stretch); 1610 (m); 1570; 1450 (s.sh); 1420 (s); 1378 (w); 1365 (sh); 1322; 1290 (s) (C-O stretch); 1235 (sh); 1194 (w); 1130 (m); 1074; 1022 (m); 1010 (sh); 975 (w.sh); 965 (w.sh); 930 (br); 902 (m); 863 (m); 813; 801; 788; 770; 732; 705 (s); 629; 581; 540 (m.br); 571 (w); 482; 472 (w); 462 (w).

1H NMR 250.134 MHz, solvent D_6 acetone, referenced externally to TMS at 0.00 ppm (ppm): 7.88-7.72 Integral 8H, (Aromatic Protons in an $AA'XX'$ pattern 7.88-7.84 H(3); 7.76-7.72 (m) H(2)); 4-3 (br,m), Integral 10H, (BH).

Mass Spectrum A highest mass peak was observed at m/e 386 corresponding to the species $^{12}\text{C}_{16}^{1}\text{H}_{20}^{11}\text{B}_{10}^{16}\text{O}_4$, accompanied by the usual carborane isotope distribution pattern between m/e 380 and 386. Other intense fragments were also observed at:



3.5.9 Preparation of 1,2 bis(4-phenoxyphenyl) ortho carborane (XX) (See Scheme 10)

i) Preparation of 4 iodo-diphenylether

4-bromo-diphenylether (25 g, 0.1 mmoles) in dry THF (50 mls) was added dropwise to a refluxing mixture of THF (50 mls) and magnesium turnings (4.86 g, 0.2 mmoles) (activated with iodine) under nitrogen. The mixture was refluxed with stirring under nitrogen for 6 hours, cooled and filtered through a grade 3 sinter. The brown Grignard solution was then added dropwise to a solution of iodine (25.6 g, 0.101 mmoles) in THF, under nitrogen using a cannula wire. The resultant mixture was refluxed under nitrogen for 2 hours, cooled and 100 mls of distilled water added dropwise. The mixture was agitated and the THF layer isolated.

The remaining aqueous layer was extracted with diethyl ether and the ether washings added to the THF solution. This mixture was washed three times each with 10% sodium thiosulphate and distilled water, dried over anhydrous magnesium sulphate, filtered and the solvents removed under reduced pressure. The resulting wet solid was recrystallised from methanol giving off white crystals identified as 4-iodo-diphenyl ether. Yield 22.23 g (75.1 mmol) 75.1%. Melting point 48°C (lit. 48°C). Characterised as follows:
Analysis Found: C, 49.0; H, 3.1; I, 42.7% $C_{12}H_9OI$
 Requires: C, 48.6; H, 3.0; I, 42.9%.

Infra Red (Nujol) (cm^{-1}): 3030 (w.sh) (Aromatic CH stretch); 1595 (sh); 1587 (sh); 1575 (s); 1555 (sh); 1474 (s); 1455 (sh); 1390 (w.sh); 1375; 1330 (w); 1295 (w); 1270 (m); 1240 (s) (C-O-C Asymmetric stretch); 1197; 1168 (s); 1092 (w); 1069 (w); 1055; 1020; 1005 (m); 890 (w.br); 867 (m); 822 (m); 835 (br); 750 (s); 690 (s); 585 (w); 497 (m); 484.

ii) Preparation of (4-phenoxy)phenyl ethynyl copper

4-(phenoxy phenyl) acetylene (18.17 g, 94 mmol) was converted to its ethynyl copper derivative in exactly the same way as outlined for the preparation of phenyl ethynyl copper (Section 3.5.7ii). The product was isolated as a bright yellow infusible powder. Yield 14.40 g (56.1 mmol), 59.7%. Characterised as follows:

Analysis Found: C, 63.7; H, 3.4; Cu, 24.3% $C_{12}H_9CuO$
 Requires: C, 65.5; H, 3.4; Cu 24.8%.

iii) Preparation of bis-(4-phenoxyphenyl)-acetylenea) The reaction of 4(phenoxyphenyl)ethynyl copper with 4-iodo diphenylether

4-iodo-diphenyl ether (8.52 g, 28.7 mmoles) dissolved in pyridine (20 mls) was added to a stirred suspension of 4-(phenoxyphenyl) ethynyl copper (7.38 g, 28.7 mmoles) in 100 mls of pyridine under nitrogen. The mixture was heated under reflux and under nitrogen for 18 hours producing a dark brown solution which was cooled and poured into 300 mls of distilled water. The mixture was extracted five times with toluene and the toluene extracts combined and washed three times each with 2M hydrochloric acid, 10% aqueous sodium bicarbonate and distilled water. The toluene solution was dried, filtered and the solvent removed under reduced pressure leaving an amber solid which was recrystallised from methanol/toluene (decolourised with activated charcoal) to give pale amber plates identified as bis(4-phenoxyphenyl) acetylene. Yield 4.80 g (13.26 mmoles) 46.2%. Melting point 169-170°C (lit 171°C). Characterised as follows:

Analysis Found: C, 86.0; H, 4.6 $C_{26}H_{18}O_2$

Requires: C, 86.2; H, 5.0%

Infra Red (Nujol) (cm^{-1}): 3030 (w.sh) (Aromatic C-H stretch), 1584 (m); 1503 (sh); 1482 (sh); 1298 (w); 1272 (m); 1252 (s) (C-O-C asymmetric stretch); 1192; 1163 (m); 1145 (w); 1102; 1067; 1019 (w); 1009 (2); 895 (w); 873; 847 (m); 835 (s); 822; 770 (m); 735 (s); 720 (sh); 688 (m); 518 (m); 480 (w).

- b) The reaction between 4 iodo-diphenylether and acetylene in the presence of bis(triphenyl phosphine) palladium dichloride and cuprous iodide

A mixture of 4 iodo-diphenylether (4.41 g, 14.9 mmoles), bis(triphenylphosphine) palladium dichloride (0.104 g, 0.15 mmoles) and cuprous iodide (14.3 mg, 0.075 mmoles) was dissolved in dry, degassed diethylamine (in apparatus purged with nitrogen and assembled in a well ventilated fume hood). Welding grade acetylene (dried by passing through concentrated sulphuric acid, and scrubbed with soda lime) was bubbled slowly through the stirred solution for 6 hours. (After 2 hours a red oil appeared, this disappeared as the reaction progressed leaving a dark brown solution and a small amount of crystalline solid). All volatile material present was then removed under vacuum and distilled-water (20 mls) added to the residue. This mixture was extracted three times with toluene, the toluene extracts combined, dried over anhydrous magnesium sulphate filtered and concentrated under reduced pressure.

The resulting residue was passed down a short alumina column (eluted with toluene), to remove residual catalyst, producing an amber solution. The toluene was removed under reduced pressure leaving a brown solid which was recrystallised from methanol/toluene (decolourised with activated charcoal) affording pale amber plates identified as bis 4-(phenoxyphenyl) acetylene. Yield 0.79 g (2.18 mmoles) 29.3%. Melting point 168-170°C.

Analysis Found: C, 85.71; H, 4.9 (infra red as

in the previous section.

iv) Preparation of 1,2 bis(4-phenoxyphenyl)-ortho-carborane (XX)

bis(4-phenoxyphenyl) acetylene (4.59 g, 12.68 mmoles) dissolved in warm toluene (45 mls) was added to a suspension of bis(acetonitrole)decaborane (2.57 g, 12.72 mmoles) in toluene (20 mls) under nitrogen. The mixture was stirred and heated under reflux for 24 hours, cooled and worked up as normal (see Section 2.4.5). The crude product was recrystallised from methanol (decolourised using activated charcoal) affording colourless plates identified as 1,2 bis(4-phenoxyphenyl)-ortho-carborane. Yield 1.49 g (3.1 mmoles), 24.4%. Melting point 119–120°C (lit 120–122⁴³). Characterised as follows:

Analysis Found: C, 65.4; H, 5.5; B, 20.7% $C_{26}H_{28}B_{10}O_2$
Requires: C, 65.0; H, 5.4; B, 22.5%.

Infra Red (Nujol) (cm^{-1}) 3040 (w.sh) (Aromatic CH stretch); 2570 (s) (B-H stretch); 1605 (sh); 1588 (s); 1502 (m); 1488 (s); 1414 (w.sh); 1312 (w.sh); 1305 (w.sh); 1295 (sh); 1287 (m); 1252 (s) (C-O-C asymmetric stretch); 1200 (m); 1180 (m); 1160; 1130; 1121 (w); 1074; 1023; 1005; 983 (w); 960 (w); 941 (w); 927 (w); 905; 892; 882 (m); 872 (sh); 842 (s); 815 (w); 790 (m); 770 (w); 753 (s); 733; 717; 693 (s); 581; 568; 525; 520 (m); 484 (m); 440 (w).

¹³C NMR {¹H broad band noise} 60 MHz solvent $CDCl_3$.
References externally to TMS at 0.00 ppm. See Figure 3.5.

¹¹B NMR {¹H broad band noise} 115.552 MHz, solvent C_6D_6 .
Referenced externally to BF_3Et_2O at 0.00 ppm. See Figure 3.5.

XX - $\delta(^{13}\text{C})$

C atom	$\delta(^{13}\text{C})$ ppm
a	85.26
b	124.99
c	132.29
d	119.70
e	155.63
f	159.22
g	117.40
h	129.23
i	125.35

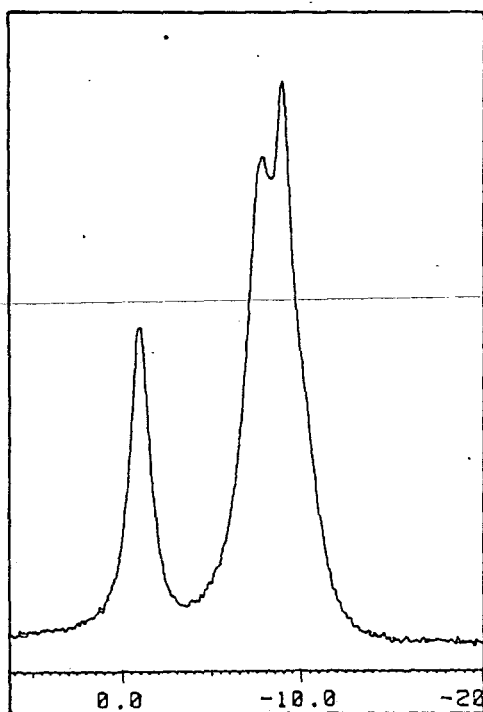
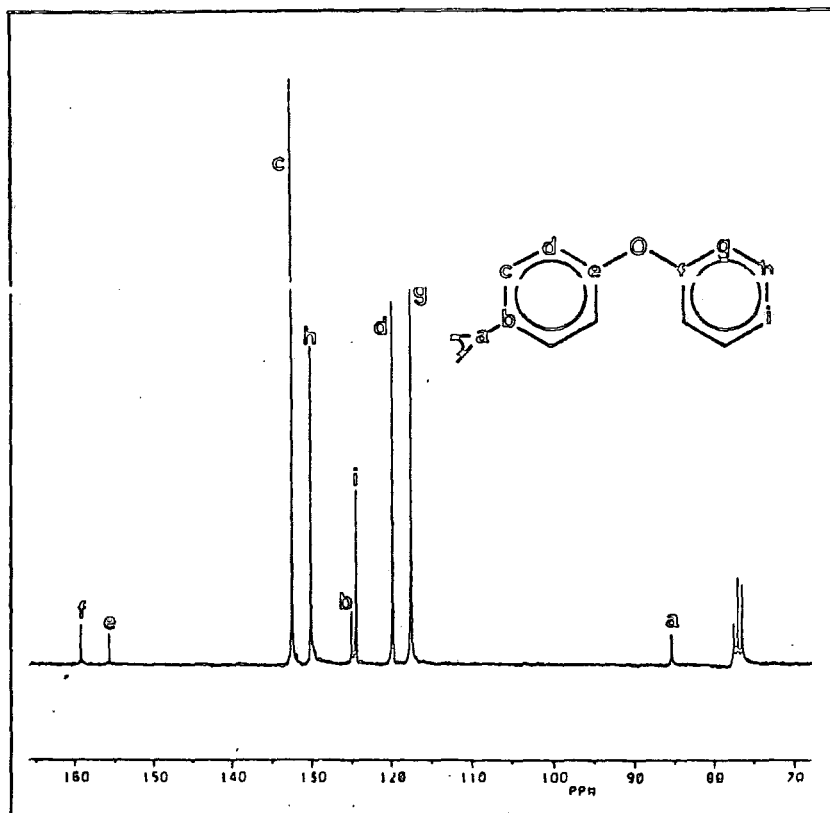


Figure 3.5 ^{13}C and ^{11}B NMR spectra of (XX)

Mass Spectrum (E.I) A highest mass peak was observed at m/e 484 corresponding to the M+2 peak of the species $^{12}\text{C}_{26}^{1}\text{H}_{28}^{11}\text{B}_{10}^{16}\text{O}_2$ due to the 1% abundance of the ^{13}C . This was accompanied by the characteristic carborane isotope distribution pattern between m/e 476 and 484. A cluster of half mass peaks were observed between m/e 239 and 241 (m/2e 478-482). A fragment at m/e 77 was also observed ($[\text{C}_6\text{H}_5]^+$).

3.5.10 Preparation of 1,4-(methylcarboxy)phenyl-2-(4-phenoxyphenyl) ortho carborane (XXII) (See Scheme 11)

i) Preparation of 1,4-(methylcarboxy)-2-(4-phenoxyphenyl)-acetylene

1-(4-carboxyphenyl)-2-(4-phenoxyphenyl) acetylene was prepared using the same procedure as for 1-(4-carboxyphenyl)-2-(phenyl) acetylene (Section 3.5.7 (iii)) from 4-iodo-methylbenzoate (5.54 g, 21.1 mmoles) and (4-phenoxyphenyl) ethynyl copper (5.41 g, 21.1 mmoles). Extraction of the product from the water quenched reaction mixture was carried out with toluene. The product was recrystallised from methanol/toluene affording pale amber plates identified as 1-(4-carboxy phenyl)-2-(4-phenoxyphenyl) acetylene. Yield 3.65 g (11.1 mmoles) 52.7%. Melting point 168°C. Characterised as follows:

Analysis Found: C, 79.6; H 4.3% $\text{C}_{22}\text{H}_{16}\text{O}_3$. Requires: C, 80.5; H, 4.8%.

Infra Red (Nujol) (cm^{-1}): 2210 (m) ($\text{C}\equiv\text{C}$ stretch); 1717 (s) ($\text{C}=\text{O}$ stretch); 1588 (s); 1510; 1485 (m); 1456 (m); 1432 (m); 1402; 1374; 1308; 1285 (s.ch); 1278 (s) ($\text{C}-\text{C}(=\text{O})-\text{O}$ and $\text{O}-\text{C}-\text{C}$ asymmetric stretch); 1255 (s) ($\text{C}-\text{O}-\text{C}$ asymmetric stretch); 1910; 1176 (m); 1165; 1156

(sh); 1135; 1105 (m); 1072 (w); 1017 (w); 957 (w); 905 (w); 873; 862; 855; 840 (s); 830 (w); 783; 770 (sh); 768 (m); 755 (m); 720; 697 (m); 685 (sh); 520; 485.

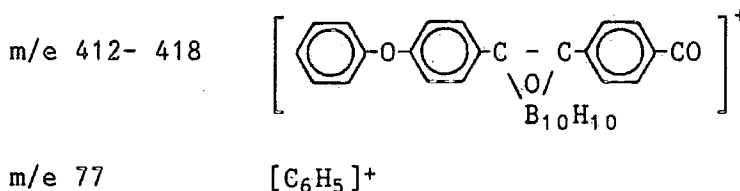
ii) Preparation of 1,4-(methylcarboxy)-2-(4-phenoxy phenyl)-ortho-carborane (XXII)

(XXII) was prepared by the reaction between 1,4-(methylcarboxy)phenyl-2-(4-phenoxyphenyl) acetylene (2.65 g, 8.05 mmoles) and bis(acetonitrile) decaborane (1.64 g, 8.1 mmoles) in toluene (50 mls) as normal (see Section 3.5.9(iv)). The product was recrystallised from hexane affording off white crystals identified as (XXII). Yield 0.79 g, (1.78 mmoles), 22%. Melting point 124-125°C. Characterised as follows:

Analysis Found: C, 59.0; H, 6.3; B, 24.8% $C_{22}H_{26}B_{10}O_3$
Requires: C, 59.2; H, 6.3; B, 24.3%.

Infra Red 3020 (w.sh) (Aromatic C-H stretch); 2580 (s.sh); 2570 (s) (B-H stretch); 1723 (s) (C=O stretch); 1605 (sh); 1585 (m); 1560 (sh); 1500 (sh); 1483 (m); 1455 (m.br); 1434 (m); 1404 (w); 1375 (w); 1305 (sh); 1276 (s) (Ester C-O stretches); 1255 (s) (C-O-C asymmetric stretch); 1196 (m); 1177 (m); 1160 (w); 1115 (s); 1070 (m); 1020; 1005 (sh); 965; 927 (w); 906 (w); 898; 880; 860; 842 (m); 825; 791; 779 (w); 766; 752 (m); 738; 730 (sh); 693 (m); 581; 570 (w); 520; 488.

Mass Spectrum (E.I) A highest mass peak was observed at m/e 450 corresponding to the M+2 signal of the species $^{12}C_{22}^{1}H_{26}^{11}B_{10}^{16}O_3$ due to the abundance of ^{13}C . This was accompanied by the characteristic carborane isotope distribution pattern between m/e 442-448 (base peak m/e 446). Other major fragments were seen at:



3.5.11 Preparation of 1-(4-methylphenyl)-2-(4-phenoxyphenyl) ortho-carborane (XXIII) (See Scheme 12)

i) Preparation of 1-(4-methylphenyl)-2-(4-phenoxyphenyl acetylene

The above acetylene derivative was prepared as standard by the reaction of (4-methylphenyl) ethynyl copper (4.68 g, 26.2 mmoles) and 4 iodo-diphenylether (7.76 g, 26.2 mmoles) in pyridine (130 mls) (see Section 3.5.9(iii)). The product was recrystallised from methanol (decolourised with activated charcoal) to give amber crystals identified as 1-(4-methylphenyl)-2-(4-phenoxyphenyl) acetylene. Yield 3.42 g (12.04 mmoles) 46%. Melting point 102-104°C. Characterised as follows:

Analysis Found: C, 90.1%, H, 5.6%. $\text{C}_{21}\text{H}_{16}\text{O}$.

Requires: C, 88.7, H, 5.6%.

Infra Red (Nujol) (cm^{-1}): 3030 (w.sh) (Aromatic CH stretch); 1590 (m) (C-C stretch); 1510 (sh); 1488 (m); 1408 (w); 1302 (w); 1281 (m); 1260 (s) (C-O-C. Asymmetric stretch); 1245 (sh); 1198; 1168 (m); 1150 (w); 1108; 1075; 1023 (w); 1015 (w); 951 (w); 900; 877; 855; 843 (s); 830; 822 (s); 795; 770 (m); 742 (m); 718 (w); 712 (w); 695 (m); 522 (m); 490; 473 (w). $^1\text{H NMR}$ 60 MHz. Solvent CDCl_3 Referenced externally to TMS at 0.00 ppm (ppm): 7.73-6.92 (m) Integral 13H (Aromatic H); 2.45 (s) Integral 3H (Methyl H).



ii) Preparation of 1-(4-methylphenyl)-2-(4-phenoxyphenyl) ortho-carborane (XXIII)

(XXIII) was prepared by the reaction between 1-(4-methylphenyl)-2-(4-phenoxyphenyl) acetylene (2.90, 10.21 mmols) and bis(acetonitrile) decaborane (2.06 g, 10.21 mmols) as standard (see Section 3.5.9(iv)). The crude product was recrystallised from methanol (discoloured with activated charcoal) affording colourless needles identified as 1-(4-methylphenyl)-2-(4-phenoxyphenyl)-ortho-carborane. Yield 0.93 g (2.31 mmols) 22.7%. Melting point 110°C. Characterised as follows:

Analysis Found: C, 62.8; H, 6.9; B, 26.7% $C_{21}H_{26}B_{10}O$. Requires: C, 62.7; H, 6.5; B, 26.9%.

Infra Red (Nujol) (cm^{-1}): 3050 (w) (Aromatic CH stretch); 2650 (sh); 2635 (sh); 2590 (s); 2565 (s) (B-H stretches); 1607 (sh); 1590 (m) (C-C stretch); 1504 (m); 1488; 1415 (w); 1315 (w); 1305 (w); 1284; 1252 (s) (C-O-C asymmetric stretch); 1205 (s); 1178 (s); 1164 (m); 1135 (w); 1122; 1076 (m); 1040 (w); 1026 (w); 1018 (w); 1007 (w); 980 (w); 930 (w); 907; 898; 883; 870 (w); 849 (s); 840 (w); 830; 790; 755 (m); 743; 735; 720; 710 (w); 692 (m); 587; 575 (w); 551; 524 (w); 502 (m); 589; 435; 404 (w).

Mass Spectrum (E.I) A highest mass peak was observed at m/e 405 (M+1). The peak at m/e 404 corresponding to $^{12}C_{21}^{1}H_{26}^{11}B_{10}^{16}O$ was observed accompanied by the usual carborane isotope distribution pattern (base peak at m/e 402) between m/e 398-404.

3.5.12 Preparation of 1-(4-bromophenyl)-2-(4-phenoxyphenyl)-ortho-carborane (XXIV) (See Scheme 13)

i) Preparation 4-bromophenylacetylene

4-bromoacetophenone (34.65 g, 0.174 moles) was treated with phosphorous pentachloride (40.00 g, 0.19 moles) see Section 2.4.6(i)). The residue from this reaction was dissolved in 20 mls of ethanol and added dropwise to a solution of potassium hydroxide (48 g, 0.86 moles) in ethanol (200 mls). The mixture was heated under reflux for 2½ hours and then poured into 500 mls of ice/water. The suspension produced was extracted five times with diethyl ether; the ether extracts combined and dried over potassium hydroxide, and then over anhydrous magnesium sulphate. The solution was filtered and the ether removed under reduced pressure leaving a dark brown oil from which a low melting solid was distilled (70-80°C, 0.025 mmHg). This was recrystallised from ethanol producing yellow crystals identified as 4-bromophenylacetylene. Yield 10.68 g (59 mmoles) 34%. Melting point 62-64°C (lit 64-65°C). Characterised as follows:

Analysis Found: C, 52.0; H, 2.7; Br, 42.0% C₈H₅Br.

Requires C, 53.0; H, 2.8; Br, 44.2%.

Infra Red (Nujol) (cm⁻¹): 3290 (s) (Acetylenic CH stretch); 3060 (w.sh) (Aromatic C-H stretch); 2110 (w) (C≡C stretch); 1896 (w); 1770 (w.br); 1682 (w); 1682 (w); 1635 (w); 1605 (m); 1586 (m); 1560 (w); 1483 (s); 1440 (w.sh); 1395 (s); 1294 (w); 1264; 1220; 1192 (w); 1175; 1125 (sh); 1113; 1097; 1080 (sh); 1071 (s); 1061; 1050 (sh); 1010 (s); 950; 885 (m); 830 (s); 774; 750 (w); 723; 718 (w); 697; 660; 630; 620 (sh); 556; 527 (m); 516; 457 (w.br); 404.

¹H NMR 60 MHz. Solvent CDCl₃ Referenced externally to TMS at 0.00 ppm: (ppm); 7.20-7.44 (m) Integral 4H (Aromatic H); 3.07 (s) Integral 1H (Acetylenic H).

ii) Preparation of (4-bromophenyl)ethynyl copper

4-bromophenyl acetylene (10.60 g, 58.6 mmoles) was converted to the ethynyl copper derivative as standard (see Section 3.5.7(ii)). The product was isolated as a yellow infusible powder. Yield 9.27 g (38.1 mmoles), 65%. Characterised as follows:

Analysis Found: C, 39.2; H, 1.7; Br, 29.0; Cu, 24.8% C₈H₄BrCu. Requires: C, 39.6; H, 1.7; Br, 32.8; Cu, 26.1%.

Infra Red (KBr disc) (cm⁻¹): 1575 (w); 1478 (s); 1389 (m); 1181 (w); 1105 (w); 1090 (w); 1068 (s); 1012 (s); 1004; 817 (s); 778; 695; 595; 515 (s); 450 (w.br) 400 (w.br); 315.

iii) Preparation of 1-(4-bromophenyl)-2-(phenoxyphenyl) acetylene

The above acetylene derivative was prepared by the reaction between (4-bromophenyl)ethynyl copper (7.09 g, 29 mmoles) and (4-iodo)-diphenylether (8.53 g, 29 mmoles) in 140 mls of pyridine, as standard (see Section 3.5.9(iii)). The product was recrystallised from methanol/toluene affording an amber powder identified as 1-(4-bromophenyl)-2-(4-phenoxyphenyl) acetylene. Yield, 7.29 g (20.9 mmoles) 72%. Melting Point 142-145°C. Characterised as follows:

Analysis Found: C, 68.9; H, 3.8; Br, 22.4% C₂₀H₁₃BrO. Requires: C, 68.8; H, 3.7; Br, 23.1%.

Infra Red (Nujol) (cm⁻¹): 3065 (w) 3039 (w) (Aromatic C-H stretch); 2220 (w) (C≡C stretch); 1580 (m) (C-C

stretch); 1500 (sh); 1490 (sh); 1480 (s); 1392 (w); 1365 (sh); 1330 (w); 1297; 1275; 1245 (s) (C-O-C Asymmetric stretch); 1199 (w); 1170 (m); 1155 (w); 1139 (w); 1105 (w); 1097 (w); 1072; 1058; 1025; 1010 (m); 905 (w); 870; 850 (sh); 840; 827 (m); 785; 757 (s); 722; 692; 582 (w); 537 (w); 530 (w); 520 (w); 505.

iv) Preparation 1-(4-bromophenyl)-2-(4-phenoxyphenyl)-ortho-carborane (XXIV)

The above carborane derivative was prepared by the reaction between 1-(4-bromophenyl)-2-(4-phenoxyphenyl acetylene) (6.10 g, 18 mmols) and bis(acetonitrile) decaborane (3.57 g, 18 mmols) as standard (see Section 3.5.9(iv)). The crude product was recrystallised from methanol (discoloured with activated charcoal) affording an off white powder identified as 1-(4-bromophenyl)-2-(4-phenoxyphenyl)-ortho-carborane. Yield 2.86 g (6.12 mmols) 34%.

Melting point 117-120°C. Characterised as follows:

Analysis Found: C, 53.4; H, 5.2; B, 24.6; Br, 16.1% $C_{20}H_{23}B_{10}BrO$. Requires: C, 51.4; H, 4.9; B, 23.1; Br, 17.1%

Infra Red (Nujol) (cm^{-1}): 3050 (w.sh) (Aromatic CH stretch); 2670 (w) 2640 (m) 2590 (s) 2560 (s) (B-H stretches); 1602 (w); 1582 (s) (C-C stretch); 1500 (m); 1484 (s); 1403 (w); 1391 (m); 1360 (w.sh) 1328 (w); 1300; 1285 (w.sh); 1275; 1242 (s) (C-O-C Asymmetric stretch); 1203 (m); 1170 (s); 1160; 1150 (w); 1115; 1064 (m); 1020; 1008; 1000 (sh); 923; 890; 875; 863; 849; 824 (m); 777 (w); 753 (s); 738 (w); 722; 689; 600; 572; 520; 497; 489; 403 (w.br).

Mass Spectrum (E.I) A highest mass peak was seen at m/e 472 (M+2 due to abundance of the ^{13}C isotope). A

peak at m/e 469 was observed corresponding to the species $^{12}\text{C}_{20}^{1}\text{H}_{23}^{11}\text{B}_{10}^{80}\text{Br}^{16}$) accompanied by the usual carborane isotope distribution pattern (base peak at m/e 467). Another intense peak was observed at m/e 77 ($[\text{C}_6\text{H}_5]^+$).

3.6 REFERENCES

1. T.E. Attwood, P.C. Dawson, J.L. Freeman, L.R.J. Hoy, J.B. Rose, P.A. Staniland, Polymer, 1981, 22, 1096.
2. J. Miller, J. Amer. Chem. Soc. 1954, 76, 448.
3. P. Hughes, Guidebook to Mechanism in Organic Chemistry 5th Ed. Longmans, London, 1981, 166. See also: Reaction mechanisms in organic chemistry, Monograph 8, J. Miller, Aromatic Nucleophilic Substitution, Elsevier, 1968.
4. J.B. Rose, Chem. Ind. 1967, 461.
5. R.L. Heppollette, J. Miller, J. Chem. Soc. 1956, 2329.
6. H.M. Colquhoun, Polymer Preprints, 1984, 25, 17.
7. F. Effenberger, E. Sohn, G. Epple, Chem. Ber. 1983, 116, 1195.
8. R.M.G. Roberts, A.R. Sadri, Tetrahedron, 1983, 39, 137.
9. S. Papetti, B.B. Schaeffer, H.J. Troscianiec, T.L. Heying, Inorg. Chem. 1964, 3, 1444.
10. L.I. Zakharkin, Yu. A. Chapovskii, V.A. Brattsev, V.I. Stanko, J. Gen. Chem. U.S.S.R. 1966, 36, 892.
11. L.I. Zakharkin, A.V. Grebannikov, Bull. Acad. Sci. U.S.S.R. Chem. Div. 1967, 1331.
12. M.F. Hawthorne, T.E. Berry, P.A. Wegner, J. Amer. Chem. Soc. 1965, 87, 4746.
13. R.G. Alder, M.F. Hawthorne, J. Amer. Chem. Soc. 1970, 92, 6174.
14. L.I. Zakharkin, V.N. Kalinin, A.P. Snyakin, B.A. Kvasov, J. Organomet. Chem. 1969, 18, 17.
15. J. March, Advanced Organic Chemistry. Reactions, Mechanism and Structure, Wiley Interscience, 1984, 247.
16. L.A. Leites, L.E. Vinogradova, V.N. Kalinin, L.I. Zakharkin, Bull. Acad. Sci. U.S.S.R. Chem. Div. 1970, 2437.
17. R.A. Wiesbock, M.F. Hawthorne, J. Amer. Chem. Soc. 1964, 86, 1642.
18. D. Grafstein, J. Bobinski, J. Dvorak, H. Smith, N. Schwartz, M.S. Cohen, M.M. Fein, Inorg. Chem. 1963, 2, 1120.
19. L.I. Zakharkin, V.N. Kalinin, Tetr. Letts. 1965, 7, 407.

20. M.F. Hawthorne, D.C. Young, P.M. Garrett, D.A. Owen, S.G. Schwerin, F.N. Tebbe, P.A. Wagner, J. Amer. Chem. Soc. 1968, 90, 862.
21. J. Plesek, S. Hermanek, Chem. Ind. 1973, 381.
22. L.I. Zakharkin, A.V. Kazantsev, Bull. Acad. Sci. U.S.S.R. Chem. Div. 1966, 541.
23. V.I. Stanko, T.V. Klimova, I.P. Beletskaya, Doklady. 1974, 216, 329.
24. D.A. Brown, Ph.D. Thesis, Durham 1985.
25. L.I. Zakharkin, A.I. Kovvedov, Bull. Acad. Sci. U.S.S.R. Chem. Div. 1978, 1483.
26. L.I. Zakharkin, A.I. Kovvedov, Bull. Acad. Sci. U.S.S.R. Chem. Div. 1974, 23, 710.
27. G. Drehfahl, G. Plotner, Chem. Ber. 1958, 91, 1280.
28. S. Trippett, D.M. Walker, J. Chem. Soc. 1960, 2676.
29. W. Trados, A.B. Sakla, M.S. Ishak, J. Chem. Soc. 1958, 4210.
30. M.M. Telyakov, I.A. Khotina, A.I. Kalachev, P.M. Valyetski, S.V. Vinogradova, V.V. Korshak, Russ. Pat. 1982, 888462.
31. J. Makaiyama, H. Namku, T. Kumamoto, J. Org. Chem. 1964, 29, 2243.
32. M.S. Newman, D.E. Reid, J. Org. Chem. 1958, 23, 665.
33. R.D. Stephens, C.E. Castro, J. Org. Chem. 1963, 28, 3313.
34. N. Ya. Kronvod, Zh. Obsch. Khim. 1956, 26, 1876.
35. T. Tsuda, T. Hashimoto, T. Saegusa, J. Amer. Chem. Soc. 1972, 94, 658.

36. L. Cassar, J. Organomet. Chem. 1975, 93, 253.
37. H.A. Dieck, F.R. Heck, J. Organomet. Chem. 1975, 93, 259.
38. K. Sonogashira, Y. Tohda, N. Hagihara, Tetr. Letts. 1975, 4467.
39. V.I. Stanko, V.A. Brattser, N.N. Ovsyannikov, T.P. Klimova, J. Gen. Chem. U.S.S.R. 1974, 44, 2441.
40. L.G. Wade Jr. Compendium of Organic Synthetic Methods, 1981, 4, 15; 1984, 5, 15.
41. J.J. Brunet, C. Sidot, P. Caubere, Tetr. Letts. 1981, 22, 1013.

42. R.M. Silverstein, G.C. Bassler, T.C. Morrill, Spectrometric Identification of Organic Compounds, 4th Ed. John Wiley, 1981, 264.
43. M.M. Teplyakov, I.A. Khotina, Ts.L. Gelashvili, V.V. Korshak, Dokl. Acad. Nauk. S.S.S.R. 1983, 271, 874.

CHAPTER 4

THE SYNTHESIS AND CHARACTERISATION
OF POLY(CARBORANYLETHETERKETONES)

4.1 INTRODUCTION

The work described in this chapter has involved the preparation and characterisation of poly(carboranyletherketones), by electrophilic polycondensation of the monomers described in the previous chapter. in TFSA. The preparation of PEEK, by a route similar to that used in its commercial production, is also outlined and illustrates the nucleophilic polycondensation technique.

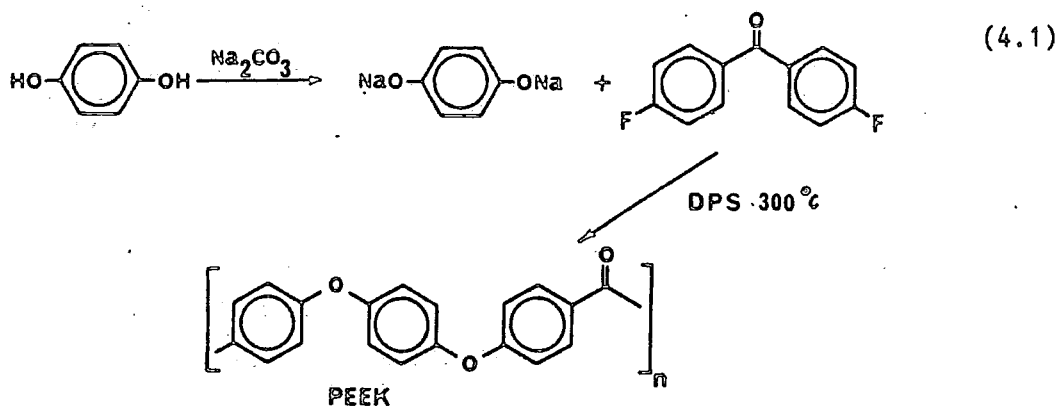
The results from attempted molecular weight determinations, and from spectroscopic, calorimetric and thermogravimetric analysis of the poly(carboranyletherketones) are also described. These show that the incorporation of the 1,2-diphenyl-ortho-carborane unit into poly(etherketone) chains, disrupts the crystallinity commonly found in these polymers. This results in the carborane polymers being much more soluble in common organic solvents. The glass transition temperatures are raised by the incorporation of the 1,2-diphenyl-ortho-carborane unit, which is attributed to the increase in chain rigidity imposed by this link. The presence of the cage has also been shown to inhibit the thermal weight loss that poly(etherketones) undergo at elevated temperatures, both in air and nitrogen atmospheres. This is thought to be due to the condensation of carborane polyhedra at elevated temperatures producing three dimensional networks in the polymers. Weight changes seen on polymer thermolysis in air are attributed to the oxidation of the BH cage to give heavier, non-volatile BO compounds.

The chapter is concluded with some proposals for future study.

4.2 POLYMER PREPARATION

The preparation of poly(etherketones) on a commercial scale, is currently carried out using the nucleophilic ether forming reaction discussed in Section 3.2.1. The main problem involved in preparing

materials such as PEEK is that they are insoluble in common organic solvents. A suitable solvent for nucleophilic polycondensation needs to be aprotic and sufficiently dipolar to ensure solvation of the polymer. Sulpholane and dimethylsulphoxide products crystallise out of solution before high molecular weight material can be produced¹. Diphenylsulphone was found to be a good solvent for these polymers at temperatures approaching their melting points. It also has high thermal stability and is unreactive towards the monomers used and thus makes a good solvent for nucleophilic polycondensation reactions to be performed in². PEEK has been prepared during this study by a route similar to that used for its commercial production (equation 4.1) and details of the procedure are given in Section 4.4.1.



The other most effective route to poly(etherketones), using the polycondensation of aromatic carboxylic acids and ethers in TFSA (see Section 3.2.2) requires very mild conditions in comparison to the previous method (reactions occur readily at room temperature). This route may also be used to prepare very small amounts of material and therefore constitutes a convenient method for preparing material on the laboratory scale. Large scale production is not carried out using this procedure because of the expense of the solvent and catalyst TFSA, and because of the difficulties associated with using TFSA in large amounts, and removing traces of it from large quantities of polymer.

Owing to the reactivity of the carborane cage towards phenoxide ion

(see Section 3.3.3) the only effective route to poly(carboranylether ketones) is through electrophilic polycondensation. All the carborane polymer preparations that have been successfully carried out in this study are summarised in Schemes 1-4 (full details of each are given in Sections 4.4.2-4.4.5).

In using both routes, it is important to ensure that all the reactive functional groups present at the start of a polymer synthesis have completely reacted. End capping of polymers with non-reactive groups is therefore necessary. This is conveniently achieved by having a small excess (ca. 1%) of the less reactive monomer species present in the reaction mixture. In nucleophilic polycondensations, the fluoro derivative is added in excess, and in the electrophilic polycondensations the ether is present in excess. This end capping procedure also provides a fairly reliable means of controlling the molecular weight of polymer produced.

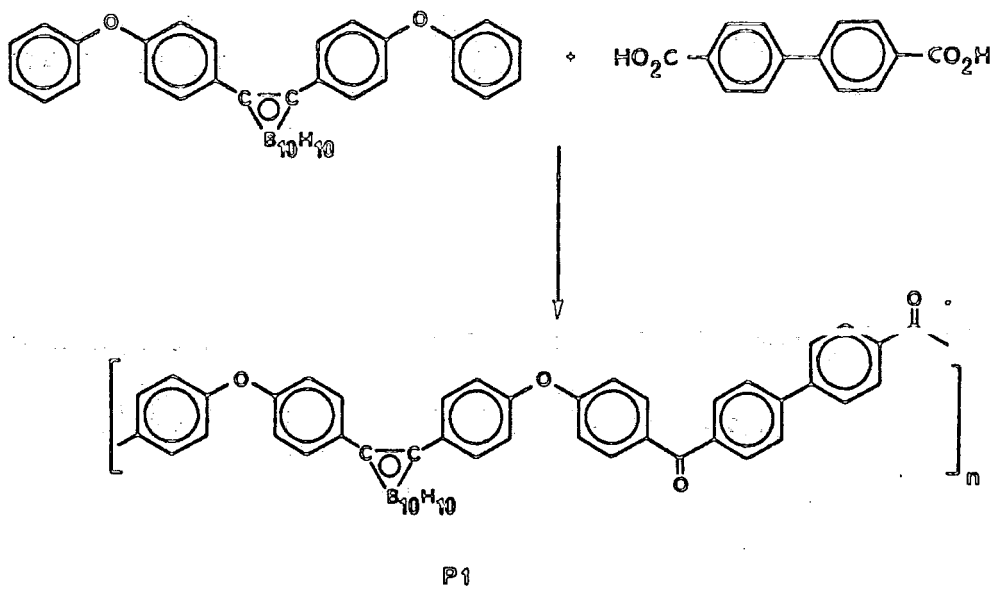
4.3 POLYMER CHARACTERISATION

All the carborane polymers produced in this study have been isolated as white solids. One striking difference between these materials and the poly(etherketones) from which they are derived is their solubility in organic solvents. P1, P2 and P3 are readily soluble in dichloromethane, chloroform, toluene, DMF and THF and appear to be swelled in acetone. P4 is less affected by organic solvents, only being slightly soluble in toluene.

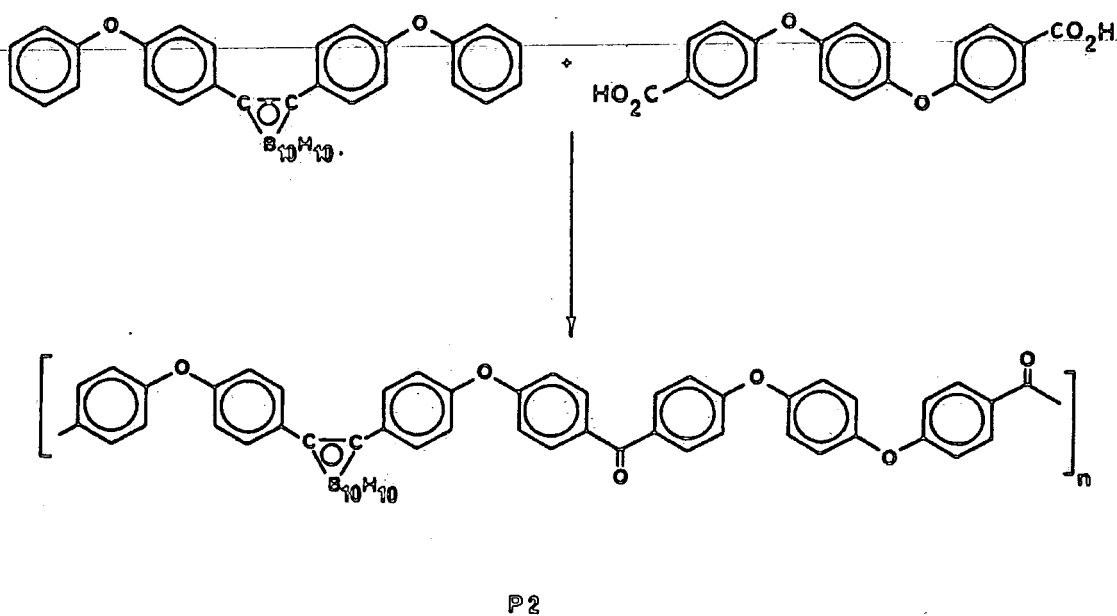
4.3.1 Molecular weight determination

Solution viscosity and light scattering measurements have been most commonly employed to monitor the molecular weight of poly(etherketones) using solution of polymers in 98% sulphuric acid^{2,3}. Problems associated with this solvent are its tendency to sulphonate phenylene rings and to protonate the ketone links when the polymer is dissolved. Sulphonation causes steric

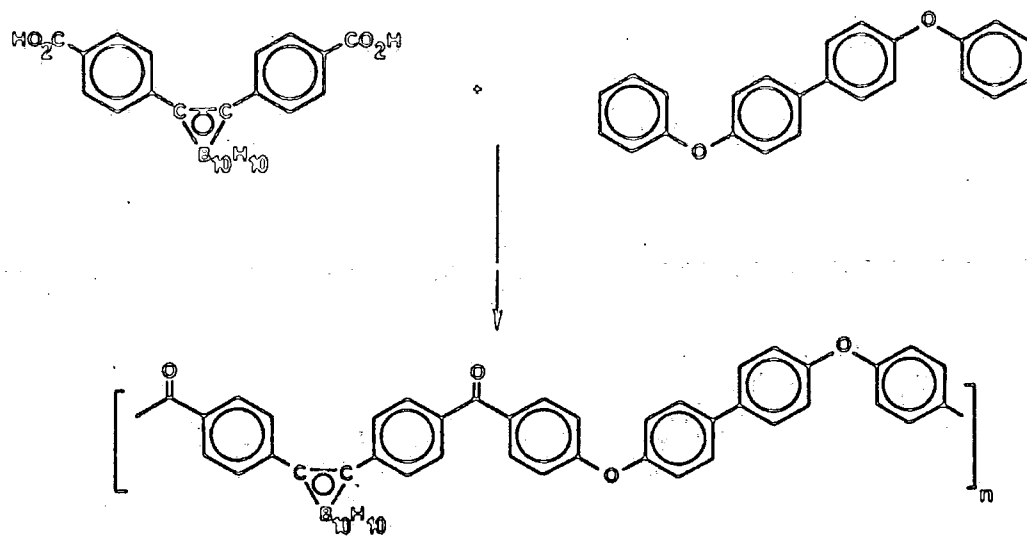
Scheme 1



Scheme 2

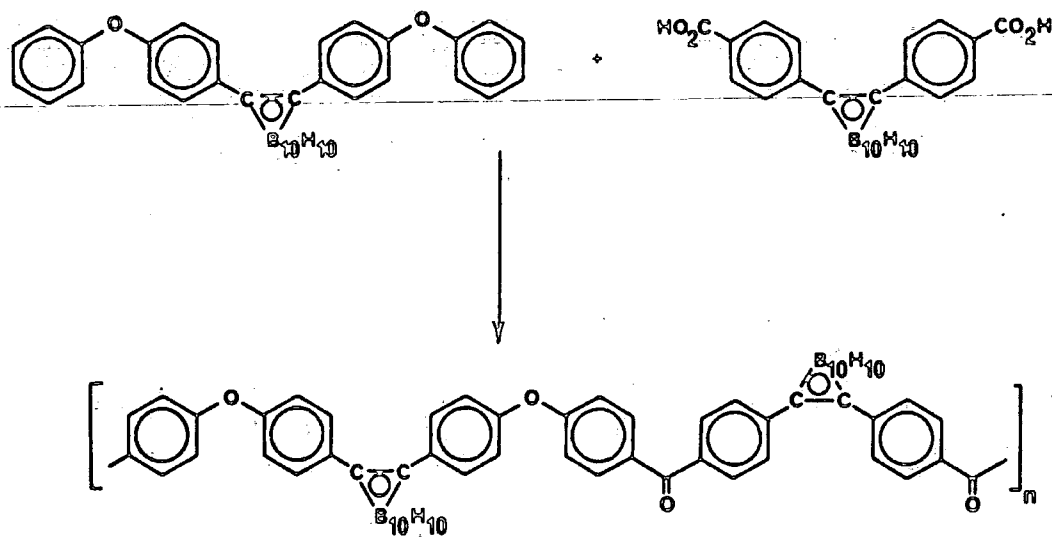


Scheme 3



P3

Scheme 4



P4

strain and intramolecular electrostatic repulsions in polymer molecules. Also there will be a tendency for phenylene rings and COH⁺ groups to remain co-planar so as to delocalise the excess charge produced by the protonation. These effects will substantially modify the solution characteristics of these polymers and so allowances for them need to be made when determining absolute molecular weights^{3,4}. Solution viscosity is routinely used to give qualitative information about polymer molecular weight by comparing values obtained for a polymer in question with those of polymers that possess the required degree of stability, solvent resistance and toughness.

Poly(etherketones) available commercially have inherent viscosities typically between 1.0 and 2.0⁵. Finally, a 1:1 mixture of 1,2,4-trichlorobenzene and phenol has been found to be an effective solvent for amorphous PEEK at 115°C and so viscosity and G.P.C. data are available on this material in this solvent system³. This solvent mixture has not been widely used however.

4.3.1.1 Solution viscosities

The inherent viscosities (η_{inh}) (equation 4.2) of 0.1% polymer solutions have been measured. η_{inh} of the PEEK sample prepared was determined in 98% sulphuric acid, η_{inh} of P1, P2 and P3 were measured in DMF solution, a value for P4 could not be obtained as this sample was insoluble in DMF.

$$\eta_{inh} = \frac{\ln\left(\frac{\eta}{\eta_0}\right)}{c}, \quad \frac{\eta}{\eta_0} \approx \frac{t}{t_0} \quad (4.2)$$

c = Polymer solution concentration (%)

t = time for a fixed volume of polymer solution to pass down a capillary

t₀ = time for a fixed volume of solvent to pass down the same capillary

The values obtained are given in Table 4.1.

The fact that most of the carborane polymers synthesised in this study are soluble in unreactive organic solvents means that, in principle, molecular weight studies on the unchanged polymers can be readily performed. The main difficulty encountered in this work however is that the techniques employed all require calibration using polymers of similar structure and known molecular weight, which are not available. Structurally related poly(ethersulphones) are soluble in many conventional organic solvents and so qualitative comparisons may be made between data obtained for these and for the poly(carboranyleterketones). However absolute molecular weights cannot be deduced from these comparisons with any certainty.

Table 4.1

Polymer	$\eta_{inh} \text{ dLg}^{-1}$
PEEK	1.01
P1	0.24
P2	0.59
P3	0.24

Comparing the values obtained for P1-P3 with values obtained for commercial samples of PES determined under the same conditions which lie in the range 0.35-0.45⁵, suggests these materials are of quite high molecular weight with P2 having a substantially higher molecular weight than P1 and P3. The much higher value for the PEEK is possibly more indicative of the much more rigid polymer chain produced by dissolution in sulphuric acid, than of a much greater molecular weight.

4.3.1.2 Gel Permeation Chromatography

G.P.C. has been carried out using solutions of P1, P2 and P3 in THF, the traces obtained are shown in figure 4 (P4 was not examined as it is insoluble in THF). The main problem with using this method is the need to calibrate the apparatus with standard polymer samples of known molecular weight and similar structure to those being analysed. Superimposed on each of the traces in figure 4.1 is the trace produced by a commercial polystyrene standard of molecular weight 72,900. The fact that this sample has a retention volume of the same order as the peaks produced by the carborane polymers cannot be taken as an indication that the various samples have molecular weight of the same value. The G.P.C. technique allows the determination of molecular weight through differentiating between polymer molecules by their size in solution. This occurs through absorption of polymer molecules into the porous stationary phase used in the chromatograph columns. Small molecules are absorbed readily into, and retained in the pores of the stationary phase, with the high molecular weight material being eluted first. The molecule size in solution depends on the polymer chain flexibility. Polystyrene has a very flexible aliphatic backbone and so tends to coil up tightly in solution. The poly(etherketones) backbone on the other hand is much more rigid therefore it will not coil up as tightly as the polystyrene chain and so a poly(etherketone) sample would be expected to be eluted more rapidly than a sample of polystyrene with a similar molecular weight. Hence using polystyrene standards to calibrate the apparatus would lead to an over estimation of molecular weight of the carborane polymers.

The traces do show that P1 and P2 appear to have similar molecular weight distribution and that both appear to be

contaminated with lower molecular weight material as indicated by the smaller peaks at the high retention volume end of the G.P.C. traces. P3 appears to be of lower molecular weight and more highly contaminated with lower molecular weight material suggesting a lower degree of polymerisation in this sample. This may be as a result of the carboranyl carboxylic acid monomer (XVII) used in the formation of P3 being deactivated towards the acylation reaction (see Section 3.3.4) causing the polymerisation to fail to go to completion. The fact that all three polymers seem to be contaminated with low molecular weight material suggests that they will have relatively low number average molecular weights and therefore quite high molecular weight distribution.

G.P.C. data obtained from poly(ethersulphone) samples in DMF solution⁶, prepared by the nucleophilic polycondensation route, showed evidence of chain branching occurring. This was indicated by the presence of peaks in the G.P.C. traces of unrealistically low retention volume (high M.W). The lack of these peaks in the traces in figure 4.1 confirm that the polymers prepared are straight chain polymers.

4.3.2. Spectroscopic Characterisation

The chemical composition of the carborane polymers, P1, P2 and P3 have been confirmed using I.R., ¹³C NMR and ¹H NMR spectroscopy. The insolubility of P4 in suitable solvents means that it has not been possible to obtain NMR data on this sample. These polymers do not give satisfactory microanalysis data, with carbon analysis falling between 20 and 50% lower than expected. This is believed to be because the combustion products of these polymers include large amounts of refractory material which is not indicated in the micro-analysis data obtained.

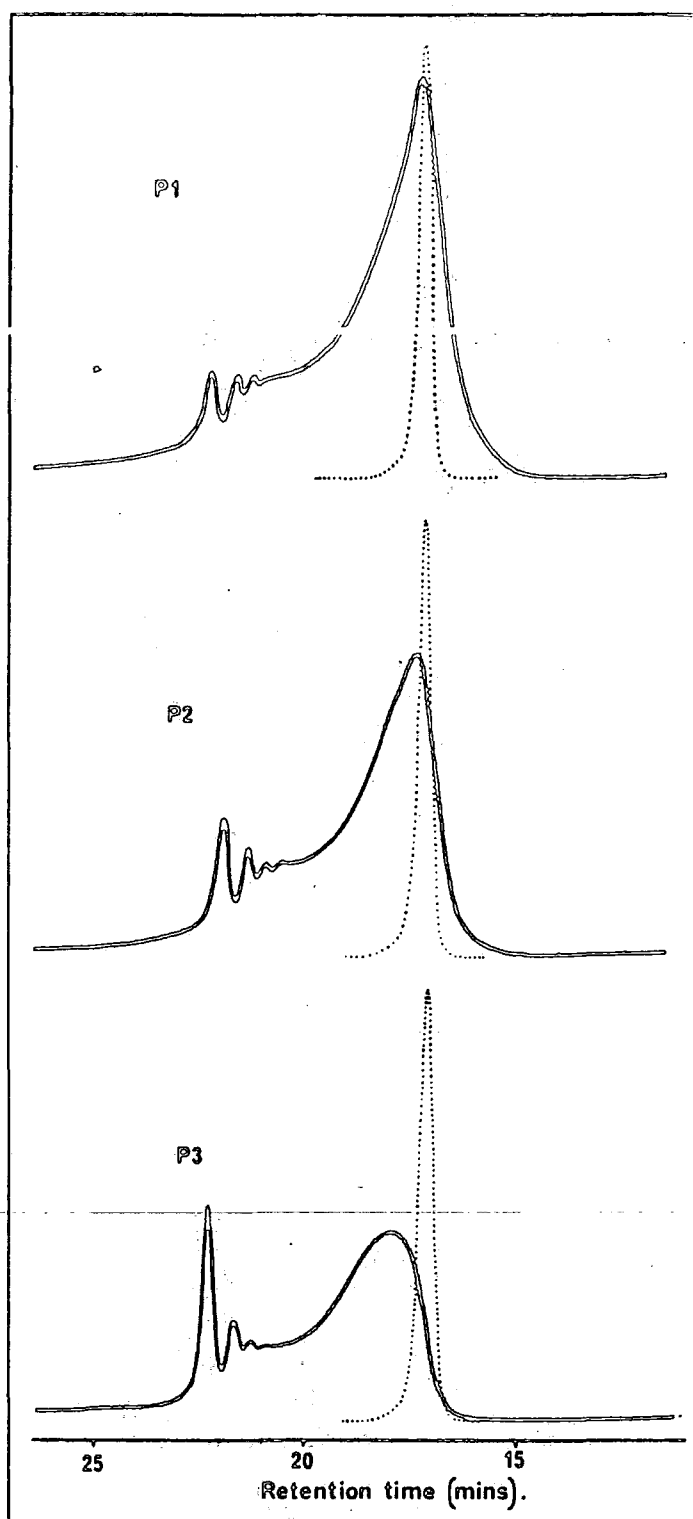
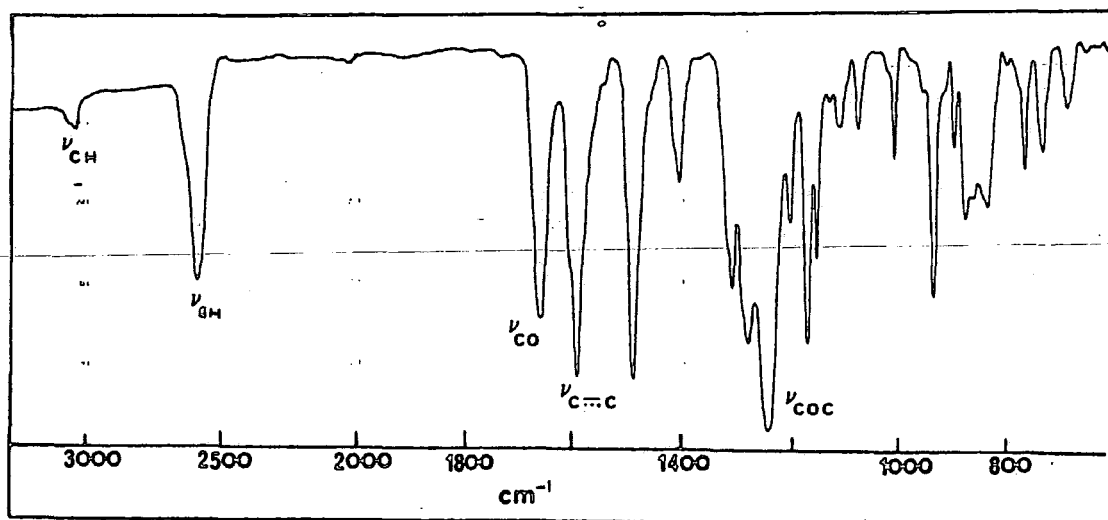


Figure 4.1 GPC traces of P1-P3

4.3.2.1 Infra Red Spectroscopy

Dichloromethane solutions of P1, P2 and P3, when poured onto a flat surface and allowed to evaporate to dryness, deposit brittle transparent films of polymer which give extremely good I.R. spectra. The spectrum shown in Figure 4.2 is that obtained from a film of P1. This clearly indicates that the polymer sample is free of carboxylic acid material by virtue of the lack of OH stretching frequencies and the position of the C=O stretching absorbance (the carboxylic acid C=O absorbance occurs at 1700 cm^{-1}). The spectrum also clearly shows the BH stretching vibrations of the carborane cage and the presence of C-C and C-O-C vibrations all consistent with the expected polymer structure. The I.R. spectra of P4 was obtained as a nujol mull. (Details of the other spectra are given in Sections 4.4.2 to 4.4.5).



4.3.2.2 ^{13}C NMR

The proton decoupled ^{13}C NMR spectra of P1, P2 and P3 in chloroform have been obtained and are shown in Figures 4.3-4.5. The assignments of the non-phenyl resonances are straightforward. The phenyl resonances have been assigned as shown using the assignments made for the compounds (XV), (XVII) and (XIX) given in Sections 2.4.7 and 3.3.4. Additionally $\delta(^{13}\text{C})$ data from the model compounds benzophenone, biphenyl, diphenyl ether and 1-phenyl-ortho carborane have been used to calculate approximate $\delta(^{13}\text{C})$ values of phenyl carbon resonances in the polymers, using the principle of substituent additivity (as for the spectra for (XIV) and (XX) in Section 3.3.4). These spectra confirm that the exclusive para substitution pattern expected is present in the polymers, and that the polymer structures are as shown in Schemes 1-3 and Figures 4.3-4.5.

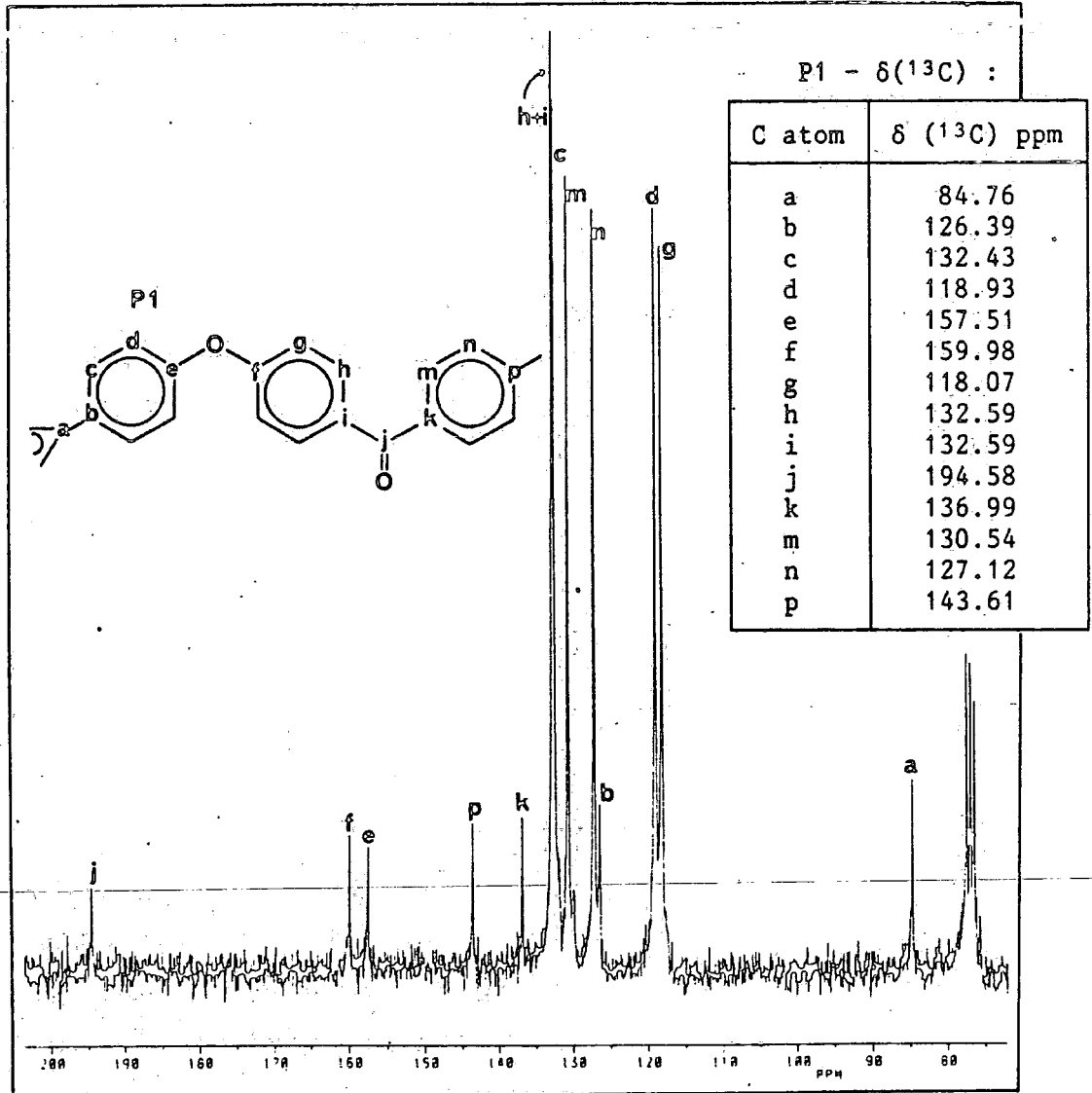


Figure 4.3 ^{13}C Spectrum of P1

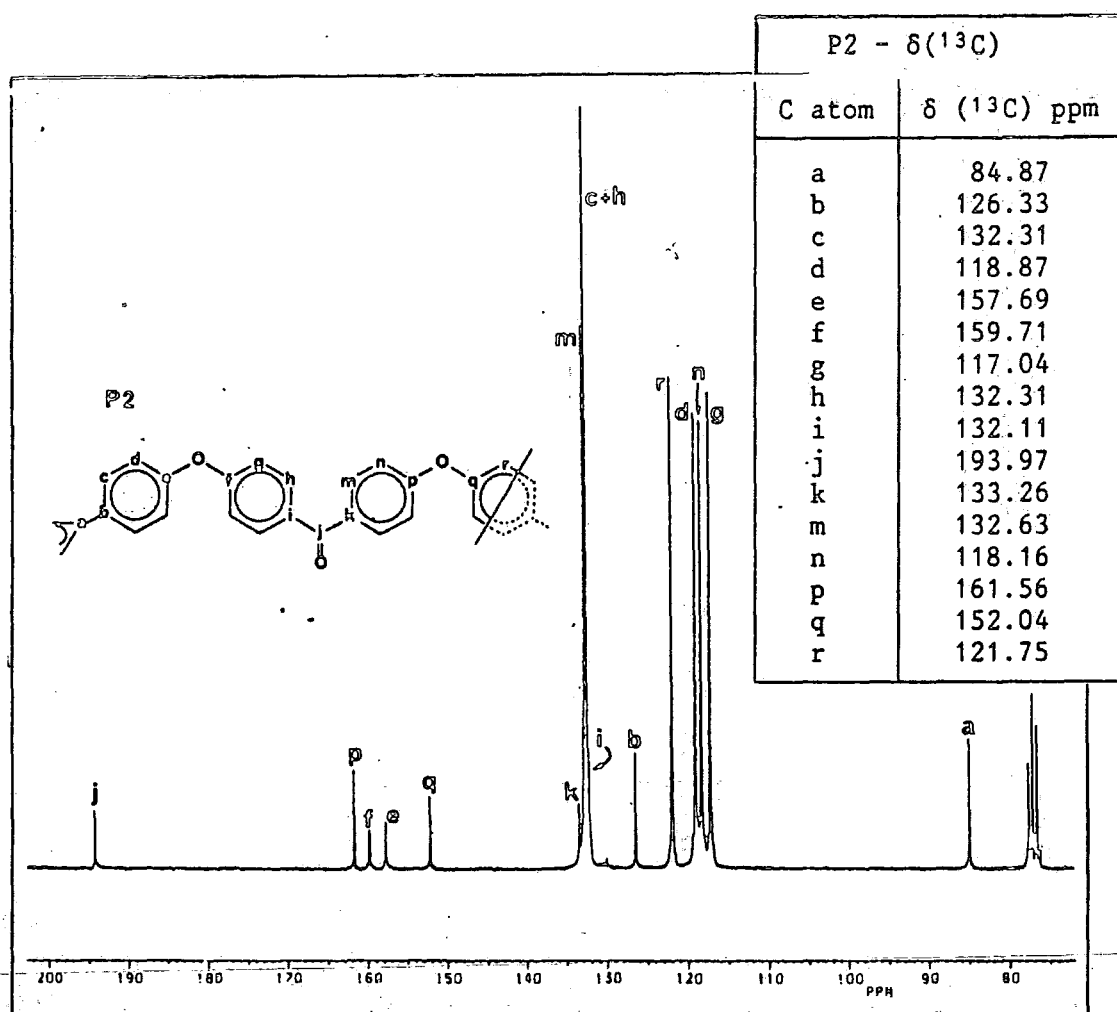


Figure 4.4 ^{13}C NMR Spectrum of P2

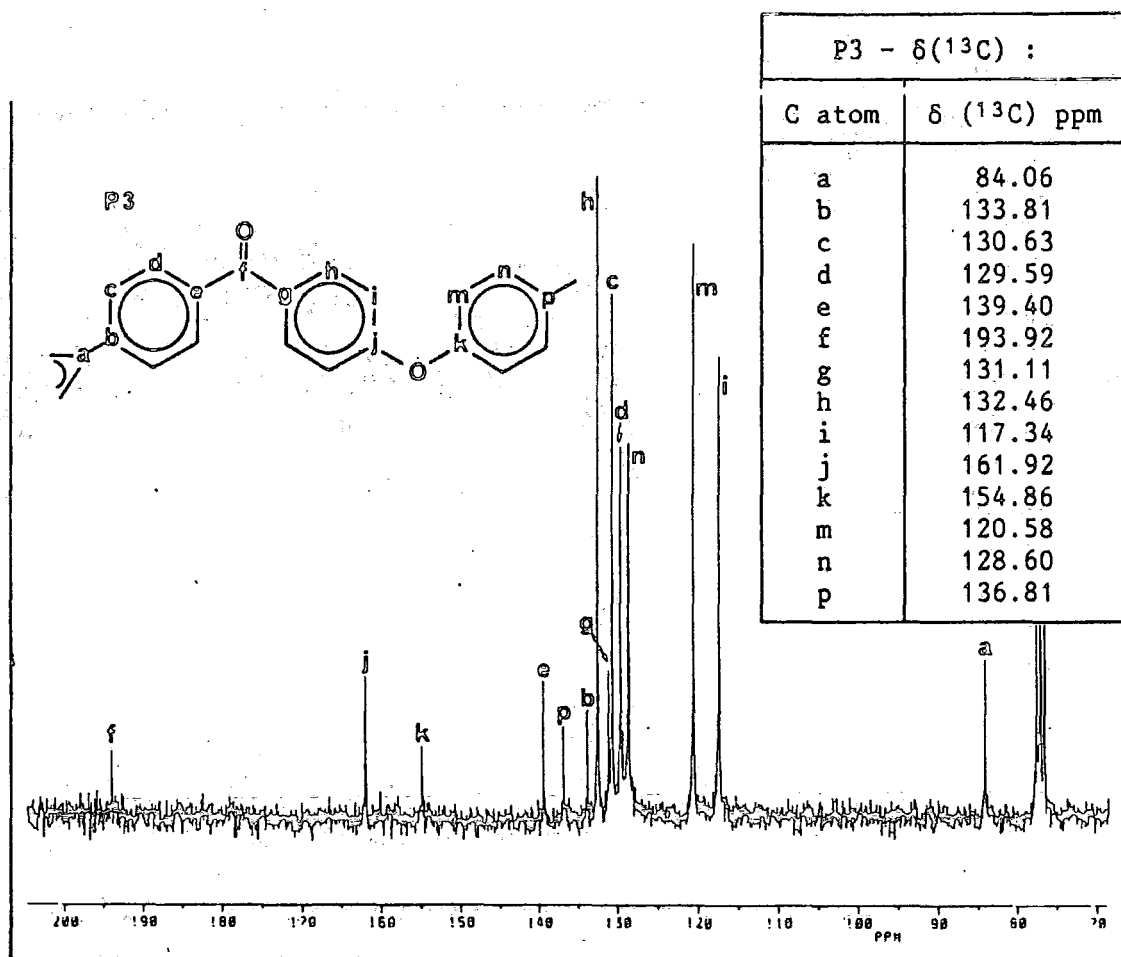


Figure 4.5 ^{13}C NMR Spectrum of P3

4.3.2.3 ^1H NMR

The ^1H spectra for P1, P2 and P3 were recorded in CDCl_3 solution. The phenyl protons resonance region of each spectrum are shown in Figures 4.6 to 4.8 respectively. The proton resonances of the carborane cage in each polymer are visible as a broad hump between ~ 4.0 and 2.5 ppm these are not included. Although in principle integration of the BH signal - vs- the phenyl H signal should give confirmation of the chemical composition of these polymers, obtaining accurate integration data on the BH signal is difficult because the signal is so broad. $^1\text{H}\{^{11}\text{B}$ broad band noise} spectra would possibly be of more use in this context because of the improved resolution that is produced on heteronuclear decoupling of the cage protons.

The phenyl ^1H resonances in each case consist of a series of superimposed $\text{AA}'\text{XX}'$ spin systems characteristic of 1,4 di-substituted benzene, thus these spectra once again confirm that all para substitution present in these polymers. Complete resolution of the full $\text{AA}'\text{XX}'$, couplings are not seen, only first order coupling being visible, hence resonances of ring protons on asymmetrically substituted rings appear as doublets ($J = 7.8$ Hz). Pairs of signals associated with particular rings have been located using selective ^1H homonuclear decoupling and tentative assignments have been made with the help of the principle of substituent additivity to calculate approximate chemical shifts⁷.

Figure 4.6

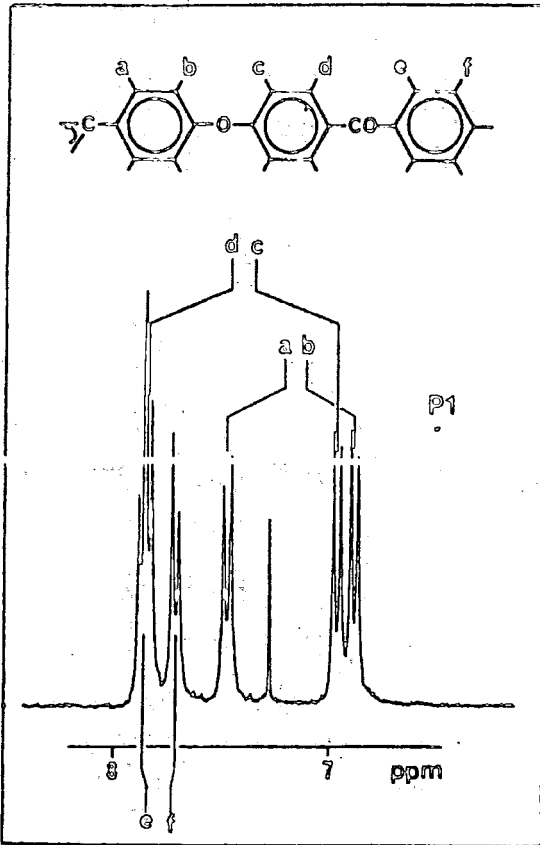


Figure 4.7

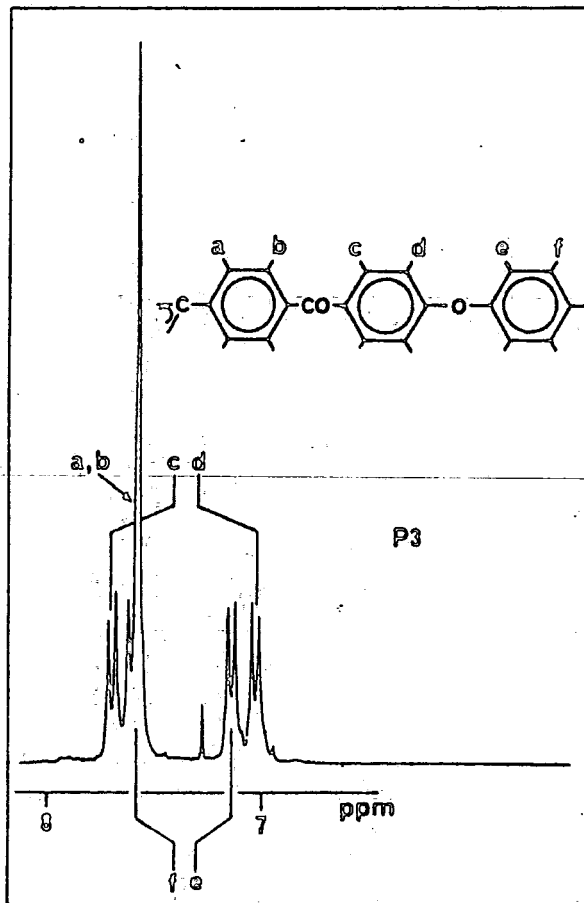
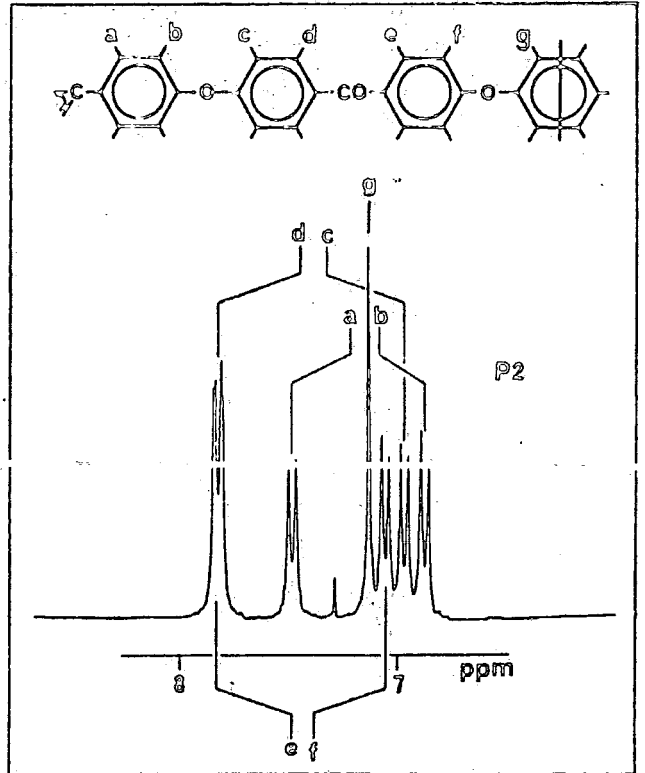


Figure 4.8

¹H Spectra of P1, P2 and P3

4.3.3. Calorimetric and Thermal characterisation of polymers

This section describes the results obtained from Differential Scanning Calorimetry (DSC) and Thermogravimetric Analysis (TGA) studies carried out on P1 to P4.

4.3.3.1 Determination of Glass Transition Temperatures (T_g) and Melting Points (T_m) : DSC Studies

The determination of the T_g and T_m is an essential part of the characterisation of a thermoplastic material. If a prerequisite for suitability of a polymer for a particular application is rigidity, as is the case in many of the current and potential applications of poly(etherketones), then the T_g determines the maximum temperature to which the polymer may be taken to under stress. The T_g is defined as the temperature at which an amorphous polymer (or the amorphous phase of a partially crystalline polymer) is transformed from a glass to a rubbery solid. That is to say, segmented movement of a polymer molecules reactive to each other becomes possible (it is also referred to as the softening temperature). T_m is the temperature at which the crystallites of a crystalline or partially crystalline polymer melt. Amorphous polymers therefore do not have a T_m .

At its T_g a polymer undergoes a number physical changes as a result of the increased molecular motion within it, allowing the T_g to be observed. In particular the greater motion increases the number of degrees of freedom of the polymer molecules and so the heat capacity (C_p) rises markedly. It is this change in C_p that is

monitored in the DSC experiment. The DSC technique involves supplying heat energy to the sample and a reference simultaneously so that the temperatures of the two increase but remain equal. As the temperature of the sample passes through its T_g , its C_p increases meaning that more energy is required to keep it at the same temperature as the reference, enabling the T_g to be measured. The T_m is registered as an endothermic peak produced by the temporary increase in C_p of the sample as a result of the latent heat required to break down the crystallinity of the polymer.

The DSC traces produced by P1-P4 are shown in Figure 4.9. The trace produced by the PEEK sample synthesised is also shown. The traces of P1-P4 all show very prominent glass transitions but no T_m , indicating that these polymers are totally amorphous. In contrast, the PEEK sample has a much smaller glass transition and a pronounced melting endotherm since it is a highly crystalline material. It is this crystallinity that gives PEEK its remarkable solvent resistance. The fact that P1-P4 are completely amorphous is consistent with their much greater solubility in organic solvents.

The values of T_g for these polymers are given in Table 4.2 (values quoted are the onset temperatures of the glass transition features). It is obvious that the incorporation of the cage into the poly(etherketone) backbone has resulted in an increase in the T_g of these polymers.

The factors that will influence the T_g of these polymers are the strength of interaction between polymer chains, the rigidity of the polymer chain and the M.W. of the sample.

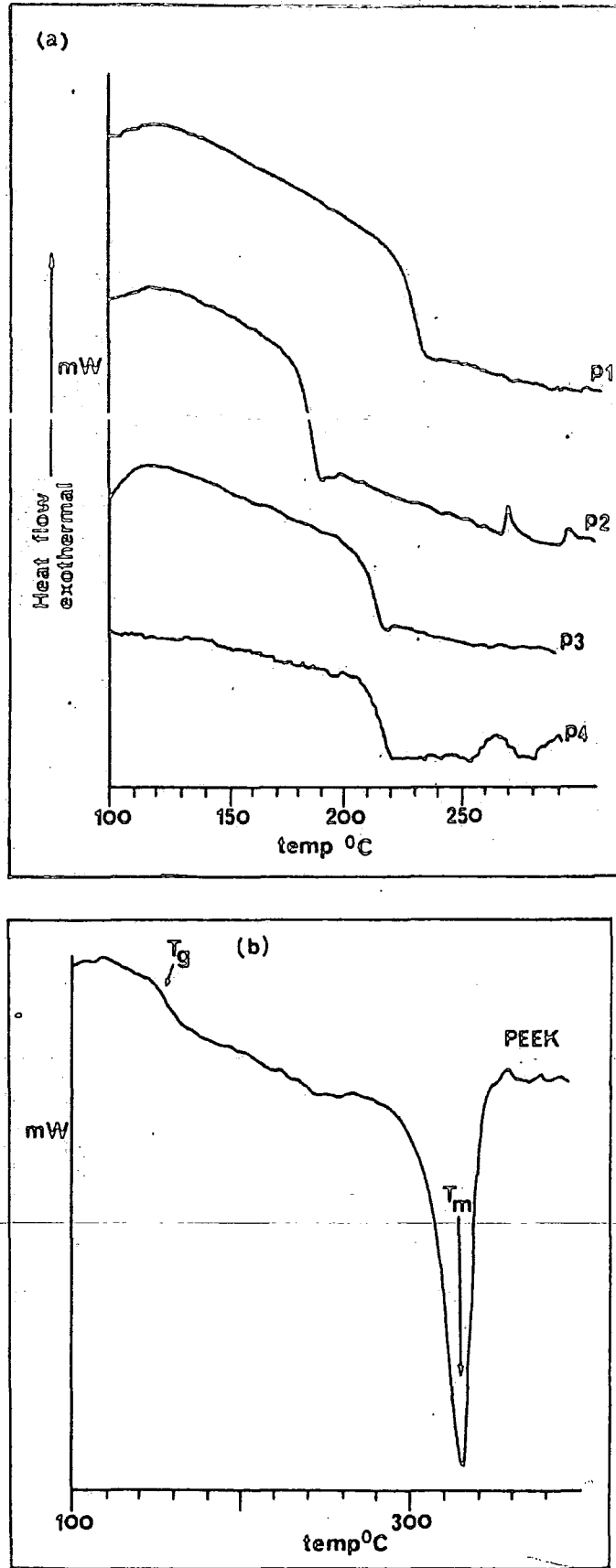
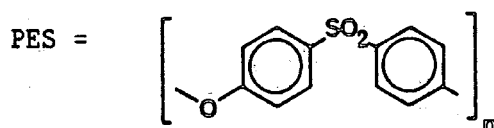
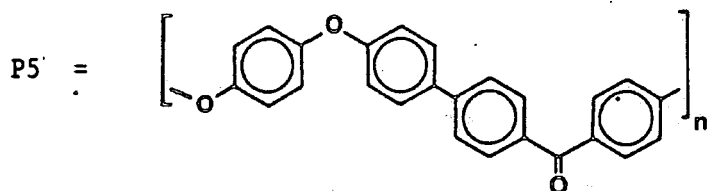


Figure 4.9 DSC traces of (a) P1-P4 and (b) PEEK

Table 4.2

Polymer	T _g (°C)	T _m (°C)
P1	214	-
P2	174	-
P3	209	-
P4	210	-
PEEK*	147 (144)	329 (335)
PEK ²	154	367
P5 ²	167	416
PES ⁸	230	-



* Values in brackets are taken from Ref. (2)

A simplified expression relating T_g to the number average molecular weight of a polymer M_n ⁹ is given by:

$$T_g = T_g^\infty - \frac{K}{M_n}, \quad T_g^\infty = T_g \text{ of a sample containing molecules of infinite M.W.}$$

K = a positive constant

From this it can be seen that as the M_n increases, so the T_g becomes less dependent on it. Therefore above a certain M_n it seems reasonable to assume that T_g is independent of the M_n . Hence in interpreting the trends seen in the T_g of the polymers prepared, the effect of M_n has been assumed to be negligible. It can be seen from Table 4.2 that if the proportion of the ketone links in the PEEK chain is increased to give PEK, the T_g rises. This is probably largely the result of a strengthening of the interchain forces brought about by an increase in the dipole interactions between chains. Also introduction of a biphenyl link into the PEEK chain to give P5 causes a rise in T_g because of the increased chain rigidity imposed by this linkage. Replacement of the CO group in PEK with the sulphone group to give PES greatly enhances the T_g , again because the tetrahedral SO_2 group is a much more rigid linkage.

The fact that the carborane polymers are totally amorphous indicates that the introduction of the 1,2 diphenyl-ortho-carborane unit disrupts interactions between polymer chains. Clearly the feature determining the high T_g of these carborane polymers is the chain rigidity. On examining the geometry of the 1,2 diphenyl-ortho-carborane unit (see Figure 4.10) it can be seen that rotation of the phenylene rings attached to the cage will be sterically hindered.

Also rotation about the C(1) C(2) bond will not be possible. Hence an abundance of these links in the polymer chain would be expected to substantially increase the chain rigidity, thus restricting its face movement and raising the T_g of the polymer as is observed. This observation is reinforced by comparing the T_g of the different carborane polymers. The T_g of P2 is expected to be lower than those of P1, P2 and P4 as this species has a larger proportion of the flexible ether linkages in the polymer repeat unit. This is observed.

From the regularity of the chain conformation and the stiffness of the polymer chains in PEEK and PEK it is fairly easy to see how these polymers readily crystallise. X-ray diffraction data on these polymers obtained by several workers^{2,10,11} show that the fibre repeat unit (10 \AA^2 , 9.72 \AA^{10}) does not correspond to the chemical repeat unit. Instead it consists of two phenylene rings joined either by two ether links or one ether and one carbonyl link. Hence the crystal structures of PEEK and PEK are virtually identical and are very similar to that of polyphenylene oxide¹². Incorporating the 1,2(diphenyl)-ortho-carborane will introduce an ortho link in the polymer chain which will severely disrupt this regularity in the chain conformation.

Figure 4.10 shows a schematic representation of the chain conformation of PEEK and of P1 to illustrate visually the ortho kink produced by the 1,2 diphenyl-ortho-carborane unit. It is clear to see how the major irregularity introduced by this link disrupts the polymer chain interactions prohibiting polymer crystallisation.

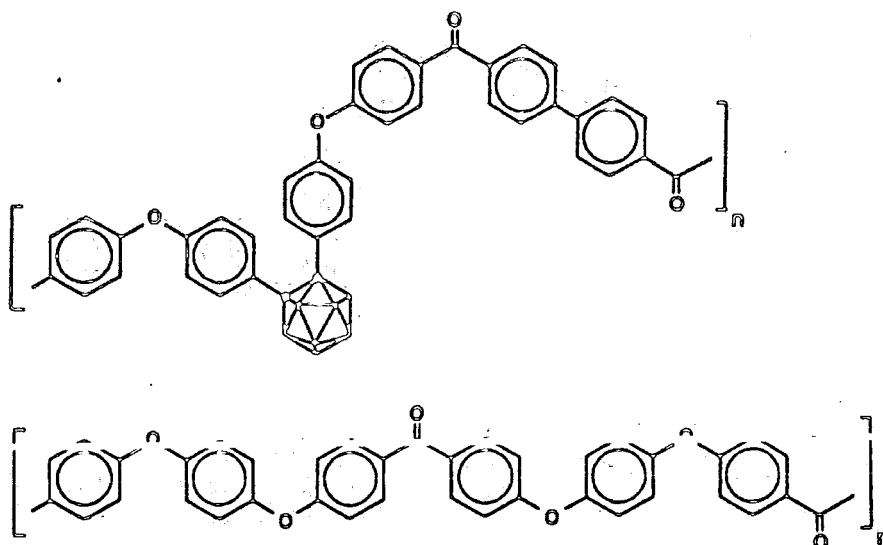


Figure 4.10

The observations seen here suggest that incorporation of links of similar geometry to the 1,2 diphenyl-ortho-carborane unit, may have the same influence on the T_g and crystallinity of these polymers. Thus polymers incorporating the 1,2 diphenyl-benzene unit may exhibit solution and calorimetric properties similar to those of the poly(carboranyl-etherketones) discussed here.

4.3.3.2 Thermal stability of polymers: TGA Studies.

The TGA technique involves measuring the % or fractional weight change of a polymer whilst it is heated at a certain rate to a given temperature. As such it gives an indication of the thermal stability of a polymer, with weight changes at particular temperatures highlighting chemical changes in the material (usually decomposition or oxidation).

The TGA plots obtained for P1-P4 in both air and nitrogen are shown in Figures 4.11-4.14. The plots obtained in nitrogen show that P1 and P3 have very similar decomposition rates and % weight losses

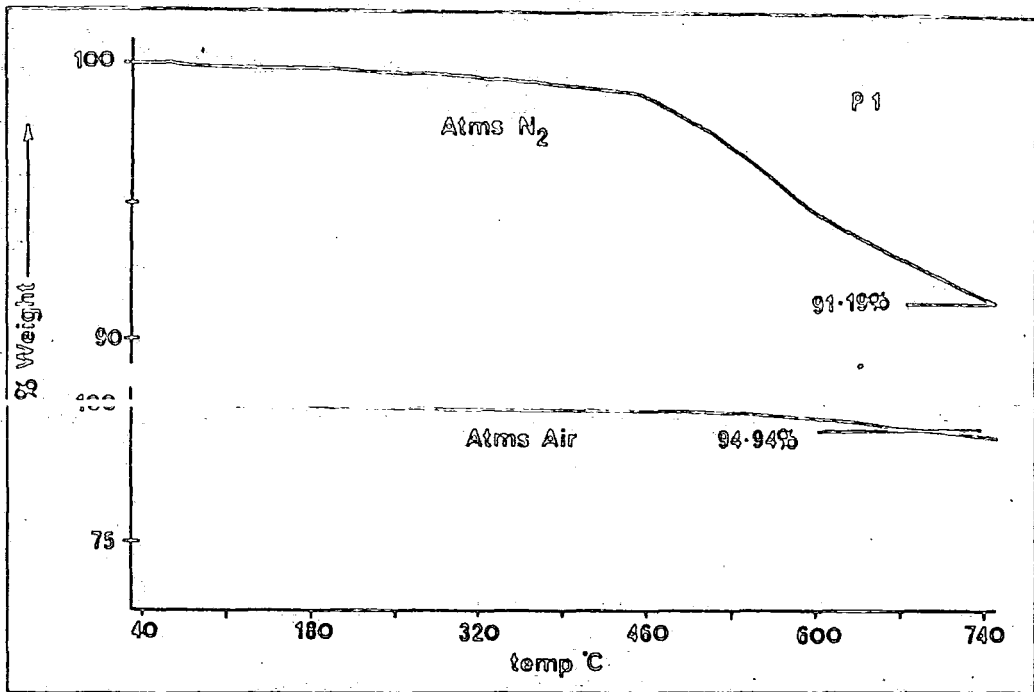


Figure 4.11 TGA plots from P1

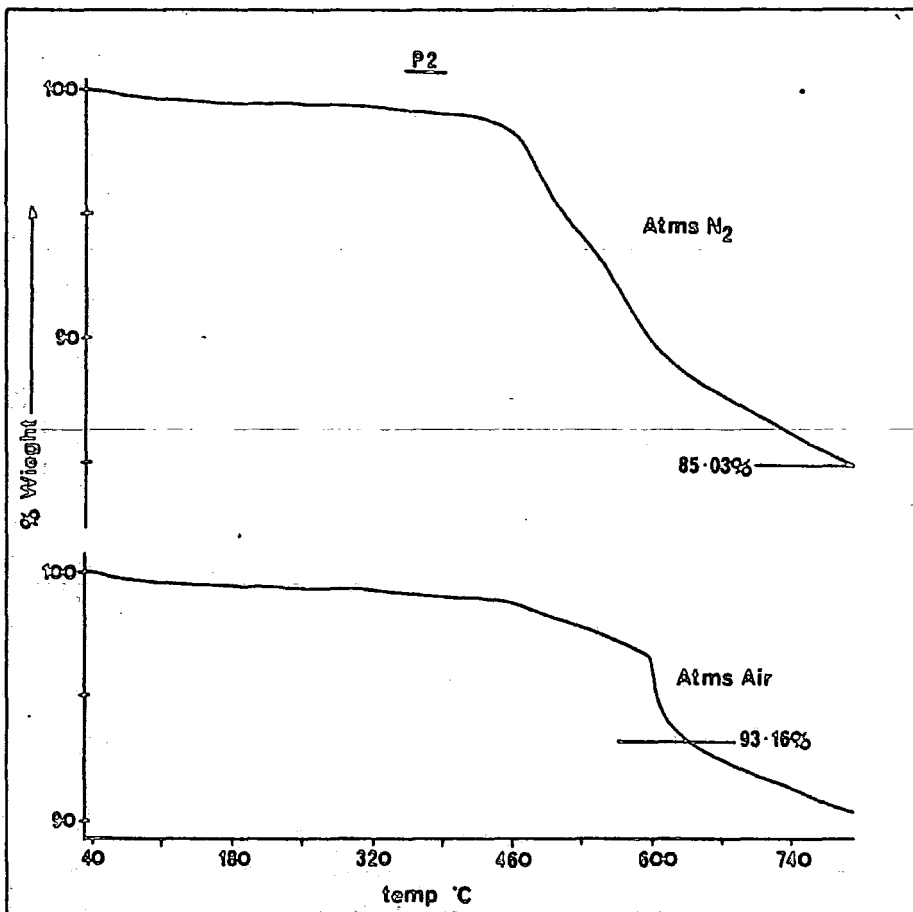


Figure 4.12 TGA plots from P2

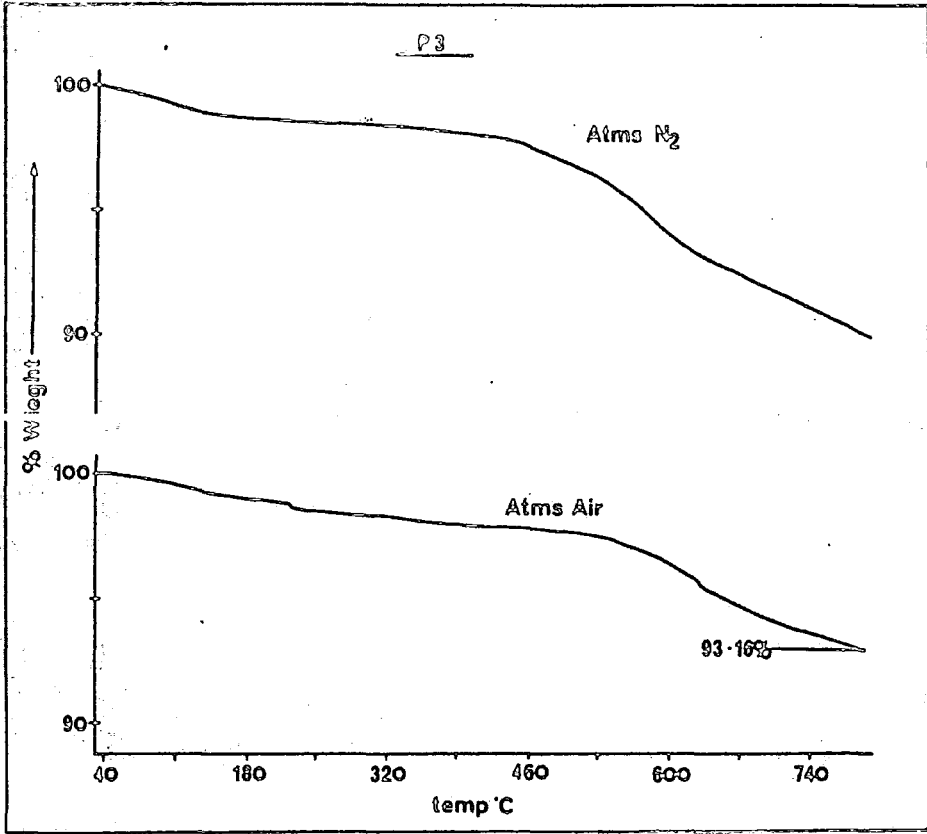


Figure 4.13 TGA plots from P3

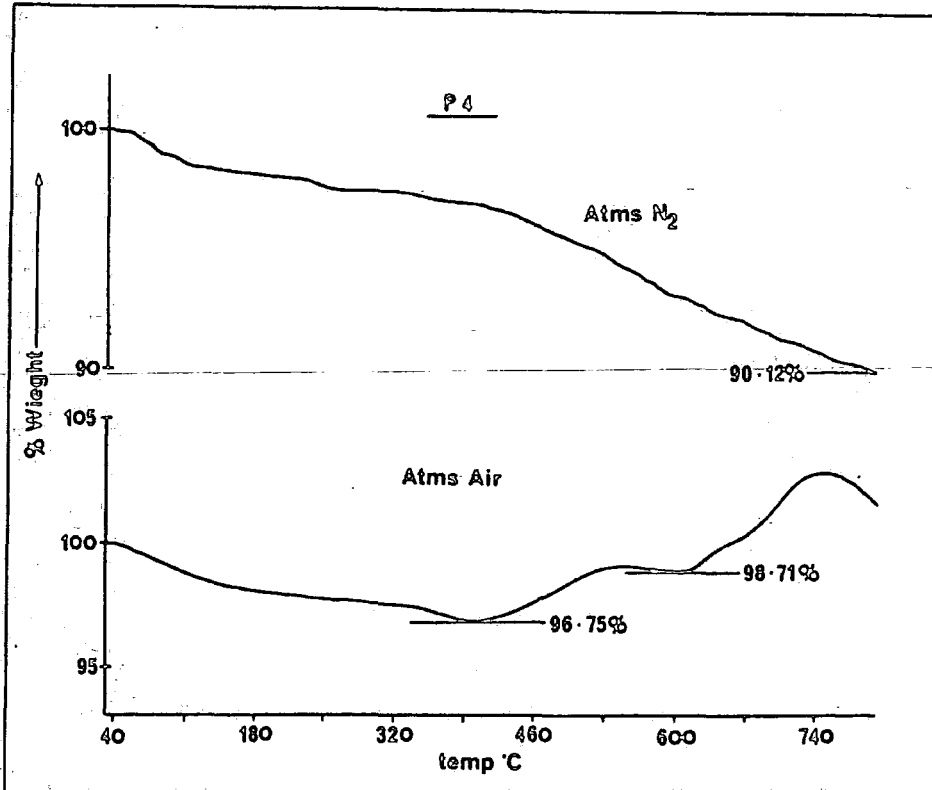


Figure 4.14 TGA plots from P4

(approximately 9% at 798°C). This is to be expected since these polymers have the same chemical composition even though they have slightly different structures. P4 also shows a similar % weight loss (~9%) at 798°C. P2 which has the lowest proportion of carborane in the polymer chain shows the most pronounced decomposition at 798°C with a weight loss of approximately 15%. All polymers show a 1-2% weight loss between 40 and 250°C and this is attributed to the evaporation of residual solvent (water and methanol) trapped in the polymer.

The TGA plots from runs carried out in air are substantially different, with weight losses decreasing for P1 (~5%), P2 (~10%) and P3 (~5%). The plot for P4 (figure 4.14) shows an initial decrease followed by an increase in weight.

PEEK has been shown to undergo approximately 40% weight loss, on heating from 50-800°C at a rate of 20°C min⁻¹, between 550 and 700°C in a nitrogen atmosphere¹³. Obviously taking PEEK to be representative of all poly(etherketones) is a slight over simplification, nevertheless comparing this observation with the results obtained for the carborane polymers P1-P4 clearly indicates that the presence of the ortho-carborane cage inhibits both the loss and rate of loss of volatile material from the poly(etherketone) backbone.

Studies on the related poly(ethersulphones)¹⁴ have shown that both in air and nitrogen the primary cause of weight loss is chain scission at linkages between phenylene rings. This gives rise to the primary products of pyrolysis comprising derivatives of phenol

and diphenyl sulphone with sulphur dioxide being evolved as well. It has been proposed that the thermal decomposition of poly(etherketones) proceeds through a similar mechanism¹³. This would lead to the production of derivatives of phenol and benzophenone accompanied by the evolution of carbon monoxide (and carbon dioxide in air).

The presence of carboranes in polymer backbones causing a decrease in thermally induced weight loss has been observed in a number of other polymer systems¹⁵. Some examples include siloxanes (Dexsils) (see Section 1.2.2), polybenzimidazoles¹⁶, polyurethanes¹⁷ and phenol formaldehyde networks¹⁸. In some cases, the most notable being the Dexsil series, the electronic influence of the cage has a marked stabilising effect on the polymer backbone.

Considering the polymers studied here, the carborane to phenyl ring linkage, used to incorporate the cage into the polymer backbone, is of the same order of thermal stability as the other links in the polymer chain. This is confirmed by thermolysis studies carried out on carboranyl C phenyl derivatives, which show that the C phenyl linkage starts to leave at temperatures above 500°C¹⁹. This suggests that the inductive effect of the cage is not likely to have an overriding influence on the polymer stability. More important seems the transformation that the cage itself begins to undergo at 450°C and above (see Section 2.2.2)¹⁹. At these temperatures the cage starts to liberate hydrogen causing the icosahedra to condense through B-B links producing polycarborane material. In polymers containing carborane cages this process will cause crosslinking between polymer

chains, creating a three dimensional network throughout the polymer thus inhibiting the loss of volatile material. This phenomena would be most predominant for materials with a high carborane content and is a possible explanation for the more pronounced weight loss exhibited by P2 compared to that by P1, P3 and P4. The hydrogen liberated by carborane decomposition has also been reported to have a stabilising effect on carborane polymers²⁰, by its reaction with reactive chain ends produced by chain scission.

The smaller % weight loss from these polymers in air is due to weight loss in the organic sections of the polymer being compensated by a gain in weight produced by the oxidation of the carborane cage which gives non volatile boron oxygen compounds. This oxidation of the cage is expected to take place above 300°C in a gradual manner. As indicated by studies on other carborane polymers^{15,18}, it proceeds through intermediate B-hydroxy compounds to B-O-B bridged species ultimately producing boric oxide B₂O₃. Clearly this oxidation will have a greater influence on polymers with a high boron content. Hence P4 with the highest boron content shows an increase in weight at 798°C in air and P2, which has the lowest boron content, shows the greatest weight loss in air.

This observation of mass increase on heating in air has been observed for other carborane polymers^{15,16,18}. In addition the oxidation of the cage has been proposed as a further mechanism for the stabilisation of polymers^{16,18}. One proposal suggests that B₂O₃ formed on the outer layers of a polymer forms a protective coating¹⁶. The crosslinking of

partially oxidised material in intermediate layers ° within polymers, is also thought to act as a barrier both to oxygen diffusing into the polymer and to volatiles, evolved in the thermolysis of inner polymer layers, which diffuse out of the polymer. It has also been shown that the presence of B_2O_3 alone will stabilise organic polymers also¹⁸, although the reasons for this are not absolutely clear.

4.4 EXPERIMENTAL

4.4.1 The preparation of P.E.E.K.

4,4' difluorobenzophenone (11.00 g, 50.4 mmoles), hydroquinone (5.50 g, 50.0 mmoles weighed out rapidly as this compound is air and moisture sensitive), sodium carbonate (5.31 g, 50.0 mmoles) and diphenylsulphone (70.00 g) were placed in a reaction vessel. The solid mixture was stirred mechanically and purged with dry nitrogen for 12 hours. A heating jacket was then placed around the vessel and the apparatus heated up to 170°C. This temperature was maintained for 30 minutes. The apparatus was then heated to 250°C and maintained at this temperature for 30 minutes and finally the temperature was raised to 300°C which was maintained for 5 hours causing the reactants to form a viscous, pale amber liquid. The apparatus was allowed to cool to room temperature and its solidified contents chipped out and crushed. The reaction mixture was then milled to a fine powder, extracted three times each with boiling acetone, water and methanol. The resultant polymer, an off white solid was dried on a vacuum oven (120°C), yield 14 g, 97%, η_{inh} 1.01 (in 98% sulphuric acid). For DSC results see Section 4.3.3.1.

4.4.2 Preparation of Polymer 1

Finely divided 1,2-bis-(4-phenoxyphenyl)-ortho-carborane (XX) (0.4765 g, 0.993 mmoles) and 4,4' biphenyldicarboxylic acid (XI) (0.2400 g, 0.991 mmoles) were mixed in a flask purged with nitrogen. 15 mls of TFSA were added and the mixture stirred vigorously for 20 hours producing a clear viscous orange solution. This was then added dropwise to 100 mls of vigorously stirred distilled water producing off white polymer globules which were filtered off and refluxed three times each with water, water/methanol (50/50) and finally once with methanol. The white solid was filtered and dried in a vacuum oven (120°C)

and identified as polymer 1, yield; 0.65 g, 95.6%.
Characterised as outlined in Section 4.3.

4.4.3 Preparation of P2

A mixture of 1,2 bis(4-phenoxyphenyl)-ortho-carborane (0.4849 g, 1.01 mmoles), 4,4' (1,2 diphenoxybenzene)dicarboxylic acid (XVIII) (0.35 g, 1.00 mmoles) and TFSA (16 mls) was stirred vigorously under nitrogen for 24 hours producing a viscous clear orange solution. The polymer was isolated as in Section 4.4.2 and identified as P2, yield 0.76 g, 95.7%. Characterised as outlined in Section 4.3 and as follows:

Infra Red (Polymer film from CH_2Cl_2 solution) (cm^{-1}) 3050 (w) (Aromatic CH stretch); 2620 (sh) 2580 (s) (BH stretch); 1650 (m) (C=O stretch); 1590 (s) (C=C stretch); 1495 (sh); 1490 (s); 1410 (m); 1305; 1277; 1245 (s) 1230 (s) (C-O-C asymmetric stretch); 1188; 1174; 1160; 1145 (sh); 1105; 1070; 1010; 950; 938 (m); 906 (w); 893 (w); 882 (w); 861; 840; 765 (m); 730 (m); 680; 592 (w); 577 (w); 534 (w); 510.

4.4.4 Preparation of P3

1,2-bis-(4-carboxyphenyl)-ortho-carborane (0.3763 g, 0.98 mmoles) and 4,4' diphenoxy-biphenyl (0.3330 g, 0.985 mmoles) were dissolved in TFSA (14 mls) and the solution left to stand under nitrogen for 60 hours, producing a dark red solution. Polymer 3 was isolated from the TFSA solution as in Section 4.4.2 as a white powder (repeated extraction with boiling methanol was required to remove residual TFSA). Yield 0.54 g, 80%. Characterised as outlined in Section 4.3 and as follows:

Infra Red (Polymer film) (cm^{-1}): 3050 (w.sh) 3030 (w) (Aromatic CH stretch); 2580 (s) (B-H stretch); 1655 (s) (C=O stretch); 1600 (sh); 1578 (s) (C=C stretch); 1486 (s); 1400; 1303; 1275 (m); 1240 (s) (C-O-C asymmetric stretch); 1197; 1167; 1148; 1123 (w); 1103 (w); 1070 (w); 1003; 948 (w.sh); 930 (m); 889; 870;

855 (sh); 830; 792 (w); 760; 727; 680; 646 (w); 592 (w); 500.

4.4.5 Preparation of P4

Finely divided 1,2 bis(4-phenoxyphenyl)-ortho-carborane (XX) (0.2092 g, 0.436 mmoles) and 1,2 bis(4-carboxyphenyl)-ortho-carborane (XVIII) (0.1672 g, 0.435 mmoles) were mixed in a flask purged with nitrogen. TFSA (5 mls) was added and the mixture stirred until all the reactants had dissolved producing a clear orange solution. This was allowed to stand for 24 hours producing an orange, opaque gelatinous solid. 10 mls of TFSA were added to liquify the reaction mixture. This solution was treated as standard (see Section 4.4.2) producing P4 as a white powder, yield 0.278 g, 77%. Characterised as follows:

Infra Red (Nujol) (cm^{-1}); 3050 (w.sh) (Aromatic CH stretch); 2640 (w.sh) 2590 (s) (BH stretch); 1730 (w); 1665 (s) (C=O stretch); 1610 (w.sh); 1594 (s) (C=C stretch); 1500 (s); 1463 (s); 1428 (w.sh); 1409; 1390 (m); 1370 (sh); 1328 (sh); 1308 (m); 1280 (m); 1247 (s) (C-O-C asymmetric stretch); 1220 (sh); 1178 (m); 1153; 1120 (w.br); 1076; 1018; 1005; 976 (w); 957 (w); 933 (m); 896; 885; 875 (sh); 860; 843; 767; 730; 688; 645 (w); 612 (w); 598 (w); 583 (w); 510.

4.4.6 Solution Viscosities

Inherent viscosities (η_{inh}) of 0.1% solutions were measured using an Ubbelohde viscometer at 30°C. The η_{inh} of PEEK was determined in 98% sulphuric acid and the η_{inh} of P1, P2 and P3 in DMF.

4.4.7 Gel Permeation Chromatography

GPC was carried out using a Perkin Elmer 601 liquid chromatograph equipped with three 30 cm PL gel columns of pore size 10^5 , 10^3 and 300 Å. Sample detection was carried out using

a Perkin Elmer LC-55 U.V. Spectrophotometer operating at 254 nm. The chromatograph was operated using THF as the solvent at a flow rate of 1 cm³/min. The sample concentrations used were 0.5% by weight, injected in 10 μ l aliquots.

4.4.8 Differential Scanning Calorimetry

DSC studies were carried out using a Mettler TA3000 system. Samples of between 10-20 mg were analysed in pellet form by heating at 20°C/min to approximately 40°C above the melting endotherm or T_g were appropriate, cooling and reheating at 20°C/min (values T_g and T_m quoted are taken from the second run).

4.4.9 Thermogravimetric Analysis

TGA studies were carried out on a Perkin Elmer PGF-2 Thermobalance interfaced to a System 4 programmer. Data was processed and presented using a Perkin Elmer TDAF Data Station (equipment kindly lent and operated by D. Goodall, N. Boswell, I.C.I. plc, Runcorn).

Samples of 5-13 mg were analysed in pellet form because of difficulties encountered with handling the polymers powders due to static. Runs were carried out using a heating rate of 10°C min⁻¹ from 40°C to ~800°C.

4.5. CONCLUSIONS AND FUTURE WORK

The incorporation of the ortho-carborane cage into the backbone of several poly(etherketones) has been accomplished by using suitably substituted 1,2-diphenyl-ortho-carborane derivatives as co-monomers in electrophilic polycondensation reactions performed in TFSA. The characterisation of these polymers has shown that the physical and chemical properties differ quite markedly from those of the poly(etherketones) from which they are derived.

The incorporation of the cage has rendered these usually highly crystalline polymers, completely amorphous. This means that unlike poly(etherketones) in general, the carborane polymers are readily soluble in organic solvents. This phenomenon has been explained in terms of the disrupting influence that the 1,2-diphenyl-ortho-carborane group has on the regular chair conformation of the poly(etherketone) chain. The T_g of these polymers increases markedly as a result of the introduction of the 1,2 diphenyl-ortho-carborane moiety which has been attributed to the increase in chain rigidity imposed by this unit. TGA studies on these polymers have shown that weight loss from poly(etherketones) as a function of temperature, is substantially reduced on incorporating carboranes into the polymer chain. This is believed to be due to the crosslinking between polymer chains produced by carborane dehydrogenation and condensation at elevated temperatures. The conservation of mass observed when these polymers are heated in air has been attributed to the oxidation of the carborane cage, yielding heavier non-volatile boron oxygen compounds.

This study has been mainly concerned with the development of synthetic routes to and the subsequent chemical characterisation of poly(carboranyl-etherketones). Clearly changing the physical state of the parent materials by destroying their crystallinity, whilst substantially increasing the chain rigidity, will have quite pronounced effects on the mechanical properties of these

thermoplastics. Therefore in order to comment on the total effect of the presence of the ortho-carborane cage in these polymers, a more detailed study into the mechanical properties of these materials is needed. This would require the scaling up of the monomer and polymer preparations described in this and the preceding chapter. The bulk properties of these polymers could then be conveniently assessed by monitoring the toughness of films produced by melt pressing.

A more absolute indication of molecular weights of these polymers would be of use both for determining the optimum conditions required for producing high quality samples and in explaining the physical properties of the polymers to a certain extent. Because of the unique nature of these polymers, calibration of the techniques more conveniently and routinely carried out, such as measurement of solution viscosities, is required. Determination of number average and weight average molecular weights of a few samples, and relating these to η_{inh} values obtained for the same samples, would allow this to be done.

Caution has to be exercised when saying whether or not the thermal stability of the poly(etherketone) chain has been enhanced by the presence of carboranes using TGA alone. Chemical changes such as crosslinking, which are not highlighted by TGA can have pronounced effects on the physical and mechanical properties of polymers.

Further information confirming the nature of the chemical changes that the polymers undergo and the temperatures at which these changes occur, would both complement the data already obtained and provide a more complete picture of the thermal characteristics of these materials. Differential Thermal Analysis (DTA) studies would allow this by supplying information concerning the enthalpic changes accompanying the chemical and physical transformations the polymers undergo, as a function of temperature. Identification of the products of polymer pyrolysis would also be informative.

The destruction of the polymer crystallinity by the presence of the

1,2-diphenyl-ortho-carborane unit will have increased the permeability of the polymers (hence their increased solubility) which may reduce their chemical resistance. Therefore the preparation of poly(carboranyletherketones) which retain a degree of crystallinity would be favourable. A possible way of achieving this would be by using meta carborane isomers in the polymerisation reactions employed in this study. The approximate geometry of the 1,7-diphenyl-meta-carborane unit is shown in Figure 4.15. It demonstrates that the

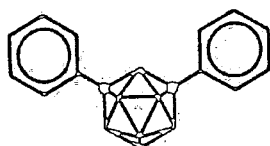
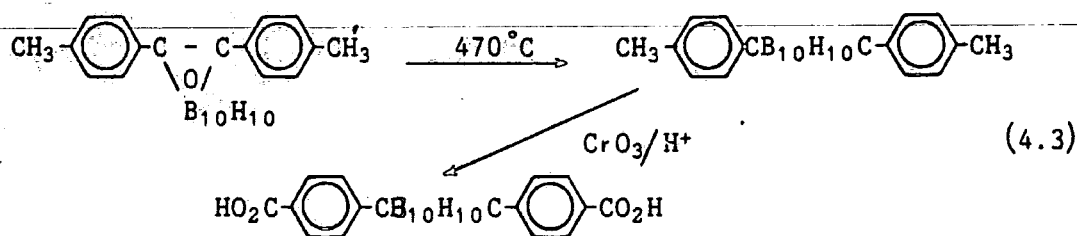


(Figure 4.15)

kink produced by this link in a poly(etherketone) would be less disruptive on the chain conformation and therefore may allow some crystallisation to occur. An additional advantage in using this isomer would be that it is slightly more thermally and chemically stable than its ortho parent¹⁹. The preparation of suitable monomers could be carried out by the synthesis of corresponding ortho-carborane derivatives followed by their thermal isomerisation. For instance the monomer 1,7-bis-(4-carboxy phenyl)-meta-carborane can be prepared as in equation 4.3²¹.

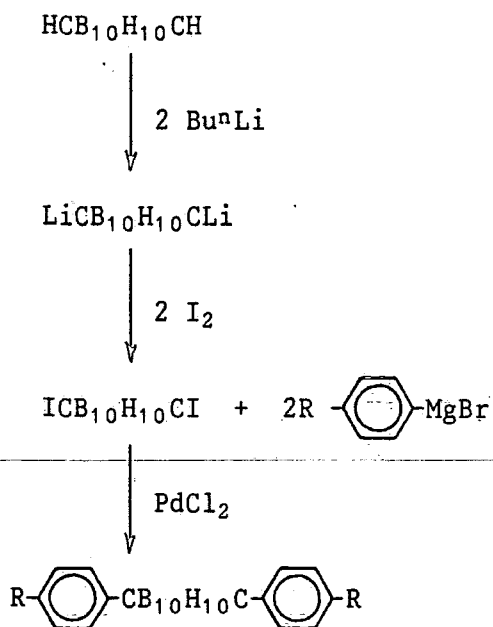


Isomerisation of 4-phenoxyphenyl-ortho-carborane derivatives may be hampered by the scission of the ether linkage under the isomerisation conditions used.

Another potential route into these derivatives that could be both

very useful and academically interesting to develop would be the substitution of the preformed cage with aryl substituents. Meta carborane is commercially available and so functionalising this in one step would greatly reduce the time spent in monomer synthesis. Possible ways of achieving this would be through adaptation of coupling reactions between aryl iodides and aryl Grignards to give biphenyls, catalysed by $(\text{Ph}_3\text{P})_2\text{Ph}(\text{Ph})\text{I}$ ²² and PdCl_2 ²³ (see Scheme 5). Alternatively a variation of the $(\text{Ph}_3\text{P})_2\text{PdCl}_2/\text{CuI}$ (see Section 3.5.9 (iii)) catalysed coupling of aryl iodides to acetylenes may be effective in the one step preparation of aryl derivatives of meta carborane.

Scheme 5



R = substituent reactive towards electrophilic polymerisation

4.6 References

1. R.A. Clendinning, A.G. Farnham, W.F. Hall, R.N. Johnson, C.N. Merriam, J. Polym. Sci. A.1., 1967, 5, 2375.
2. T.E. Attwood, P.C. Dawson, J.L. Freeman, L.R.J. Hoy, J.B. Rose, P.A. Staniland, Polymer., 1981, 22, 1096.
3. J. Devaux, D. Delimov, D. Daoust, R. Legras, J.P. Mercier, C. Strazielle, E. Nield, Polymer, 1985, 26, 1994.
4. M.T. Bishop, F.E. Karasz, P.S. Russo, Macromolecules, 1985, 18, 86.
5. H.M. Colquhoun, J.A. Daniels, I.C.I. plc, private communication.
6. T.E. Attwood, T. King, I.D. McKenzie, J.B. Rose, Polymer, 1977, 18, 365.
7. R.M. Silverstein, G.C. Bassler, T.C. Morrill, Spectrometric Identification of Organic Compounds, 4th Ed. John Wiley, 1981, 231.
8. J.B. Rose, Polymer, 1974, 15, 456.
9. J.A. Brydson in Polymer Science, Ed. A.D. Jenkins, N. Holland, Publ. Co. 1972, 1, 198. T.G. Fox, P.J. Flory, J. Polym. Sci. 1954, 14, 315.
10. D.R. Rueda, F. Ania, R. Richardson, I.M. Ward, F.J.B. Calleja, Polym. Commun. 1983, 24, 258.
11. J.N. Hay, D.J. Kemmish, J.I. Langford, A.I.M. Rae, Polym. Commun. 1985, 26, 283.
12. J. Boom, E.P. Magre, Markromol. Chem. 1969, 126, 130.
13. X. Jin, M.T. Bishop, T.S. Ellis, F.E. Karasz, Brit. Polym. J. 1985, 17, (1), 4.
14. B. Crossland, G.J. Knight, W.W. Wright, Brit. Polym. J. 1986, 18 (3), 156.
15. N.I. Bekasova, Russ Chem. Rev. 1984, 53, (1), 61.
16. J. Green, N. Mayes J. Macromol. Sci. (Chem), A1, 1967, 135.
17. A.D. Delman, J.J. Kelly, B.B. Simms, J. Polym. Sci. A1. 1970, 8, 111.
18. Yu M. Rodionov, S.I. Danilov, Dokl. Akad. Nank. S.S.S.R., 1986, 288, 143 (Engl 132).
19. L.I. Zakharkin, V.N. Kalinin, T.V. Balkykova, P.N. Gribkova, V.V. Korshak, J. Gen. Chem. U.S.S.R., 1973, 43, 2249.

20. L.S. Strel'chenko, P.M. Valetskii, P.A. Pshenichkin, T.M. Abramova, L.I. Golubenkova, S.V. Vinogradova, Vysokomol. Soed. 1979, 21B, 135.
21. V.I. Stanko, P.M. Valetskii, S.V. Vinogradova, T.N. Vostrikova, A.I. Kalechev. J. Gen. Chem. U.S.S.R., 1969, 39, 542.
22. A. Sekiya, N. Ishikawa, J. Organomet. Chem. 1976, 118, 349.
23. A. Sekiya, N. Ishikawa, J. Organomet. Chem. 1977, 125, 281.

CHAPTER 5

STUDIES ON C-HYDROXY CARBORANES

5.1 INTRODUCTION

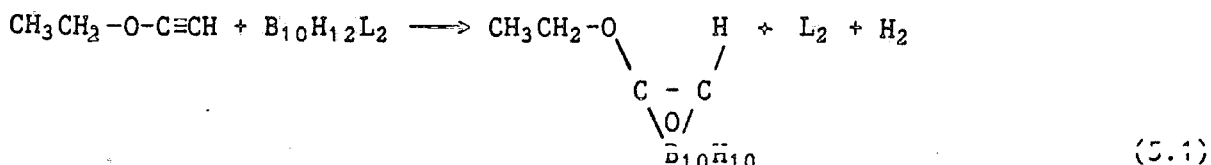
Despite the fact that the derivative chemistry of icosahedral carboranes is now extensive (see Chapter 1), surprisingly little attention has been paid to the C-hydroxy carboranes. Our original interest in these compounds stemmed from their being considered as potential monomers for the preparation of poly(carboranyletherketones). However for reasons already discussed, this potential has not been developed (see Section 3.3.5.2).

This chapter describes the methods of preparation of C-oxygen and C-hydroxy carborane derivatives, and outlines the various syntheses of C-hydroxy carboranes carried out in this study. Also described are investigations into the effects of delocalisation of electron density into the carborane cage, occurring in anions produced by the deprotonation of C-hydroxy derivatives using various amine bases. These effects are manifest, to a certain extent, in the spectroscopic properties of these compounds. Unequivocal evidence for delocalisation into the cage is provided by the molecular structure of the anion $\text{PhC}_2\text{B}_{10}\text{H}_{10}\text{O}^-$, produced by deprotonation of 1-hydroxy-2-phenyl-ortho-carborane with proton sponge. The recently published structure¹ shows this anion effectively consisting of a nido shaped $\text{PhCB}_{10}\text{H}_{10}^-$ residue capped by a μ_5 carbonyl group whose CO bond length and position over the open face of the nido shaped residue are rationalised by frontier orbital considerations. These considerations have allowed predictions to be made about structures of related systems, and these are discussed as a basis for some proposals for further study.

5.2 C-oxygen derivatives of icosahedral carboranes

Pioneering workers attempting to prepare C-oxygen derivatives of carboranes found great difficulty in doing so². Original efforts to synthesise hydroxy derivatives by the oxidation of C-lithio and C-magnesium species failed. In fact the first C-oxygen derivative made

was 1-ethoxy-ortho-carborane, prepared with great difficulty, by the reaction between ethoxyacetylene and bis Lewis base adducts of decaborane² (equation (5.1)).

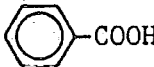
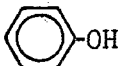


The tendency of the decaborane to polymerise the ethoxyacetylene meant that a stabiliser was needed and isolation of only minute quantities (1% of theory) of the pure carborane derivative was possible.

Other workers have reported the successful preparation of C-hydroxy derivatives using the air or oxygen oxidation of lithio derivatives of ortho and meta-carboranes, although yields quoted are quite low (at best 20-30%) and difficult to reproduce routinely^{3,4}. A much more convenient route has been devised using the benzoyl peroxide oxidation of carboranyl lithio derivatives⁵. All the C-hydroxy derivatives examined in this study were prepared exclusively by this method which is discussed in detail in the following sections.

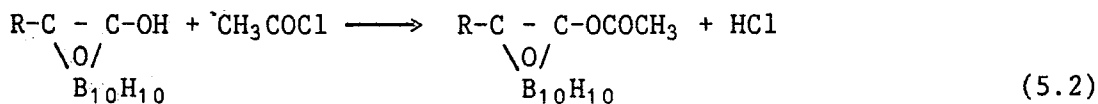
The C-hydroxy carboranes are acidic compounds on account of the electron withdrawing influence of the cage, as shown by their pK_a values given in Table 5.1 (taken from reference 5).

Table 5.1

Compound	pK _a
$\begin{array}{c} \text{H}-\text{C} - \text{C}-\text{OH} \\ \diagdown \text{O} / \\ \text{B}_{10}\text{H}_{10} \end{array}$	5.25
$\begin{array}{c} \text{CH}_3-\text{C} - \text{C}-\text{OH} \\ \diagdown \text{O} / \\ \text{B}_{10}\text{H}_{10} \end{array}$	5.30
	5.55
H-CB ₁₀ H ₁₀ C-OH	8.24
CH ₃ -CB ₁₀ H ₁₀ C-OH	8.33
	9.95

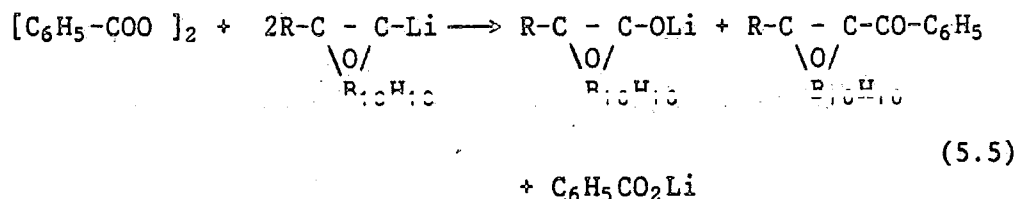
These values show the 1-hydroxy-ortho derivatives to be of the same order of acidity as benzoic acid. The meta derivatives are less acidic because of the less electron withdrawing nature of the meta-carborane cage (see Section 3.3.1). As a result of this acidity the 1-hydroxy-ortho-carboranes can be readily deprotonated by bases such as triethylamine or ammonia⁵ producing salts.

A limited derivative chemistry of these compounds has been developed⁵. Esters are formed by their reaction with acyl chlorides such as acetyl chloride (equation (5.2)).

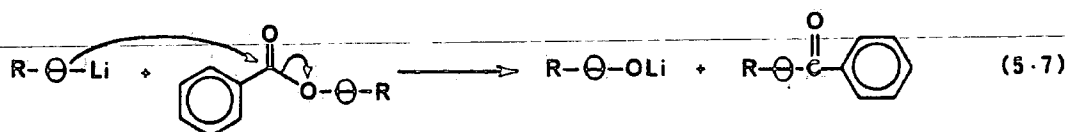
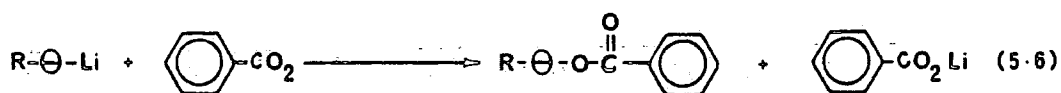


Their triethylammonium salts will also react with benzoyl chloride generating the corresponding benzoates (equation (5.3)).

The reaction with lithio-carboranes follows a different course however, with two equivalents apparently reacting with one equivalent of the peroxide as in equation (5.5).



This stoichiometry is believed to arise because the reaction takes place in two steps. The first (equation 5.6) produces the benzoate derivative as expected. This intermediate is extremely reactive towards nucleophiles as suggested in the previous section, and is therefore more readily attacked by further lithio derivative than is the residual benzoyl peroxide. This results in the formation of the lithiated hydroxy species and the carboranyl benzoate side product (equation 5.7).

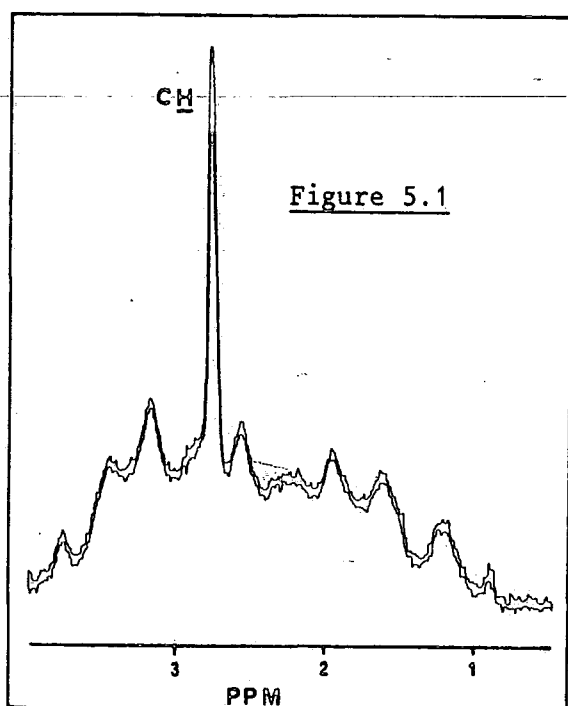


This reaction scheme is confirmed by the fact that the benzoyl intermediate prepared as in equation 5.3 reacts readily with \underline{C} -lithio derivatives as in equation 5.7.

Clearly a major limitation of this reaction is that only 50% of the carborane reactant is converted into the desired product. This is somewhat compensated by the fact that the benzoyl side product can be readily converted back to the carborane starting material by treatment with alkali.

5.3.2 Properties of C-hydroxy carboranes

The \underline{C} -hydroxy derivatives crystallise from hexane as white air stable solids. As expected their infra red spectra show characteristic O-H stretching absorbances between 3500 and 3000 cm^{-1} , and C-O stretching absorbances at approximately 1200 cm^{-1} . The O-H stretching modes are more complicated than expected in some cases. Spectrum A in figure 5.2 is that of 1-hydroxy-2-phenyl-ortho-carborane (XXVII), which shows the most complicated pattern in the O-H stretching region of the spectrum. The three absorbances seen might suggest that the species is present as a



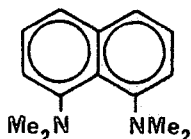
hydrate although results from other analytical methods do not show this to be the case. The occurrence of these separate absorptions has not been explained yet.

The ^1H NMR of these derivatives fail to show the resonance of the hydroxy proton clearly as this tends to be masked by the broad BH resonances of the cage. Figure 5.1 shows the ^1H spectrum of (XXV) highlighting this problem.

The mass spectra of the C(2) substituted 1-hydroxy derivatives are as expected for normal carborane derivatives, showing strong molecular ion peaks (accompanied by the usual isotope distribution pattern) and a small amount of cage fragmentation. The spectrum of 1-hydroxy-ortho-carborane is slightly different in that the base peak in the spectrum occurs at m/e 159 corresponding to $[\text{M} - \text{H}]^+$. Also a weak ion fragment is observed at m/e 318 corresponding to $[2(\text{M}-\text{H})]^+$. This smaller signal is possibly due to elimination of H_2 from two molecules which then dimerise in the spectrometer. The mode of dimerisation is unclear however with intermolecular bonding possibly occurring through C-C, B-B or O-O bonds or any combination of these.

5.3.3 The effects of deprotonation on C-hydroxy derivatives

As mentioned previously, the acidity of the 1-hydroxy-ortho-carboranes allows them to be easily deprotonated by bases. In fact their isolation depends on the solubility of these compounds in aqueous alkali. Deprotonation by amine bases occurs instantaneously on mixing hexane solutions of the hydroxy derivative and base, usually causing the corresponding salt to precipitate. Bases that have been used in this study include triethylamine, pyridine and latterly NNN^1N^1 tetramethyl-1-1,8-diaminonaphthalene (proton sponge)⁸:



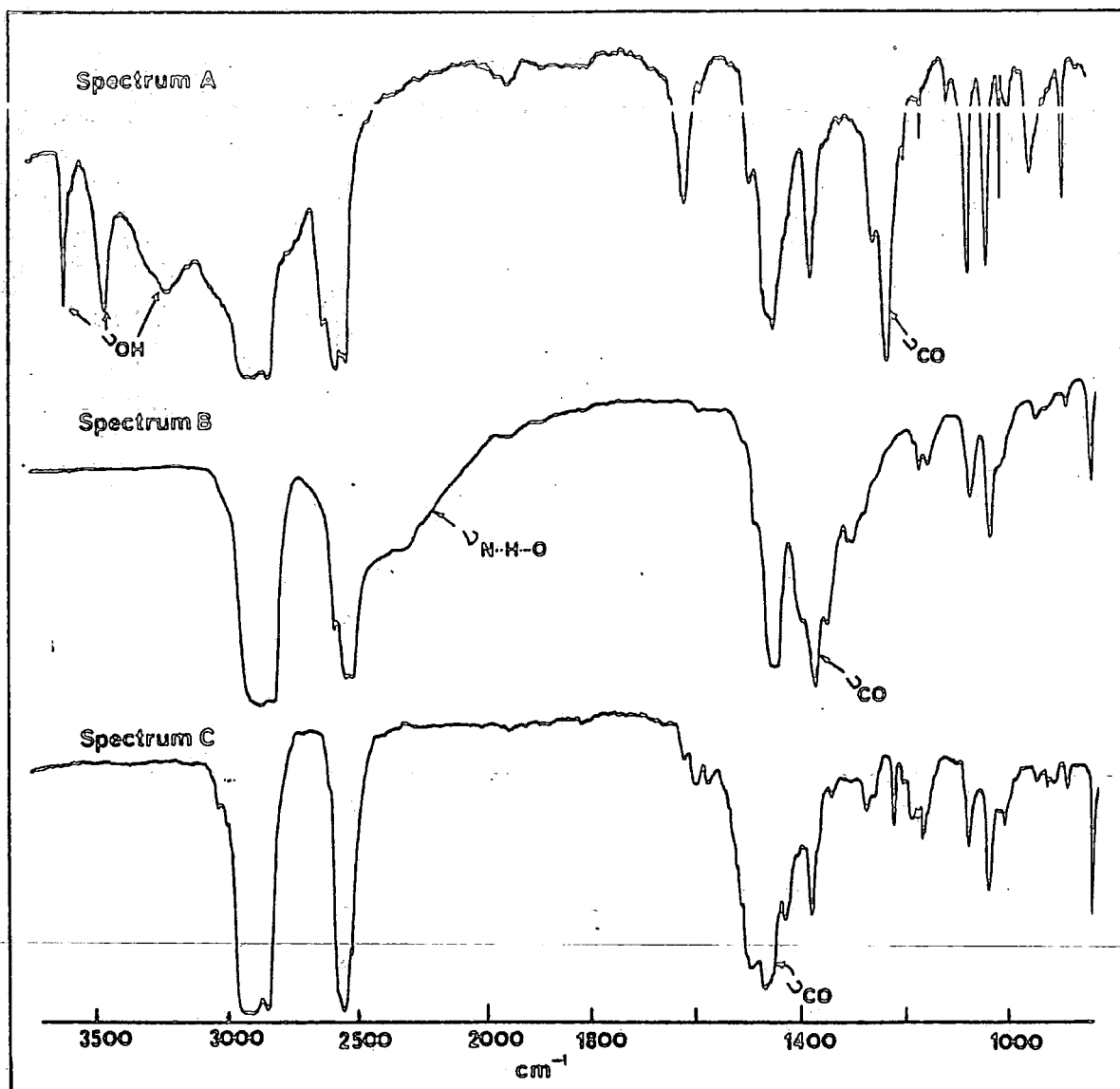
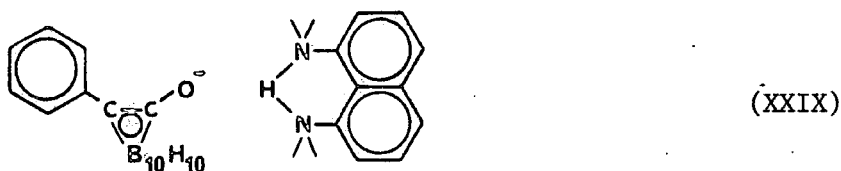


Figure 5.2 I.R. spectra of A. (XXVII), B. (XXVIII) and C. (XXIX)

system⁹. The relief of this molecule strain upon protonation and the strong hydrogen bonding that holds the proton tightly between the two nitrogen atoms, are believed to give rise to the strong basicity of this compound¹⁰. In addition, the steric restrictions imposed by the methyl groups and the naphthalene ring in this compound mean it is a very weak nucleophile. This is important as some amine bases are sufficiently nucleophilic to degrade the ortho-carborane cage (see Section 3.3.2).

Deprotonation of the 1-hydroxy-ortho-carboranes by this species occurs readily and the salt of 1-hydroxy-2-phenyl-ortho-carborane (XXIX) has been studied in detail.



This species is different from other salts in that it appears to be completely insoluble in aliphatics, dissolving readily in only more polar solvents such as THF and acetone (the compound was recrystallised from boiling toluene). The I.R. spectrum of this compound (spectrum C, figure 5.2) shows marked differences from that of the triethylammonium salt. The broad N.....H.....O absorption has disappeared. This together with the solubility characteristics of the proton sponge salt indicate that (XXIX) is a much more ionic species. On comparing the C-O stretching frequencies in (XXVII) and (XXIX) it can be seen that the shift to higher wavenumber in (XXIX) is even greater (ν_{C-O} , 1460 cm^{-1} $\Delta\nu$ 230 cm^{-1}).

The marked increase in ν_{C-O} on deprotonation is an indication that the C-O bond order in the salts has increased giving a linkage with substantial multiple bond character in the case of (XXIX). This phenomena can be rationalised by noting that the

anion produced on deprotonation consists of a substituent carrying a unit negative charge attached to a highly electron withdrawing and formally electron deficient cage. This negative charge is thus readily delocalised via the C-O bond, into the cage (therefore increasing the C-O bond order and giving the CO unit carbonyl character). Two canonical forms for the anions can be drawn as a result (structures 2 and 3 in figure 5.3).

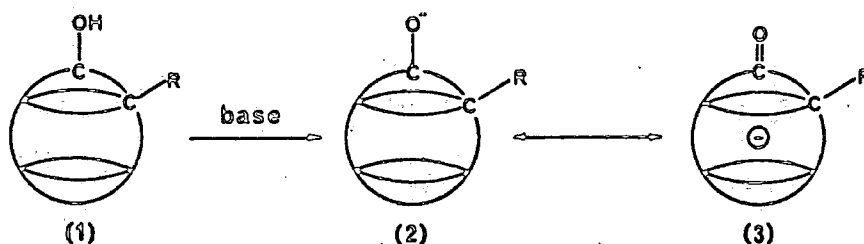


Figure 5.3

The increased carbonyl character of the CO unit is further confirmed by the $\delta(^{13}\text{C})$ of the carbon atom accommodating the oxygen substituent (C(1)), which is substantially deshielded upon deprotonation. Table 5.2 gives the $\delta(^{13}\text{C})$ of this carbon atom in 1-phenyl-ortho-carborane, (XXVII) and (XXIX) showing the deshielding of this carbon atom both on attaching OH and O^- .

Table 5.2

R	$\delta(^{13}\text{C})$	C* (ppm)
H		77.06
OH		106.78
O^-		136.52

The attachment of hydroxy and oxo substituents onto the carbon atoms of the cage have quite substantial effects on the ^{11}B NMR of the cage boron atoms. These effects have formed the basis of a separate investigation carried out in this study, the results

from which are presented in Chapter 6.

1-hydroxy-meta carborane derivatives are not sufficiently acidic to allow the easy isolation of the corresponding triethylammonium salts. The increased basicity of proton sponge however should in principle allow the salts of these derivatives to be prepared. Attempts to isolate the salt of 1-hydroxy-7-phenyl meta-carborane have been made although the identity of the material obtained from the reaction has not yet been completely established.

In an effort to obtain unequivocal evidence for charge delocalisation from the oxygen atom in the oxo salts of 1-hydroxy-ortho-derivatives, X-ray diffraction studies were attempted on several salts of 1-hydroxy-ortho-carborane. These systems proved to have disordered lattices at ambient temperature. The salt (XXIX) is ideally suitable for X-ray diffraction studies however. This is because the pendant phenyl group on the anion firstly serves as a label for the carbon atom to which it is attached and secondly because it prevents disordering of the lattice by locking the cage rigidly in place. Also as mentioned before, this compound is the most ionic of any salts studied to date and so any effects produced by the delocalisation of charge on the molecular structure of anions will be most clearly shown by this compound.

5.4 The crystal and molecular structure of the proton sponge salt of 1-hydroxy-2-phenyl-ortho-carboranes (XXIX)

The structure of (XXIX) is shown in figure 5.4 and represents the first structurally characterised C-oxygen derivative of ortho-carborane. Selected distances and bond angles are given in Table 5.3 (full crystallographic details are given in Section 5.5.11). The ionic nature of (XXIX) is clearly established by this structure. The planar configuration of the naphthalene ring in the protonated proton

sponge molecule is clear, as is the way the methyl groups on the nitrogen atom of the cation sterically restrict any N...H...O hydrogen bonding interaction between the cation and the anion.

In the anion, strong evidence for the delocalisation of the negative charge on the oxygen atom into the cage is provided by the C-O bond length. This is 1.245(3) Å and lies in the region typical for the bond lengths of carbonyl groups in ketones. A C-O single bond would be expected to be c.a. 1.43 Å in length. The cage itself is substantially distorted from ideal icosahedral geometry. The C-B and B-B bond lengths in the nido shaped $\text{PhC(2)B}_{10}\text{H}_{10}$ residue (1.65 - 1.85 Å) are typical of those found in other carborane derivatives. However the CO group is shifted away from C(2) towards B(2) and B(3) so that the C(1) - C(2) bond length (2.001 (3) Å) is substantially longer than the C-C bond in ortho carborane (1.64 Å)¹⁹. Figure 5.5 shows an alternative projection of the anion viewed down the C-O bond, illustrating more clearly the movement of the CO unit away from C(2) towards B(2) and B(3).

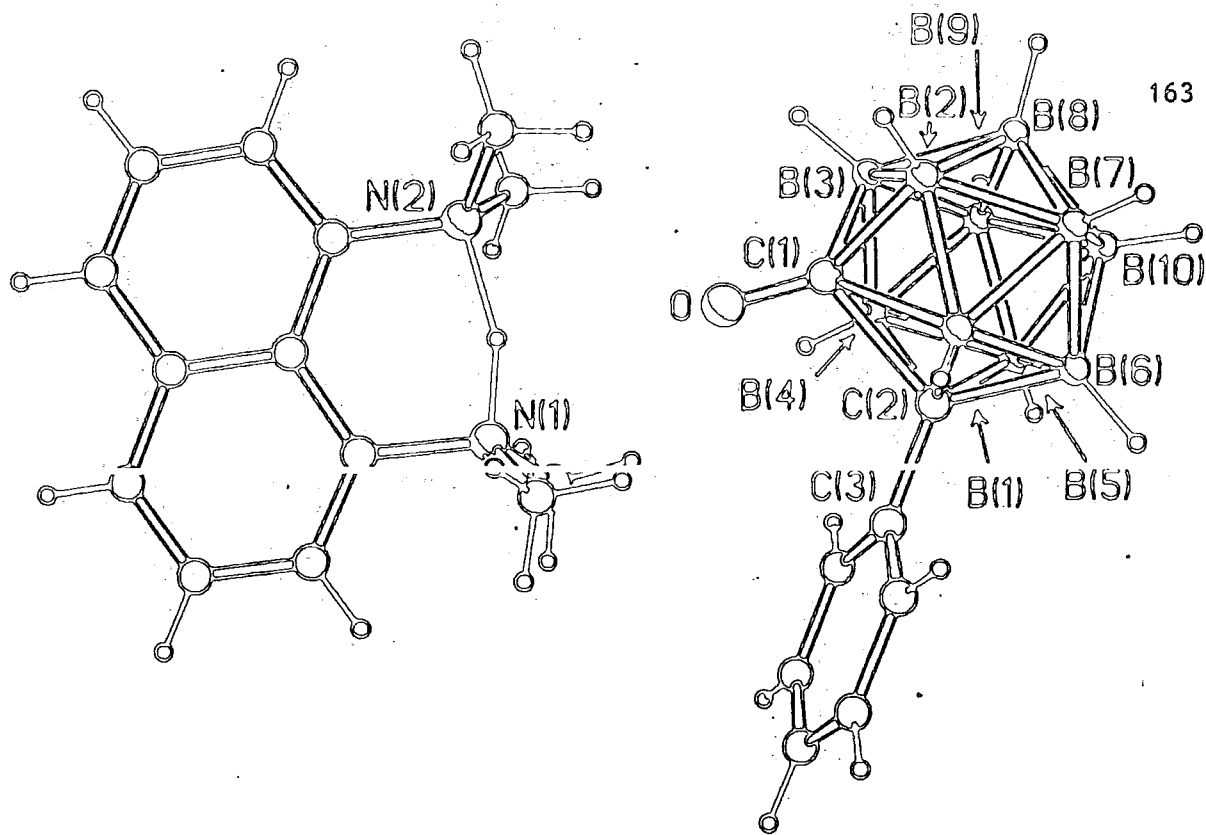


Figure 5.4 Molecular structure of (XXIX)

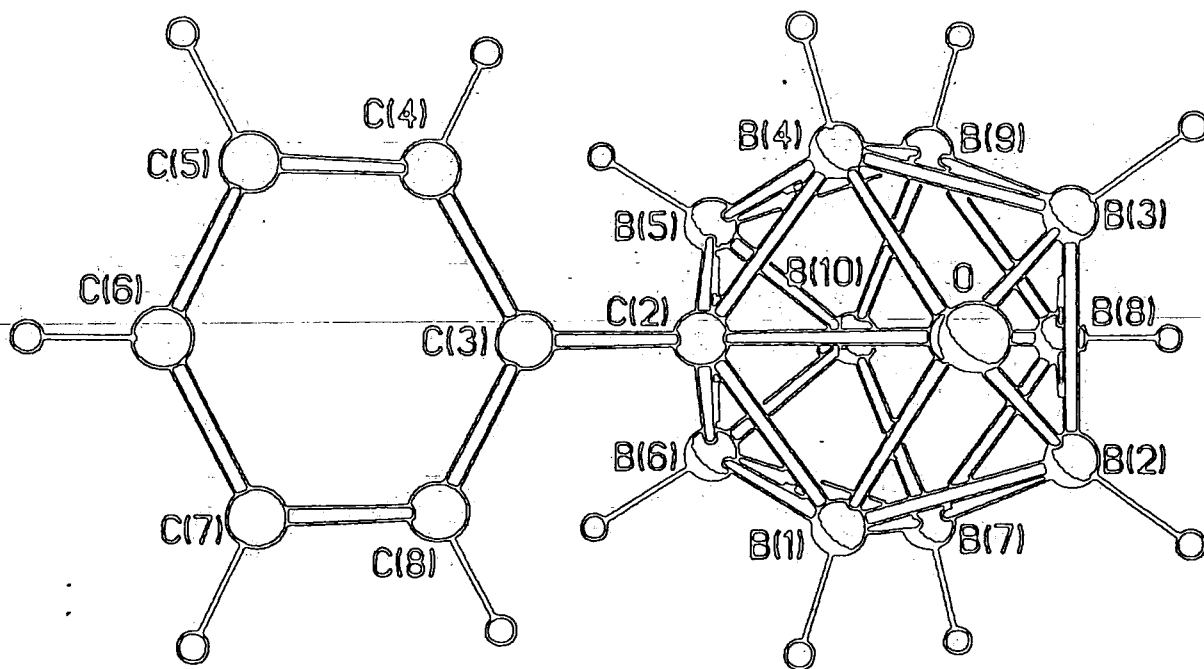


Figure 5.5 Alternative projection of (XXIX)

Table 5.3

Interatomic Distances (Å)		Bond Angles (°C)	
C(1)-O	1.245 (3)	O-C(1)-C(2)	117.7 (2)
C(1)-C(2)	2.001 (3)	O-C(1)-B(1)	119.7 (2)
C(1)-B(1)	1.62 (5)	O-C(1)-B(2)	130.0 (2)
C(1)-B(2)	1.684 (3)	O-C(1)-B(3)	130.3 (3)
C(1)-B(3)	1.683 (4)	O-C(1)-B(4)	120.1 (3)
C(2)-B(1)	1.697 (5)	B(1)-C(2)-B(4)	108.1 (2)
B(1)-B(2)	1.771 (4)	C(2)-B(1)-B(2)	110.0 (2)
B(2)-B(3)	1.801 (6)	C(2)-B(4)-B(3)	110.6 (3)
B(3)-B(4)	1.770 (5)	B(1)-B(2)-B(3)	105.5 (3)
B(4)-C(2)	1.686 (4)	B(2)-B(3)-B(4)	105.2 (2)
C(2)-C(3)	1.502 (4)		
N(1)-H	1.222 (32)		
N(2)-H	1.519 (25)		
O....H	2.603 (60)		
N(1).....O	3.115 (12)		
N(2).....O	3.208 (12)		

Molecular Orbital Bond Index (MOBI) calculations have been carried out using orthogonalised atomic coordinates obtained from the crystal structure of the compound. This has firstly been with a view to estimate the extent of the hydrogen bonding between cation and anion by calculating the bond index between the O and hydroxyl H atoms, and secondly to monitor the distortion within the cage once again from calculated bond indices.

The bond index calculated for the O....H bond is 0.004 which is

virtually negligible and thus re-emphasises the ionic nature of (XXIX). As a result of this, the MOBI calculation to monitor the cage distortions was performed on the discrete anion. The C-B and B-B bond indices in the nido shaped $\text{PhC}(2)\text{B}_{10}\text{H}_{10}$ residue lie in the region (0.45 - 0.59) expected for icosahedral carboranes. The bond indices for bonds between C(1) and the rest of the cage are given in Figure 5.6. They clearly reflect the distortion of the cage seen in Figure 5.5, showing a strengthening of the C(1) to B(2) and B(3) bonds and a weakening of the C(1)-C(2) bond (C-C bond index 0.66 in ortho-carborane).

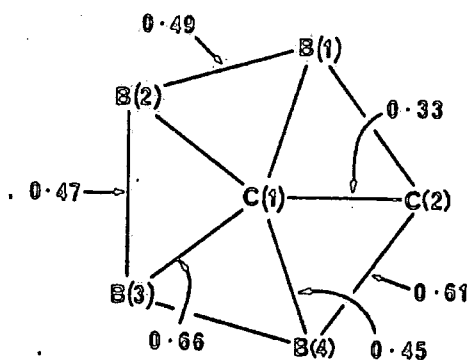


Figure 5.6

A qualitative explanation of the distortions in the anion is provided by treating the system as a nido shaped $\text{PhCB}_{10}\text{H}_{10}^-$ residue which is stabilised by co-ordinating through its open μ_5 face to a molecule of carbon monoxide, and examining the frontier orbitals involved in such an interaction. Like the cyclopentadiene (Cp) anion, and other species such as nido shaped $\text{B}_{11}\text{H}_{12}^{2-}$, the $\text{PhCB}_{10}\text{H}_{10}^-$ residue has three orbitals with which to interact with atoms or groups lying over the pentagonal face^{11,12}. The orbitals of the borane and carborane fragments differ slightly from those of the Cp unit in their uncoordinated forms, in that the lobes of the π orbitals protruding from the μ_5 face of the cage fragments are not perpendicular to the plane

of the face but are tilted inwards. This is as a result of rehybridisation caused by the hydrogen atoms or substituents attached to the atoms defining the face, which do not lie in that plane but above it. The form of these orbitals is shown in Figure 5.7 (labelled as by Mingos¹¹). The $6a_1$ orbital functions as the one into which the lone pair electrons on the carbon atom of the CO molecule are formally donated. The e_1 pair undergo back π -bonding into the CO π^* orbital. In the case of the Cp or $B_{11}H_{11}^{2-}$ this e_1 pair are degenerate and would therefore participate equally in the back π -bonding. However the inclusion of the carbon heteroatom in the face causes a lowering of the energy of the $5e_1(x)$ orbital relative to that of the $5e_1(y)$ orbital because of the greater electronegativity of the carbon atom relative to boron. The $5e_1(y)$ orbital is not stabilised because the carbon atom lies in the nodal plane of this orbital and so makes no bonding contribution. These energy differences are clearly illustrated by the calculated eigenvalues of $5e_1(x)$ and $5e_1(y)$ in $B_{11}H_{11}^{2-}$ and $CB_{10}H_{11}^-$ obtained from Extended Huckel M.O. calculations¹¹: in $B_{11}H_{11}^{2-}$, $5e_1(x) = 5e_1(y) = -9.4912$ eV; in $CB_{10}H_{11}^-$ $5e_1(x) = -10.2128$ eV, $5e_1(y) = -9.5573$ eV.

The removal of the degeneracy of the e_1 pair means that $5e_1(y)$ becomes the orbital most effective for back π -bonding because of its higher energy. Hence, as this orbital contains no contribution from C(2), the CO unit moves towards B(2) and B(3) to allow a stronger interaction between $5e_1(y)$ and the p_y orbital on the carbonyl carbon atom, producing the distortion seen in the anion. Because of the position of the CO group and the length of the C(1)-C(2) bond, its bonding could arguably be more aptly described as μ_4 , however MOBI calculations give the C(1)-C(2) bond a bond index of 0.33 indicating there is still a significant bonding interaction between C(1) and C(2). The back π donation from the cage into the CO π^* orbital is expected to leave the oxygen atom slightly negatively charged although with less than the full negative charge that canonical form 2 implies (see Figure 5.3).

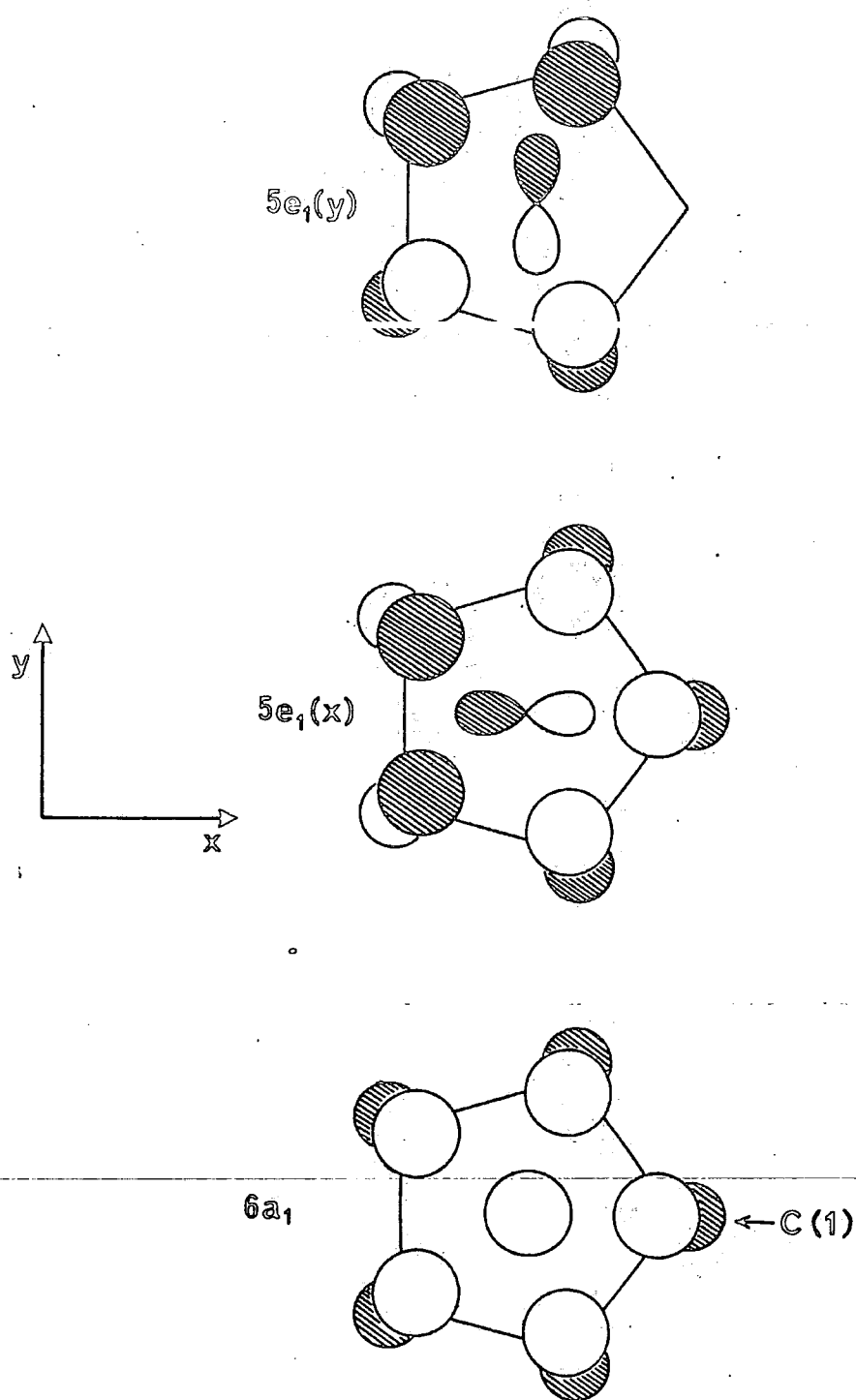
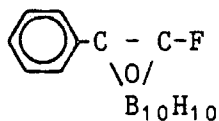


Figure 5.7 Frontier orbitals of the $\text{PhCB}_{10}\text{H}_{10}^-$ residue

Finally the bond index of the CO link (1.20) is lower than might be expected emphasising the carbocationic nature of C(1) (the total valencies of C(1) and C(2) are 3.76 and 3.95 respectively, as indicated by the MOBI calculations).

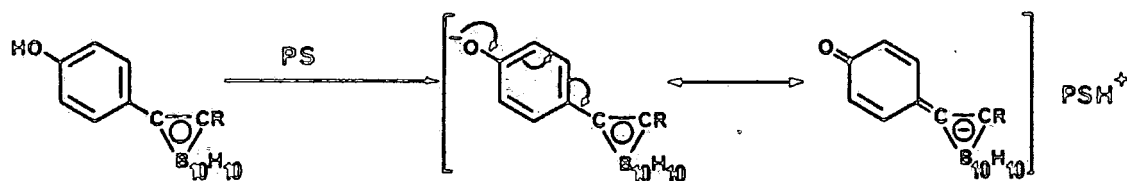
Looked at in the way described above, this 'carbonylate' anion shows carbon monoxide in a μ_5 bonding role unprecedented in its coordination chemistry^{13,14}. It should be noted however that \underline{C} -hydroxy¹⁵, \underline{C} -diethylether¹⁶ and \underline{C} -carboxylato^{17,18} metalla-carboranes, formed by the migration of carbonyl ligands into cage sites, have been reported although none of these examples show multiple bonding between the cage carbon atom and the attached oxygen atoms. It is also interesting to note that the C(1)-C(2) bond length of 2.001(3) Å in (XXIX) is to our knowledge the longest C-C bonding interaction recorded, the previous record apparently being held by ortho-carborane¹⁹.

Regarding the anion as a substituent attached to the C atom of the icosahedral cage, this compound, contrary to the results obtained from studies into the interaction between the cage and aryl π system (see Section 3.3.1), shows the carborane deltahedron undergoing π overlap with a substituent. This has implications for other carborane derivatives possessing substituents capable of such interactions. For instance, 1-fluoro-2-phenyl-ortho-carborane:



would be isoelectronic with the $\text{PhC}_2\text{B}_{10}\text{H}_{10}\text{O}^-$ anion. Despite the extreme electronegativity of the fluorine atom, its lone pairs are ideally situated for π overlap. The molecular structure of this neutral fluorine derivative may therefore show distortion similar to those seen in (XXIX). Deprotonation of \underline{C} -thiols using proton sponge may also generate anions showing appreciable π overlap between the anionic sulphur atom generated and the cage.

By preparing \underline{C} -carboranyl aryl derivatives with suitable substituents attached to the aryl ring, it may be possible to induce π overlap between the ring and the cage. The most likely systems envisaged to show this effect are 1-(4-hydroxyphenyl)-ortho-carborane derivatives which upon deprotonation could afford a system showing π overlap as summarised by the canonicals in equation 5.8.



(5.8)

Such π overlap would be detected in the molecular structure of the above anion by a shortening of the C-O bond, the ortho to meta C-C bonds and the ring to cage C-C bond, as well as distortions in the cage similar to those in (XXIX). The propensity of the dimethylamino group to overlap strongly with aryl π systems has long been known²⁰. Hence the corresponding 4-(NN-dimethylamino)phenyl-ortho-carborane way might activate the aryl π system to overlap with the cage as well. This too would be detected through monitoring the molecular structure of the compound, or in principle by determining the pKa of this species. The basicity of this species would be inhibited by strong π interaction between the dimethylamino group and the phenyl ring, enhanced by interaction with the cage.

The frontier orbital approach used to rationalise the distortions of the cage seen in (XXIX) allow predictions to be made about the molecular structures of other related compounds. For instance in the meta analogue of (XXIX), the CO unit would be situated over a B₅ face. This would mean that the 5e₁(x) and 5e₁(y) orbitals back π bonding into the CO π^* orbital would be of virtually the same energy (slight perturbations may occur as a result of the asymmetry of the

residue). Thus they would be expected to contribute more equally to back bonding producing only very slight distortions in the shape of the cage. Clearly in the case of the para analogue of (XXIX), the nido shaped $\text{RCB}_{10}\text{H}_{10}^-$ has a C_5 rotation axis through the open pentagonal face making $5e_1(x)$ and $5e_1(y)$ degenerate. Both would therefore be expected to participate equally in back π -bonding, meaning the CO unit would lie on the C_5 axis of the residue.

Figure 5.8 shows an alternative view of the π interaction between $5e_1(y)$ and π^* orbitals of $\text{PhCB}_{10}\text{H}_{10}^-$ and CO respectively, to emphasise the plane in which the orbital accommodating back donated π electron density lies. Because of its energy, this orbital is clearly the one through which the oxygen atom will be expected to coordinate to other species. Thus we can predict that the $\underline{\text{C}}$ -hydroxy carboranes would show the H-O-C group lying in a plane perpendicular to the plane of the O-C-C atoms. Similarly, metal salts such as lithium- $\underline{\text{C}}$ -oxides would be expected to show the same feature, i.e. the Li-O-C plane lying perpendicular to the O-C-C plane.

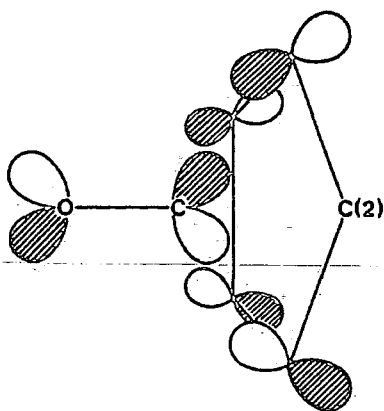


Figure 5.8

Considering the interaction of the aryl π system with the cage, shown in equation 5.8, the aryl residue interacting with the $\text{CB}_{10}\text{H}_{10}^-$ fragment will be as in Figure 5.9.



Figure 5.9

in theory, this residue will have a lone pair on the co-ordinating carbene like carbon atom which can interact with the $6a_1$ orbital of the nido residue (as CO does in (XXIX)). Again π backdonation will be mainly from the $5e_1(y)$ orbital causing an elongation of the carboranyl C-C bond. The p orbital on the co-ordinating carbon atom of the aryl residue, lying perpendicular to the plane of the ring, will be occupied through its conjugation with the aryl π system. Hence π backdonation will occur from the $5e_1(y)$ into the p orbital on the co-ordinating carbon atoms which lies in the same place as the ring. Thus we can predict that the molecular structure of the anion in equation 5.8 will show the aryl ring lying in a plane perpendicular to the plane of the quaternary aryl and carboranyl carbon atoms. Similarly, if strong π overlap between the 4-dimethylamino-phenyl substituent and the cage occurs, the ring would be expected to take up the same configuration in this compound also. Interestingly, this prediction is confirmed by the structure of (XXIX) in which the pendant aryl ring takes up this configuration. It should be noted however, that the weak steric interactions between the ortho-aryl and cage hydrogen atoms, and the interaction between the ring and the methyl groups of the cation may also be influential in the alignment of the phenyl ring.

5.5 EXPERIMENTAL

5.5.1 The use of benzoyl peroxide

Benzoyl peroxide is an extremely hazardous material when in anhydrous solid form being liable to detonate under shock. As a result, commercially available material is supplied with 25% (by weight) of water added to stabilise the material during transit. Clearly in reactions with carboranyl lithium species, the peroxide needs to be free of water. Dry benzoyl peroxide was prepared as needed by dissolving the correct weight of material + 25% water in toluene. This solution was then dried first with anhydrous magnesium sulphate, filtered and further dried over A4 molecular sieve. All apparatus and materials exposed to the peroxide solution were soaked in acidified potassium iodide solution prior to conventional washing to degrade any residual material (degradation indicated by a brown colouration produced by the oxidation of iodide ions to iodine).

5.5.2 Preparation of 1-hydroxy-2-phenyl-ortho-carborane (XXVII)

5.7 mls (9.1 mmoles) of a solution of n-butyl lithium (1.61 M in hexane) was added to a solution of 1-phenyl-ortho-carborane (prepared as in Section 2.4.4, 2.00 g, 9.1 mmoles) in dry toluene (20 mls) under a dry nitrogen atmosphere. This mixture was stirred under reflux for 2 hours, cooled to 0°C and dry diethyl ether (20 mls) added taking the precipitated C-lithio carborane derivative into solution. A dry solution of benzoyl peroxide (1.10 g, 4.57 mmoles) in toluene (20 mls) was added via syringe to the stirring reaction mixture affording a precipitate and turning the solution yellow. This mixture was refluxed under nitrogen for a further 3 hours, cooled to room temperature and distilled water (30 mls) added dropwise. 10% aqueous sodium hydroxide was also added and the mixture transferred to a separating funnel. The organic layer was isolated and washed a

further two times with sodium hydroxide solution*. The aqueous extracts were combined and acidified with hydrochloric acid producing a white precipitate. This suspension was washed three times with diethyl ether, taking the precipitate into the organic layer (Silica t.l.c. plates spotted with this solution, containing the hydroxy derivative and benzoic acid, failed to give good separation of the two materials on eluting with the following: dichloromethane, methanol, hexane, toluene and 1:1 dichloromethane/methanol. As a result, isolation of pure hydroxy material by column chromatography was not attempted). The organic layer was washed three times with 5% aqueous sodium bicarbonate and dried over anhydrous magnesium sulphate (acidification of the bicarbonate washings afforded a precipitate of benzoic acid, identified by I.R). The ether solution was then filtered and the solvent removed under reduced pressure affording a viscous oil which solidified to give an off white material on prolonged exposure to vacuum. This solid was recrystallised from hexane affording opaque white needles identified as 1-hydroxy-2-phenyl-ortho-carborane. Yield 0.84 g, (3.55 mmoles), 78%.

Melting Point 84-86°C. Characterised as follows:

Analysis. Found: C, 40.1; H, 6.6; B, 45.1% $C_8H_{16}B_{10}O$. Requires: C, 40.7; H, 6.8; B, 45.7%.

Infra Red: See Figure 5.2A

1H -NMR: 360.134 MHz solvent C_6D_6 , referenced internally to the solvent (C_6D_5H) at 7.1619 ppm (ppm): 7.36-7.33 (m), Integral 2H (aromatic H (ortho)); 6.99-6.92 (m), Integral 1H (aromatic H (para)); 6.91-6.88 (m), Integral 2H (aromatic H (meta)); 2.83 (s) Integral 1H (C-OH); 3.5-1.5 (br.m) (BH).

^{11}B NMR This is discussed in Section 6.3.2.

^{13}C NMR { 1H } 62.896 MHz, solvent CD_3COCD_3 referenced externally to TMS at 0.00 ppm (ppm): 131.60 (aryl quaternary ortho C); 130.96 (meta C); 129.13, (para C); 106.78 (C(1)); 85.38 (C(2)).

Mass Spectrum E.I. The mass spectrum show a highest mass peak at m/e 239 (M+1) with the peak at m/e 238 corresponding to

$^{12}\text{C}_8^{1}\text{H}_{16}^{11}\text{B}_{10}^{16}\text{O}$. This was accompanied by the expected carborane isotope distribution pattern between m/e 228-238 and cage fragmentation. An intense fragment (seen only in E.I) was observed between m/e 187-207. $\frac{1}{2}$ mass peaks were also seen between m/e 114-119 ($m/2e$ 228-238).

- * The ether solution produced here can be stirred with 20% aqueous sodium hydroxide for 48 hours at room temperature. Isolation of the resulting organic layer followed by evaporation of the solvent and ether vacuum sublimation or recrystallisation of the residue from hexane, affords the unreacted carborane starting material.

5.5.3 Preparation of triethylammonium 1-oxo-2-phenyl-ortho-carborane (XXVIII)

Triethylamine (0.3 mls) was added dropwise to a solution of 1-hydroxy-2-phenyl-ortho-carborane (0.46 g, 2.1 mmoles) affording a white precipitate which coagulated giving an opaque gum like material. The solvent was decanted off, the residue washed with fresh hexane and recrystallised from boiling hexane/toluene (4:1) affording colourless crystals identified as triethylammonium 1-oxo-2-phenyl-ortho-carborate, yield 0.5 g (1.48 mmoles), 70.7%. Melting point 125-126°C. Characterised as follows:

Analysis Found: C, 47.2; H, 8.9; N, 3.3%. $\text{C}_{14}\text{H}_{31}\text{B}_{10}\text{NO}$.

Requires: C, 46.4; H, 9.2, N, 4.2%.

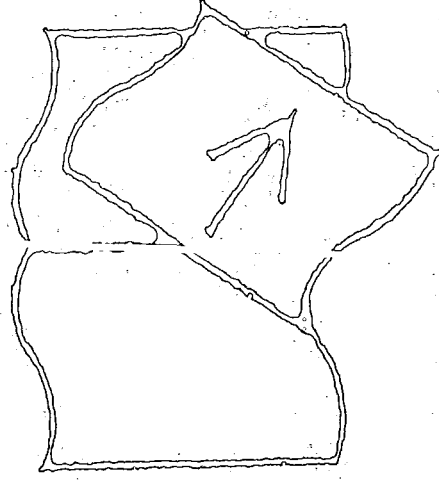
Infra Red : See Figure 5.2B (Section 5.3.2)

^1H NMR: 250.133 MHz. Solvent C_6D_6 referenced externally to TMS at 0.00 ppm; (ppm): 10.5, vbr.s. Integral ^1H (N...H...O); 7.98-7.95, m, Integral 2H (aromatic H(ortho)); 7.12-7.07 (m), Integral 3H, (aromatic H (meta & para); 4-2 (br), (BH); 1.77-1.68, q, $J=7.3$ Hz Integral .6H, (ethyl CH_2); 0.38-0.32, t, $J=7.3$ Hz, Integral 9H (ethyl CH_3).

^{11}B NMR. This is discussed in Chapter 6, (Section 6.3.2).

PAGE(S) MISSING
NOT AVAILABLE

175



5.5.4 Preparation of 1,8 N,N,N',N'-tetramethylnaphthalenediammonium-1-oxo-2-phenyl-ortho-carborate (XXIX)

A solution of proton sponge (0.104 g, 0.48 mmoles) in hexane (10 ml) was added dropwise to a solution of 1-hydroxy-2-phenyl-ortho-carborane (0.114 g, 0.48 mmoles) in hexane affording a white precipitate. This was filtered off, washed with fresh hexane and recrystallised from hot toluene affording off which crystals identified as (XXIX), yield 0.14 g, (0.312 mmoles) 65%. Melting point 146-148°C. Characterised as follows:

Analysis Found: C, 59.0; H, 7.4; N, 6.5% $C_{22}H_{34}B_{10}N_2O$.

Requires: C, 58.8; H, 7.6; N, 6.2%.

Infra Red (see Figure 5.2C, Section 5.3.2)

1H NMR: 250.134 MHz, solvent CD_3COCD_3 , referenced externally to TMS at 0.00 ppm (ppm): 18.95, (br.s), Integral 1H, (N...H...N), 8.13-8.1 (m), 7.77-7.70 (m), 7.29-7.26 (m), total integral 11H (naphthelene ring and phenyl ring H); 3.5-1.0 (br.m), (BH); 3.27 (s), integral 12H (N- CH_3).

^{11}B NMR. This is discussed in Chapter 6, Section 6.3.2.

^{13}C NMR [1H], 62.896 MHz, solvent CD_3COCD_3 , referenced externally to TMS at 0.00 ppm, (ppm): (C^1 denotes carbon atoms of the cation, C denotes carbon atoms of the anion), 145.48 ($C^1(1,8)$); 138.25 ($C^1(9)$); 136.42, (C(1)); 130.29, 128.59, 122.91 (resolution poor, naphthelene and phenyl ring carbons); 122.57, ($C^1(4,5)$); 120.20 ($C^1(10)$); 88.12, (C(2)); 46.62, (N- C^1H_3).

Mass Spectrum (E.I) A highest mass peak was seen at m/e 239 corresponding to M+1 ($m = ^{12}C_8^1H_{16}^{11}B_{10}O$), the anion apparently being re-protonated. This peak was accompanied by the usual carborane isotope distribution pattern between m/e 228-238 and characteristic cage fragmentation. Superimposed on this was the E.I. spectrum of proton sponge, which showed a strong molecular ion peak at m/e 214 and fragmentation through loss of CH_3 and $N(CH_3)_2$ groups.

5.5.5 Preparation of pyridinium 1-oxo-2-phenyl-ortho-carborate from the corresponding triethylammonium salt

2M hydrochloric acid (25 mls) was added to a vigorously stirred solution of triethylammonium 1-oxo-2-phenyl-ortho-carborate. This mixture was stirred for a further 10 minutes and allowed to settle. The ether layer was then isolated and the remaining aqueous extract washed three times with diethyl ether. The ether extracts were all combined, washed with distilled water, dried over anhydrous magnesium sulphate and filtered. The solvent was removed under reduced pressure leaving an off white solid, identified by I.R. as 1-hydroxy-2-phenyl-ortho-carborane. This solid was dissolved in hexane (30 mls). Pyridine (0.5 mls) was added to the resulting solution which was stirred for a few minutes. All the solvents were removed in vacuo leaving a white solid which when recrystallised from hexane afforded colourless needles identified as pyridinium 1-oxo-2-phenyl-ortho-carborate. Melting point 143-145°C. Characterised as follows:

Analysis. Found C, 47.8; H, 7.0; N, 3.0% $C_{13}H_{21}B_{10}NO$ Requires: C, 49.7; H, 6.7; N, 45%.

Infra Red (Nujol) (cm^{-1}): 3060 (aromatic C-H stretch); 2600 (sh) 2570 (s) (B-H stretch); ~2500-2200 (br) (N...H...O vibration); 1491 (w.sh); 1484 (sh); 1280 (sh); 1210 (s) (C-O stretch) 1199; 1174; 1076 (m); 1034 (m); 1023; 1007; 1096; 937; 885 (w); 805 (w); 778 (w); 752 (s); 730; 687 (m); 681 (m); 602; 572 (w.sh); 562; 538 (w); 505 (w); 490 (w).

1H NMR 250.133 MHz, solvent C_6D_6 , referenced externally to TMS at 0.00 ppm (ppm): 7.73 (s.br), Integral 1H (phenyl H, para); 7.64-7.59 (m), Integral 2H (phenyl H, meta); 7.07-6.93 (m) (phenyl H ortho); 7.49-7.47 (m) Integral 2H (ortho pyridinium H); 6.76-6.70 (m) Integral 1H (para pyridinium H); 6.34-6.29 (m) Integral 2H (meta pyridinium H); 4-2.5 (br.m) Integral 10H (BH). ^{11}B NMR { 1H broad band noise}, 80.239 MHz, solvent C_6D_6 referenced externally to $BF_3 \cdot Et_2O$ at 0.00 ppm (ppm): -10.37 (br.s); -12.49 (br.s), -14.67 (br.s). Spectral assignment was

prohibited by the broadness of the resonances relative to the spectrum width, which produced substantial coincidental combination of different signals.

5.5.6 Preparation of 1-hydroxy-ortho-carborane (XXV)

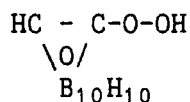
Freshly sublimed commercial ortho-carborane (1.73 g, 12 mmoles) was lithiated and treated with anhydrous benzoyl peroxide (1.45 g, 6 mmoles) as outlined in Section 5.5.2. 1-hydroxy-ortho-carborane, recrystallised from hexane was obtained in 70% yield. Melting point 308-310 (lit. 308-310). Characterised as follows: Analysis Found: C, 15.9; H, 7.9; B, 67.1% $C_2H_{12}B_{10}O$. Requires: C, 15.0; H, 7.5; B, 67.5%.

Infra Red (Nujol) (cm^{-1}): 3522 (w) 3580-3200 (s,br) (OH stretching frequencies); 3059 (s) (CH stretch); 2560 (s) (B-H stretch); 1590 (w) (O-H stretch overtone); 1325 (sh); 1230 (s) (C-O stretch); 1118 (m); 1068 (m); 1006 (m); 927 (w); 940; 915 (sh); 900 (w.sh); 870 (w); 801; 772; 730 (sh); 723 (s) (cage vibration); 691 (w); 675 (w); 540 (w).

1H NMR 250.133 MHz, solvent C_6D_6 , referenced externally to TMS at 0.00 ppm - see Figure 5.1, Section 5.3.2.

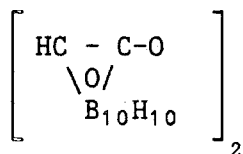
^{11}B NMR This is discussed in detail in Chapter 6, Section 6.3.2.

Mass spectrum (E.I) The mass spectrum showed a strong molecular ion signal (highest peak at m/e 162 corresponding to the species $^{12}C_2^{1}H_{12}^{11}B_{10}^{16}O$, accompanied by the standard carborane isotope distribution pattern). The base peak occurred at m/e 159 due to the lability of the hydroxy proton under E.I. Fragments of weak intensity gave rise to characteristic carborane signals centered at m/e 176 ($M+16$) and m/e 318. The former peak may be due to a trace of the peroxy species being present



The highest mass peak is most probably a product of

dehydrogenation giving a dimeric species



5.5.7 Preparation of triethylammonium 1-oxo-ortho-carborate

1-hydroxy-ortho-carborane (0.50 g, 6.3 mmoles) was treated with triethylamine as outlined in Section 5.5.3. Triethylammonium 1-oxo-ortho-carborate was isolated as colourless crystals. Yield 69%.

Melting point 125-7°C Characterised as follows:

Analysis Found: C, 38.6; H, 12.8; N, 55% $\text{C}_8\text{H}_{27}\text{B}_{10}\text{NO}$. Requires: C, 36.8; H, 10.3; N, 5.3%.

Infra Red (Nujol) (cm^{-1}): 3060 (w.br) (carboranyl C-H stretch); 2700-1800 (v.br) (N...H...O vibration); 2560 (s) (B-H stretch); 1362; 1340 (s) (C-O stretch); 1270 (m); 1230 (sh); 1171; 1160 (sh); 1092; 1069; 1006; 940 (w.br); 840 (m); 810 (w); 751 (w); 721 (m); 695 (w); 674 (w); 648 (w); 547 (m)

^1H NMR 360.134 MHz solvent C_6D_6 referenced internally to $\text{C}_6\text{D}_5\text{H}$ at 7.16 ppm (ppm): 9.72 (br.s) Integral 1H (N...H...O); 3.86 (s), Integral 1H (carboranyl CH); 3.5-1.8 (br.m), Integral ~10H, (B-H); 1.99-1.93 (q), $J=7.2$ Hz, Integral 6H (ethyl CH_2); 0.56-0.52 (t) $J=7.2$ Hz, Integral 9H (ethyl CH_3).

^{11}B NMR This is discussed in Section 6.3.2.

5.5.8 Preparation of 1-hydroxy-2-methyl-ortho-carborane

1-methyl-ortho-carborane (see Section 2.4.3) (2.35 g, 15.00 mmoles) was lithiated and treated with anhydrous benzoyl peroxide (1.82 g, 7.5 mmoles) as outlined in Section 5.5.2. 1-hydroxy-2-methyl-ortho-carborane was isolated as colourless crystals, yield 0.89 g (5.1 mmoles), 68%.

Melting point Sublimed 250-265°C. Characterised as follows:

Analysis Found: C, 20.9; H, 8.7; B, 59.9% $C_3H_{14}B_{10}O$. Requires: C, 20.7; H, 8.0; B, 62.1%.

Infra Red (Nujol) (cm^{-1}): 3630 (br) 3500 (s.br) 3300 (sh,br) (O-H stretch); 2570 (s) (B-H stretch); 1597 (O-H stretch overtone); 1319 (w); 1274 (w.sh); 1219 (s) (C-O stretch); 1196 (sh); 1080 (m); 1038 (m); 1016 (m); 947; 917 (w); 900 (w.sh); 797; 767; 735 (sh); 723 (s) (cage vibration); 695 (w); 675 (w); 568 (w); 510 (w).

1H NMR 360.134 MHz, solvent C_6D_6 referenced internally to C_6D_5H at 7.16 ppm (ppm): 3.5-1.2 (m.br) Integral $\sim 11H$ (B-H + O-H); 1.38 (s) Integral 3H ($-CH_3$).

^{11}B NMR this is discussed in Section 6.3.2.

Mass Spectrum (E.I) The mass spectrum showed a highest mass peak at m/e 176 corresponding to $^{12}C_3^{1}H_{14}^{11}B_{10}^{16}O$ accompanied by the usual characteristic carborane isotope distribution pattern between m/e 166-176. $\frac{1}{2}$ mass peaks were observed between m/e 83-88 (m/e 166-176). The usual fragmentation of the cage was also seen.

5.5.9 Preparation of triethylammonium 1-oxo-2-methyl-ortho-carborate

The above compound was prepared as outlined in Section 5.5.3.
Yield 72%.

Melting Point 136-138°C (lit. 120-122°C). Characterised as follows:

Analysis Found: C, 37.6; H, 10.6; N, 3.4% $C_9H_{29}B_{10}NO$.

Requires: C, 39.2; H, 10.5; N, 5.1%.

Infra Red (Nujol) (cm^{-1}): 2715-1900 (v.br) (N...H...O vibration); 2580 (s) 2545 (s) (B-H stretch); 1474 (sh); 1390 (m); 1374 (m); 1337 (s) (C-O stretch); 1290 (m); 1260 (sh); 1240 (w); 1220; 1170; 1155 (w); 1075; 1032 (m); 1017 (m); 946 (w); 925 (w); 911 (w); 897 (w); 837; 808 (w); 891 (w); 738 (w); 726 (m); 698 (w); 679 (w); 657 (w); 625 (w); 565 (m); 541.

1H NMR 360.134 MHz, solvent C_6D_6 , referenced internally to C_6D_5H at 7.1619 ppm (ppm): 12.54 (br.s), integral 1H,

(N...H...O); 2.03 (s), integral 3H (carboranyl CH₃); 1.96-1.92 (q), J 7.2 Hz, integral 6H (Ethyl CH₂); 0.57-0.53, (t), J=7.4 Hz, integral 9H (Ethyl CH₃).

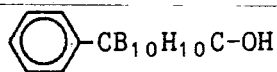
¹¹B NMR See Section 6.3.2.

5.5.10 (i) Preparation of 1-hydroxy-7-phenyl-meta-carborane

1-phenyl-meta-carborane (see Section 2.4.8) (1.197 g, 5.44 mmoles) was lithiated and treated with anhydrous benzoyl peroxide (0.658 g, 2.72 mmoles) as outlined in Section 5.5.2. Crude 1-hydroxy-7-phenyl-meta-carborane was isolated as an oily solid, yield 70 mg (0.3 mmoles), 10.9%. Characterised as follows:

Infra Red (contact film): 3700-3100 (v.br,s) (O-H stretch); 3060 (w) 2940 (w) (Aromatic C-H stretch); 2600 (s) (B-H stretch); 1948 (w); 1598 (w) (O-H overtone + C-C stretch?); 1580 (w); 1492; 1448 (m); 1360 (m.br); 1203 (s) (C-O stretch); 1072; 1028 (s); 1005; 940 (w.br); 917 (w); 901 (w); 870; 850; 805; 762; 743; 692 (s); 662 (w); 600 (w); 580 (w); 520 (w); 490.

Mass Spectrum The mass spectrum showed a strong molecular ion signal with the characteristic carborane isotope distribution pattern, between m/e 228 and 238 expected for the species:



The characteristic carborane cage fragmentation pattern was also observed below this signal.

ii) Preparation of 1,8 N,N,N¹,N¹-tetramethylnaphthalene diammonium-1-oxo-7-phenyl-ortho-carborate

Proton sponge (63 mg, 0.29 mmoles) dissolved in hexane (5 mls) was added to a solution of crude 1-hydroxy-7-phenyl-ortho-carborane (68.4 mg, ~29 mmoles) in hexane (5 mls)

affording a white precipitate which rapidly coagulated on stirring to give an opaque gum like material. The solvents were decanted off and the residue washed with fresh hexane. The residue was then dissolved in a minimum amount of hexane/toluene (1:1) and the solution chilled (-30°C) affording colourless crystals.

Melting point $102-103^{\circ}\text{C}$ Partially characterised as follows:

Infra red Nujol mull (cm^{-1}): 3040 cm (w.sh) (Aromatic C-H stretch); 2590 (s) (B-H stretch); 2600-2000 (w.br) (N...H...O vibration?); 1060 (w); 1580 (w); 1210 (m) (C-O stretch?); 1182 (m); 1165 (sh); 1131 (m); 1005 (sh); 940 (w.br); 872; 834; 809 (w); 770 (m); 744; 700; 665 (w); 580 (w.sh); 538 (w); 520 (w); 480 (w.br).

^{11}B { ^1H broad band noise} 80.239 MHz, solvent C_6D_6 , referenced externally to $\text{BF}_3\text{Et}_2\text{O}$ at 0.00 ppm: (ppm); -6.64 (s) Integral 1B (B(5)); -11.05 (s); Integral 2B; -13.13, (s) Integral 7B (includes the resonance of B(12), antipodal to the C atom carrying the oxygen substituent).

The preparation of this material was carried out at the end of the study, insufficient time was available to obtain a sufficient quantity to obtain elemental analysis data.

5.5.11 Crystallographic data for (XX1X)

Bond lengths (Å)

O-C(1)	1.246(3)	C(1)-C(2)	2.091(3)
C(1)-O(1)	1.622(5)	C(1)-O(2)	1.694(6)
C(1)-O(3)	1.693(4)	C(1)-O(4)	1.813(4)
C(2)-O(1)	1.697(5)	C(2)-O(4)	1.853(4)
C(2)-O(5)	1.653(4)	C(2)-O(6)	1.692(5)
C(2)-C(3)	1.502(4)	D(1)-H(1)	1.113(15)
D(1)-O(2)	1.771(4)	D(1)-O(6)	1.776(4)
D(1)-O(7)	1.762(5)	D(2)-H(2)	1.106(27)
D(2)-O(3)	1.601(6)	D(2)-O(9)	1.760(6)
D(2)-O(8)	1.797(5)	O(3)-H(3)	1.129(26)
D(3)-O(4)	1.770(5)	D(3)-O(8)	1.763(4)
D(3)-O(9)	1.761(5)	D(4)-H(4)	1.097(20)
D(4)-O(2)	1.772(5)	D(4)-O(6)	1.766(5)
D(5)-O(9)	1.760(4)	D(5)-O(6)	1.773(5)
D(6)-H(6)	1.118(21)	D(5)-O(10)	1.762(6)
D(6)-O(10)	1.778(4)	D(6)-O(7)	1.767(5)
D(7)-O(8)	1.769(5)	D(7)-H(7)	1.092(24)
D(8)-H(8)	1.052(29)	D(7)-O(10)	1.774(5)
D(8)-O(10)	1.748(5)	D(8)-O(9)	1.772(6)
D(9)-O(10)	1.771(6)	O(9)-H(9)	1.110(24)
C(3)-C(4)	1.384(5)	D(10)-H(10)	1.121(28)
C(4)-C(5)	1.384(5)	C(3)-C(8)	1.375(5)
C(6)-C(7)	1.363(7)	C(5)-C(6)	1.354(5)
H(1)-H	1.222(32)	C(7)-C(8)	1.350(4)
H(1)-C(10)	1.481(4)	H(1)-C(9)	1.495(4)
H(2)-H	1.519(25)	H(1)-C(11)	1.476(4)
H(2)-C(21)	1.494(3)	H(2)-C(19)	1.462(4)
C(11)-C(12)	1.358(4)	H(2)-C(22)	1.462(5)
C(12)-C(13)	1.363(5)	C(11)-C(20)	1.426(3)
C(14)-C(15)	1.420(5)	C(13)-C(14)	1.361(5)
C(15)-C(20)	1.434(5)	C(15)-C(16)	1.419(4)
C(17)-C(18)	1.391(6)	C(16)-C(17)	1.337(7)
C(19)-C(20)	1.414(4)	C(18)-C(19)	1.366(4)

Anisotropic thermal parameters (Å² × 10³)

The anisotropic temperature factor exponent takes the form
 $-2\pi^2(h^2 a^{*2} U_{11} + \dots + 2hka^*b^*U_{12})$

	U ₁₁	U ₂₂	U ₃₃	U ₁₂	U ₁₃	U ₂₃
O	56(1)	50(1)	117(2)	0(1)	39(1)	6(1)
C(1)	46(2)	49(1)	83(2)	3(1)	30(1)	-3(1)
C(2)	46(1)	40(1)	49(1)	3(1)	24(1)	1(1)
D(1)	46(2)	61(2)	60(2)	19(2)	27(2)	4(2)
H(1)	64					
D(2)	45(2)	63(2)	102(3)	19(2)	34(2)	-2(2)
H(2)	82					
O(3)	46(2)	78(2)	76(2)	-8(2)	17(2)	-12(2)
H(3)	82					
D(4)	53(2)	63(2)	53(2)	-1(2)	23(2)	-4(2)
H(4)	67					
D(5)	58(2)	54(2)	61(2)	16(2)	27(2)	11(2)
H(5)	69					
D(6)	57(2)	59(2)	63(2)	4(2)	35(2)	8(2)
H(6)	67					
D(7)	58(2)	89(3)	80(2)	22(2)	44(2)	13(2)
H(7)	83					
D(8)	36(2)	83(3)	36(3)	17(2)	25(2)	4(2)
H(8)	50					
D(9)	48(2)	89(3)	66(2)	13(2)	14(2)	6(2)
H(9)	64					
D(10)	53(2)	76(2)	83(2)	20(2)	33(2)	24(2)
H(10)	83					
C(3)	46(1)	37(1)	62(2)	-2(1)	27(1)	-5(1)
C(4)	67(2)	69(2)	84(2)	-18(2)	47(2)	-20(2)
C(5)	64(2)	65(2)	137(3)	-37(2)	78(2)	-31(2)
C(6)	54(2)	62(2)	173(4)	-28(2)	54(2)	-13(2)
C(7)	50(2)	66(2)	115(3)	4(2)	10(2)	-8(2)
C(8)	53(2)	61(2)	77(2)	6(1)	18(1)	-9(1)
C(9)	53(1)	45(1)	46(1)	-1(1)	22(1)	-2(1)
H(1)	65(1)	51(1)	52(1)	0(1)	31(1)	-8(1)
H(2)	102(10)					
H	89(2)	55(2)	110(3)	15(2)	61(2)	6(2)
C(9)	66(2)	102(2)	58(2)	-18(2)	18(2)	11(2)
C(10)	50(2)	57(2)	46(1)	4(1)	21(1)	1(1)
C(11)	60(2)	88(2)	79(2)	-3(2)	28(2)	4(2)
C(12)	68(2)	118(3)	91(2)	1(2)	35(2)	17(2)
C(13)	93(2)	100(3)	65(2)	20(2)	51(2)	50(2)
C(14)	99(2)	54(2)	59(2)	16(1)	43(2)	23(2)
C(15)	145(4)	46(2)	84(2)	13(2)	65(3)	25(2)
C(16)	156(4)	42(2)	63(2)	-12(2)	64(3)	-13(2)
C(17)	103(2)	51(2)	70(2)	-9(1)	43(2)	-22(2)
C(18)	79(2)	39(1)	46(1)	0(1)	30(1)	-5(1)
C(19)	66(2)	47(2)	42(1)	7(1)	25(1)	5(1)
C(20)	69(2)	94(2)	66(2)	0(2)	15(2)	7(2)
C(21)	107(3)	82(2)	110(3)	-16(2)	75(2)	-28(2)

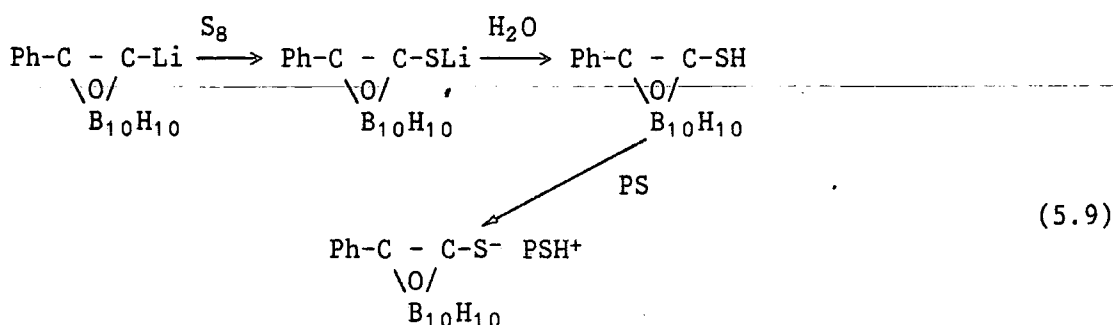
O-C(1)-C(2)	117.7(2)	O-C(1)-O(1)	119.7(2)
C(2)-C(1)-O(1)	92.5(2)	O-C(1)-O(2)	130.0(3)
C(2)-C(1)-O(2)	100.0(2)	O(1)-C(1)-O(2)	60.9(2)
O-C(1)-O(3)	120.3(3)	C(2)-C(1)-O(3)	100.9(2)
O(1)-C(1)-O(3)	103.4(2)	O(2)-C(1)-O(3)	64.7(2)
O-C(1)-O(4)	120.1(3)	C(2)-C(1)-O(4)	92.3(1)
O(1)-C(1)-O(4)	97.0(2)	O(2)-C(1)-O(4)	100.0(2)
O(3)-C(1)-O(4)	69.7(2)	C(1)-C(2)-O(1)	58.3(2)
C(1)-C(2)-O(4)	101.1(2)	O(1)-C(2)-O(4)	108.1(2)
C(1)-C(2)-O(5)	110.0(2)	O(1)-C(2)-O(5)	113.0(2)
O(4)-C(2)-O(5)	63.5(2)	C(1)-C(2)-O(6)	110.2(2)
O(1)-C(2)-O(6)	63.4(2)	O(4)-C(2)-O(6)	114.0(2)
O(5)-C(2)-O(6)	63.9(2)	C(1)-C(2)-C(3)	117.3(2)
O(1)-C(2)-C(3)	117.0(2)	O(4)-C(2)-C(3)	110.8(2)
O(5)-C(2)-C(3)	122.6(2)	O(6)-C(2)-C(3)	121.0(2)
C(1)-O(1)-C(2)	68.2(2)	C(1)-O(1)-O(1)	115.3(14)
C(2)-O(1)-O(1)	117.9(14)	O(1)-O(1)-O(2)	96.0(2)
C(2)-O(1)-O(2)	110.0(2)	O(1)-O(1)-O(2)	122.0(12)
C(1)-O(1)-O(6)	114.6(2)	C(2)-O(1)-O(6)	87.5(2)
O(1)-O(1)-O(6)	121.0(13)	O(2)-O(1)-O(6)	109.3(2)
C(1)-O(1)-O(7)	103.4(2)	C(2)-O(1)-O(7)	106.7(2)
O(1)-O(1)-O(7)	127.4(16)	O(2)-O(1)-O(7)	99.0(2)
O(6)-O(1)-O(7)	99.9(2)	C(1)-O(2)-O(1)	63.6(2)
C(1)-O(2)-O(2)	112.7(17)	O(1)-O(2)-O(2)	119.7(11)
C(1)-O(2)-O(3)	97.8(2)	O(1)-O(2)-O(3)	103.5(3)
O(1)-O(2)-O(7)	122.9(19)	C(1)-O(2)-O(7)	112.9(4)
O(3)-O(2)-O(7)	99.9(2)	H(2)-O(2)-O(7)	120.0(17)
O(1)-O(2)-O(8)	107.5(3)	C(1)-O(2)-O(8)	108.3(3)
O(3)-O(2)-O(8)	105.3(2)	H(2)-O(2)-O(8)	128.1(13)
D(3)-O(2)-O(8)	99.4(2)	O(7)-O(2)-O(8)	60.0(2)
C(1)-O(3)-O(2)	97.7(2)	C(1)-O(3)-O(3)	114.2(12)
O(2)-O(3)-O(3)	121.9(18)	C(1)-O(3)-O(4)	63.3(2)
D(2)-O(3)-O(4)	105.2(2)	H(3)-O(3)-O(4)	121.5(17)
C(1)-O(3)-O(8)	108.0(3)	O(2)-O(3)-O(8)	59.1(2)
H(3)-O(3)-O(8)	126.3(15)	D(4)-O(3)-O(8)	105.2(3)
C(1)-O(3)-O(9)	113.0(2)	O(2)-O(3)-O(9)	107.7(3)
H(3)-O(3)-O(9)	124.2(12)	D(4)-O(3)-O(9)	60.0(2)
O(8)-O(3)-O(9)	60.4(2)	C(1)-O(4)-C(2)	69.7(2)
C(1)-O(4)-O(3)	96.0(2)	C(2)-O(4)-O(3)	110.6(3)
C(1)-O(4)-O(4)	112.4(12)	C(2)-O(4)-O(4)	118.2(10)
D(3)-O(4)-O(4)	120.4(12)	O(1)-O(4)-O(5)	115.1(3)
C(2)-O(4)-O(5)	50.3(2)	D(3)-O(4)-O(5)	109.1(3)
H(4)-O(4)-O(5)	124.6(12)	C(1)-O(4)-O(9)	105.8(3)
C(2)-O(4)-O(9)	105.1(3)	D(3)-O(4)-O(9)	59.0(2)
H(4)-O(4)-O(9)	129.3(10)	H(5)-O(4)-O(9)	59.7(2)
C(2)-O(5)-O(4)	50.3(2)	C(2)-O(5)-O(5)	117.0(12)
O(4)-O(5)-O(5)	119.0(16)	C(2)-O(5)-O(6)	58.1(2)
O(4)-O(5)-O(6)	105.6(2)	H(5)-O(5)-O(6)	121.2(13)
C(2)-O(5)-O(9)	105.3(2)	D(4)-O(5)-O(9)	59.9(2)
H(5)-O(5)-O(9)	125.5(11)	O(6)-O(5)-O(9)	108.4(3)
C(2)-O(5)-O(10)	106.5(2)	O(4)-O(5)-O(10)	106.7(3)
H(5)-O(5)-O(10)	128.0(15)	O(6)-O(5)-O(10)	60.3(2)
D(9)-O(5)-O(10)	60.3(2)	C(2)-O(6)-O(1)	58.7(2)
C(2)-O(6)-O(5)	58.3(2)	O(1)-O(6)-O(5)	106.0(2)
C(2)-O(6)-O(6)	117.4(19)	O(1)-O(6)-O(6)	119.6(11)
D(5)-O(6)-O(6)	121.2(14)	C(2)-O(6)-O(7)	105.1(2)
O(1)-O(6)-O(7)	59.6(2)	D(5)-O(6)-O(7)	107.7(2)
H(6)-O(6)-O(7)	126.2(16)	C(2)-O(6)-O(10)	105.2(2)
O(1)-O(6)-O(10)	105.5(2)	D(5)-O(6)-O(10)	59.6(2)
H(6)-O(6)-O(10)	128.9(12)	O(7)-O(6)-O(10)	60.1(2)
O(1)-O(7)-O(2)	60.4(2)	O(1)-O(7)-O(6)	60.4(2)
O(2)-O(7)-O(6)	110.2(3)	O(1)-O(7)-O(7)	120.7(12)
D(2)-O(7)-O(7)	118.4(14)	O(6)-O(7)-O(7)	121.7(13)
O(1)-O(7)-O(8)	106.6(2)	O(2)-O(7)-O(8)	59.9(2)
O(6)-O(7)-O(8)	108.0(3)	H(7)-O(7)-O(8)	123.0(12)
O(1)-O(7)-O(10)	107.1(3)	O(2)-O(7)-O(10)	108.5(3)
D(6)-O(7)-O(10)	60.3(2)	H(7)-O(7)-O(10)	124.4(14)
O(8)-O(7)-O(10)	59.3(2)	O(2)-O(8)-O(3)	61.5(2)
O(2)-O(8)-O(7)	60.1(2)	D(3)-O(8)-O(7)	109.3(2)
O(2)-O(8)-O(8)	117.9(14)	O(3)-O(8)-O(8)	118.3(17)
O(7)-O(8)-O(8)	122.2(17)	O(2)-O(8)-O(9)	109.1(3)
D(3)-O(8)-O(9)	59.8(2)	O(7)-O(8)-O(9)	108.5(3)
H(8)-O(8)-O(9)	122.7(15)	O(2)-O(8)-O(10)	109.0(2)
D(3)-O(8)-O(10)	109.4(2)	O(7)-O(8)-O(10)	60.0(2)
H(8)-O(8)-O(10)	123.8(15)	D(9)-O(8)-O(10)	60.4(2)
D(3)-O(9)-O(4)	60.3(2)	D(3)-O(9)-O(5)	110.1(2)
D(4)-O(9)-O(5)	60.4(2)	D(3)-O(9)-O(8)	59.9(2)
D(4)-O(9)-O(8)	106.0(2)	H(5)-O(9)-O(8)	107.5(3)
D(3)-O(9)-O(9)	117.7(14)	D(4)-O(9)-O(9)	123.0(18)
O(5)-O(9)-O(9)	123.7(14)	O(8)-O(9)-O(9)	121.0(17)
D(3)-O(9)-O(10)	108.4(3)	D(4)-O(9)-O(10)	108.9(2)
O(5)-O(9)-O(10)	60.0(2)	H(8)-O(9)-O(10)	59.1(2)
H(9)-O(9)-O(10)	123.7(16)	B(5)-B(10)-O(6)	60.0(2)
B(5)-O(10)-O(7)	107.7(2)	O(6)-B(10)-O(7)	59.7(2)
B(5)-O(10)-O(8)	108.3(3)	B(6)-B(10)-B(8)	108.0(2)
B(7)-O(10)-O(8)	59.9(2)	B(5)-B(10)-B(9)	59.7(2)
B(6)-O(10)-O(9)	107.7(3)	B(7)-O(10)-B(9)	107.9(3)
B(8)-O(10)-O(9)	60.5(2)	B(5)-B(10)-B(10)	121.4(16)
O(6)-O(10)-H(10)	118.0(12)	D(7)-B(10)-H(10)	119.8(16)
B(8)-O(10)-H(10)	123.9(14)	B(9)-O(10)-H(10)	125.5(13)
C(2)-C(3)-C(4)	120.5(2)	C(2)-C(3)-C(8)	121.6(3)
C(4)-C(3)-C(8)	117.8(3)	C(3)-C(4)-C(5)	121.0(3)
C(4)-C(3)-C(6)	120.1(4)	C(5)-C(6)-C(7)	120.2(3)
C(6)-C(7)-C(8)	119.7(3)	C(3)-C(8)-C(7)	121.1(3)
H-N(1)-C(9)	120.7(13)	H-N(1)-C(10)	97.3(15)
C(9)-H(1)-C(10)	110.4(2)	H-N(1)-C(11)	101.3(15)
C(9)-H(1)-C(11)	112.7(3)	C(10)-H(1)-C(11)	115.5(2)
H-N(2)-C(19)	93.8(13)	H-N(2)-C(21)	116.6(11)
C(19)-H(2)-C(21)	111.8(2)	H-N(2)-C(22)	106.9(15)
C(19)-H(2)-C(22)	114.0(2)	C(21)-H(2)-C(22)	108.6(2)
H(1)-H-N(2)	104.0(29)	H(1)-C(11)-C(12)	119.6(2)
H(1)-C(11)-C(20)	118.1(2)	C(12)-C(11)-C(20)	122.3(3)
C(11)-C(11)-C(13)	120.4(3)	C(12)-C(13)-C(14)	120.3(3)
C(13)-C(11)-C(15)	121.6(4)	C(14)-C(13)-C(16)	122.6(4)
C(14)-C(11)-C(20)	118.8(3)	C(16)-C(15)-C(20)	118.6(3)
C(15)-C(11)-C(17)	121.3(4)	C(16)-C(17)-C(18)	120.7(3)
C(17)-C(11)-C(19)	120.6(3)	H(2)-C(19)-C(18)	120.9(3)
H(2)-C(19)-C(20)	118.2(2)	C(18)-C(19)-C(20)	120.9(3)
C(11)-C(20)-C(15)	116.6(3)	C(11)-C(20)-C(19)	125.7(3)
C(15)-C(20)-C(19)	117.8(2)		

			[C14 H16 N2] [PhC2 B10 H10 O]		
1					
2	O	5	.00000	.00000	.00000
3	C1	1	-.87059	.84746	.27275
4	C2	1	-.27265	2.75598	.44019
5	B1	3	-.72376	1.83315	1.79750
6	H1	2	.08624	1.51787	2.49192
7	B2	3	-2.10859	.79838	1.41291
8	H2	2	-2.20386	-.19106	1.89626
9	B3	3	-2.42387	1.04882	-.34282
10	H3	2	-2.76752	.20812	-1.01387
11	B4	3	-1.20045	2.21332	-.87234
12	H4	2	-.69172	2.08409	-1.83610
13	B5	3	-1.51731	3.77948	-.10515
14	H5	2	-1.23275	4.66902	-.59147
15	B6	3	-1.27827	3.33007	1.02401
16	H6	2	-.68194	4.31816	2.23400
17	B7	3	-2.35661	2.34253	2.22071
18	H7	2	-2.69114	2.33777	3.26250
19	B8	3	-3.39235	1.87273	.87805
20	H8	2	-4.39690	1.55742	1.02145
21	B9	3	-2.85828	2.73996	-.57249
22	H9	2	-3.57104	2.98387	-1.38724
23	B10	3	-2.86692	3.53459	1.00956
24	H10	2	-3.53797	4.38152	1.30874
25	C3	1	1.16435	3.05550	.23016
26	C4	1	1.63596	3.41135	-1.02093
27	H4A	2	1.01883	3.48725	-1.75242
28	C5	1	2.98068	3.66255	-1.23168
29	H5A	2	3.29070	3.90621	-2.10701
30	C6	1	3.85953	3.56437	-.20592
31	H6A	2	4.79448	3.71863	-.35980
32	C7	1	3.41959	3.24608	1.05044
33	H7A	2	4.03926	3.20250	1.78233
34	C8	1	2.07007	2.99190	1.26297
35	H8A	2	1.76494	2.76375	2.14423
36	N1	4	2.44614	-1.12445	-1.56782
37	N2	4	.34835	-2.59568	-1.85317
38	H	2	1.46027	-1.76528	-1.23514
39	C9	1	2.30409	.15151	-2.33217
40	H9A	2	1.98252	-.05708	-3.21224
41	H9B	2	3.15598	.58902	-2.39811
42	H9C	2	1.67908	.73251	-1.89240
43	C10	1	2.96490	-.85496	-.20679
44	H10A	2	3.02990	-1.66960	.29686
45	H10B	2	2.39560	-.23665	.25703
46	H10C	2	3.83986	-.47104	-.30852
47	C11	1	3.21817	-2.14367	-2.30039
48	C12	1	4.54120	-1.94432	-2.53317
49	H12	2	4.96329	-1.14019	-2.22208
50	C13	1	5.28572	-2.89620	-3.21252
51	H13	2	6.21764	-2.73993	-3.38202
52	C14	1	4.70466	-4.03715	-3.64262
53	H14	2	5.23959	-4.68827	-4.10252
54	C15	1	3.32480	-4.29686	-3.42712
55	C16	1	2.69575	-5.49267	-3.86062
56	H16	2	3.21122	-6.15305	-4.32965
57	C17	1	1.39903	-5.71905	-3.62849
58	H17	2	.99779	-6.53645	-3.93257
59	C18	1	.62210	-4.77943	-2.95150
60	H18	2	-.30457	-4.96376	-2.78180
61	C19	1	1.16811	-3.60392	-2.52424
62	C20	1	2.53811	-3.32043	-2.73181
63	C21	1	-.55991	-1.89224	-2.80881
64	H21A	2	.01446	-1.52661	-3.48531
65	H21B	2	-1.00239	-1.17826	-2.34426
66	H21C	2	-1.21509	-2.46172	-3.21886
67	C22	1	-.45366	-3.11984	-.74927
68	H22A	2	-.15980	-3.55357	-1.15179
69	H22B	2	-1.13345	-3.74242	-1.01737
70	H22C	2	-.86100	-2.37357	-.30338

5.6 CONCLUSIONS AND FUTURE WORK

Several \underline{C} -hydroxy carborane derivatives have been prepared. On deprotonation with amine bases, these derivatives yield salts which show evidence of delocalisation of electron density from the negative oxygen atom into the cage. This has been manifest in the spectroscopic (IR and NMR) properties of these compounds, and in the molecular structure of the anion $C_6H_5C_2B_{10}H_{10}O^-$ generated by deprotonation of 1-hydroxy-2-phenyl-ortho-carborane with proton sponge. Electron delocalisation into the cage in this species is shown by a short CO bond and substantial cage distortion, which are quantitatively explained by treating the system as a μ_5 CO ligand stabilising a nido shaped $PhCB_{10}H_{10}^-$ residue.

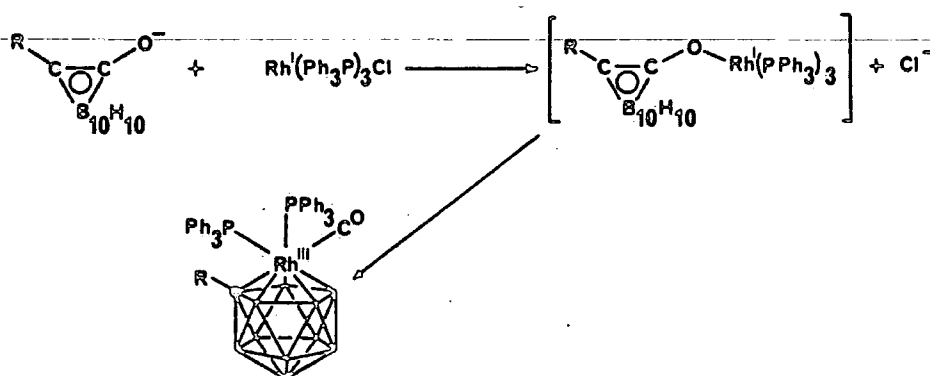
As discussed in the previous section, the frontier orbital considerations used to rationalise the distortions in (XXIX) have implications for the structures of a number of other systems providing much scope for further study. Firstly the meta and para analogues of (XXIX) clearly need to be structurally characterised to verify the predictions made about the possible cage distortions likely to be seen in these compounds. The sulphur analogue of 1-hydroxy-2-phenyl-ortho-carborane²¹



should in principle be deprotonated by proton sponge to give the anion shown in equation 5.9. The molecular structure of this species would be expected to show similar distortions in the cage to those seen in (XXIX).

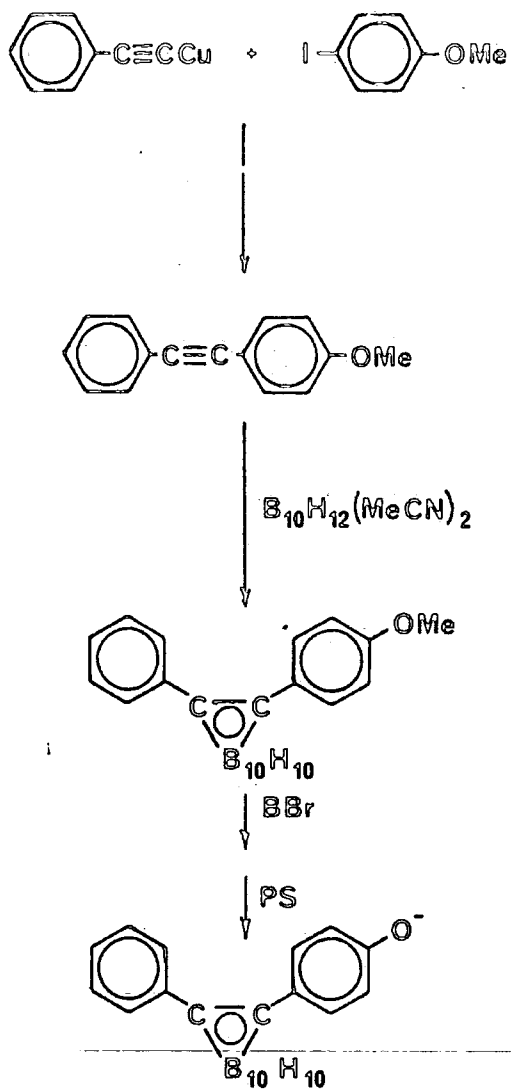
The preparation of a 1-(4-hydroxy-phenyl)-ortho-carborane derivative and its deprotonation with proton sponge will undoubtedly yield a species worthy of structural characterisation. For this purpose, a derivative possessing a substituent on the other carbon atom is necessary to act as a label for this carbon atom (indistinguishable from boron in X-ray analysis). Scheme 1 gives a proposed route to the species 1-(4-hydroxyphenyl)-2-phenyl-ortho-carborane from commercially available precursors. Deprotonation of this species would produce a salt that could be readily structurally characterised. Also the 4-dimethylamino analogue would be worthy of study. A proposed route to this material is given in Scheme 2.

Finally, the carbonyl like nature of the CO group in the anion of (XXIX) suggests that it may be possible to abstract CO from this species. Simply removing CO thermally, or chemically by the action of decarbonylating agents such as trimethylamine *N*-oxide would leave the $\text{PhCB}_{10}\text{H}_{10}^-$ residue. This would be expected to close, giving the eleven vertex closo mono carbaborane. Alternatively the action of a suitable transition metal substrate might induce an oxidative insertion of the metal accompanied by CO abstraction to give a metalla-carborane derivative. One reaction that could be envisaged is shown in equation 5.10.

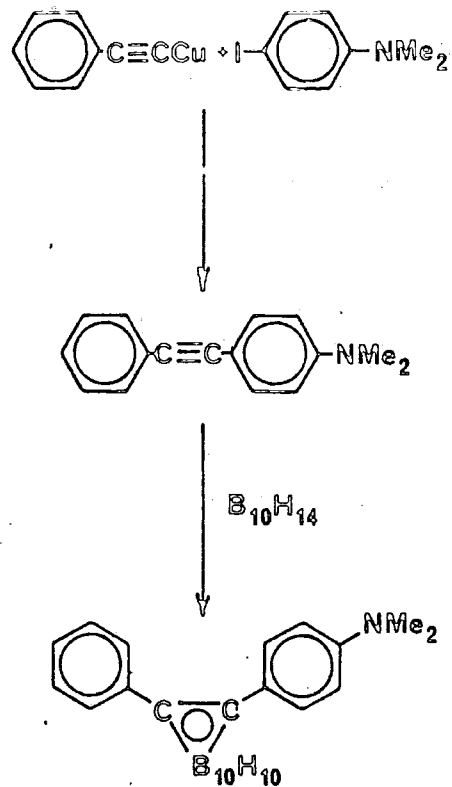


(5.10)

Scheme 1



Scheme 2



5.7 REFERENCES

1. D.A. Brown, W. Clegg, H.M. Colquhoun, J.A. Daniels, I.R. Stephenson, K. Wade, J. Chem. Soc. Chem. Commun. 1987, 889.
2. V. Gregor, S. Hermanek, J. Plesek, Collect. Czech. Chem. Commun., 1968, 33, 980.
3. L.I. Zakharkin, G.G. Zhigerava, J. Gen. Chem. U.S.S.R. 1970, 40, 2318.
4. D.A. Brown, PhD Thesis, Durham, 1985.
5. L.I. Zakharkin, G.G. Zhigerava, Bull. Acad. Sci. U.S.S.R. Chem. Div., 1970, 2153.
6. R.M. Silverstein, C.G. Bassler, T.C. Morrill, Spectrometric Identification of Organic Compounds, John Wiley, 1981, p 117.
7. H. Gilman, E. Adams, J. Amer. Chem. Soc. 1925, 48, 2816.
8. W.R.S. Steele, D.R. Winterman, Chem Commun. 1968, 723.
9. H. Einspahr, J.B. Robert, R.E. Marsh, J.D. Roberts, Acta. Cryst., 1973, B29, 1611.
10. R.W. Alder, J.E. Anderston, J. Chem. Soc. Perkin II, 1973, 2086.
11. D.M.P. Mingos, J. Chem. Soc. Dalton Trans. 1977, 602.
12. H.M. Colquhoun, T.H. Greenhough, M.G.H. Wallbridge, J. Chem. Soc. Dalton Trans., 1979, 619.
13. Transition Metal Clusters, e.d. B.F.G. Johnson, John Wiley, New York, 1980.
14. Metal Clusters, e.d. M. Muskovits, John Wiley, New York, 1986.
15. J.E. Crook, N.N. Greenwood, J.D. Kennedy, W.S. McDonald, J. Chem. Soc. Chem. Commun. 1981, 933.
16. R.V. Shultz, F. Sato, L.J. Todd, J. Organomet. Chem. 1977, 125, 115.
17. P.A. Wagner, L.J. Guggenberger, E.L. Muetterties, J. Amer. Chem. Soc. 1970, 92, 3473.
18. J.E. Crook, N.N. Greenwood, J.D. Kennedy, W.S. McDonald, J. Chem. Soc. Chem. Commun. 1983, 83.
19. V.I. Bregadze, O. Yu. Okhlobystin, Organomet. Chem. Rev. 1969, 4, 345.

20. G.W. Wheland, Resonance in Organic Chemistry, 1955, Wiley, New York.
21. L.I. Zakharkin, G.G. Zhigareva, A.K. Kazantsev, J. Gen. Chem. U.S.S.R. 1968, 38, 86.

CHAPTER 6

NMR AND THEORETICAL STUDIES ON
ICOSAHEDRAL CARBORANES

6.1 INTRODUCTION

This chapter describes the complete assignment of resonances in the ^{11}B spectra of a series of ortho carborane derivatives, including the C-hydroxy carboranes and their trialkylammonium salts described in Chapter 5. These assignments have been made using the recently developed ^{11}B - ^{11}B 2D COSY NMR technique.

Explanation of the effects of substitution on the ^{11}B spectra of these compounds, identified as a result of making the assignments, are proposed in terms of:

- i) The π donating ability of the substituents attached. This is manifest in changes of the average chemical shift calculated for each spectrum.
- ii) The extent to which the polarity of the cage is distorted by the substituent. This has been found to be largely due to the electronegativity of the substituent and has been monitored using molecular orbital calculations on model systems.

Finally the assignment of the proton NMR spectra of several carborane derivatives have been made using ^{11}B heteronuclear decoupling. The trends identified as a result are also discussed.

N.B. The 'highfield negative' sign convention for chemical shift is used in this chapter. It should be noted that much of the earlier literature (pre 1976) uses the 'high field positive' sign convention.

6.2 ^{11}B NMR studies on icosahedral carborane derivatives

One technique that has played a major part in the development of boron chemistry is ^{11}B NMR. The ^{11}B nucleus (spin 3/2) is of high relative abundance (81.7%) and sensitivity (0.165 relative to ^1H), therefore data may be readily obtained using conventional Continuous Wave and Fourier Transform techniques¹. As a result this area is covered quite extensively in the literature^{2,3}. In polyhedral boron hydride chemistry, the main use of ^{11}B NMR has been in confirming the formation of new compounds by comparing patterns seen in spectra with patterns exhibited by fully characterised species^{4,5}.

Relationships do exist between ^{11}B chemical shift values ($\delta(^{11}\text{B})$) and co-ordination number in structurally related compounds⁶, i.e. atoms of higher co-ordination number resonate at lower frequency (higher field) than atoms of lower co-ordination number. (E.g. the spectrum of $\text{B}_{10}\text{H}_{10}^{2-}$, where the signal of the eight tropical boron atoms are shielded relative to the signal of the two polar atoms⁵). The position of bridging hydrogen atoms also consistently affects $\delta(^{11}\text{B})$ values⁷, and atoms bonded to substituents other than hydrogen may easily be identified by comparing proton coupled and decoupled spectra (boron atoms with terminally bound hydrogen atoms are split into a doublet due to coupling with ^1H , spin $\frac{1}{2}$). The attachment of substituents onto, and the inclusion of hetero atoms into borane frameworks can predictably influence $\delta(^{11}\text{B})$ values of certain boron atoms. The most common effect is the perturbation of the $\delta(^{11}\text{B})$ of the atom diametrically opposite (antipodal to) the hetero atom, or the point of substitution. This is called the Antipodal Effect^{8,9,10,11}. Considering ^{11}B NMR of boranes and carboranes as a whole however, there is no generally applicable theory for explaining $\delta(^{11}\text{B})$ values quantitatively. Therefore assignments of individual resonances in ^{11}B NMR spectra is more often than not a difficult task.

Another problem associated with the spectra of polyhedral boron

hydrides is the broadening of signals caused by unresolved ^{11}B - ^{11}B coupling (typically 50-150 Hz¹²). Therefore in many cases where line widths are broad relative to spectrum width, resolution may be hampered by coincidental overlap of signals from inequivalent boron atoms.

Enhancement of resolution may be achieved in some cases by using line narrowing techniques¹³, or increasing the relaxation times of nuclei by running spectra at elevated temperatures. Assignments can, in principle, be made using substitution and isotopic labelling experiments, however these are time consuming and not possible in many cases. Double resonance techniques can also be used, as in the assignment of the spectrum of 8-iodo-ortho-carborane¹⁴. Distinctions can be made between atoms in a cage on the basis of variations in relaxation times using partial relaxation¹⁵. More recently the application of two dimensional techniques¹⁶ in the form of ^{11}B - ^{11}B 2D COSY NMR^{17,18} has been helpful in many cases. This is demonstrated in the present study where without it, unambiguous assignments of ^{11}B resonances would not have been possible.

In the carborane derivatives studied here, all the boron atoms are six co-ordinate, all possess terminally bound hydrogen atoms (all cage substitution has been carried out at the carbon atoms) and obviously there are no bridging hydrogen atoms present. However the antipodal effect occurs very clearly as a shielding of the atom opposite the substituted carbon atom, and so by using it in conjunction with the ^{11}B - ^{11}B 2D COSY technique, assignments of ^{11}B spectra of a series of compounds have been made.

6.3 RESULTS

6.3.1 Experimental

The synthesis of all the compounds studied here have been described in previous chapters (Chapters 2 and 5). All spectra were run on a Brüker WH.360 Fourier Transform NMR spectrometer operating at 115.548 MHz, unless otherwise stated. The solvent used, unless otherwise stated, was C_6D_6 (lock - C_6D_5H 7.16 ppm) and all spectra were referenced externally to $BF_3 \cdot Et_2O$ at 0.00 ppm.

6.3.2 Assignment of Spectra - The use of ^{11}B - ^{11}B 2D COSY NMR

The following text starts by outlining the use of the ^{11}B - ^{11}B COSY technique in making spectral assignments. The ^{11}B - ^{11}B COSY spectrum (see figures 6.2-6.10) consists of a two dimensional contour plot in which the x and y directions represent $\delta(^{11}B)$ and the contours represent the resonance intensities. The signals along the central diagonal carry exactly the same chemical shift information as the conventional 1D spectrum (also shown in figures 6.2-6.10).

The off diagonal cross peaks arise from ^{11}B - ^{11}B spin coupling which, in the case of boron hydride cage systems, is only significant for adjacent nuclei. This means that cross peaks will only occur between signals on the diagonal of atoms that are directly bonded to each other. Hence all the cage connectivities may be deduced from information displayed by these cross peak signals. Assignments can be made by comparing the B-B and C-B connectivities in the ortho-carborane cage, shown in figure 6.1, with the cross peak information shown in the ^{11}B - ^{11}B COSY plots and noting the following points:

- i) B(8,10) is the only pair of boron atoms bonding to every

other boron environment in the cage. Consequently the COSY plot should have one resonance of integral 2B showing cross peaks with every other resonance on the diagonal.

- ii) On substitution of the cage carbon atoms, the molecule loses a plane of symmetry so that B(9) and B(12) become unique atoms. Also B(4,5) and B(7,11) are no longer equivalent. B(9) and B(12) may be identified from integration data given by the 1D spectra, and the two may be distinguished through a knowledge of the antipodal effect, i.e. substitution at C(1) causes the signal of B(12) to be shielded (resonate at lower frequency, or higher field) relative to that of B(9). Being able to differentiate between the signals of B(9) and B(12) in this manner is an essential handle. The information supplied by the COSY plot alone does not allow this to be done.
- iii) B(3,6) is the only pair not bonding to either B(9) or B(12). Therefore the B(3,6) signal can be assigned because it is the only one showing no cross peaks with the signals from B(9) or B(12) in the COSY plot.
- iv) A distinction can be made between B(4,5) and B(7,11) since B(4,5) is bonded to B(9) but not B(12) and B(7,11) is bonded to B(12) but not to B(9). This again is shown up in the information supplied by the cross peaks in the COSY plot.

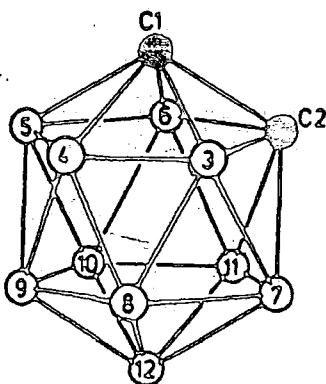


Figure 6.1

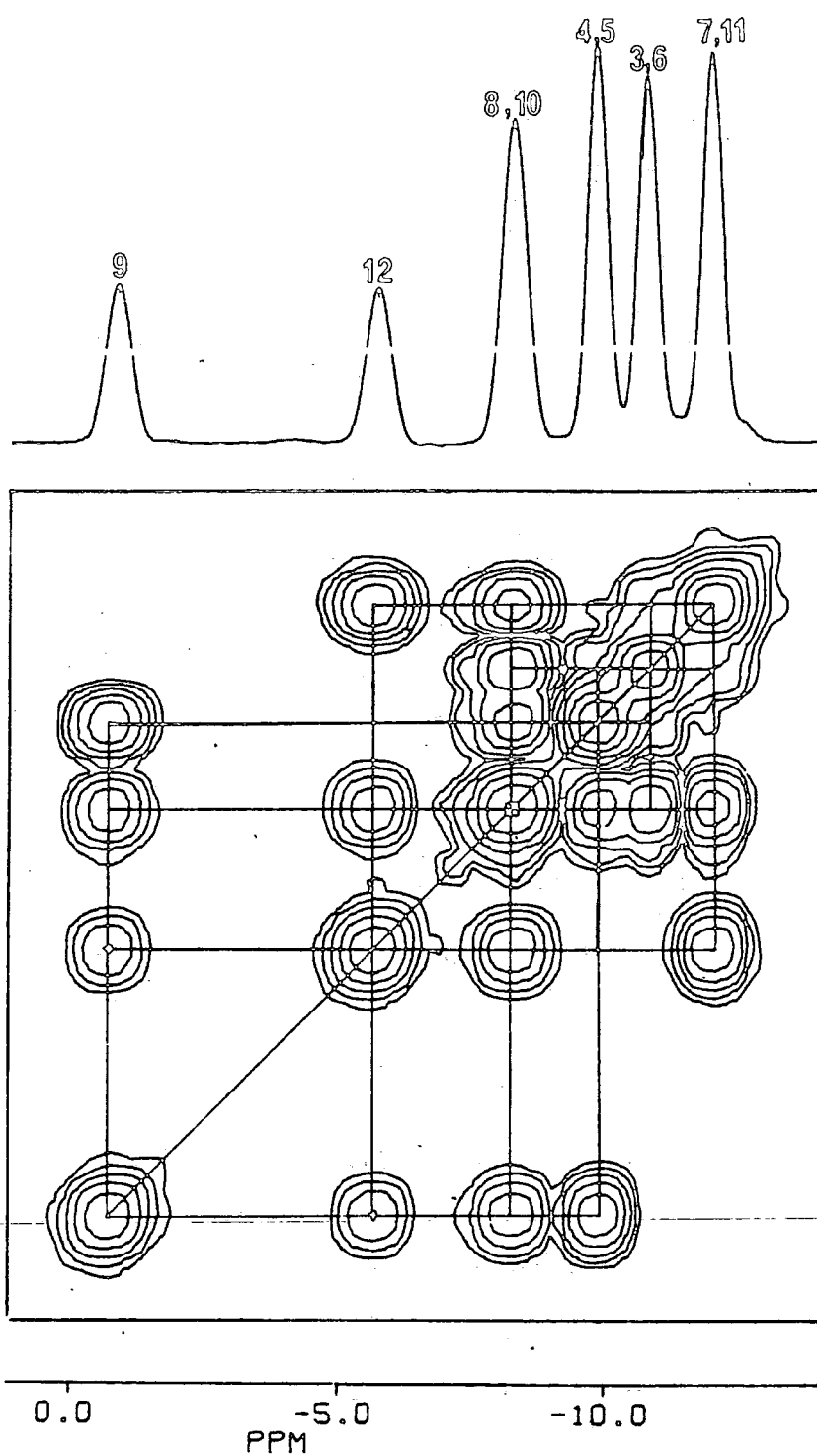


Figure 6.2 $^{11}\text{B}\{^1\text{H broad band noise}\}$ and $^{11}\text{B } ^{11}\text{B}$ 2D COSY NMR spectra of 1-methyl-ortho-carborane

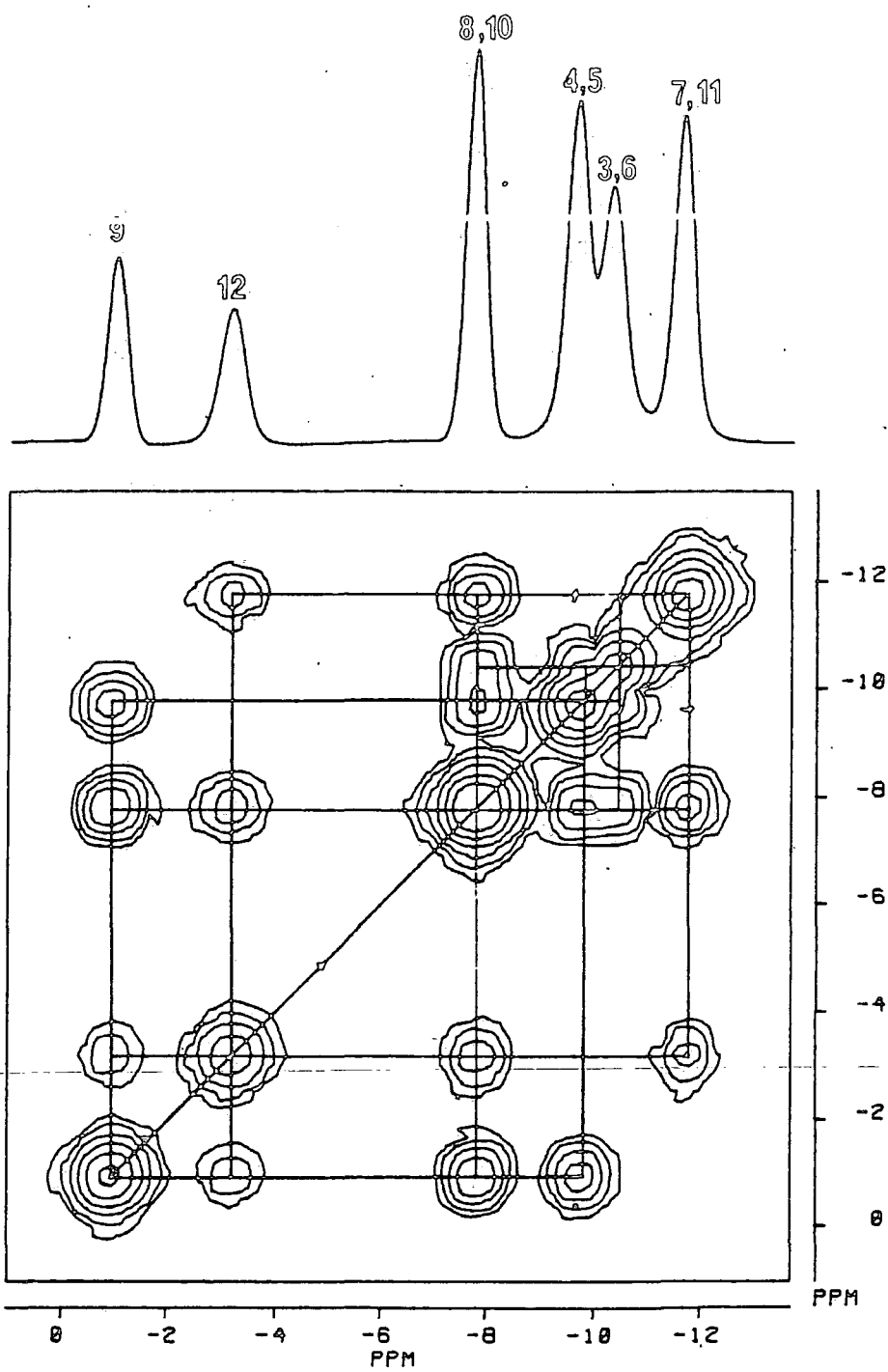


Figure 6.3

The $^{11}\text{B}\{^1\text{H}$ broad band noise $\}$ and ^{11}B ^{11}B 2 D COSY NMR spectra of 1-phenyl-ortho-carborane

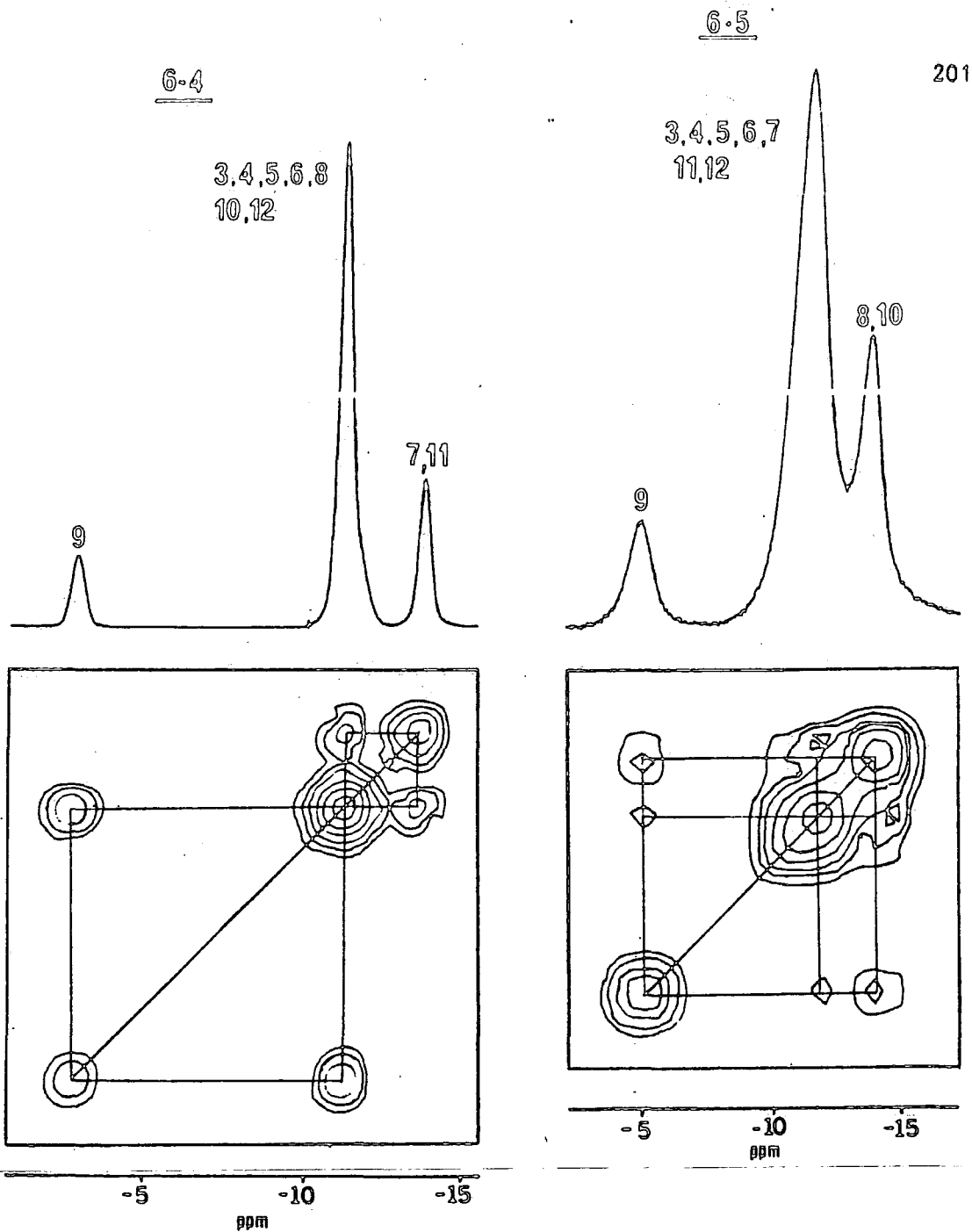


Figure 6.4

$^{11}\text{B}\{^1\text{H broad band noise}\}$ and $^{11}\text{B } ^{11}\text{B}$ 2D COSY NMR spectra of 1-hydroxy-ortho-carborane

Figure 6.5

$^{11}\text{B}\{^1\text{H broad band noise}\}$ and $^{11}\text{B } ^{11}\text{B}$ 2D COSY NMR spectra of 1-hydroxy-2-phenyl-ortho-carborane

(Spectra run on an AC 250 machine at 80.24 MHz)

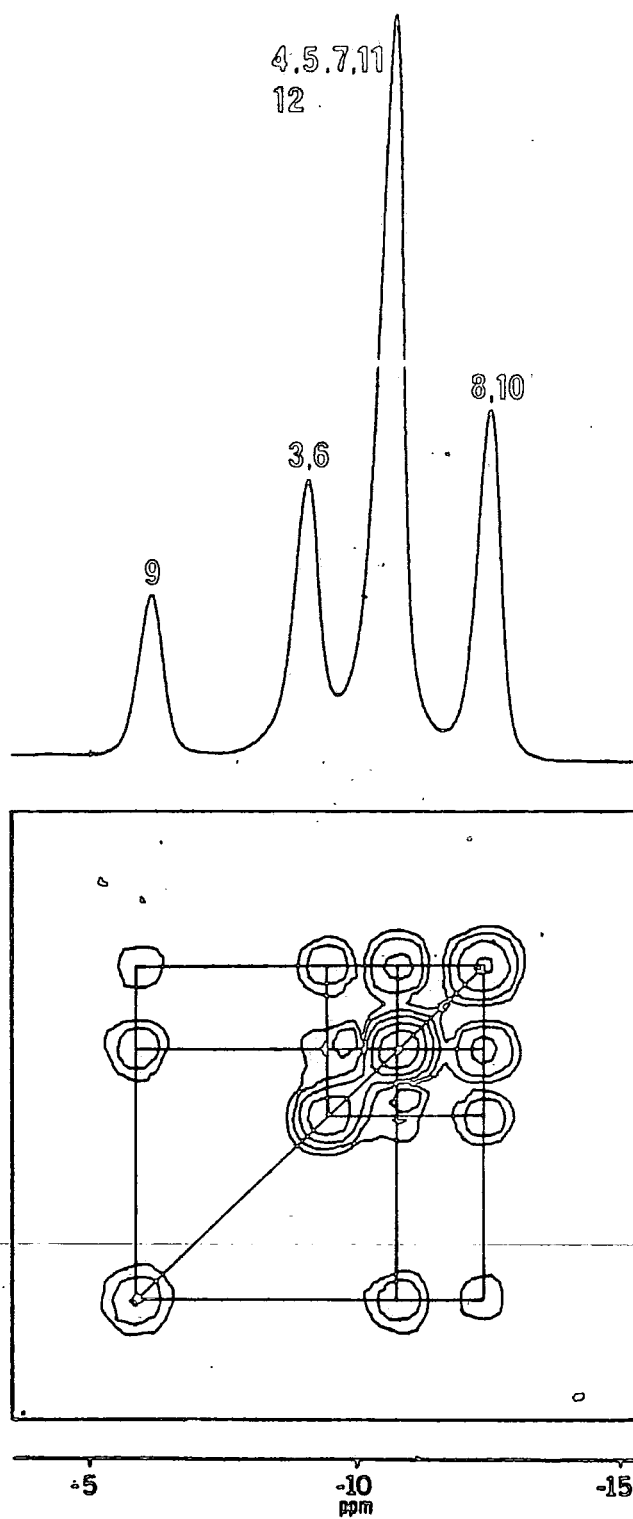


Figure 6.6

$^{11}\text{B}\{^1\text{H}$ broad band noise $\}$ and ^{11}B ^{11}B 2D COSY NMR spectra of
1-hydroxy-2-methyl-ortho-carborane

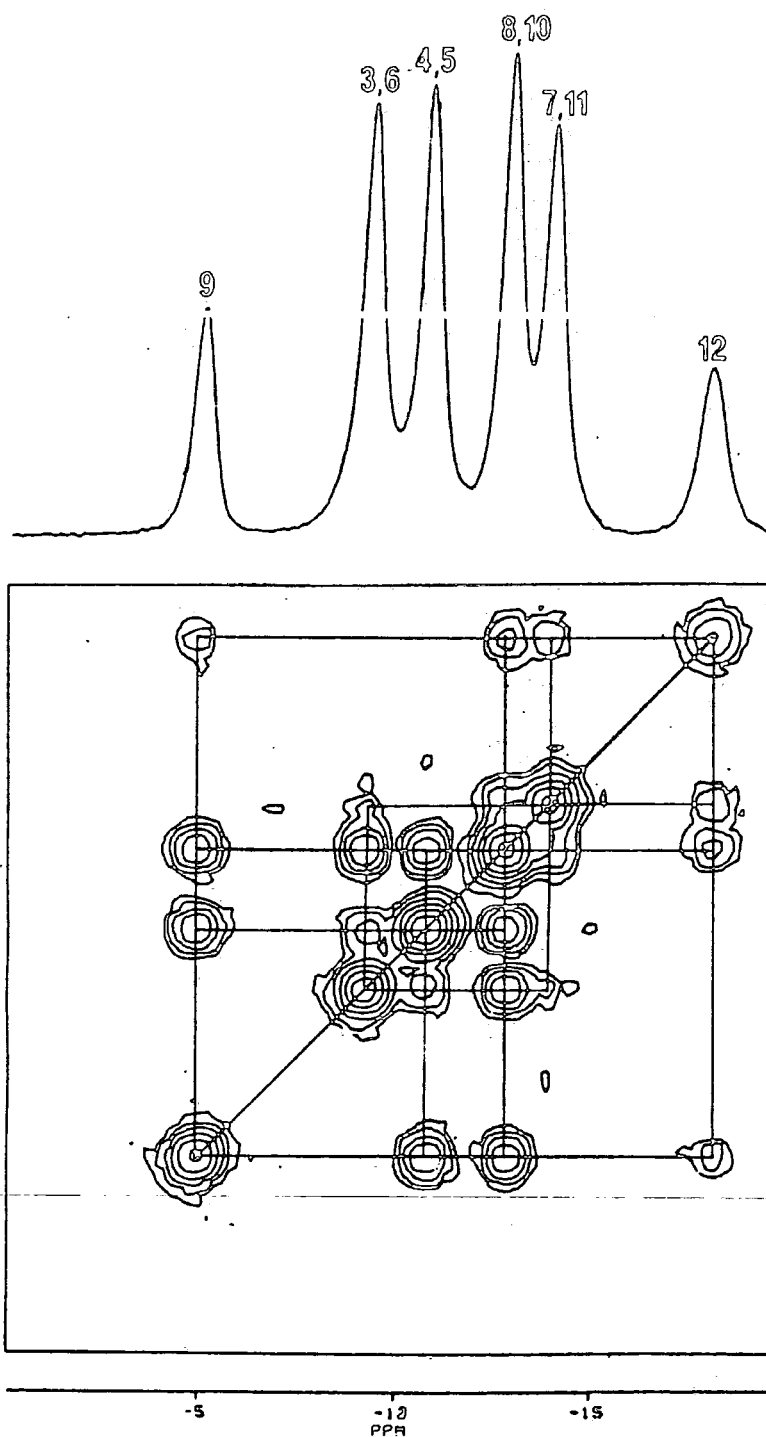
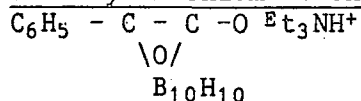


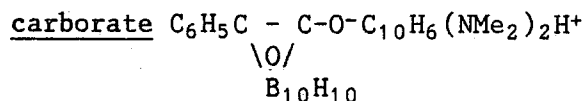
Figure 6.7

$^{11}\text{B}\{^1\text{H}$ broad band noise $\}$ and ^{11}B ^{11}B 2D COSY NMR spectra of triethylammonium 1-oxo-ortho-carborate

ix) Triethylammonium 1-oxo-2-phenyl-ortho-carborate

Resonance Pattern { ¹ H}	$\delta(^{11}\text{B})$ (ppm)	Integral	Assignment
S	-6.87	1B	B(9)
S	-8.82	2B	B(3,6)
S	-12.36	4B	B(4,5,7,11)
S	-16.21	2B	B(8,10)
S	-18.92	1B	B(12)

The spectrum of the 1-oxo-2-phenyl derivative was run on a Bruker AC250 MHz machine operating at 80.24 MHz. At room temperature on this instrument, the resolution of the COSY spectrum was not sufficient to allow unambiguous assignments to be made, resolution was therefore enhanced by running the spectrum 325K.

x) 1,8 NNN'N' tetramethylnaphthalene diammonium 1-oxo-2-phenyl ortho carborate

Resonance Pattern { ¹ H}	$\delta(^{11}\text{B})$ (ppm)	Integral	Assignment
S	-5.43	2B	B(3,6)
S	-6.51	1B	B(9)
S	-11.12	2B	B(7,11)
S	-14.04	2B	B(4,5)
S	-16.97	2B	B(8,10)
S	-21.06	1B	B(12)

Coincidental overlap occurs once again in the spectra of triethylammonium 1-oxo-2-methyl and 1-oxo-2-phenyl-ortho-carborate (figures 6.8 and 6.9 respectively) resulting in resonances of integral 4B in both cases. The resonances of B(9), B(12) and B(8,10) can be assigned for both compounds as before, however identifying the remaining signals is not quite as straightforward. The resonance at -10.96 ppm of integral 4B in figure 6.8 (the 1-oxo-2 methyl derivative) shows cross peak correlations with all other signals on the diagonal in the COSY plot which leads to an assignment of B(4,5,7,11). Therefore by elimination the remaining resonance at -7.06 ppm would be assigned to B(3,6). This resonance on the other hand, shows no cross peak signal with the resonance of B(12) but does show one with B(9). This suggests it should be assigned to B(4,5), leaving the resonance at -10.96 ppm as a combination of B(7,11) and B(3,6). This assignment is impossible because a strong cross peak signal occurs between the resonances of B(9) and of integral 4B. The spectrum of the 1-oxo-2-phenyl derivative (figure 6.9) poses the same problem, however the position and extremely weak intensity of the apparent cross peak signal between the resonances at -6.87 and -8.82 ppm casts much doubt on this reflecting a direct linkage between the two sites.

The final spectrum (figure 6.10) was run in an effort to observe this apparently spurious cross peak signal again. The effect of running the ^{11}B NMR spectrum of the same anion ($\text{C}_6\text{H}_5\text{C}_2\text{B}_{10}\text{H}_{10}\text{O}^-$ - see figure 6.9) with a more basic counterion, and in a more polar solvent, has been to spread the resonances in the spectrum and also to resolve the signals of B(4,5) and B(7,11). The assignment of the spectrum is once again easily achieved using the COSY plot and shows that no cross peak signal occurs between the high frequency resonance at -5.43 ppm due to B(3,6) (now deshielded relative to B(9)) and the resonance at -6.51 due to B(9). The lack of an apparent cross peak signal between the resonances of B(9) and B(3,6) and the similarity in the positions of the resonances of B(3,6), B(4,5) and B(7,11) in the spectrum compared to those seen in the spectra of the triethylammonium 1-oxo-2-methyl and

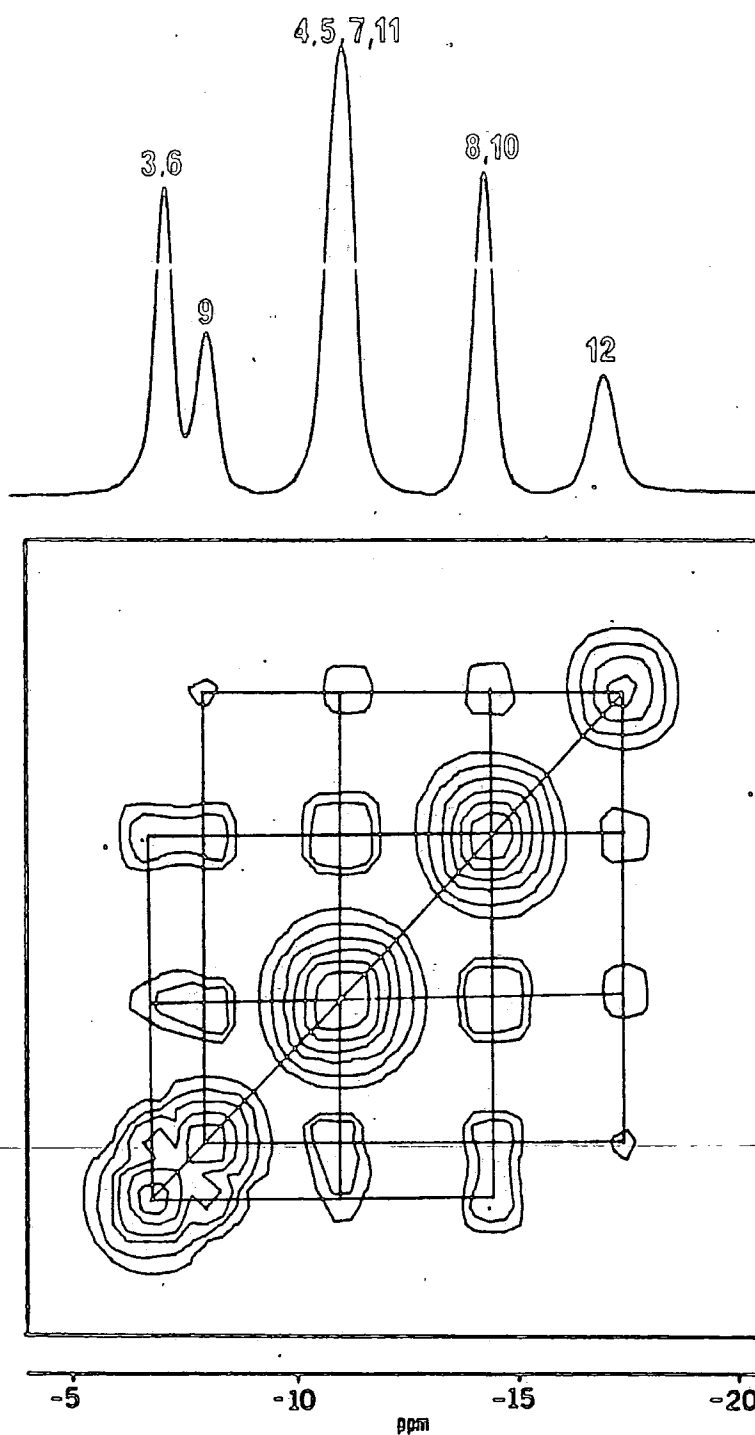


Figure 6.8

$^{11}\text{B}\{^1\text{H}$ broad band noise $\}$ and ^{11}B ^{11}B 2 D COSY NMR spectra
of triethylammonium-1-oxo-2-methyl-ortho-carborate

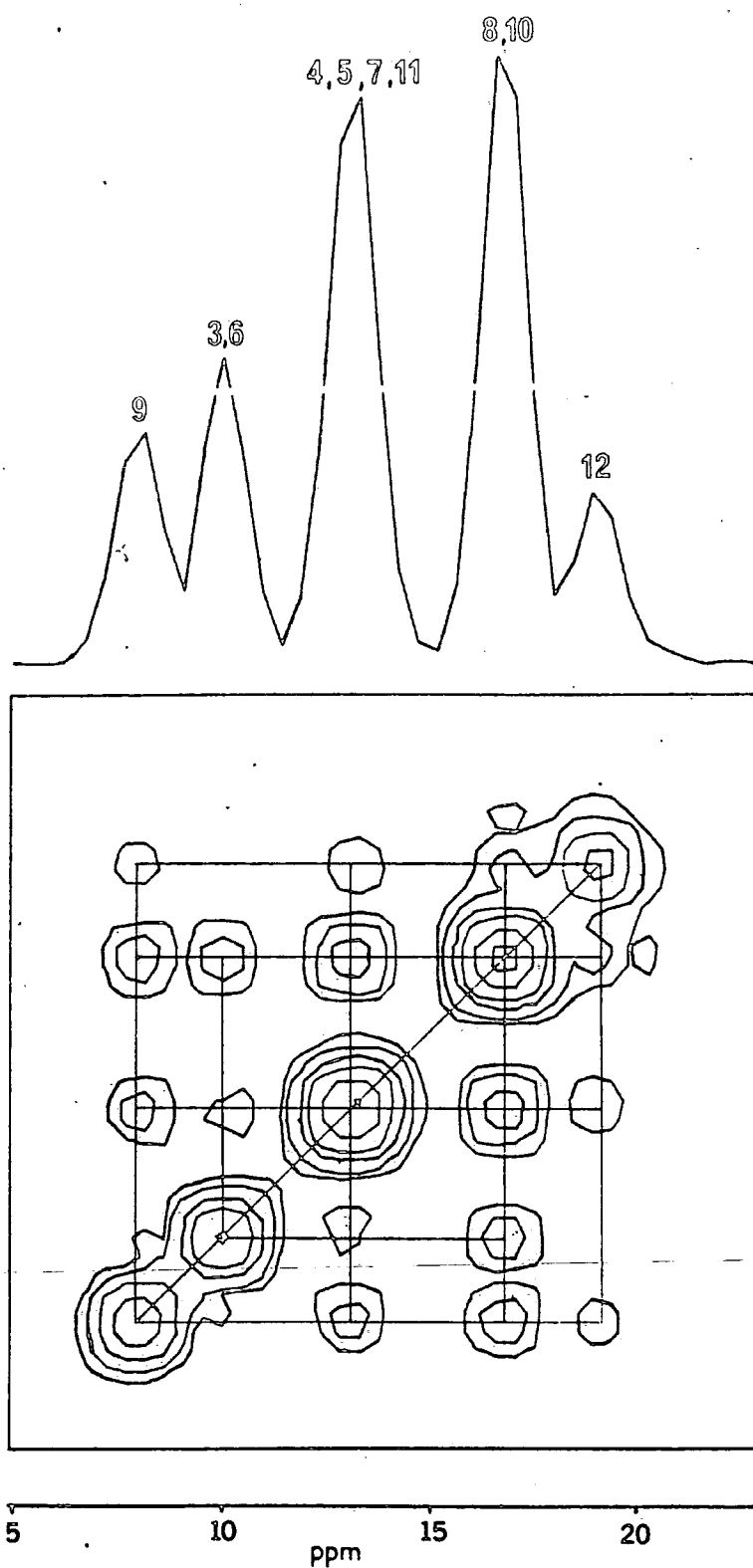


Figure 6.9

$^{11}\text{B}\{^1\text{H}$ broad band noise $\}$ and ^{11}B ^{11}B 2D COSY NMR spectra of triethylammonium-1-oxo-2-phenyl-ortho-carborate

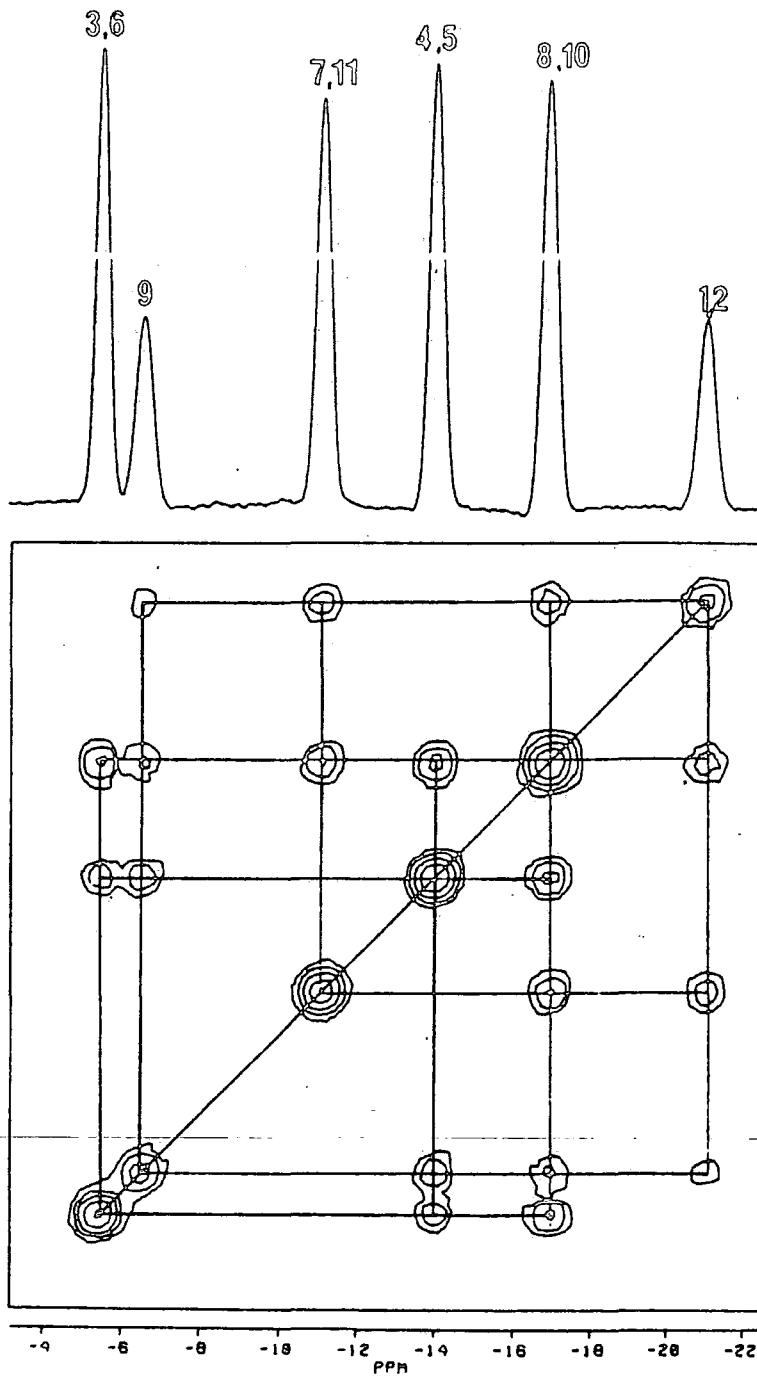


Figure 6.10

^{11}B $\{^1\text{H}$ broad band noise $\}$ and ^{11}B ^{11}B 2D COSY NMR spectra of 1,8 NNN'N' tetra-naphthalenediammonium 1-oxo-2-phenyl-ortho-carborate

1-oxo-2-phenyl derivatives (figures 6.8 and 6.9) confirm the spectral assignments made for these two latter compounds. The occurrence of these weak cross peak signals may be due to noise which, superimposed on the authentic resonances, gives rise to signals of sufficient intensity to be detected.

6.3.3. Discussion

In explaining spectral assignments not all the cross peak signals occurring in the COSY plots have been mentioned mainly for brevity's sake. Table 6.1 summarises all the connectivities within the cage and therefore all the atoms that should couple to give a cross peak signal, provided all inequivalent ^{11}B resonances are resolved.

Table 6.1 x denotes connectivities

Atoms	B(3,6)	B(4,5)	B(7,11)	B(8,10)	B(9)	B(12)
B(3,6)		x	x	x		
B(4,5)	x			x	x	
B(7,11)	x			x		x
B(8,10)	x	x	x		x	x
B(9)		x		x		x
B(12)			x	x	x	

In virtually all the fully resolved spectra shown, the resonances of B(3,6) and B(4,5,7,11), which are expected to produce a cross peak signal, either show consistently weak signals or none at all. For instance in the spectra of 1-methyl- and 1-phenyl-ortho-carborane (figures 6.2 and 6.3) the cross peak signals between the resonances of B(3,6) and both B(4,5) and B(7,11) are barely visible, and in figure 6.10 the expected cross peak signal between the resonances of B(3,6) and B(7,11) is absent altogether. A cross peak signal will

occur only when¹⁸ :

- a) there is sufficient electron density between nuclei to permit scalar coupling;
- b) the longitudinal relaxation time (spin - spin) T_1 , is long enough to prevent decoupling of the nuclei;
- c) the transverse relaxation time (spin - lattice) T_2 , is long enough to prevent signal decay.

Therefore the weak intensity or absence of these cross peak signals may be an indication that bonding to the relatively electronegative carbon atoms of the cage has diminished the electron density between B(3,6) and B(4,5,7,11), or that bonding to carbon has altered the relaxation times of these boron atoms so as to prevent visible coupling.

Figure 6.11 gives schematic plots of all the spectra described in Section 6.3.2. arranged in sequences according to substitution pattern to allow visual comparisons to be made. The only really predictable trend that emerges on looking at these schemes is in the shielding of the antipodal atom B(12) on substitution at C(1). This gets progressively greater according to the sequence Ph<Me<OH<O⁻ which suggests a correlation between the magnitude of the shielding produced and the electron donating capability of the substituent. (In disubstituted species both B(9) and B(12) experience antipodal shielding). The magnitude and direction of the changes in $\delta(^{11}\text{B})$ at other atoms appear to be more random. An interesting pattern does emerge however if the average chemical shifts, $\delta(^{11}\text{B})_{\text{AVE}}$, of each spectrum are calculated and compared (see Table 6.2). The dotted lines in figure 6.11 cross each spectrum base line at the $\delta(^{11}\text{B})_{\text{AVE}}$, highlighting how this value changes on substituting

Figure 6-11

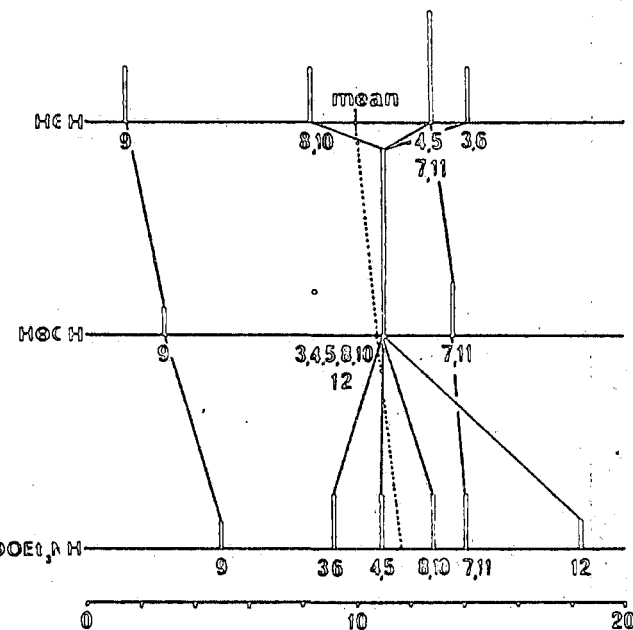
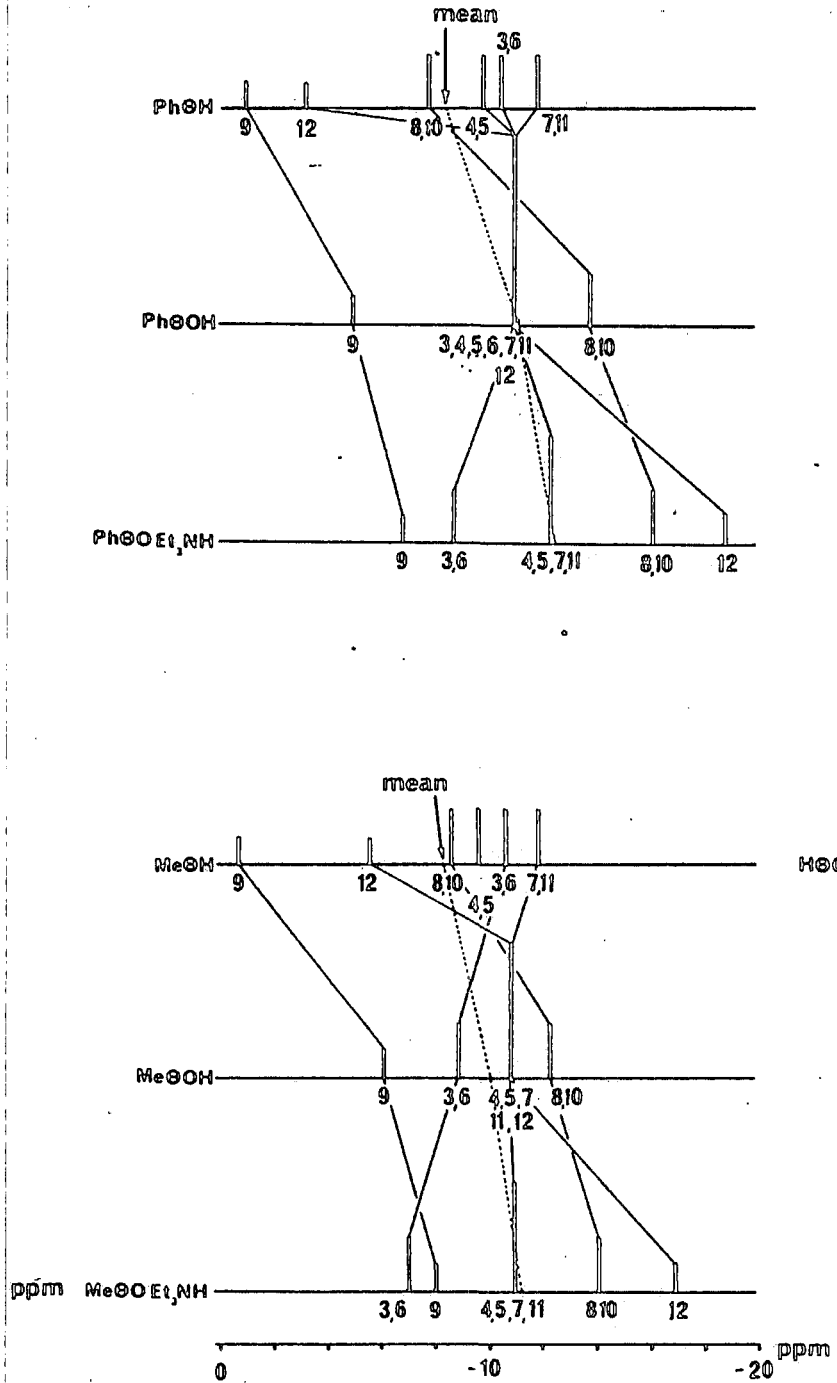
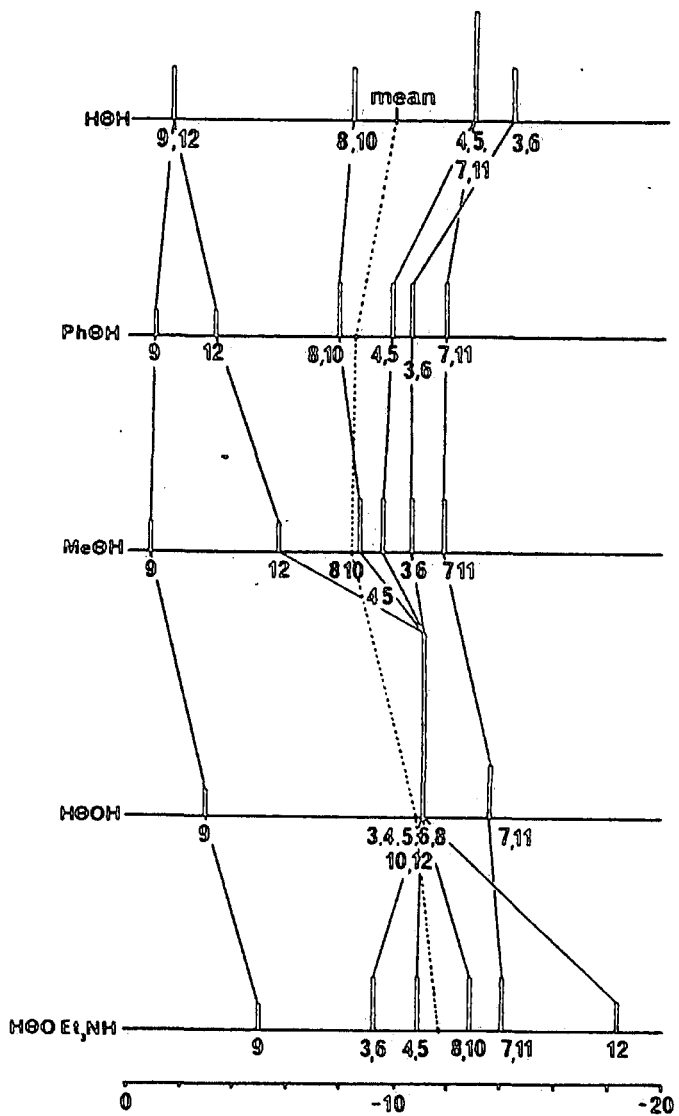


Table 6.2 $\delta(^{11}\text{B})_{\text{AVE}}$ calculated from ^{11}B spectra of ortho-carborane derivatives studied

Derivative	$\delta(^{11}\text{B})_{\text{AVE}}$ (ppm)
H @ H	-9.92
Ph @ H	-8.42
CH ₃ @ H	-8.31
HO @ H	-10.98
HO @ Ph	-11.24
HO @ CH ₃	-10.7
Et ₃ NH ⁺ O ⁻ @ H	-11.74
" O ⁻ @ CH ₃	-11.22
" O ⁻ @ Ph	-12.53

the carbon atoms. Hence attaching a methyl substituent causes $\delta(^{11}\text{B})_{\text{AVE}}$ to be deshielded relative to the parent system as does the phenyl group whereas the hydroxy or oxo (O⁻) substituents produce a marked shielding in the $\delta(^{11}\text{B})_{\text{AVE}}$.

A very similar trend occurs in the $\delta(^{11}\text{B})$ of tricoordinate boron compounds with the same substituents attached to the boron atom. In these tervalent derivatives the $\delta(^{11}\text{B})$ observed is strongly influenced by the π electron donating ability of the substituents attached. This means that a low frequency signal can be observed when a high frequency resonance is expected on electronegativity grounds²¹. Figure 6.12 shows a plot of $\delta(^{11}\text{B})$ values for the series of compounds obtained by replacing methyl groups in $\text{B}(\text{CH}_3)_3$ and phenyl groups in $\text{B}(\text{Ph})_3$ with the more electronegative but stronger π donating substituents -OH and F, to illustrate the shielding this causes. The methyl group is commonly

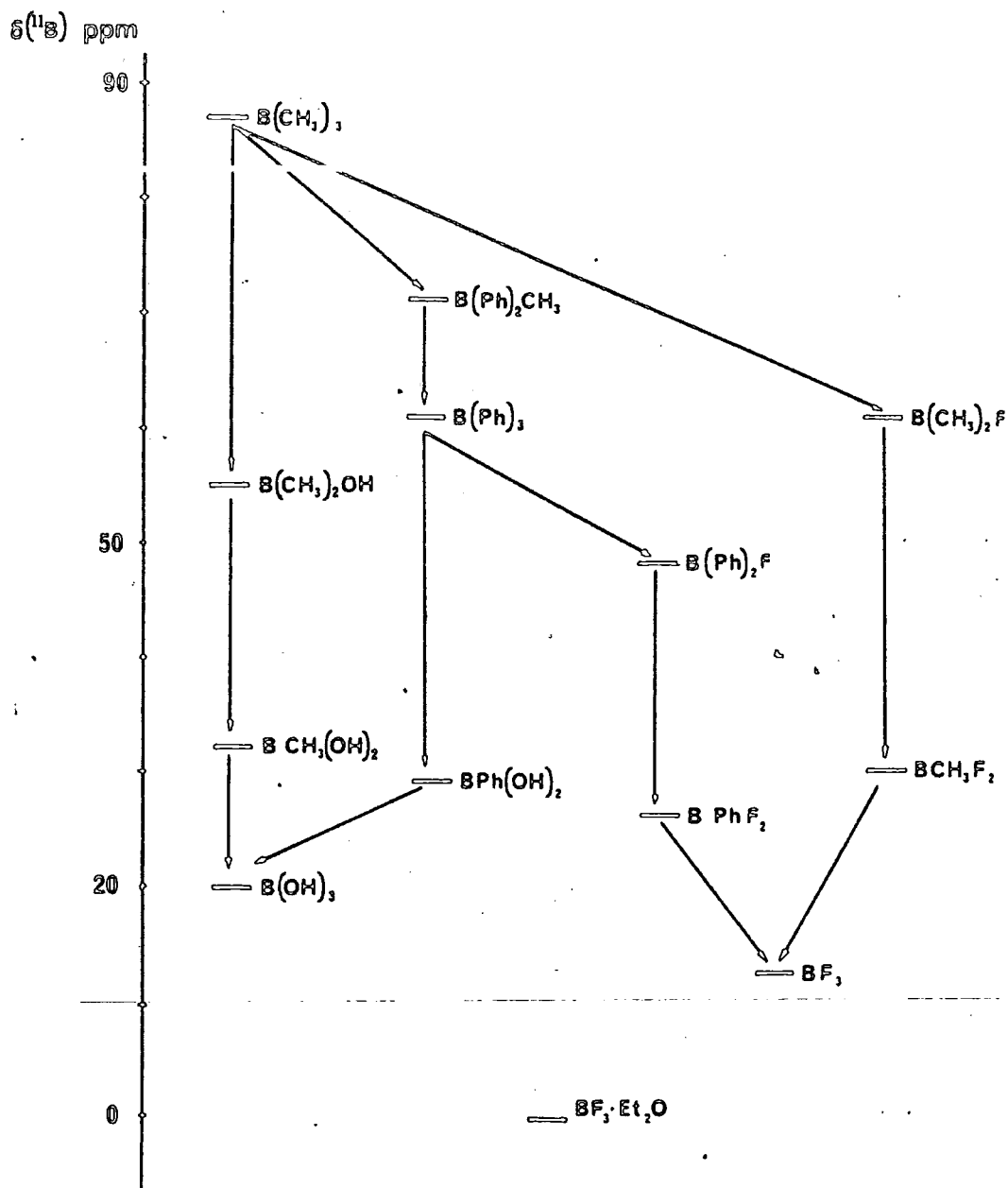


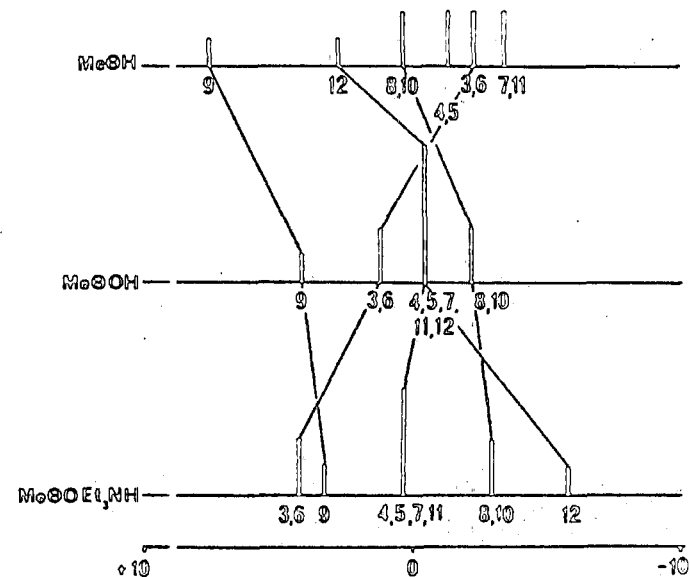
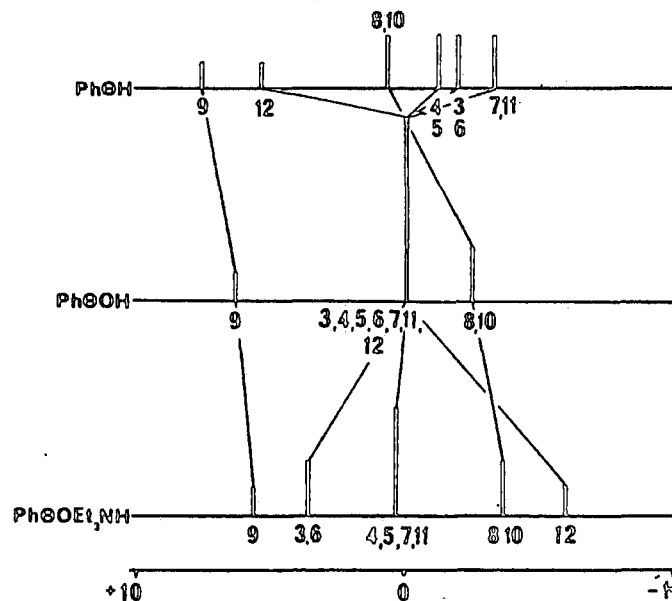
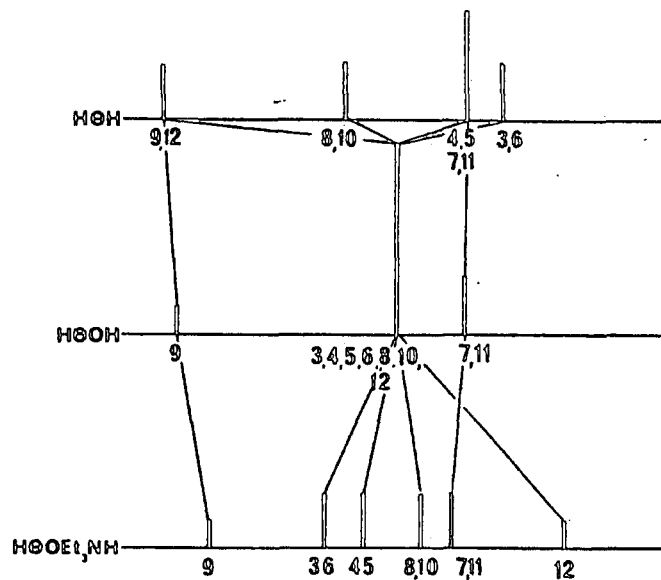
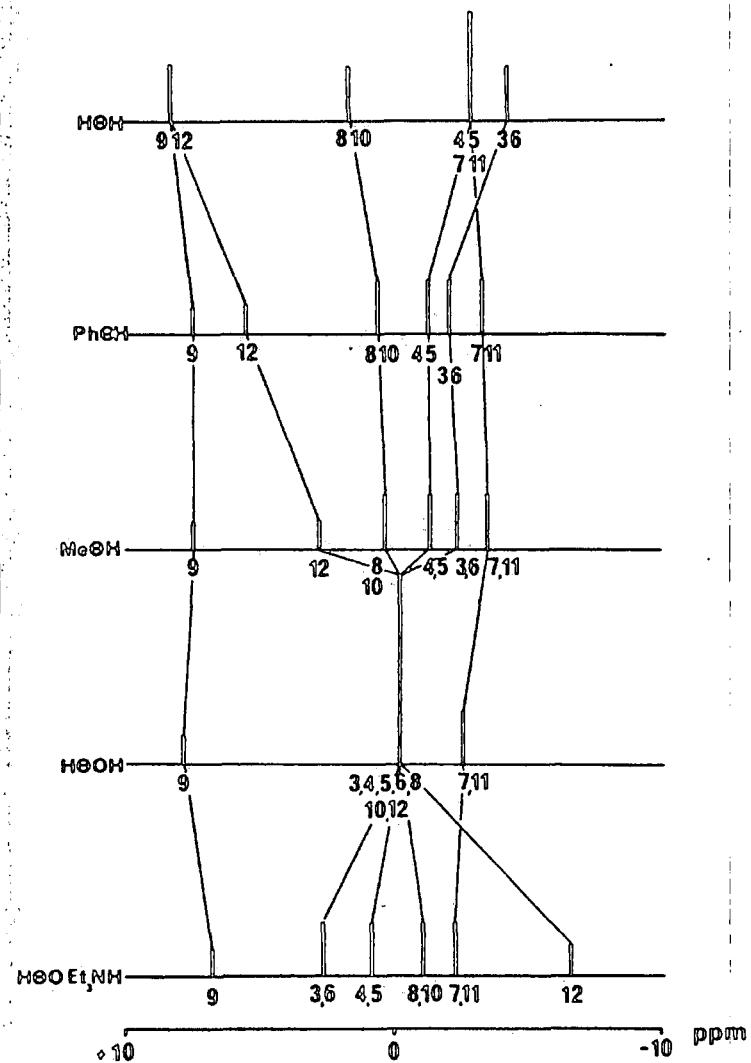
Figure 6.12 A plot of $\delta(^{11}\text{B})$ for various B^{11} compounds

thought of as a σ donor in organic systems, however carbon is more electronegative than boron and this coupled with the negligible π back donation from the sp^3 carbon atoms means that $B(CH_3)_3$ has a high $\delta(^{11}B)$. The more shielded values of $\delta(^{11}B)$ for $B(Ph)_3$ and other phenyl derivatives, relative to the corresponding methyl analogues, are presumably due to the phenyl ring acting as a weak π donor to boron.

The similarity between the trends in $\delta(^{11}B)$ of these tricoordinate boron compounds and the $\delta(^{11}B)_{AVE}$ values of the carborane derivatives suggests that, like the tricoordinate boron atom, the cage is acting as a π acceptor. The extra π electron density from the substituent is delocalised into the three dimensional π system within the cage causing a net shielding of all ^{11}B resonances as shown by the shielding of $\delta(^{11}B)_{AVE}$. The magnitude of this shielding is therefore directly dependant on the π donating ability of the substituent. Hence the 1-oxo-anions show a greater shielding of $\delta(^{11}B)_{AVE}$ than the hydroxy compounds they are derived from. The relatively large shieldings for the 1-hydroxy-2-phenyl ortho-carborane and its triethylammonium salt, may be an indication that the phenyl substituent has improved the π accepting ability of the cage.

Having identified this "bulk effect" on the ^{11}B NMR spectra produced by substitution, we are in a position to simplify the sequences shown in figure 6.11 by plotting the spectra so that all the chemical shift averages are aligned vertically thus cancelling out the shift in $\delta(^{11}B)_{AVE}$. This is shown in figure 6.13 from which it can be seen not only that the shielding at the antipodal atoms is still clearly visible, but also that the correction has highlighted trends occurring in $\delta(^{11}B)$ of all the other boron atoms. In the mono-substituted species the B(9) resonance is shielded slightly, as is the B(8,10) resonance in both the mono- and disubstituted derivatives. (B(9) is more shielded in disubstituted species because of the antipodal effect). It can also be seen that the resonances of B(4,5) and B(7,11) tend to be slightly deshielded and the resonance of B(3,6) is quite markedly deshielded upon substitution of the cage carbon atoms.

Figure 6-13



Finally the magnitudes of each of these shifts in $\delta(^{11}\text{B})$ seem to vary in a fairly predictable manner suggesting these effects may be useful in making assignments of ^{11}B spectra of structurally related compounds. This is clearly demonstrated by comparing the spectra of 1-hydroxy-ortho-carborane and 1-hydroxy-2-phenyl-ortho-carborane in figure 6.13 with other spectra in their respective series. The COSY plots of each compound (figures 6.4 and 6.5 respectively) did not provide sufficient information to allow complete assignments to be made because of the occurrence of coincidental overlap. The low frequency resonance

(-13.58 ppm) in the spectrum of 1-hydroxy-ortho-carborane (figure 6.4) was assigned to either B(3,6) or B(7,11) on the basis of the COSY data. On examining figure 6.13 it is obvious that if this spectrum is to conform to the pattern exhibited by the other spectra in its series, this resonance must be due to B(7,11). Hence by elimination the resonance at -13.13 ppm is assigned to B(3,6,4,5,8,10,12). Similarly for the 1-hydroxy-2-phenyl derivative (figure 6.5), the lowest frequency resonance at -13.78 ppm is assigned to B(8,10) using the same argument, and so the remaining signal has to be that of B(3,6,4,5,7,11,12).

Obviously the highlighting of the trends discussed here, by introducing a correction for the shift in $\delta(^{11}\text{B})_{\text{AVE}}$, has been useful in assigning ^{11}B resonances. It is also useful in confirming those already made, for instance, the assignment of the B(3,6) resonances in the spectra of the triethylammonium salts of 1-hydroxy-2-methyl- and 1-hydroxy-2-phenyl-ortho-carborane (figures 6.8 and 6.9 respectively). These are backed up by the trends shown in figure 6.13.

The most prominent substituent effect seen here, the antipodal effect, has been observed before⁸⁻¹¹ and has been likened to the shielding in $\delta(^{13}\text{C})$ of the para carbon atom in monosubstituted benzenes¹⁰, where the mesomeric effect causes localisation of π electron density at this site. In some of the compounds studied here

the antipodal shielding is remarkably large considering it is a through cage effect produced as a result of substitution at the atom diametrically opposite. (B(12) in the 1-oxo-ortho-carborane derivatives is shielded by 17-20 ppm relative to B(12) in the parent ortho-carborane). The most likely medium through which this, and other substituent effects are probably being transmitted, is the electron cloud delocalised through the carborane cage. Therefore an estimate of the polarisation of this cloud may give some insight into how the trends seen in the ^{11}B NMR of these carborane derivatives are produced. The following theoretical study outlines an effort to do this by looking at the changes in charge distribution in various directions within the cage, on attaching substituents to C(1) and C(2).

6.4 Theoretical Studies on icosahedral carboranes

Owing to the interesting bonding that occurs in polyhedral boron hydrides, they have commanded much theoretical interest²². It was demonstrated at an early stage that there was little correlation between $\delta(^{11}\text{B})$ and the electron density at particular boron atoms in borane polyhedra²³. The chemical shift of any nucleus depends on the amount the nucleus is screened from an external magnetic field by its surrounding electrons, so that:

$$\nu = \frac{\gamma B_0}{2\pi} (1-\sigma)$$

where ν = NMR frequency (from which chemical shift is derived)

γ = Magnetogyric Ratio

B_0 = Applied magnetic field strength

σ = Nuclear screening constant

σ is made up of two components, the diamagnetic contribution σ_d and the paramagnetic contribution σ_p ¹. σ_d reflects the free rotation of electron density around the nucleus, and is important for free ions and for atoms whose electron density resides mainly in spherical s orbitals. The σ_p component describes the hinderance of this rotation of electron density, through interaction with electrons and nuclei of other atoms, and so is important for heavier atoms involved in chemical bonding. The cluster bonding in boron hydrides will obviously restrict the free rotation of electrons around individual boron nuclei, resulting in the σ_p contribution to σ being large²³. Although the electron density around a nucleus is important in the determination of σ_p , other factors such as the separation of electronic energy states in the molecule and the asymmetry of the electron distribution about a nucleus can be equally important¹. This is a possible indication of why the correlation between electron density and $\delta(^{11}\text{B})$ in polyhedral boron hydride compounds is a poor one.

The fact that there are a number of components making up the σ_p contribution means that it is a complicated parameter to determine and so only a few attempts have been made to calculate absolute $\delta(^{11}\text{B})$ values in polyhedral boranes and carboranes^{24,25}.

The compounds studied in Section 6.3 however are all closely related structurally in that they are C derivatives of ortho-carborane. All the boron atoms are six co-ordinate and they all have terminally attached hydrogen atoms. Therefore it seems reasonable to expect that the patterns seen in the ^{11}B NMR of these compounds are caused by the position of the boron atoms relative to the points of substitution, and the change in charge distribution around the boron atoms. Using the Molecular Orbital Bond Index calculations (MOBI) devised by Armstrong et al²⁶, an estimate of the atomic charges in all the molecules studied in the previous section have been made. This has enabled a picture of the charge distribution within the cage for the various derivatives to be built up.

The calculations operate at the CNDO level, using the orthogonalised atomic co-ordinates and atomic number of each atom making up the molecule. The lack of available crystal data on the compounds studied here (as their lattices have proved to be disordered at ambient temperatures²⁷) has meant that the molecular co-ordinates for all the derivatives investigated have been calculated manually using the following assumptions:

1. In all derivatives studied the cage has identical dimensions and ideal icosahedral geometry. The bond length between cage atoms (C-B, C-C, B-B) is taken as 1.7 Å, and the cage atom to terminal hydrogen bond length is taken as 1.19 Å. Bond angles are as for the icosahedral geometry. The bond angles and lengths of substituents are as standard²⁸. The dimensions of the phenyl ring in 1-hydroxy-2-phenyl-ortho-carborane and in the 1-oxo-2-phenyl-ortho-carborate anion are taken as being the same as those found for the pendant phenyl group in the molecular structure of $\text{C}_6\text{H}_5\text{C}_2\text{B}_{10}\text{H}_{10}\text{O}^-\text{C}_{14}\text{H}_{19}\text{N}_2^+$ (see Chapter 5, figure 5.4).

2. The triethylammonium salts are assumed to be completely ionic and so calculations were carried out on the discrete singly charged anions. The C-O bond distance in these derivatives was set at 1.245 Å in accordance with that found in the molecular structure of $C_6H_5C_2B_{10}H_{10}O^-C_{14}H_{19}N_2^+$ (see Chapter 5, figure 5.4).

6.4.1. Results from theoretical calculations

Table 6.3. Charges, calculated by the MOBI method, at each atom of the cage (numbering as in figure 6.1)

CPD ATOM	H ⊕ H	Ph ⊕ H	Me ⊕ H	H ⊕ OH	Ph ⊕ OH	Me ⊕ OH	H ⊕ O ⁻	Ph ⊕ O ⁻	Me ⊕ O ⁻	Xtal Data
C(1)	0.039	0.055	0.082	0.172	0.159	0.155	0.235	0.222	0.219	0.223
C(2)	0.033	0.015	0.022	0.025	0.043	0.074	0.002	0.027	0.056	0.001
B(3)	0.088	0.087	0.084	0.082	0.078	0.076	0.049	0.050	0.050	0.040
B(4)	0.037	0.035	0.033	0.028	0.027	0.029	0.002	0.003	0.004	-0.008
B(5)	0.037	0.035	0.035	0.028	0.027	0.028	0.002	0.002	0.002	-0.013
B(6)	0.088	0.087	0.083	0.082	0.078	0.077	0.049	0.048	0.045	0.041
B(7)	0.039	0.037	0.038	0.040	0.036	0.036	0.027	0.027	0.025	0.011
B(8)	-0.015	-0.017	-0.015	-0.015	-0.016	-0.015	-0.023	-0.024	-0.024	-0.038
B(9)	0.000	-0.001	-0.001	0.002	0.003	0.002	-0.007	-0.004	-0.005	-0.024
B(10)	-0.015	-0.017	-0.016	-0.015	-0.016	-0.015	-0.023	-0.024	-0.023	-0.039
B(11)	0.039	0.037	0.039	0.040	0.036	0.034	0.027	0.028	0.024	0.021
B(12)	0.001	0.001	0.001	-0.001	-0.004	-0.004	-0.011	-0.015	-0.005	-0.027
ΣeB	0.299	0.284	0.281	0.271	0.247	0.248	0.092	0.091	0.093	-0.036

Table 6.4 Dipole contributions along each pseudo C_5 axis for all derivatives studied

Cpd Axis	H ⊕ H	Ph ⊕ H	Me ⊕ H	H ⊕ OH	Ph ⊕ OH	Me ⊕ OH	H ⊕ O ⁻	Ph ⊕ O ⁻	Me ⊕ O ⁻	Xtal Data
1,12	-0.163	-0.160	-0.177	-0.260	-0.257	-0.268	-0.293	-0.294	-0.306	-0.309
2,9	-0.144	-0.136	-0.153	-0.200	-0.206	-0.231	-0.192	-0.227	-0.250	-0.234
6,8 (3,10)	-0.089	-0.089	-0.101	-0.142	-0.143	-0.154	-0.155	-0.163 (-0.160)	-0.176 (-0.168)	-0.169 (-0.167)
4,11 (5,7)	-0.000	-0.013	-0.020	-0.050	-0.042	-0.004	-0.070	-0.056 (-0.058)	-0.044 (-0.050)	+0.063 (+0.062)

Table 6.5 The change in dipole contribution along each pseudo C_5 axis (ΔP) upon substitution of the cage (taken relative to the dipole contributions in ortho-carborane)

Cpd Axis	Me ⊕ H	Ph ⊕ H	H ⊕ OH	Me ⊕ OH	Ph ⊕ OH	H ⊕ O ⁻	Me ⊕ O ⁻	Ph ⊕ O ⁻	Xtal Data
(1,12)	-0.034	-0.017	-0.117	-0.124	-0.113	-0.150	-0.162	-0.150	-0.165
(2,9)	-0.009	+0.008	-0.056	-0.088	-0.063	-0.048	-0.107	-0.184	-0.091
(6,8)	-0.012	0.000	-0.053	-0.065	-0.054	-0.066	-0.079	-0.071	-0.079
(4,11)	-0.020	-0.013	-0.050	-0.004	-0.042	-0.074	-0.050	-0.058	+0.062

Table 6.6

The change in $\delta(^{11}\text{B})$ at each boron atom upon substitution of the cage (relative to the corresponding atom in ortho carborane). These values are all adjusted so as to cancel out the shifts in $\delta(^{11}\text{B})_{\text{AVE}}$ observed for each derivative. This eliminates the bulk effect the substituents have on the cage as a whole and allows realistic comparisons between neutral and charged species to be made.

Atom \ Cpd	Me @ H	Ph @ H	H @ OH	Me @ O	Ph @ OH	H @ O ⁻	Me @ O ⁻	Ph @ O ⁻
	B(9)	-0.87	-0.97	-0.56	-4.47	-2.20	-1.68	-5.31
B(12)	-5.72	-3.20	-8.75	-8.79	-8.58	-14.85	-14.21	-14.81
B(3,6)	+1.87	+2.12	+3.87	+5.32	+4.04	+6.60	+8.26	+7.91
B(4,5)	+1.52	+1.54	+3.16	+2.55	+2.76	+3.81	+3.08	+3.09
B(7,11)	-0.60	-0.49	+0.57	+2.55	+2.76	+0.62	+3.08	+3.09
B(8,10)	-1.46	-1.05	-1.23	-3.79	-4.14	-2.76	-4.64	-5.28

6.4.2 Discussion

The assumption that the cage has ideal icosahedral geometry in all these derivatives is obviously a reasonably major one in the light of the distortions that have been shown by the $C_6H_5C_2B_{10}H_{10}O^-C_{14}H_{19}N_2^+$ salt (figure 5.4). Before proceeding therefore the effects of this assumption should be noted. It is obvious from Table 6.3 that the main difference in using the theoretically and crystallographically determined co-ordinates for the $PhC_2B_{10}H_{10}O^-$ anion, is that the total charge on the boron atoms (ΣeB) is more negative for the authentic structure. As the main source of negative charge is from the oxygen atom, this is possibly due to the distortion in the structure allowing more effective delocalisation of this negative charge into the cage. This is backed up by the charge on the oxygen atom for the theoretical structure (-0.473) being greater than for the authentic structure (-0.444). Despite this difference however the charge distribution within the two cage systems is essentially the same, and since this study is setting out to monitor changes in charge distribution rather than quantitative changes in individual atomic charges, the assumption is believed to be a valid one.

As expected²³, the calculated charges at particular boron atoms in various derivatives bear no correlation with their $\delta(^{11}B)$. This is illustrated in figure 6.14 which shows a plot of charge at individual boron atoms (eB) vs $\delta(^{11}B)$, from which it can be seen that the relatively small change in charge can accompany substantial changes in $\delta(^{11}B)$.

If the charge on each atom of the cage is treated as a vector, whose magnitude is given by the size of the charge, and whose direction is determined by the position of the atom relative to the centre of the cage and the sign of the charge, then these charge vectors can be resolved in various directions. If this is done along the pseudo C_5 rotational axes of the icosahedral cage, then the result is an estimate of the polarity of the cage as a whole, along axes which

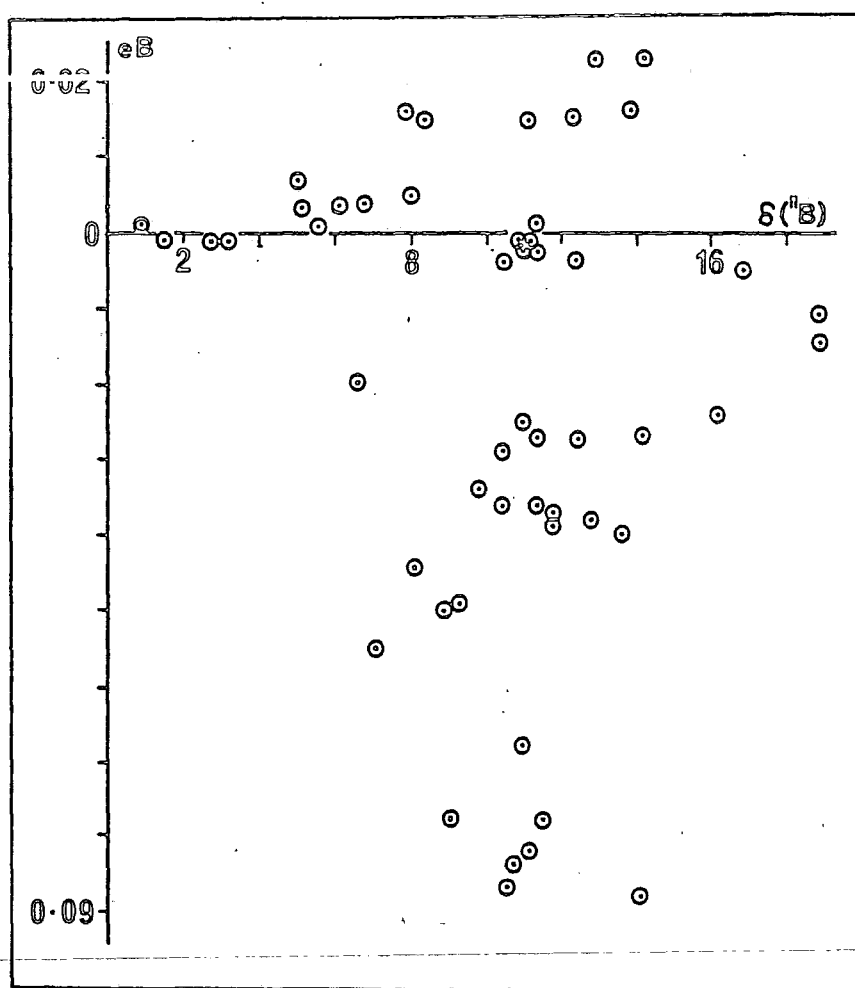
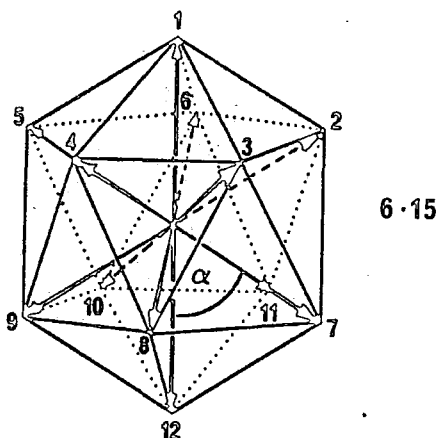


Figure 6.14 Charge (eB) -vs- $\delta(^{11}\text{B})$ for B atoms of derivatives analysed in Section 6.3

pass directly through the cage atoms. This can be thought of alternatively as the contribution along these axes, made by the cage atom charges, to the dipole moment of the molecule. This calculation is summarised in figure 6.15. The icosahedron has six C_5 axes and so this process can be carried out in six directions. The axes are defined here by the atoms through which they pass. Thus axis (1,12) passes from C(1) through B(12) and so on for axes (2,9), (6,6), (3,10), (4,11) and (5,7). In the derivatives studied here, axes (6,8) and (3,10) are equivalent as are (4,11) and (5,7) because of the symmetry of the molecules.



$$p(1,12) = [e_{12} + (e_7 + e_8 \dots + e_{11}) \cos \alpha] - [e_1 + (e_2 + e_3 + \dots + e_6) \cos \alpha]$$

$e = \text{charge}$

This calculation has been performed along each of these axes for all the carborane derivatives whose ^{11}B NMR spectra were assigned in Section 6.3, and the results are given in Table 6.4. The dipole contributions calculated for ortho-carborane are most negative down axes (1,12) and (2,9). This is in agreement with the direction of the dipole moment of the molecule (4.31 D with the carbon atoms situated at the positive end of the molecular dipole²⁹). The dipole contribution down axis (6,8) (and (3,10)) is still negative but smaller than in the previous cases because these axes point

diagonally across the polar axis of the cage. Finally the dipole contributions along (4,11) and (5,7) are zero because these axes are perpendicular to the dipole axis of the cage. On substituting the carbon atoms, these dipole contributions are obviously changed. The most dramatic changes are seen along axis (1,12) where substitution at C(1) causes the dipole contribution through B(12) to become markedly more negative, particularly on attaching the hydroxy and oxo substituents. In fact the magnitude of the change in this dipole contribution relative to the value in ortho-carborane clearly follows the sequence $-\text{C}_6\text{H}_5 < -\text{CH}_3 < -\text{OH} < \text{O}^-$. It also corresponds to the marked shielding of B(12) in the ^{11}B spectra of these compounds. On substitution, the contributions along (6,8) and (3,10) become more negative also, which again is in agreement with the trends seen in the ^{11}B NMR (see figure 6.13) which show that B(8,10) tend to be shielded as well. If this same dipole contribution is considered in the opposite direction, i.e. along axis (8,6) or (10,3), it becomes in effect a positive dipole contribution. This means that substitution causes the dipole contribution along these axes to become more positive. The NMR trends show that B(3,6) are deshielded on cage substitution so again the change in the dipole contribution through a particular atom is agreeing with the change in $\delta(^{11}\text{B})$ at that atom. The same comparisons may be drawn between changes in dipole contribution along axes (4,11) and (5,7) ((11,4) and (7,5) also), and the shifts in $\delta(^{11}\text{B})$ of B(4,5,7,11) where in some cases the correlation between the two is good.

To demonstrate the extent of the correlation between change in $\delta(^{11}\text{B})$ of a particular atom and the change in dipole contribution through it, a plot of $\delta(^{11}\text{B})$ versus the change in dipole contribution (Δp) for all the boron atoms of each derivative studied has been drawn. This is shown in figure 6.16. The changes in $\delta(^{11}\text{B})$ and dipole contribution are all relative to ortho-carborane. The chemical shifts used in this plot have all been adjusted to cancel out the changes in $\delta(^{11}\text{B})_{\text{AVE}}$. This figure shows that the correlation is a fairly good one, with most points falling near a straight line

(correlation coefficient 0.88). Some disagreements in the correlation do occur for B(4,5,7,11) in the anionic species. Using this approach we generally predict that B(4,5) will deshielded and B(7,11) shielded since these pairs are at opposite ends of axes (4,11) and (5,7). In reality however both pairs of atoms are deshielded. Explaining this disagreement as a result of errors incurred by the assumptions made in calculating the dipole contributions seems unlikely. This is because the same phenomenon occurs if the dipole contributions along (4,11) and (5,7) are calculated using charges on the atoms of the authentic $C_6H_5C_2B_{10}H_{10}O^-$ structure. Nevertheless the degree of correlation between $\delta(^{11}B)$ and Δp suggest that that the distortions in the polarity of the cage are important in determining the magnitude and direction of shifts in $\delta(^{11}B)$.

Focusing on the antipodal shielding. Interpreting this in terms of a mechanism similar to the mesomeric effect seen in benzene derivatives does not seem feasible as the planar π system in benzene, which transmits the mesomeric effect, is not present in the cage. It seems much more likely that the electron cloud within the cage, proposed as being partly made up of a complicated series of interpenetrating π systems³⁰ (which because of its highly delocalised nature is going to be readily polarisable), is being distorted by the attachment of substituents to the cage carbon atoms. The magnitude of the polarisation will obviously be greatest for substituents which lie on or near the dipole axis of the cage and which act to reinforce this dipole. Hence we see the greatest change in dipole contributions, or the most polarisation, along axes (1,12) and (2,9). Further still, the polarisation along axes whose angles with the dipole axis increase, will necessarily become smaller. This is backed up by the observation made by Hermanek et al¹⁰ that the magnitude of the antipodal shift depends directly on the position of a substituent X (in their case Br), and decreases with increasing angle between the B-X or C-X bond and the dipole axis of the carborane derivative. This is a clear indication of the delocalised electron cloud in the

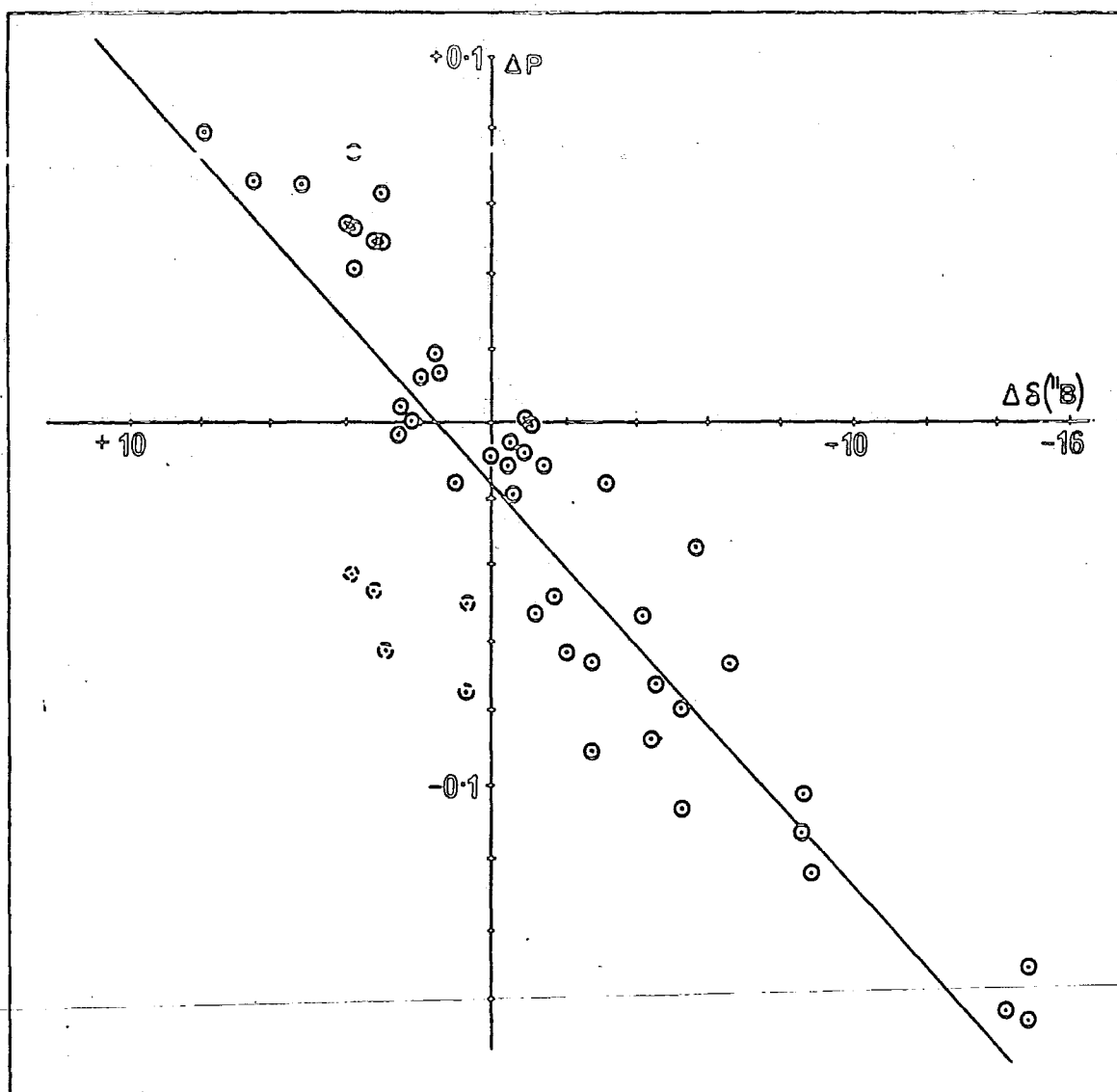


Figure 6.16 $\delta(^{11}\text{B})$ -vs- $-\Delta p$ (Change in $\delta(^{11}\text{B})$ -vs- change in dipole moment contribution)

cage becoming less polarisable on moving away from the dipole axis of the cage.

To explain this polarisation of the cage, two properties of the substituents need to be considered. Firstly the ability of the substituent to donate π electron density into the cage, and secondly the electronegativity of the substituent. It has been suggested that π back donation from a substituent into the cage causes transfer of electron density down the polar axis to the antipodal position¹⁰. This study seems to indicate however that π donation into the cage does not cause localisation of electron density at any particular position but that it affects all boron atoms in the same way, resulting in the shifts in $\delta(^{11}\text{B})_{\text{AVE}}$ shown in Table 6.2. On the other hand, the electronegativity of the substituent has a very pronounced effect on the charge of the cage atom to which it is attached. Table 6.3 clearly shows that all substituents cause the charge on the substituted carbon to become more positive and moreover, the change in charge at this atom is much greater than the change at any other atom in the cage, particularly on attaching the -OH and O^- substituents. This increase in positive charge is backed up by the $\delta(^{13}\text{C})$ of these substituted carbon atoms, which are deshielded accordingly. This suggests that the antipodal shielding is due to a build up of positive charge at the substituted carbon atom, which produces an increase in the negative dipole contribution through the antipodal atom, as opposed to a dramatic build up of negative charge at the antipodal atom. The smaller shielding produced at B(8,10) is due to the negative dipole contribution through these atoms increasing but by less because they lie on axes offset from the polar axis of the cage. Similarly the atoms at the other end of the molecule will experience an increase in positive dipole contribution, accounting for the deshielding of B(3,6) on substitution. The lack of correlation in some cases, between the $\delta(^{11}\text{B})$ and ρ at B(4,5,7,11) may be a result of axes (4,11) and (5,7) falling virtually perpendicular to the polar axis of the cage. This means the effect of polarisation in these directions is diminished and is therefore not great enough to have a consistent effect on $\delta(^{11}\text{B})$.

6.5 Proton NMR studies on icosahedral carboranes

Proton NMR is of obvious importance in polyhedral boron hydride chemistry, however it has not been as widely used as ^{11}B NMR because the spectra obtained tend to be very complicated even for smaller cage species. Coupling to the ^{11}B nucleus ($I = 3/2$) splits the proton signal into a widely spaced quartet and the quadrupole moment of the ^{11}B nucleus decreases the relaxation time of the proton resulting in broad signals. (Coupling to the less abundant ^{10}B nucleus ($I = 3$) is usually obscured by background noise³¹). This means that in some cases, ^1H spectra of boranes and carboranes show little more than an apparent increase in baseline noise.

Useful information may be obtained however using $\{^{11}\text{B}\}$ heteronuclear decoupling which takes two forms. The first ^{11}B broad band noise decoupling ($\{^{11}\text{B}$ broad band noise $\}$), involves irradiating all the boron nuclei present in the molecule at their resonance frequencies while looking at the ^1H spectrum. This collapses all the ^1H signals to singlets ($^2\text{J}(\text{H}-\text{H})$ coupling is seldom resolved) and allows each resonance to be clearly seen, provided coincidental overlap does not occur. The second allows assignments of each proton signal to be made, provided the ^{11}B spectrum of the compound is fully assigned. It involves selectively irradiating each boron atom in turn, ($\{^{11}\text{B}$ (selective) $\}$) and looking at the resulting ^1H spectrum. Protons may be thermally decoupled from boron nuclei³², however in the case of carboranes, the improved resolution is still not sufficient to allow individual resonances to be seen. Therefore heteronuclear decoupling is the only really effective method for assigning polyhedral borane ^1H spectra unambiguously^{33,34,35,36}. More recently, two dimensional $^1\text{H}-^1\text{H}$ COSY NMR (with $\{^{11}\text{B}$ (broad band noise) $\}$) has been shown to be very effective in not only providing connectivity data complementary to that supplied by the $^{11}\text{B}-^{11}\text{B}$ COSY method, but also in showing up longer range $^1\text{H}-^1\text{H}$ coupling information (up to $^5\text{J}(\text{H}-\text{H})$)³⁷.

Solvent effects on $\delta(^1\text{H})$ values are quite pronounced and one, the

Aromatic Solvent Induced Shift (ASIS)³⁸ caused by solvents such as benzene, has been shown to correlate well with the charges on terminal hydrogens. As a result, this effect has been used to calculate charges on individual hydrogen atoms in several boranes and carboranes^{36,39}.

As it has been possible to assign all the resonances in the ^{11}B NMR of several carborane derivatives, shown in Section 6.3, all the ^1H spectra of these compounds can in principle be assigned using ^{11}B heteronuclear decoupling. This final section describes and analyses several such assignments.

6.5.1 Results - Interpretation of ^1H NMR spectra

Figures 6.17 and 6.18 are included to demonstrate the effects of ^{11}B broad band noise decoupling and selective ^{11}B decoupling, respectively. The former shows how each ^1H resonance is resolved, however this does not permit individual assignments to be made. Selective irradiation of one boron atom at its resonance frequency however causes only the signal of the proton bound to it to collapse to a singlet. This makes it visible in the ^1H NMR spectrum and therefore allows it to be assigned. Figure 6.18 shows the ^1H $\{^{11}\text{B}$ selective $\}$ spectra of ortho-carborane produced by irradiating each boron atom in turn while accumulating the ^1H spectrum of the compound. This therefore illustrates how assignments of all ^1H resonances may be deduced.

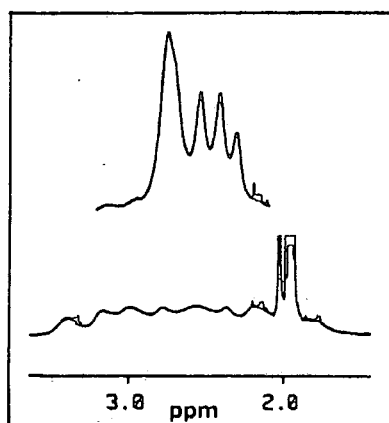


Figure 6.17 ^1H and $^1\text{H}\{^{11}\text{B}$ broad band noise $\}$ spectra of 1 trimethyl ammonium 1-oxo-2-methyl-ortho-carborate

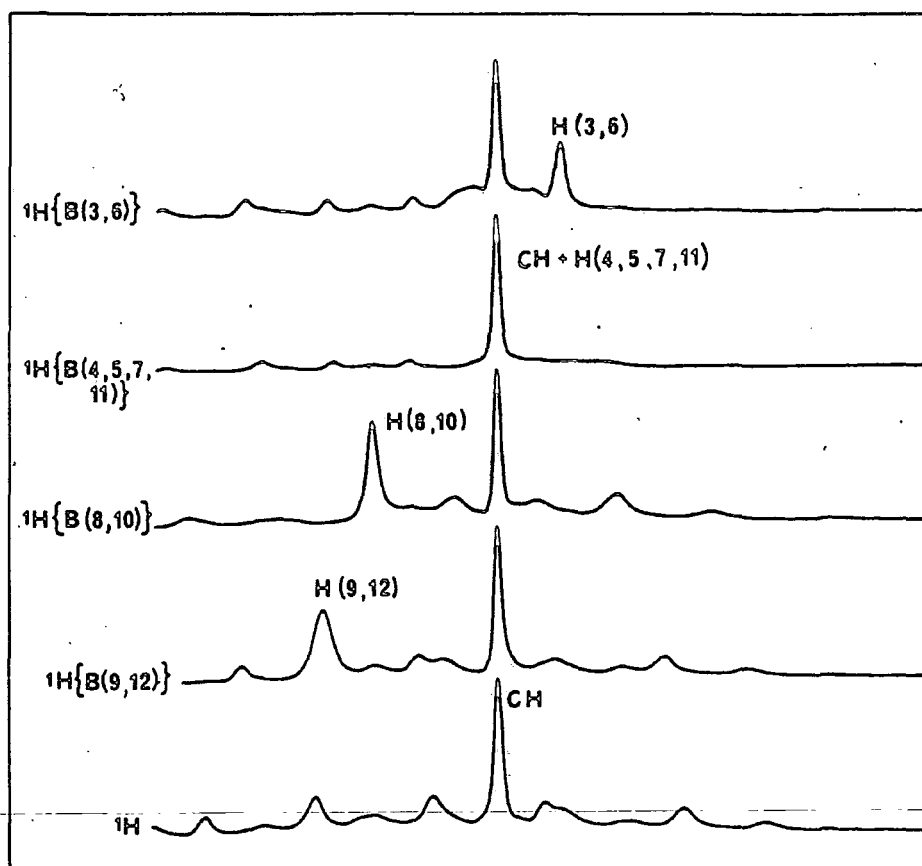


Figure 6.18 ^1H $\{^{11}\text{B}$ selective $\}$ spectra of ortho-carborane

Table 6.7

The $\delta(^1\text{H})$ values of protons terminally bound to the icosahedral cage atoms, as determined by ^1H $\{^{11}\text{B}$ (selective) $\}$ NMR spectra. The numbering system used is identical to that used for the cage boron atoms (see figure 6.1) so that H(1) is bound to C(1), H(3) to B(3), etc.

Atom Compound	H(1,2)	H(3,6)	H(4,5)	H(7,11)	H(8,10)	H(9)	H(12)	$\delta(^1\text{H})_{\text{AVE}}$
H \ominus H	2.14	1.90	2.14	2.14	2.60	2.78	2.78	2.31
PH \ominus H	2.92	2.38	2.66	2.36	2.82	3.02	2.92	2.64
Me \ominus H	2.27	2.20	2.27	2.23	2.61	2.84	2.63	2.41
Et ₃ NH ⁺ -O \ominus H		2.89	2.76	2.57	2.65	2.90	2.25	2.67
HO \ominus Me		2.17	2.59	2.35	2.29	2.48	2.32	2.36
Et ₃ NH ⁺ -O \ominus Me		2.46	2.77	2.77	2.67	2.90	2.45	2.69

Table 6.8

Changes in $\delta(^1\text{H})$ (ppm) relative to $\delta(^1\text{H})$ values in ortho-carborane. Values have been adjusted to allow for changes in $\delta(^1\text{H})_{\text{AVE}}$.

Atom Compound	H(3,6)	H(4,5)	H(7,11)	H(8,10)	H(9)	H(12)
Ph \ominus H	0.13	0.17	-0.13	-0.13	-0.11	-0.21
Me \ominus H	0.2	0.04	-0.01	-0.09	-0.04	-0.25
Me \ominus OH	0.22	0.38	0.16	-0.36	-0.35	-0.51
Me \ominus O ⁻ -Et ₃ NH ⁺	0.2	0.27	0.27	-0.29	-0.24	-0.78
H \ominus O ⁻ -Et ₃ NH ⁺	0.6	0.24	0.05	-0.33	-0.26	-0.85

Table 6.9

Charges on terminally bound hydrogen atoms as calculated by the MOBI method

Cpd Atom	H ⊙ H	Ph ⊙ H	Me ⊙ H	Me ⊙ OH	Me ⊙ O-	H ⊙ O-
H(1)	0.047	-	-	-	-	-
H(2)	0.047	0.046	0.044	-	-	-
H(3)	-0.045	-0.047	-0.047	-0.038	-0.074	-0.075
H(4)	-0.044	-0.049	-0.047	-0.042	-0.076	-0.075
H(5)	-0.044	-0.049	-0.047	-0.042	-0.076	-0.075
H(6)	-0.045	-0.047	-0.047	-0.038	-0.074	-0.075
H(7)	-0.045	-0.048	-0.047	-0.045	-0.087	-0.089
H(8)	-0.048	-0.050	-0.049	-0.048	-0.092	-0.092
H(9)	-0.051	-0.055	-0.053	-0.052	-0.097	-0.096
H(10)	-0.048	-0.050	-0.049	-0.048	-0.092	-0.092
H(11)	-0.045	-0.048	-0.047	-0.045	-0.087	-0.089
H(12)	-0.051	-0.054	-0.053	-0.051	-0.095	-0.095
ΣeH	-0.466	-0.497	-0.486	-0.449	-0.850	-0.853

6.5.2 Discussion

The $\delta(^1\text{H})$ values given in Table 6.7 show that they vary fairly randomly on substitution of the cage. The values of $\delta(^1\text{H})_{\text{AVE}}$ for each spectrum have also been included in the table and can be seen to vary quite substantially also. Understanding these shifts in $\delta(^1\text{H})_{\text{AVE}}$ in terms of the π donating ability of the ligands attached seems feasible in view of the changes in $\delta(^{11}\text{B})_{\text{AVE}}$ seen in these compounds, although it should be noted that the two values do not correlate exactly. For instance, the attachment of methyl and phenyl substituents cause a shielding in $\delta(^1\text{H})_{\text{AVE}}$ (they cause a deshielding in $\delta(^{11}\text{B})_{\text{AVE}}$), the phenyl group shielding $\delta(^1\text{H})_{\text{AVE}}$ by the same order as the oxo- substituent.

Figure 6.19 shows schematic plots of the ^1H spectra in two sequences, once again according to substitution pattern, and with $\delta(^1\text{H})_{\text{AVE}}$ for each, aligned vertically. The trends seen in these plots are not as clear cut as the ^{11}B NMR spectra. However, if the change in $\delta(^1\text{H})$ at each atom upon substitution is calculated (relative to the same atom in the parent ortho carborane) then it can be seen that the general trends seen in the ^{11}B NMR are repeated here. Table 6.8 gives the values of $\delta(^1\text{H})$ showing that H(12) attached to the antipodal B(12) is generally relatively strongly shielded on substitution. H(8,10) and H(9) are somewhat less shielded, and H(4,5) and H(7,11) are in the main slightly deshielded. Finally H(3,6) is consistently deshielded on substitution of the cage.

Plotting $\delta(^{11}\text{B})$ -vs- $\delta(^1\text{H})$ shows that there is a good correlation between the variation in δ for the two nuclei, demonstrated by figure 6.20. This correlation is interesting since the screening of the ^1H nucleus is often described as being largely dependant on σ_d^{40} , as the valence electron associated with the proton resides in a spherical s orbital. If this is the case here then it seems reasonable to expect that $\delta(^1\text{H})$ will correlate with the charge density around the nucleus. Table 6.8 gives the charges at the hydrogen atoms for these derivatives, as calculated by the MOBI method. The variation in the

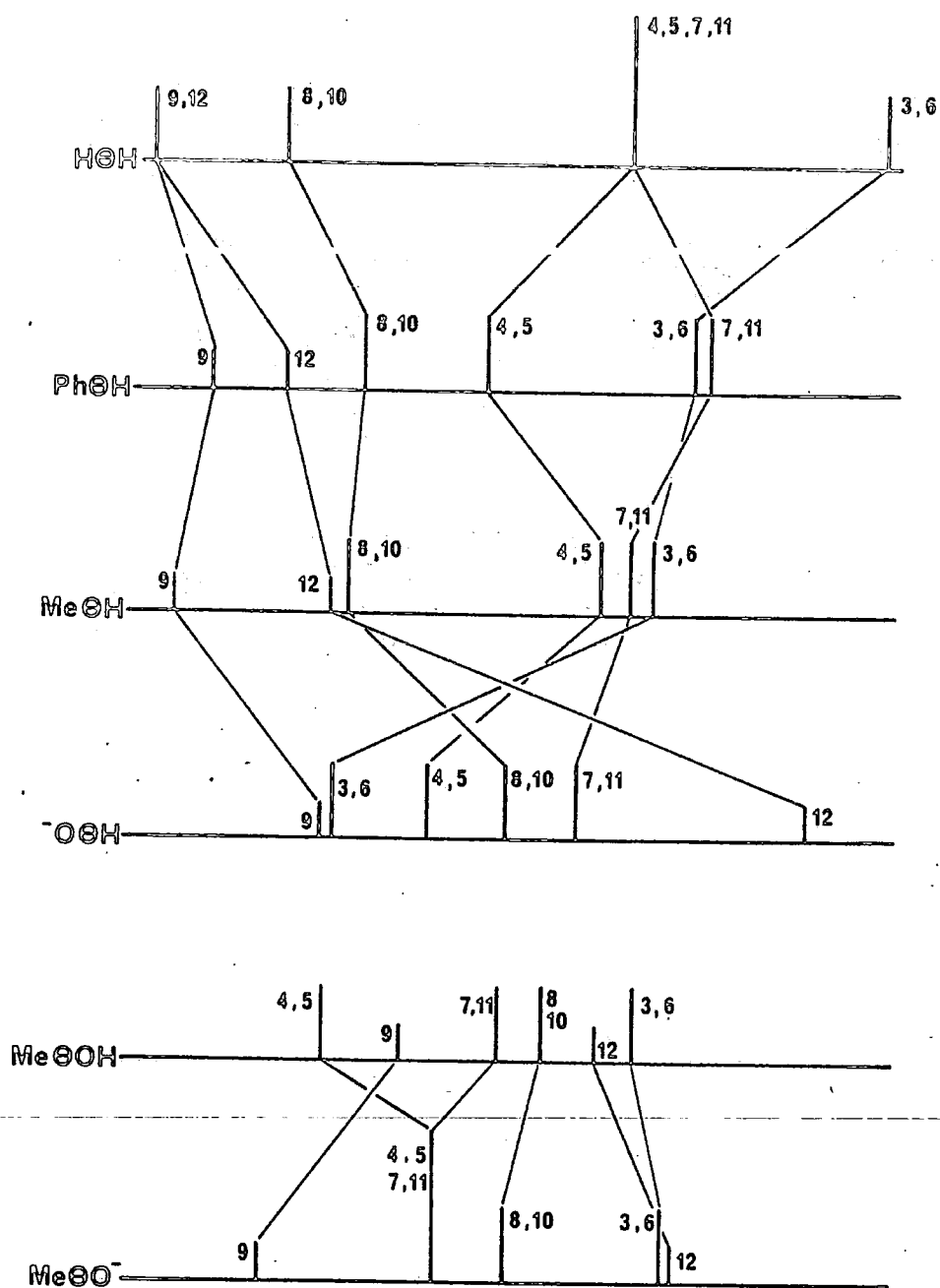


Figure 6.19 Schematic plots of ^1H spectra

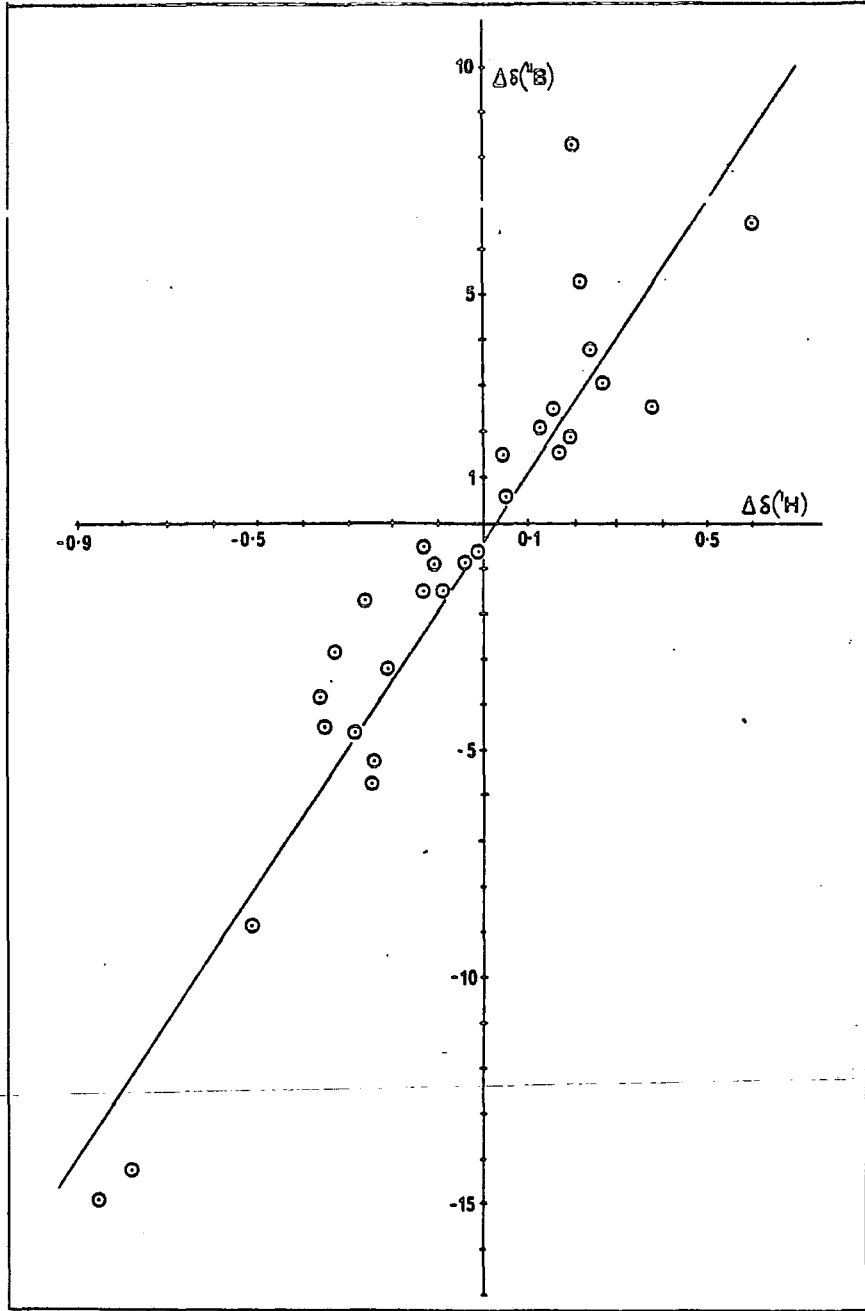


Figure 6.20 Plot of $\delta(^{13}\text{B})$ -vs- $\delta(^1\text{H})$

charge at particular atoms is very small for all the neutral species, however on deprotonation of hydroxy derivatives to give the $\text{CH}_3\text{C}_2\text{B}_{10}\text{H}_{10}\text{O}^-$ and $\text{HC}_2\text{B}_{10}\text{H}_{10}\text{O}^-$ anions, there is a dramatic increase in negative charge on the hydrogen atoms of the cage. This increase in negative charge is not reflected in the ^1H NMR of the anions, whose $\delta(^1\text{H})_{\text{AVE}}$ would be expected to be far more shielded. This implies that the σ_d contribution does not dominate the screening of the cage protons and so σ_p must be important in determining $\delta(^1\text{H})$ values in these carborane derivatives.

The fact that the change in $\delta(^{11}\text{B})$ correlates well with the change in $\delta(^1\text{H})$ is an indication that these shifts are being brought about by the same factors. Hence the polarisation of the cage is determining changes in $\delta(^1\text{H})$ of the cage protons in these carborane derivatives.

6.6 Conclusions and Future Work

It has been shown that by using ^{11}B - ^{11}B COSY 2D NMR in conjunction with the occurrence of the antipodal effect, that it is possible to assign the ^{11}B NMR spectra of a series of ortho-carborane derivatives. The substituent effects that are subsequently identified have been explained in terms of two separate factors:

- a) The effect of π donation from a substituent into the cage, producing a net shielding of ^{11}B resonances, monitored by observing shifts in $\delta(^{11}\text{B})_{\text{AVE}}$ of each spectrum.
- b) The polarisation of the cage produced by an inductive effect, the magnitude of which is largely dependent on the electronegativity of the substituent. This strongly influences the shifts in $\delta(^{11}\text{B})$ seen at individual atoms.

Finally the complete assignments of the ^{11}B resonances of these compounds have facilitated the assignment of the cage proton resonances using selective boron decoupling. The changes in $\delta(^1\text{H})$ resulting from cage substitution have been found to correlate quite well with changes in the corresponding $\delta(^{11}\text{B})$ values, suggesting that the two parameters are being influenced by similar factors.

~~The relationship between $\delta(^{11}\text{B})_{\text{AVE}}$ for the ^{11}B spectra of these derivatives, and the extent of the π donation into the cage has been proposed because of the way the changes in $\delta(^{11}\text{B})_{\text{AVE}}$ follow trends seen in $\delta(^{11}\text{B})_{\text{O}}$ of BIII compounds possessing the same substituents. Obviously the data from this preliminary study is limited and so a more in depth investigation into this relationship is needed. This could encompass not only carbon substituted derivatives of ortho-carborane, but also boron substituted derivatives, derivatives of other carboranyl isomers and indeed of other carborane and borane systems. This would test whether this phenomenon occurs more widely in electron deficient boron compounds.~~

The method used to monitor the cage polarity in these derivatives has involved fairly substantial simplifications of molecular structures. Nevertheless quite effective qualitative predictions can be made on the basis of calculations of dipole contributions along the pseudo C_5 rotational axes of the cage. Small improvements might possibly be made by performing calculations on less simplified structures. The correlation between Δ_p and $\delta(^{11}\text{B})$ might also be improved by using other molecular orbital calculation methods to devise the atomic charges within this cage. It seems unlikely however that this simplistic model will allow reliable quantitative predictions to be made about changes seen in the ^{11}B NMR of carboranes. The chemical shift is undoubtedly influenced by other factors as well as this polarity effect, something that is perhaps reflected in the spread of points shown in the plot of Δ_p -vs- $\delta(^{11}\text{B})$ (figure 6.16). The main advantage of the simplistic nature of these calculations is that they are relatively straightforward to carry out since they do not require extremely detailed knowledge of molecular dimensions only available from X-ray diffraction, etc. This means that they could easily be applied to a much wider range of carboranes and boranes to investigate whether relationships between distortion of polyhedral cage polarity by substituents and changes in $\delta(^{11}\text{B})$ are more widespread.

6.7 References

1. R.K. Harris, B.E. Mann, N.M.R. and the Periodic Table. Academic Press, London 1978.
2. J.D. Kennedy, N.M.R. in Inorganic and Organometallic Chemistry. Chapter 8. Ed. J. Mason Plenum Press 1986 (in Press).
3. A.R. Siedle, Ann. Rep. Royal Soc. Chem. 1982, 12, 177.
4. L.J. Todd, A.R. Siedle, Prog. Nucl. Magn. Reson. Spectr. 1979, 13, 87.
5. G.R. Eaton, W.N. Lipscomb, N.M.R. Studies of Boron Hydrides and Related Compounds. Benjamin, N.Y., 1969.
6. R.E. Williams, Progr. Boron Chem. 1970, 2, 103.
7. S. Hermanek, J. Plesek, Z. Anorg. Allgem. Chem. 1974, 409, 115.
8. A.R. Siedle, G.M. Bodner, A.R. Garber, D.C. Beer, L.J. Todd, Inorg. Chem. 1974, 10, 2321.
9. S. Hermanek, V. Grigor, B. Stibr, J. Plesek, Z. Janousek, V. Anatovich, Collect. Czech. Chem. Commun. 1976, 41, 1492.
10. J. Plesek, S. Hermanek, V. Gregor, B. Stibr, J. Chem. Soc. Chem. Commun. 1977, 561.
11. F. Teixidor, C. Vinas, R.W. Rudolph, Inorg. Chem. 1986, 25, 3339.
12. R. Weiss, R.N. Grimes, J. Amer. Chem. Soc. 1978, 100, 1401.
13. A.O. Clouse, D.C. Moody, R.R. Rietz, T. Roseberry, R. Schaeffer, J. Amer. Chem. Soc. 1973, 95, 2496.
14. B.E. Auferhiede, R.F. Sprecher, Inorg. Chem. 1974, 13, 2286.
15. A. Allerhand, A.O. Clouse, R.R. Rietz, T. Roseberry, R. Schaeffer, J. Amer. Chem. Soc. 1972, 94, 2445.
16. R. Benn, H. Gunther, Angew. Chem. Ind. Ed. Engl. 1983, 22, 350.
17. D. Reed, J. Chem. Res. Synop. 1984, 198.
18. T.L. Venable, W.C. Hutton, R.N. Grimes, J. Amer. Chem. Soc. 1984, 106, 29.
19. J.A. Potenza, W.N. Lipscomb, G.D. Vickers, H. Schroeder, J. Amer. Chem. Soc. 1966, 88, 628.
20. J.A. Potenza, W.N. Lipscomb, Inorg. Chem. 1966, 5, 1471.
21. H. Noth, B. Wrackmeyer, N.M.R. Spectroscopy of Boron Compounds. Springer Verlag, 1978.
22. W.N. Lipscomb, Pure and Appl. Chem. 1972, 29, 493.

23. F. Boer, R.A. Hegstrom, M.D. Newton, J.A. Potenza, W.N. Lipscomb, J. Amer. Chem. Soc. 1966, 88, 5340.
24. J. Kromer, B. Wrackmeyer, J. Chem. Soc. Farraday Trans. 1976, 2, 2283.
25. P.D. Ellis, V-C. Chon, P.A. Dobosh, J. Magn. Reson. 1980, 39, 529.
26. D.R. Armstrong, P.C. Perkins, J.J.P. Stewart, J. Chem Soc. Dalton Trans. 1973, 838 and 2273.
27. R.H. Baughman, J. Chem. Phys. 1970, 53, 3781.
28. CRC Handbook of Chemistry and Physics, 63rd ed. 1982-1983.
29. R. Maruca, H. Schroeder, A.W. Laubengayer, Inorg. Chem. 1967, 6, 572.
30. A.J. Stone, Polyhedron, 1984, 3, 1299.
31. V.R. Miller, R.N. Grimes, Inorg. Chem. 1977, 16, 15.
32. H. Beall, A.T. Elvin, C.H. Bushweller, Inorg. Chem. 1974, 13, 2031.
33. G.M. Bodner, L.G. Sneddon, Inorg. Chem. 1970, 9, 1421.
34. J.D. Kennedy, B. Wrackmeyer, J. Magn. Reson. 1980, 38, 529.
35. J.D. Kennedy, N.N. Greenwood, Inorg. Chim. Acta. 1980, 38, 93.
36. W. Inman, B. Powell, E.W. Distefano, T. Onak, J. Magn. Reson. 1981, 43, 302.
37. X.L.R. Fontaine, J.D. Kennedy, J. Chem. Soc. Chem Commun. 1986, 779.
38. A.H. Cowley, M.C. Damasco, J.A. Mosbo, J.G. Verkade, J. Amer. Chem. Soc. 1972, 94, 6715.
39. T. Onak, W. Inman, H. Rosendo, E.W. Distefano, J. Nurse, J. Amer. Chem. Soc. 1977, 99, 6488.
40. J. Mason, J. Chem. Soc. Dalton Trans. 1975, 1422.

Appendix AStudies into the interactions between lithium boron hydride anionsA.1. Introduction

This Appendix gives a brief account of some preliminary work carried out through the duration of the carborane project, to investigate the possible ways that lithium interacts and may be induced to interact with boron hydride systems. This has been done by examining some Lewis base adducts of the lithium salts of the BH_4^- and $\text{B}_{10}\text{H}_{10}^{2-}$ anions.

This work has led to the discovery of an unusual solid state structure for the complex $\text{LiBH}_4 \cdot \text{TMEDA}$ containing the BH_4^- anion in an originally unexpected μ_3 bridging role. This has implications for the rationalisations commonly invoked to explain the way BH_4^- co-ordinates to metals.

Data obtained so far on other LiBH_4 adducts is presented and briefly discussed in Sections A3 and A4. It is hoped that the work described in these sections will soon be backed up by structural information supplied by X-ray data.

A2. Discussion

Reprinted from the Journal of The Chemical Society:
 Chemical Communications 1987

Structure and Bonding of the Lithium Tetrahydroborate-Tetramethylethylenediamine Adduct (TMEDA·LiBH₄)₂, a Centrosymmetric Dimer containing Doubly and Triply Bridging Hydrogen Atoms

David R. Armstrong,^a William Clegg,^b Howard M. Colquhoun,^c J. Anthony Daniels,^c Robert E. Mulvey,^a Ian R. Stephenson,^d and Kenneth Wade^{a,d}

^a Department of Pure and Applied Chemistry, Strathclyde University, 295 Cathedral Street, Glasgow G1 1XL, U.K.

^b Department of Inorganic Chemistry, The University, Newcastle-upon-Tyne NE1 7RU, U.K.

^c ICI Chemicals and Polymers Group, The Heath, Runcorn, Cheshire WA7 4QE, U.K.

^d Department of Chemistry, Durham University Science Laboratories, South Road, Durham DH1 3LE, U.K.

The title compound, the first alkali metal tetrahydroborate complex to be structurally characterised, has been shown by an X-ray study to be dimeric in the crystal, with each μ_2, η^3 -BH₄ group bonding to two metal atoms through one μ_2 -hydrogen atom apiece and also through one μ_3 -hydrogen atom; MO calculations at the 6-31G level on unsolvated LiBH₄ and the model adducts (H₂O)_n·LiBH₄ (*n* = 1 or 2) and their dimers, with η^2 - and η^3 -BH₄ geometries, show how their stabilities reflect the number of Li --- H contacts, whilst illustrating the inadequacies of LiHB and Li₂HB 3- and 4-centre bond schemes for such compounds.

Although alkali metal tetrahydroborates MBH₄ are widely used as reducing or hydroborating agents in inorganic, organic, and organometallic chemistry,¹ and Lewis bases are known to have a significant influence on their reactivity, surprisingly little structural work has been done to probe the metal-hydroborate interactions that presumably affect their

reactions.^{1,2} Such interactions are expected to be most marked in the case of lithium tetrahydroborate, whose neglect is especially surprising in view of the structural attention other lithium systems have commanded recently.³ The structures of two lithium hydroborates, LiBH₂(mesityl)₂·2MeOCH₂CH₂OMe⁴ (1) and LiBH₃C(SiMe₂Ph)₃·3THF⁵ (2) (THF =

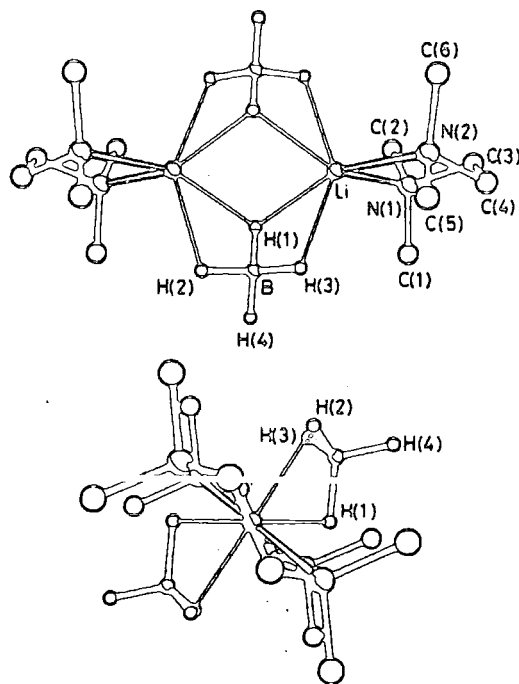
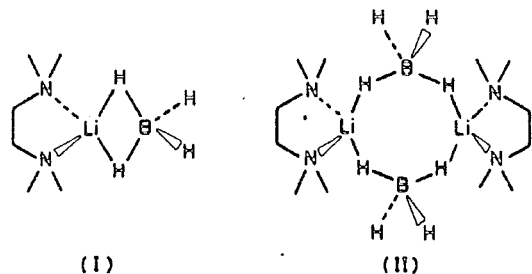


Table 1. Calculated relative electronic energies (kcal mol⁻¹)^a of LiBH₄ and its derivatives.

	$E(\eta^3 - \eta^2)^b$	ΔE (Dimerisation) ^c	ΔE (Solvation) ^d
LiBH ₄	-3.5	-	-
H ₂ O·LiBH ₄	-3.2	-	-30.9
(H ₂ O) ₂ ·LiBH ₄	-3.1	-	-54.2
(LiBH ₄) ₂	-10.6	-37.8	-
(H ₂ O·LiBH ₄) ₂	-5.8	-31.7	-55.6
[(H ₂ O) ₂ ·LiBH ₄] ₂	-3.3	-20.1	-90.7

^a 1 cal = 4.184 J. ^b Difference in energy between η^3 - and η^2 -BH₄ geometries. ^c Difference in energy between dimer and two monomers. ^d Difference in energy between adduct(H₂O)_n·LiBH₄ (n = 1 or 2) and LiBH₄ + 1 or 2 H₂O.

tetrahydrofuran) have been determined recently, but are not expected to be typical because of substituent bulk effects. We chose the title compound, TMEDA·LiBH₄ (3) (TMEDA = tetramethylethylenediamine) for structural study as a representative (indeed, commercially available) complex L₂LiBH₄, where L₂ is a bidentate Lewis base. Compound (3) is formed when LiBH₄ is treated with an excess of TMEDA, and crystallises from toluene-TMEDA as colourless hygroscopic plates whose high solubility in hydrocarbon as well as other solvents contributes significantly to its scope as a reagent. The chelating base TMEDA was expected to restrict to two AO's per metal atom the number of metal orbitals available for metal-hydroborate bonding. Possible structures envisaged were (I) and (II), each involving the metal in two 2-centre Li-N bonds and two 3-centre Li-H-B bonds.

An X-ray crystallographic study of (3) showed neither (I) nor (II) to be correct, but established the presence of the centrosymmetric dimeric molecules shown in Figure 1.† Remarkably, the BH₄ residues bond through *three* of their four hydrogen atoms, two μ_2 , one μ_3 , and the metal atoms are *six*-co-ordinate, not *four*-co-ordinate as expected in (I) or (II). Such a bonding mode for BH₄⁻ ligands has to our knowledge only one precedent in the cobalt complex [Co(BH₄)(Ph₂PC₅H₁₀PPh₂)]₂ (4)⁶ where its presence was attributed to the effect of the diphosphine ligands, and the

Figure 1. Two views of the molecular structure of (3). Key dimensions: Li-B 2.467(5), Li-B' 2.461(6), Li-Li' 3.089(9), Li-N(1) 2.125(6), Li-N(2) 2.115(6), Li-H(1) 2.07(3), Li-H(1') 2.12(3), Li-H(2') 2.06(4), Li-H(3) 2.02(3), B-H(1) 1.19(4), B-H(2) 1.17(4), B-H(3) 1.07(4), B-H(4) 1.06(4) Å; the prime denotes an atom related by the inversion centre.

electron-counting implications were obscured by uncertainties about what metal-metal interactions were involved. Borohydride anions BH₄⁻ have been considered⁷ as sources of 2, 4, or 6 electrons when they co-ordinate to metal atoms through one, two, or three hydrogen atoms, respectively, as in MeC(CH₂PPh₂)₃Cu(μ_2 -H)BH₃,⁸ (Ph₃P)₂Cu(μ_2 H)₂BH₂,⁹ or Zr[(μ_2 -H)₃BH]₄.¹⁰ However, the structures of compounds (1)–(4) show that such valence shell electron counts may be misleading, apparently requiring the metal atoms to accommodate more than the expected 8 (for Li) or 18 (for Co) electrons.

To probe the bonding in (3) we have carried out MO calculations^{11,12} at the 6-31G level on the monomers and dimers of LiBH₄, H₂O·LiBH₄, and (H₂O)₂·LiBH₄ (where H₂O molecules were mimicking the solvation effect of TMEDA). For each of the six model systems we optimised its structure with both η^2 and η^3 BH₄ geometries present (previously¹³ only monomeric, unsolvated LiBH₄ had been subjected to a theoretical study which found that the η^3 BH₄ geometry that maximises the number of B---H---Li links provided the most stable structure). Our calculations show that the η^3 BH₄ structures are preferred in *all* cases, monomers *and* dimers, and that the dimeric forms are energetically favourable (see Table 1). Repeating the geometry optimisation procedure on for example η^3 -(LiBH₄)₂ and employing only a 1s orbital in the lithium basis set had little effect on the length of the B-H and Li---H bonds which differed at most by 0.003 and 0.055 Å, respectively, when compared to the corresponding full basis set optimised distances; this underlines the predominantly ionic nature of the bonding. The Mulliken charge distribution in [(H₂O)₂·LiBH₄]₂, our model for (TMEDA·LiBH₄)₂, gives a total charge on the BH₄ group of -0.64 e with the bridging hydrogens having charges of -0.11 e (μ_3) and -0.13 e (μ_2) while the terminal hydrogen carries 0.08 excess electrons; the water

† Crystal data for (3): C₁₂H₄₀B₂Li₂N₄, triclinic, space group P $\bar{1}$, dimer, $a = 8.2201(8)$, $b = 8.3090(6)$, $c = 8.7538(10)$ Å, $\alpha = 89.583(7)$, $\beta = 88.338(6)$, $\gamma = 64.130(6)^\circ$, $U = 537.74$ Å³, $Z = 1$ (dimer), $D_c = 0.852$ g cm⁻³, $F(000) = 156$, Cu-K α radiation, $\lambda = 1.54184$ Å, $\mu = 0.33$ mm⁻¹. The structure was solved by direct methods and refined by weighted blocked-cascade least-squares [$w^{-1} = \sigma^2(F) + 0.00157F^2$]; anisotropic thermal parameters were used for all non-hydrogen atoms, isotropic for the freely refined BH₄ hydrogen atoms; other hydrogen atoms were constrained, with C-H 0.96 Å, H-C-H 109.5°, $U(H) = 1.2U_{eq}(C)$. $R = 0.089$, $R_w = 0.124$ for 1111 unique reflections with $F > 4\sigma(F)$ and 119 parameters. Atomic co-ordinates, bond lengths and angles, and thermal parameters have been deposited at the Cambridge Crystallographic Data Centre. See Notice to Authors, Issue No. 1.

molecules donate 0.13 e to lithium resulting in an overall charge of +0.38 e on the metal atoms. The preference of TMEDA·LiBH₄ for structure (3) can thus be readily understood as this arrangement offers a greater number of electron-rich hydrogen atoms for bonding to lithium than any monomeric structure. In addition, the calculations on the model species show that the η³ bonding mode with its centrosymmetric arrangement of the BH₄ groups allows closer packing of the two BH₄ moieties and thus smaller Li---H and Li---B distances than those in the corresponding η² structure [for the η³ structure Li---B = 2.584, Li---H (μ₃) = 2.147, and Li---H (μ₂) = 2.106 Å; for the η² structure Li---B = 2.861 and Li---H (μ) = 2.536 Å]. A qualitative estimate of the stabilisation of (LiBH₄)₂ by the TMEDA molecules is provided by calculations which show that the addition of four water molecules to (LiBH₄)₂ decreases the energy by 90.7 kcal mol⁻¹ (1 cal = 4.184 J).

In conclusion, the lithium environments in compounds (1)–(5), in LiDIVE₄,¹¹ and in many other molecular lithium alkyls,¹⁵ amides, and imides³ show how readily lithium can interact with more hydrogen atoms than simplistic LiHB or LiHC bond schemes might suggest. [For example, the metal co-ordination number in compounds (1),⁴ (2),⁵ and (3) is six, and is even higher than that in LiBMe₄.¹⁴] Moreover, the structures of compounds (1)–(4) reveal the dangers of treating BH₄⁻ ligands as sources of 2, 4, or 6 electrons depending on whether they are η¹, η², or η³-co-ordinated.

We thank the S.E.R.C. and ICI p.l.c. for financial support and Dr. R. Snaith for discussions.

Received, 28th November 1986; Com. 1687

References

1 H. C. Brown, 'Boranes in Organic Chemistry,' Cornell University Press, 1972.

- 2 D. E. Buck, in the supplement to 'Mellor's Comprehensive Treatise on Inorganic and Theoretical Chemistry,' 1981, V.5, Part B1, Sect. B6, p. 354–398.
- 3 For examples of recent work on organo and related lithium structures see D. Barr, W. Clegg, R. E. Mulvey, R. Snaith, and K. Wade, *J. Chem. Soc., Chem. Commun.*, 1986, 295; D. R. Armstrong, D. Barr, W. Clegg, R. E. Mulvey, D. Reed, R. Snaith, and K. Wade, *ibid.*, p. 869; L. M. Engelhardt, J. MacB. Hanowfield, M. F. Lappert, J. A. MacKinnon, B. H. Newton, C. L. Raston, B. W. Shelton, and A. H. White, *ibid.*, p. 846; A. G. Avent, C. Eaborn, P. B. Hitchcock, J. D. Smith, and A. C. Sullivan, *ibid.*, p. 988; N. H. Buttrus, C. Eaborn, S. H. Gupta, P. B. Hitchcock, J. D. Smith, and A. C. Sullivan, *ibid.*, p. 1043.
- 4 J. Hooz, S. Akiyama, F. J. Cedar, M. J. Bennet, and R. M. Tuggle, *J. Am. Chem. Soc.*, 1974, **96**, 274.
- 5 C. Eaborn, M. N. A. El-Kheli, P. B. Hitchcock, and J. D. Smith, *J. Chem. Soc., Chem. Commun.*, 1984, 1673.
- 6 D. G. Holah, A. N. Hughes, S. Maciaszek, and V. R. Magnuson, *J. Chem. Soc., Chem. Commun.*, 1983, 1308; D. H. Holah, A. N. Hughes, S. Maciaszek, V. R. Magnuson, and K. O. Parker, *Inorg. Chem.*, 1985, **24**, 3956.
- 7 M. Mancini, P. Bogear, R. C. Burns, M. Mlekuz, B. G. Sayer, J. I. A. Thompson, and M. J. McGlinchey, *Inorg. Chem.*, 1984, **24**, 1072.
- 8 C. A. Ghilardi, S. Midollini, and A. Orlandini, *Inorg. Chem.*, 1982, **21**, 4096.
- 9 S. J. Lippard and K. M. Melmed, *Inorg. Chem.*, 1967, **6**, 2223.
- 10 V. Plato and K. Hedberg, *Inorg. Chem.*, 1971, **10**, 590.
- 11 M. F. Guest, J. Kendrick, and S. A. Pope, GAMESS Documentation, Daresbury Laboratory, 1983.
- 12 M. Dupuis, D. Spangler, and J. J. Wendoloski, GAMESS, N.R.C.C. Software Catalogue, Volume 1, Program No. 2G01, 1980.
- 13 J. D. Dill, P. v. R. Schleyer, J. S. Binkley, and J. A. Pople, *J. Am. Chem. Soc.*, 1977, **99**, 6159.
- 14 W. E. Rhine, G. Stucky, and S. W. Peterson, *J. Am. Chem. Soc.*, 1975, **97**, 6401.
- 15 J. L. Wardell, 'Comprehensive Organometallic Chemistry,' eds. G. Wilkinson, F. G. A. Stone, and E. W. Abel, Pergamon, Oxford, 1982, vol. 1, ch. 2.

16. R.K. Harris, B.E. Mann, N.M.R. and The Periodic Table. Academic Press, London, 1978.

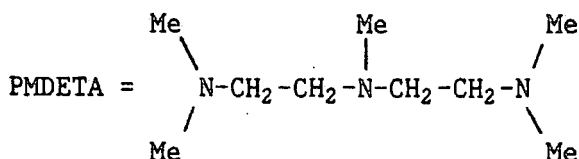
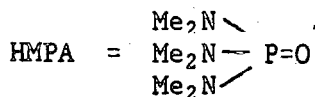
17. R.E. Mulvey, PhD Thesis, Strathclyde, 1984.

A.3 Additional studies carried out

Other adducts of LiBH_4 that have been prepared and characterised include:

$\text{LiBH}_4 \cdot 4(\text{HMPA})$, $\text{LiBH}_4 \cdot 4(\text{py})$, $\text{LiBH}_4 \cdot \text{PMDETA}$

(HMPA and pyridine being mono-dentate and PMDETA tridentate).



These adducts, with the exception of the HMPA complex, behave unremarkably in solution (full details of preparative and spectroscopic details are given in Section A4) as shown by NMR. This leads to the prediction that the solid state structures of the adducts of the monodentate species simply consist of the Li atom tetrahedrally surrounded by four ligand molecules. In the case of the PMDETA complex, two structures can be envisaged, placing Li in either 4 or 6 co-ordinate environments, as shown in Figure A1. In view of the findings discussed in Section A2, structure II would be predicted to be the preferred structure.

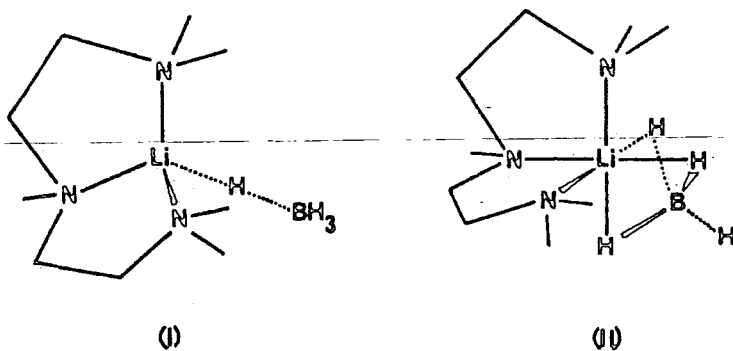


Figure A1

A particularly interesting property of the HMPA adduct is its behaviour in the ^7Li NMR spectrum at different temperatures. This is illustrated in Figure A2 which clearly shows that at -65°C , the lithium atom is present in two different environments. This is a possible indication of an increase in co-ordination number of the lithium atom, which would occur as

a result of an interaction with the BH_4^- anion. At -65°C , the two different species appear to be in equilibrium, and on cooling to -90°C , the lithium atoms are present as the higher co-ordinate complex almost exclusively.

Attempts to prepare HMPA adducts of $\text{Li}_2\text{B}_{10}\text{H}_{10}$ showing the lithium atom interacting with the cage have been unsuccessful. The only adduct isolated was the species $[\text{Li}(\text{HMPA})_6]_2\text{B}_{10}\text{H}_{10}$. This stoichiometry was determined by elementary analysis, and by measuring the $\delta(^7\text{Li})$ of the lithium atoms in this complex. At -6.33 ppm, the lithium atom in this complex is remarkably shielded for a lithium atom in a non aqueous solvent¹⁶ and is an obvious indication of the octahedral co-ordination of the metal centre. It seems unusual to find six HMPA ligands co-ordinating to a lithium cation (Li^+ would be expected to accommodate four HMPA ligands and take up tetrahedral geometry¹⁷). The Li-O bond in this complex will have to be unusually long. In other Li.HMPA adducts this bond is about 1.87 \AA ¹⁷ long. This length gives the total cone angle subtended by the ligand as 138 which is too large to allow octahedral co-ordination around the lithium cation.

To advance this work further, additional structural information from X-ray analysis is essential.

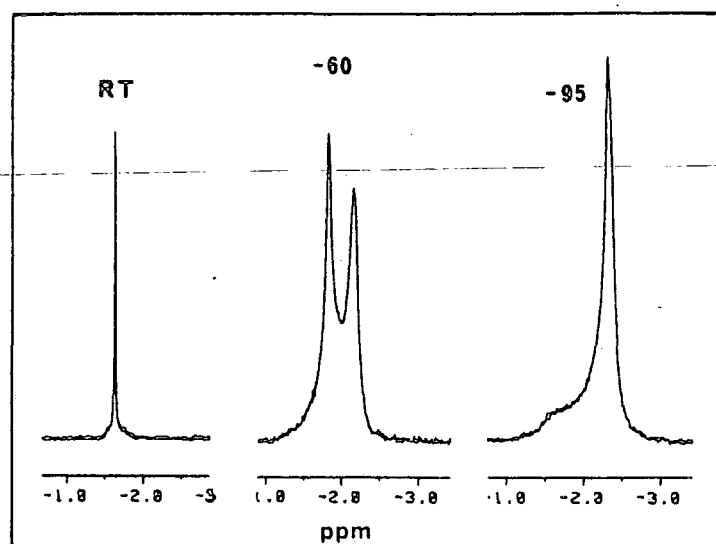


Figure A2 V.T. ^7Li NMR of $\text{LiBH}_4 \cdot 4 \text{ HMPA}$

A.4. Experimental

A.4.1 Preparation of [LiBH₄.TMEDA]₂

[LiBH₄.TMEDA]₂ was prepared quantitatively by dissolving lithium borohydride in excess dry TMEDA under nitrogen. Typically, lithium borohydride (0.50 g, 23 mmoles) was placed in a Schlenk tube purged with nitrogen. TMEDA (18 mls) were added via syringe and the mixture stirred producing an exoethermic reaction. Dry toluene (15 mls) was added and the mixture heated to boiling producing a cloudy solution. This was filtered hot under nitrogen leaving a colourless solution which on standing afforded colourless moisture sensitive crystals (isolated by filtration and washing with hexane) identified as [LiBH₄.TMEDA]. Characterised as follows:

Melting point. Decomp 160-170 °C.

Analysis. Found: C, 8.1; Li, 5.0%; C₁₂H₄₀B₂Li₂N₄. Requires: B, 8.0; Li, 5.1%.

Infra Red (Nujol) (cm⁻¹) 3000-2780 (s) (Aliphatic C-H stretch); 2700 (w); {2500 (w,sh) 2430 (sh) 2370 (sh) 2337 (s) 2297 2266 (s) 2211 (s) 2177 (sh) 2130 (sh)} (B-H stretching modes); 1460 (s); 1410 (w); 1378; 1355 (m); 1290 (s); 1257; 1230; 1180; 1153 (s); 1132; 1102; 1063 (m); 1041 (m); 1023 (m); 951 (s); 792 (m); 773; 725 (w); 587.

¹H NMR 250.133 MHz, solvent C₆D₆, referenced externally to TMS at 0.00 ppm: (ppm) 2.11 (s), Integral 12 H, (Ligand CH₂);

1.84, (s), Integral 4H, (Ligand CH₂); 0.685, 0.360, 0.035, -0.291, (1:1:1:1 q) J = 81.3 Hz, Integral 4H (¹¹BH₄).

¹¹B NMR 115.546 MHz, solvent D₈ toluene, referenced externally to BF₃.Et₂O at 0.00 ppm. (ppm): -37.34, -38.05; -38.75; -39.46; -40.16 (1:2:3:2:1 p), J = 80.9 Hz, (¹¹B coupled to 4¹H).

Variable temperature ⁷Li NMR. 139.955 MHz, solvent D₈ toluene, referenced externally to PhLi at 0.00 ppm, (ppm): Room Temperature (R.T), -1.424, (s), (½ Height line width 0.72 Hz); -60 °C, -1.233, (s); -95 °C, -1.085 (br.s) (½ height line width, 16 Hz).

A.4.2 Preparation of LiBH₄.4 HMPA

LiBH₄.4 HMPA was prepared in the same way as the TMEDA adduct, from lithium borohydride (0.40 g, 18.36 mmoles) and HMPA (16.0 mls). The adduct was isolated as a moisture sensitive, colourless crystalline solid. Characterised as follows:

Analysis Found: C, 37.9; H, 9.6; B, 1.8; Li, 0.8; N, 22.4%
C₂₄H₇₆BLiO₄P₄ Requires: C, 39.0; H, 10.3; B, 1.5; Li 0.95; N, 22.8%.

Infra Red (Nujol) (cm⁻¹): 3040-2760 (s) (Aliphatic CH stretch); {2480 (w.sh) 2290 (sh) 2260 (m) 2210 2190 (s) 2117 (sh) } (B-H stretching modes); 1480 (sh); 1455 (s); 1378 (m); 1300 (s); 1208 (s.br) (PO stretch?) 1170 (m); 985 (s.br); 754 (s); 508; 485 (m).

¹H NMR 360.134 MHz, solvent C₆D₆, referenced internally to C₆D₅H at 7.15 ppm. (ppm): 2.430, 2.434 (d), J 1.44 Hz, Integral ~72H, (Ligand CH₃ coupled to ³¹P); 1,216, 0.990, 0.764, 0.538 (1:1:1:1 q), J = 81.4 Hz, Integral 4H, (BH₄)

¹¹B NMR 115.546 MHz, solvent D₈ toluene, referenced externally to BF₃.Et₂O at 0.00 ppm. (ppm): -36.31, -37.01, -37.72, -38.42, -39.13, (1:2:3:2:1 p), J = 80.9 Mz, (¹¹B coupled to 4¹H).

V.T. ⁷Li NMR 139.963 MHz, solvent D₈ toluene, referenced externally to PhLi at 0.00 ppm. R.T., -1.633 (s); -60°C, -1.821, (s), -2.154 (s); -95°C, -1.481 to -1.869 (weak shoulder), 2.318 (s).

A.4.3 Preparation of LiBH₄.PMDETA

LiBH₄.PMDETA was prepared in the same way as for the preparation of [LiBH₄.TMEDA]₂ from lithium borohydride (0.89 g, 40.86 mmoles) and PMDETA (8.33 mls, 40.86 mmoles). The compound was isolated as a moisture sensitive, colourless crystalline solid, identified as a 1:1 adduct. Characterised as follows:

Analysis Found: C, 60.1; H, 17.9; N, 23.8%. $C_9H_{27}BLiN_3$.

Requires: C, 55.4; H, 13.9; N, 21.6%.

Infra Red (Nujol) (cm^{-1}): 3020-2700 (s) (Aliphatic CH stretch); 2315 (s), 2160 (s), 2100 (sh) (BH stretching modes); 1460 (s); 1380 (m); 1368 (m); 1358; 1304 (m); 1292; 1285 (sh); 1257; 1217 (w); 1180 (sh); 1170 (m); 1158 (m); 1115 (s); 1100; 1072 (sn); 1060 (m); 1043 (m); 1027 (m); 983; 950; 941 (m); 902; 795; 780; 755; 725; 604; 572.

1H NMR 250.133 MHz, solvent C_6D_6 , referenced externally to TMS at 0.00 ppm, (ppm): 2.071 (s), Integral 3H, (N- CH_3); 2.044 (s), Integral 12 H, ($-N(CH_3)_2$); 1.971-1.906, (m), Integral 8H (ligand CH_2); 0.733, 0.407, 0.081, -0.244, (1:1:1:1 q), Integral 4H, $J = 81.5$ Hz, (BH_4).

^{11}B NMR 80.239 MHz, solvent C_6D_6 , referenced externally to $BF_3 \cdot Et_2O$ at 0.00 ppm. (ppm): -37.17, -38.18, -39.20, -40.21, -41.23, (1:2:3:2:1 p), $J = 81.0$ Hz, (^{11}B coupled to 4 1H).

A.4.4 Preparation of $LiBH_4 \cdot 4(pyridine)$

$LiBH_4 \cdot (C_5H_5N)_4$ was prepared in the same way as $[LiBH_4 \cdot TMEDA]_2$ from lithium borohydride (0.48 g, 22.04 mmoles) and dry pyridine (7.13 mls, 88.16 mmoles). The adduct was isolated as a moisture sensitive colourless crystalline solid.

Characterised as follows:

Analysis Found: C, 67.3; H, 7.3; B, 4.2; Li, 2.3; N, 1.9% $C_{20}H_{24}BLiN_4$. Requires C, 71.0; H, 7.1; B, 3.3; Li, 2.1, N, 16.6%.

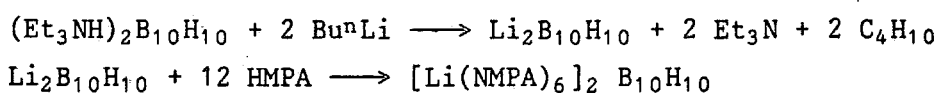
Infra Red (Nujol) (cm^{-1}): 3085 (w) 3050 (w) 3035 (w) (Aromatic CH stretch); 2460-2020 (s.br) (B-H stretching modes); 1990 (w.br); 1935 (w.br); 1880 (w.br); 1614 (w); 1590 (s) (C-C stretch); 1570 (w); 1481; 1436 (s); 1227 (w); 1212; 1192 (w); 1095 (m.br); 1065; 1033 (m); 1000 (m); 945 (w); 882 (w); 792 (w); 752 (s); 700 (s); 617 (s).

1H NMR 250.133 MHz, solvent C_6D_6 referenced to C_6D_5H at 7.17 ppm. (ppm): 8.676-8.649 (m); Integral 8H (pyridine H

(meta)); 6.998-6.931 (m); Integral 4H (pyridine H (para)); 6.677-6.624 (m); Integral 8H (pyridine H (ortho)); 1.772, 1.448, 1.123, 0.799, (1:1:1:1 q), J = 81 Hz, Integral 4H, (BH₄).

¹¹B {¹H broad band noise} Solvent C₆D₆, referenced externally to BF₃.OEt₂ at 0.00 (ppm) -38.30 (s).

A.4.5 Preparation of Li₂B₁₀H₁₀ (HMPA)₁₂



A Schlenk, purged with dry nitrogen was charged with triethylammonium decahydrodecaborate (Et₃NH)₂B₁₀H₁₀ (1.37 g, 4.25 mmoles prepared as by Hawthorne et al) and dry THF (30 mls). The mixture was cooled to -196 °C and n-butyl lithium (4.96 mls of 1.715 M solution in hexane, 8.51 mmoles) added. The mixture was allowed to warm initiating an exothermic reaction which afforded a colourless solution. The volatiles present in the reaction mixture were removed by prolonged exposure to vacuum leaving Li₂B₁₀H₁₀ as a white powder.

To this powder were added twelve equivalents of HMPA and toluene (20 mls). This mixture was heated to boiling and filtered hot leaving a colourless solution. Crystal growth was induced by adding hexane and chilling the 2 phase mixture (-30 °C). The adduct was filtered off and dried under vacuum. Characterised as follows:

Analysis Found: C, 36.9; H, 9.9; N, 21.2% C₇₂H₂₂₆B₁₀

Li₂N₃₆O₁₂P₁₂ Requires: C, 37.9; H, 9.9; N, 22.1%.

Infra Red Nujol (cm⁻¹): 2470 (sh); 2425 (s) (B-H stretching modes); 2284 (w); 2220 (w); 1475 (sh); 1460 (s); 1295 (s); 1200 (s) (P=O stretch); 1068 (m); 983 (s); 745 (s); 650 (w); 635 (w); 505 (sh); 487 (s).

¹H NMR 360.134 MHz, solvent C₆D₆, referenced internally to

C_6H_5H at 7.16 ppm (ppm): 4.16 (s),

Integral $2H$ (polar BH); 2.44 2.43

Integral (approx) $200H$ (ligand CH_3); 1.25 (s)

Integral $8H$, (Tropical BH)

^{11}B { 1H broad band noise} 115.545 MHz, solvent C_6D_6

referenced externally to $BF_3 \cdot Et_2O$ at 0.00 ppm. (ppm): 0.17

(s); Integral $2B$, (Polar B); -26.68 (s), Integral $8B$ (Tropical B).

7Li NMR 139.96 MHz, solvent C_6D_6 , referenced externally to $PhLi$ at 0.00 ppm. (ppm): -6.33 (s).

General Techniques

Nitrogen Supply

Nitrogen gas was supplied to the laboratory as boil off from a liquid nitrogen tank having been passed through a deoxygenation plant. The gas was dried at the bench by passage through columns packed with phosphorous pentoxide and A4 molecular sieve.

Solvents

Hydrocarbons and diethyl ether were dried over freshly extruded sodium wire. THF was dried by refluxing with potassium (benzophenone added as indicator). All ethers were regularly checked for peroxide content (acidified KI). Methanol was dried over A4 molecular sieve. Pyridine was distilled and dried over A4 molecular sieve. Acetonitrile was purified and dried by the following sequence: (i) reflux over aluminium trichloride distillation, (ii) reflux over alkaline permanganate-distillation, (iii) reflux over potassium bisulphate-distillation, (iv) reflux over calcium hydride distillation (middle fraction retained), yield 60%. DMA was dried over calcium hydride.

Glove box

Air and moisture sensitive compounds were handled in a Faircrest glove box purged with white spot nitrogen. The atmosphere in the box was continuously passed copper catalyst to remove oxygen (catalyst regenerated periodically with hydrogen) and over a charcoal column to remove other impurities.

Analysis

Carbon, hydrogen and nitrogen were determined on a Carlo Erba Strumentazione Elemental Analyser (Model 1106). Metals were determined on

a Perkin Elmer 5000 Atomic Absorption Spectrophotometer. Halogens were determined by oxygen flask combustion followed by potentiometric titration. Boron was determined by oxygen flask combustion followed by Atomic Absorption.

Infra Red Spectroscopy

I.R. spectra, in the range $4000-250\text{ cm}^{-1}$ were recorded on Perkin Elmer 457 or 577 grating spectrometers. Samples were mounted as nujol mulls or contact films between KBr plates or as pressed KBr plates.

Mass Spectrometry

Mass spectra were recorded on a V.G. 7070E Analytical Organic Mass Spectrometer operating at 70 eV. C.I. spectra were recorded using ammonia and isobutane as reagent gases. Source temperatures of $150-250^\circ\text{C}$ were used and samples were introduced by direct insertion.

Nuclear Magnetic Resonance Spectroscopy

N.M.R. spectra were recorded on a Hitachi/Perkin Elmer R-24B Continuous Wave spectrometer operating at 60 MHz (^1H), a Brüker AC250 Fourier Transform spectrometer (^1H , ^{11}B , ^{13}C , ^{19}F) and a Brüker WH360 Fourier Transform instrument (^1H , ^{11}B , ^7Li) (a SERC facility at Edinburgh University). Deuterated solvents for high field work were dried over A4 molecular sieve and stored in a glove box.

X-ray Crystal Structure determination

X-ray structure determinations were carried out at Newcastle University on a Siemens AED2 diffractometer with a graphite monochromator, using either CuK α or MoK α radiation ($\lambda = 1.54184/0.71073\text{ \AA}$). w/θ scan mode was used for data collection, with appropriately chosen scan width and time. Programs were SHELXTL and local software on a Data General Model 30 computer.

Appendix CCOLLOQUIA

The Board of Studies in Chemistry requires that each postgraduate research thesis contains an appendix listing:

- a) All research colloquia, research seminars and lectures arranged by the Department of Chemistry during the period of the author's residence as a postgraduate student;
 - b) All research conferences attended and papers presented by the author during the period when research for the thesis was carried out.
-

RESEARCH COLLOQUIA, SEMINARS, LECTURES, AND CONFERENCES

(A) Lectures and Seminars organised by the Department of Chemistry during the period 1984-1987.

- 19.10.84 Dr. A. Germain (Languedoc, Montpellier)
"Anodic Oxidation of Perfluoro Organic Compounds in Perfluoroalkane Sulphonic Acids"
- 24.10.84 Prof. R.K. Harris (Durham)
"N.M.R. of Solid Polymers"
- 28.10.84 Dr R. Snaith (Strathclyde)
"Exploring Lithium Chemistry: Novel Structures, Bonding, and Reagents"
- 7.11.84 Prof. W.W. Porterfield (Hampden-Sydney College, USA)
"There is no Borane Chemistry (only Geometry)"
- 7.11.84 Dr. H.S. Munro (Durham)
"New Information from ESCA Data"
- 21.11.84 Mr. N. Everall (Durham)
"Picosecond Pulsed Laser Raman Spectroscopy"
- 27.11.84 Dr. W.J. Feast (Durham)
"A Plain Man's Guide to Polymeric Organic Metals"
- 28.11.84 Dr. T.A. Stephenson (Edinburgh)
"Some recent Studies in Platinum Metal Chemistry"
- 12.12.84 Dr. K.B. Dillon (Durham)
"³¹P NMR Studies of some Anionic Phosphorus Complexes"
11. 1.85 Emeritus Prof. H. Suchitzky (Salford)
"Fruitful Fissions of Benzofuroxanes and Isobenzimidazoles (Umpolung of *o*-phenylenediamine)"
13. 2.85 Dr. G.W.J. Fleet (Oxford)
"Synthesis of some Alkaloids from Carbohydrate"
19. 2.85 Dr. D.J. Mincher (Durham)
"Stereoselective Syntheses of Some Novel Anthracyclines Related to the Anti-cancer Drug Adriamycin and to the Steffimycin Antibiotics"
27. 2.85 Dr. R.E. Mulvey (Durham)
"Some Unusual Lithium Complexes"
6. 3.85 Dr. P.J. Kocienski (Leeds)
"Some Synthetic Applications of Silicon-Mediated Annulation Reactions"

7. 3.85 Dr. P.J. Rodgers (I.C.I. plc Agricultural Division, Billingham)
"Industrial Polymers from Bacteria"
12. 3.85 Prof. K.J. Packer (B.P. Ltd./East Anglia)
"NMR Investigations of the Structure of Solid Polymers"
14. 3.85 Prof. A.R. Katritzky F.R.S. (Florida)
"Some Adventures in Heterocyclic Chemistry"
20. 3.85 Dr. M. Poliakoff (Nottingham)
New Methods for Detecting Organometallic Intermediates in Solution"
28. 3.85 Prof. H. Ringsdorf (Mainz)
"Polymeric Liposomes as Models for Biomembranes and Cells"
24. 4.85 Dr. M.C. Grossel (Bedford College, London)
"Hydroxypyridine Dyes - Bleachable One-Dimensional Metals?"
25. 4.85 Major S.A. Shackelford (U.S. Air Force)
"In Situ Mechanistic Studies on Condensed Phase Thermochemical Reaction Processes: Deuterium Isotope Effects in HMX Decomposition, Explosives and Combustion"
1. 5.85 Dr. D. Parker (I.C.I plc, Petrochemical and Plastics Division, Wilton)
"Applications of Radioisotopes in Industrial Research"
7. 5.85 Prof. G.E. Coates (formerly of Wyoming, U.S.A.)
"Chemical Education in England and America: Successes and Deficiencies"
8. 5.85 Prof. D. Tuck (Windsor, Ontario)
"Lower Oxidation State Chemistry of Indium"
8. 5.85 Prof. G. Williams (U.C.W., Aberystwyth)
"Liquid Crystalline Polymers"
9. 5.85 Prof. R.K. Harris (Durham)
"Chemistry in a Spin: Nuclear Magnetic Resonance"
14. 5.85 Prof. J. Passmore (New Brunswick, U.S.A.)
The Synthesis and Characterisation of some Novel Selenium-Iodine Cations, aided by ^{77}Se NMR Spectroscopy"
15. 5.85 Dr. J.E. Packer (Auckland, New Zealand)
"Studies of Free Radical Reactions in Aqueous Solution Using Ionising Radiation"
17. 5.85 Prof. I.D. Brown (McMaster University, Canada)
"Bond Valence as a Model for Inorganic Chemistry"
21. 5.85 Dr. D.L.H. Williams (Durham)
"Chemistry in Colour"
22. 5.85 Dr. M. Hudlicky (Blacksburg, U.S.A.)
Preferential Elimination of Hydrogen Fluoride from Vicinal Bromofluorocompounds"
22. 5.85 Dr. R. Grimmett (Otago, New Zealand)
"Some Aspects of Nucleophilic Substitution in Imidazoles"

4. 6.85 Dr. P.S. Belton (Food Research Institute, Norwich)
"Analytical Photoacoustic Spectroscopy"
13. 6.85 Dr. D. Woolins (Imperial College, London)
"Metal - Sulphur - Nitrogen Complexes"
14. 6.85 Prof. Z. Rappoport (Hebrew University, Jerusalem)
"The Rich Mechanistic World of Nucleophilic Vinylic
Substitution"
19. 6.85 Dr. T.N. Mitchell (Dortmund)
"Some Synthetic and NMR-Spectroscopic Studies of Organotin
Compounds"
26. 6.85 Prof. G. Shaw (Bradford)
"Synthetic Studies on Imidazole Nucleosides and the
Antibiotic Coformycin"
12. 7.85 Dr. K. Laali (Hydrocarbon Research Institute, University of
Southern California, U.S.A.)
"Recent Developments in Superacid Chemistry and Mechanistic
Considerations in Electrophilic Aromatic Substitutions: A
Progress Report"
13. 9.85 Dr. V.S. Parmar (Delhi)
"Enzyme Assisted ERC Synthesis"
- 17.10.85 Dr. C.J. Ludman (Durham)
"Some Thermochemical Aspects of Explosions"
- 24.10.85 Dr. J. Dewing (UMIST)
"Zeolites - Small Holes, Big Opportunities"
- 30.10.85 Dr. S.N. Whittleton (Durham)
"An Investigation of a Reaction Window"
- 31.10.85 Dr. P. Timms (Bristol)
"Some Chemistry of Fireworks"
- 5.11.85 Prof. M.J. O'Donnell (Indiana-Purdue University, U.S.A.)
"New Methodology for the Synthesis of Amino Acids"
- 7.11.85 Prof. G. Ertl (Munich, W. Germany)
"Heterogeneous Catalysis"
- 14.11.85 Dr. S.G. Davies (Oxford)
"Chirality Control and Molecular Recognition"
- 20.11.85 Dr. J.A.H. McBride (Sunderland Polytechnic)
"A Heterocyclic Tour on a Distorted Tricycle - Biphenylene"
- 21.11.85 Prof. K.H. Jack (Newcastle)
"Chemistry of Si-Al-O-N Engineering Ceramics"
- 28.11.85 Dr. B.A.J. Clark (Kodak Ltd.)
"Chemistry and Principles of Colour Photography"
- 28.11.85 Prof. D.J. Waddington (York)
"Resources for the Chemistry Teacher"

15. 1.86 Prof. N. Sheppard (East Anglia)
"Vibrational and Spectroscopic Determinations of the Structures of Molecules Chemisorbed on Metal Surfaces"
23. 1.86 Prof. Sir Jack Lewis (Cambridge)
"Some More Recent Aspects in the Cluster Chemistry of Ruthenium and Osmium Carbonyls"
29. 1.86 Dr. J.H. Clark (York)
"Novel Fluoride Ion Reagents"
30. 1.86 Dr. N.J. Phillips (Loughborough)
"Laser Holography"
12. 2.86 Dr. J. Yarwood (Durham)
"The Structure of Water in Liquid Crystals"
12. 2.86 Dr. O.S. Tee (Concordia University, Montreal, Canada)
"Bromination of Phenols"
13. 2.86 Prof. R. Grigg (Queen's, Belfast)
"Thermal Generation of 1,3-Dipoles"
19. 2.86 Prof. G. Procter (Salford)
"Approaches to the Synthesis of Some Natural Products"
20. 2.86 Dr. C.J.F. Barnard (Johnson Matthey Group)
"Platinum Anti-Cancer Drug Development"
26. 2.86 Ms. C. Till (Durham)
"ESCA and Optical Emission Studies of the Plasma Polymerisation of Perfluoroaromatics"
27. 2.86 Prof. R.K. Harris (Durham)
"The Magic of Solid-State NMR"
5. 3.86 Dr. D. Hathway (Durham)
"Herbicide Selectivity"
5. 3.86 Dr. M. Schroder (Edinburgh)
"Studies on Macrocyclic Compounds"
6. 3.86 Dr. B. Iddon (Salford)
"The Magic of Chemistry"
12. 3.86 Dr. J.M. Brown (Oxford)
"Chelate Control in Homogeneous Catalysis"
14. 5.86 Dr. P.R.R. Langridge-Smith (Edinburgh)
"Naked Metal Clusters - Synthesis, Characterisation, and Chemistry"
9. 6.86 Prof. R. Schmutzler (Braunschweig, W. Germany)
"Mixed Valence Diphosphorus Compounds"
23. 6.86 Prof. R.E. Wilde (Texas Technical University, U.S.A.)
"Molecular Dynamic Processes from Vibrational Bandshapes"
- 16.10.86 Prof. N.N. Greenwood (University of Leeds)
"Glorious Gaffes in Chemistry"

- 23.10.86 Prof. H.W. Kroto (University of Sussex)
"Chemistry in Stars, Between Stars and in the Laboratory"
- 29.10.86 Prof. E.H. Wong (University of New Hampshire, U.S.A.)
"Coordination Chemistry of P-O-P Ligands"
- 5.11.86 Prof. Döpp (University of Duisburg)
"Cyclo-Additions and Cyclo-Reversions Involving Capto-Dative Alkenes"
- 6.11.86 Dr. R.M. Scrowston (University of Hull)
"From Myth and Magic to Modern Medicine"
- 13.11.86 Prof. Sir Geoffrey Allen (Unilever Research)
"Biotechnology and the Future of the Chemical Industry"
- 20.11.86 Dr. A. Milne and Mr. S. Christie (International Paints)
"Chemical Serendipity - A Real Life Case Study"
- 26.11.86 Dr. N.D.S. Canning (University of Durham)
"Surface Adsorption Studies of Relevance to Heterogeneous Ammonia Synthesis"
- 27.11.86 Prof. R.L. Williams (Metropolitan Police Forensic Science)
"Science and Crime"
- 3.12.86 Dr. J. Miller (Dupont Central Research, U.S.A.)
"Molecular Ferromagnets: Chemistry and Physical Properties"
- 8.12.86 Prof. T. Dorfmueller (University of Bielefeld)
"Rotational Dynamics in Liquids and Polymers"
22. 1.87 Prof. R.H. Ottewill (University of Bristol)
"Colloid Science: A Challenging Subject"
28. 1.87 Dr. W. Clegg (University of Newcastle-upon-Tyne)
"Carboxylate Complexes of Zinc Charting a Structural Jungle"
4. 2.87 Prof. A. Thomson (University of East Anglia)
"Metalloproteins and Magneto-optics"
5. 2.87 Dr. P. Hubberstey (University of Nottingham)
"Demonstration Lecture on Various Aspects of Alkali Metal Chemistry"
11. 2.87 Dr. T. Shepherd (University of Durham)
"Pteridine Natural Products: Synthesis and Use in Chemotherapy"
12. 2.87 Dr. P.J. Rodgers (I.C.I. Billingham)
"Industrial Polymers from Bacteria"
17. 2.87 Prof. E.H. Wong (University of New Hampshire, U.S.A.)
"Symmetrical Shapes from Molecules to Art and Nature"
19. 2.87 Dr. M. Jarman (Institute of Cancer Research)
"The Design of Anti-Cancer Drugs"
4. 3.87 Dr. R. Newman (University of Oxford)
"Change and Decay: A Carbon-13 CP/MAS NMR Study of Humification and Coalification Processes"

(B) Research Conferences attended and papers presented

- September 1984 Intraboron III, Durham University
- April 1985 Graduate Symposium, Durham University
- September 1985 Intraboron IV, Edinburgh University
paper presented "Derivative Chemistry of Icosahedral
Carboranes"
- April 1986 Annual Chemical Congress, Warwick University,
poster presented "Carboranyl groups as bulky 'aryl'
ligands"
- September 1986 Intraboron V, Warwick University
paper presented "More Derivative Chemistry of
Icosahedral Carboranes"
- April 1987 Graduate Symposium, Durham University
paper presented "Aspects of Derivative Chemistry of
Icosahedral Carboranes"
- September 1987 Intraboron VI, Strathclyde University
paper presented "Anions $\text{Ph(O)C}_2\text{B}_{10}\text{H}_{10}^-$ and related
species"

